Design and development of an AI enhanced channel coding technique with adaptive reconfigurable intelligent surface for terahertz 6G communication

A Thesis Submitted for the Degree of Doctor of Philosophy

By

Aya Khalid Ahmed Al-Joudi

Department of Electronic and Electrical Engineering, Brunel University London

2026

To

My Idol, My First Love, The Only Man in My Life, My First Supporter, The Greatest Man in The World, Whose Early Death Made My Heart and Soul Bleed, My Handsome Great Father,

Prof. Khalid Ahmed Al-Joudi

Sacrifice, Giving, Patience, Loyalty, Generosity, Love, Tenderness, The Woman Who Gave Up Her Academic Career So That I Could Continue My Life in Comfort, My Beautiful and Great Mother,

Prof. Maysoon Mohammed Al-Hitti

The Great Mother ***Maysaloon Khalid Al-Joudi***
The Great Pharmacist ***Dr. Kawther Khalid Al-Joudi***
The Great Assistant Lecture ***Dr. Basma Khalid Al-Joudi***

My Sisters and Their Families

The One and Only, My Favourite, My Joy, Who Always Telling Me You Can Do It But Do It Faster Because I Miss You ***Khaldoon***

My Nephew

Declaration of Authorship

We declare on our honour that the work presented in this dissertation, entitled Design and Development of an AI Enhanced Channel Coding Technique with Adaptive Reconfigurable Intelligent Surface for Terahertz 6G Communication, is original and was carried out by Aya Khalid Ahmed Al-Joudi under the supervision of Professor Hamed Al-Raweshidy and Dr Take Itagaki, and Professor Maysam Abbod as a Research Development Advisor (RDA).

February 2026

Aya Khalid Ahmed Al-Joudi

Acknowledgements

لَنَجْزِيَنَّ الَّذِينَ صَبَرُوا أَجْرَهُم بِأَحْسَنِ مَا كَانُوا يَعْمَلُونَ

We will surely give those who were patient their reward according to the best of what they do

Alhamdulillah, Foremost, I would like to offer this endeavour to God Almighty for the wisdom he bestowed upon me and the strength in order to complete this research.

Furthermore, I would like to express my deepest appreciation and gratitude to my supervisor Professor Hamed Al-Raweshidy. His endless support, encouragement, care and motivation have helped me to make my Ph.D. journey more productive, and enjoyable.

I can not forget Professor Maysam Abbod (Peace be upon his sole), for his valuable support, mentoring, and guidelines with the little time I had lucky to have him as a second supervisor and research development principle.

I am grateful for my mentors through my academic years for always supporting and believing in me Professor Abdulkareem Kadhim, and Professor Mohammed Abdala.

Mostly, I am thankful and grateful for my family, my father prof. Khalid Ahmed Al-Joudi, I just wished that you are still here with me to witnesses your little girl be a Dr. My mother prof. Maysoon Mohammed Al-Hiti, no words can describe how much I am thankful to you, I wish I will be able to pay back a small amount of your sacrifices for me through these years. My lovely sisters Maysaloon, Kawther, and Basma, this journey couldn't be easier without your and your families support.

My courages nephew Khaldoon, your hugs, laughters, and endless phone calls always gave me strength.

My sisters in life Basma Al-Atia and Neaam Al-Samaraie, I wouldn't be able to continuo without your encouragement, support, and true friendship.

Brunel University of London

Thank You

Abstract

This thesis presents a novel approach to design and implement a new channel coding method combined with a Adaptive RIS (ARIS) to enhance Terahertz (THz) communication in 6G networks. The research addresses the crucial requirements of 6G communication, including ultra-fast data transmission, minimal delay, extensive connectivity, and optimal energy usage.

The innovative channel coding approaches, Polar Convolutional Serial Code (PCSC) and Polar Convolutional Parallel Code (PCPC), are specifically designed to enhance the reliability and data transfer rate of wireless communication systems operating at THz frequencies. Their performance is rigorously evaluated in congested network conditions, a common scenario in 6G applications, in conjunction with Non Orthogonal Multiple Access (NOMA) strategies.

A key achievement in this research is the integration of ARIS into the communication system, leading to the development of a ARIS Decision Making Algorithm (ARIS-DMA). This technology optimises signal strength and coverage by dynamically adjusting surface reflection and transmission properties based on the user's location and network conditions. The ARIS-DMA effectively reduces power loss and latency, providing comprehensive coverage and a 70% signal power loss reduction, instilling confidence of users about the progress in the field.

In addition, the thesis investigates the application of Deep Learning (DL) methods for decoding PCPC. It suggests a Deep Q Network (DQN) based Deep Q Network ARISDMA (DQN-ARISDMA) to improve beamforming and increase spectral efficiency. The findings exhibit significant enhancements in data transmission speeds, utilisation of the frequency spectrum, and the ability of the system to respond promptly, all of which are vital for time-sensitive applications in 6G networks.

The outcomes of this study contribute significantly to the development of communication systems that can meet the rigorous standards of future 6G networks while also being scalable, energy-efficient, and reliable. This advancement creates opportunities for progress in areas such as smart cities, autonomous vehicles, and augmented/virtual reality experiences, demonstrating the practical implications of our research.

Contents

List of Algorithms

List of Figures

List of Tables

Acronyms

1G First Generation. *(p. 2, 10, 15, 18, 21)*
2D Two Dimensional. *(p. 65)*
2G Second Generation. *(p. 2, 10, 25)*
3D Three Dimensional. *(p. 65)*
3G Third Generation. *(p. 2, 10, 25)*
3GPP 3rd Generation Partnership Project. *(p. 30)*
4G Fourth Generation. *(p. 2, 10, 11, 25)*
5G Fifth Generation. *(p. 2–5, 8, 10, 11, 13–19, 21, 22, 25, 27, 29, 30, 34, 35, 42, 54, 57, 63, 64, 66, 67, 87, 89–94, 97, 131, 155, 161–164)*
6G Sixth Generation. *(p. x, xiii, 2–8, 10, 11, 13–33, 35–40, 42, 49–52, 54–58, 60–67, 71, 72, 86–90, 92–97, 101, 106, 108–110, 128, 130, 131, 133, 137–140, 146, 148, 150, 155, 157, 160–169, 172)*

AI Artificial Intelligence. *(p. 3–8, 21, 22, 42, 47, 48, 62, 97, 162)*
AP Access Point. *(p. 34, 38, 39, 65)*
AR Augmented Reality. *(p. 3, 22, 54–56, 169)*
ARIS Adaptive RIS. *(p. iii, 7, 110, 123, 124, 140, 162, 166)*
ARIS-DMA ARIS Decision Making Algorithm. *(p. iii, ix, xi, 7–9, 110, 118–128, 130–138, 140–144, 148, 160, 163, 166–172)*
AU Aerial Users. *(p. 49, 50)*
AWGN Additive White Gaussian Noise. *(p. 74)*

BC-LDPC block code LDPC. *(p. 27)*
BCD Block Coordinate Descent. *(p. 40, 47)*
BCE Binary Cross Entropy Loss. *(p. 101)*
BCH Bose, Chaudhuri, and Hocquenghem. *(p. 26, 27, 32, 69)*
BCS Block Coordinate Searching. *(p. 40)*
BER Bit Error Rate. *(p. 8, 18, 19, 26, 27, 30–34, 44, 86, 87, 89, 92–94, 162–164)*
BLER Block Error Rate. *(p. 33, 34)*

BN Batch Normalization. *(p. 148)*
BP Belief Propagation. *(p. 25, 44, 85)*
bps bits per second. *(p. 15, 88, 99)*
BPSK Binary Phase Shift Keying. *(p. 33, 89, 90, 164)*
BS Base Station. *(p. 17, 31, 33, 34, 37, 39, 40, 47, 50, 64, 65, 72–75, 114, 118–120, 123–128, 131–138, 140–142, 144, 145, 148, 166)*

CC Convolutional Code. *(p. 27)*
CC-LDPC Convolutional Code LDPC. *(p. 27)*
CD chase detector. *(p. 31)*
CNN Convolutional Neural Networks. *(p. 44, 47, 48, 102, 140, 148, 150, 152, 154–156, 158–160)*
CP-OFDM Cyclic Prefix OFDM. *(p. 28)*
CRAN Cloud Radio Access Network. *(p. 64)*
CRC Cyclic Redundancy Check. *(p. 26–28)*
CSI Channel State Information. *(p. 30, 32, 40, 57, 75, 120, 124, 141, 143, 145, 168)*
CV convolutional layer. *(p. 146, 148)*

D2D Device to Device. *(p. xiii, 62, 63)*
DDPG Deep Deterministic Policy Gradient. *(p. 41, 140, 148, 150, 152, 154–156, 158–160)*
DL Deep Learning. *(p. iii, 4, 8, 42, 44, 99–101, 143, 149, 155, 160, 162, 163, 165, 167, 168, 170, 171)*
DL-PCPC Deep Learning PCPC. *(p. xi, xiii, 8, 97, 102–106, 108, 109, 162, 164–166, 168, 170, 172)*
DNN Deep Neural Network. *(p. 44)*
DQN Deep Q Network. *(p. iii, 9, 140, 143, 163, 169)*
DQN-ARISDMA Deep Q Network ARISDMA. *(p. iii, ix, 8, 9, 139, 143, 145, 146, 148, 150, 152, 154–160, 163, 167, 169–172)*

EC European Commission. *(p. 13)*
EE Energy Efficiency. *(p. 6, 14, 19–21, 25, 39–41, 106, 108, 109, 115, 117, 118, 162, 165)*
EM ElectroMagnatic. *(p. 112, 113)*
eMBB Enhanced Mobile Broadband. *(p. 35)*
ERLLCS Extremely high Reliability and Low Latency Communication with Security. *(p. 17)*
ES Energy Splitting. *(p. 40, 41, 115–117)*
ETP NetworldEurope. *(p. 13)*

ETSI European Telecommunications Standards Institute. *(p. 56)*

FBMC Filter Bank based Multi Carrier. *(p. 29)*
FC fully connected layers. *(p. 146, 148)*
FEC Forward Error Correcting. *(p. 32)*
FER Frame Error Rate. *(p. 18, 19, 27)*
FL Federated Learning. *(p. 42, 47)*
FSR Failed Signal Rate. *(p. 130, 135, 166)*

Gbps Gigabit per second. *(p. 15, 16)*
GFNOMA Grant Free Access with NOMA. *(p. 31, 32)*
GRAND Guessing Random Additive Noise Decoding. *(p. 26)*
GRU Gated Recurrent Unit. *(p. 48)*
GSM Global System for Mobile communications. *(p. 10)*

HMIMOS Holographic MIMO surface. *(p. 64, 65)*

IGTHz Interest Group on THz communications. *(p. 24)*
IoE Internet of Everything. *(p. 3, 4)*
IoST Internet of Smart Things. *(p. 22)*
IoT Internet of Things. *(p. 3, 5, 11, 17, 18, 22, 31, 32, 49, 57, 63, 64, 72, 90, 168, 170)*
IR Infrared. *(p. 23, 52)*
IRS Intelligent Reflecting Surfaces. *(p. 36, 39)*
ISAC Integrated Sensing and Communication. *(p. 38)*
ITU International Telecommunication Union. *(p. 24, 162)*

JSCC Joint Source Channel Coding. *(p. 25, 26)*
JSCD Joint Source-Channel Decoding. *(p. 25)*

Kbps kilobits per second. *(p. 15)*
KPIs Key Performance Indicators. *(p. xiii, 3, 4, 6–8, 12, 13, 19, 21, 25, 31, 35, 36, 57, 60, 63, 66, 71, 92, 96, 97, 110, 128, 131, 157, 161, 162, 166)*

LDPC Low Density Parity Code. *(p. 25, 27, 31, 32, 44)*
LED Light Emitting Diodes. *(p. 51, 53)*
LIS Large Intelligent Surfaces. *(p. 36)*
LLR Log Likelihood Ratio. *(p. 85)*
LLRs log-likelihood ratios. *(p. 33)*

LORD layered orthogonal lattice detector. *(p. 31)*
LoS Line of Sight. *(p. 50–53, 127, 142)*
LRs Likelihood Ratios. *(p. 80, 82)*
LTE Long Term Evolution. *(p. 10)*
LWC Low Weight Coding. *(p. 25)*

M2M Machine to Machine. *(p. 172)*
MAC Medium Access Control. *(p. 20)*
MAP Maximum Posteriori. *(p. 32, 44)*
Mbps Mega bit per second. *(p. 31, 103)*
MEC Minimum Energy Code. *(p. 25)*
MECs Mobile Edge Computing's. *(p. 56–59, 62)*
MIMO Multiple Input Multiple Output. *(p. 11, 16, 21, 27, 28, 30–32, 34, 37, 40, 47, 51, 64)*
ML Maximum Likelihood. *(p. 82)*
ML Machine Learning. *(p. 3–6, 21, 22, 26, 41, 42, 44, 48, 99, 101, 140, 162)*
mMIMO massive MIMO. *(p. 34, 35, 64)*
MMSE Minimum Mean Square Error. *(p. 139, 150)*
mMTC massive Machine Type Communication. *(p. 4, 17, 18, 22, 35, 63)*
mmWave Milimeter Wave. *(p. 23, 35, 36, 39, 41, 51, 65)*
MR Mixed Reality. *(p. 22, 54)*
MRT Maximum Ratio Transmission. *(p. 139, 150)*
MS Mode Switching. *(p. 115–117)*
MSE Mean Squared Error. *(p. 46, 47)*
MUD Multiuser Detection. *(p. 29)*

Nadam Nesterov accelerated adaptive moment estimation. *(p. 101)*
NC nulling-and-cancelation. *(p. 31)*
NLoS NoLoS. *(p. 127, 128, 131, 134, 142)*
NN Neural Networks. *(p. 48)*
NOMA Non Orthogonal Multiple Access. *(p. iii, 4, 7, 8, 27, 29–35, 39–42, 62, 63, 67, 72, 162, 163)*

OFDM Orthogonal Frequency Division Multiplexing. *(p. 11, 27–30, 47, 48)*
OMA Orthogonal Multiple Access. *(p. 30, 39, 40, 72)*
OSD Ordered Statistics Decoding. *(p. 26)*
OWC Optical Wireless Communication. *(p. 52)*

PC Polar Code. *(p. 89–94, 164)*
PCPC Polar Convolutional Parallel Code. *(p. iii, 7, 8, 75, 76, 83, 85, 89–94, 96, 97, 99, 100, 162–164, 168, 169, 172)*
PCSC Polar Convolutional Serial Code. *(p. iii, 7, 8, 75, 76, 80, 83, 89–94, 96, 97, 99, 135, 137, 162–164, 168, 169, 172)*
PD-NOMA Power Domain NOMA. *(p. 30, 73–75, 88, 89, 96)*
PDF Probability Density Function. *(p. 33)*
PER Packet Error Rate. *(p. 9, 18, 19, 150, 157, 158, 160, 167)*
PHY Physical Layer. *(p. 21, 32, 65)*
PIN Positive Intrinsic Negative. *(p. 112)*
PM Path Metric. *(p. 82, 83)*
PPO Proximal Policy Optimisation. *(p. 140, 148, 150, 152, 154–156, 158–160)*
PSM Precoded Spatial Modulation. *(p. 30)*

QAM Quadrature Amplitude Modulation. *(p. 32, 87, 89–94, 164)*
QC Quantum Communication. *(p. 61, 62)*
QCLDPC Quasi Cyclic LDPC. *(p. 26)*
QKD Quantum Key Distribution. *(p. 62)*
QoS Quality of Service. *(p. 34, 50, 63, 66, 170, 171)*
QPSK Quadratic Phase Shift Keying. *(p. 33)*
QRD QR decomposition. *(p. 31)*

ReLU Rectified Linear Unit. *(p. 99, 100, 148)*
RF Radio Frequency. *(p. 23, 51, 52)*
RIS Reconfigurable Intelligent Surfaces. *(p. 4, 6, 7, 16, 21, 33–42, 44, 47, 48, 64, 110–118, 138–140)*
RL Reinforcement Learning. *(p. 42)*
RNNs Recurrent Neural Networks. *(p. 168)*
RS Reed Solomon. *(p. 27, 69)*
RSMA Rate Splitting Multiple Access. *(p. 29)*

SC Superposition Coding. *(p. 44, 72)*
SCD Successive Cancellation Decoding. *(p. xi, 80, 99, 103–109, 165)*
SCL Successive Cancellation List. *(p. 26)*
SCLD Successive Cancellation List Decoding. *(p. 80)*
SDR Semi Definite Relaxation. *(p. 139, 150)*
SE Spectral Efficiency. *(p. 6, 39, 72, 150, 152, 154, 155, 160, 167)*
SER Symbol Error Rate. *(p. 18, 19, 32, 34)*

SIC Successive Interference Cancellation. *(p. 29, 30, 32, 33, 72–75)*
SINR Signal to Interference Noise Ratio. *(p. 39, 40, 52)*
SISO Soft Input Soft Output. *(p. 83, 99)*
SLM Spatial Light Modulator. *(p. 51)*
SNR Signal to Noise Ratio. *(p. 31, 33, 38, 39, 44, 87, 91, 93, 94, 113, 139, 142, 152, 154–158)*
SNS Smart Networks and Services. *(p. 13)*
SNS JU Smart Networks and Services Joint Undertaking. *(p. 5)*
SQ Sequential Decoding. *(p. 26)*
SRIA Strategic and Innovation Research Agenda. *(p. 13)*
STAR-RIS Simultaneously Transmitting and Reflection RIS. *(p. xi, 9, 34, 39–41, 114–122, 125–128, 131–140, 163, 166)*

Tb/J Terabit per Joule. *(p. 104)*
Tbps Terabits per second. *(p. 15, 16, 23, 25, 35, 88, 93, 94, 96, 105, 106, 150, 164, 165)*
TCM Transmission Control Mechanism. *(p. 32, 33)*
THz Terahertz. *(p. iii, 4, 6, 7, 15, 17, 21–25, 31, 35, 37–40, 51, 64, 65, 109, 110, 118, 128, 131, 133, 135, 138, 148, 154, 160, 162, 165–168)*
TLBP Turbo Like Belief Propagation. *(p. 25)*
TS Time Switching. *(p. 40, 41, 115, 117, 118)*

UAV Unmanned Aerial Vehicles. *(p. 17, 47, 49–51, 169)*
UDR Ultimate Detection Resolution. *(p. 38)*
UE User Equipment. *(p. 34, 38, 49, 50, 52, 65, 119)*
UEP Unequal Error Protection. *(p. 26)*
um-MIMO ultra mMIMO. *(p. 34, 41)*
URLLC Ultra Reliable and Low Latency Communication. *(p. 3, 4, 17, 21, 22, 26, 35, 63)*
UV Ultra Violet. *(p. 52)*

V2X Vehicle to infrastructure. *(p. 18, 56)*
VLC Visible Light Communication. *(p. 17, 18, 51–53, 65, 106)*
VLSA Very Large-Scale Antenna. *(p. 36)*
VR Virtual Reality. *(p. 3, 22, 54–56, 90, 106, 165, 169)*

Wi-Fi Wireless Fidelity. *(p. 97)*
WRD WR decomposition. *(p. 31)*

XR Extended Reality. *(p. x, 22, 54–56, 106, 165)*

List of Publications

1. A. K. Ahmed and H. S. Al-Raweshidy, "Performance Evaluation of Concatenated Rate Splitting Multiple Access for 6G Multiuser Communication System," 2025 International Conference on Computer, Information and Telecommunication Systems (CITS), Colmar, France, 2025, pp. 1-7, doi: 10.1109/CITS65975.2025.11099363.

2. A. K. Ahmed and H. S. Al-Raweshidy, "Performance Evaluation of Deep Q Networks for Hybrid Reconfigurable Intelligent Surface in 6G Networks," 2024 International Conference on Computer, Information and Telecommunication Systems (CITS), Girona, Spain, 2024, pp. 1-8, doi: 10.1109/CITS61189.2024.10608029. Contribute to Chapter 6, [1].

3. A.K. Ahmed and H.S. Al-Raweshidy, "Highly Efficient Hybrid Reconfigurable Intelligent Surface Approach for Power Loss Reduction and Coverage Area Enhancement in 6G Networks", Appl. Sci. 2024, 14, 6457, doi:/10.3390/app14156457. Contribute to Chapter 5, [2].

4. A. K. Ahmed and H. S. Al-Raweshidy, "Deep Learning Polar Convolutional Parallel Concatenated (DL-PCPC) Channel Decoding for 6G Communications," 2023 International Conference on Computer, Information and Telecommunication Systems (CITS), Genoa, Italy, 2023, pp. 01-05, doi: 10.1109/CITS58301.2023.10188712. Contribute to Chapter 4, [3].

5. A. K. Ahmed and H. S. Al-Raweshidy, "Performance Evaluation of Serial and Parallel Concatenated Channel Coding Scheme With Non-Orthogonal Multiple Access for 6G Networks," in IEEE Access, vol. 10, pp. 39681-39690, 2022, doi: 10.1109/ACCESS.2022.3166943. Contribute to Chapter 3, [4].

1 Introduction

Over the past three decades, the consecutive generations of mobile communication networks have facilitated significant advancements towards a more digitised society. Every generations has included a comprehensive cellular network structure, encompassing radio access technology, access and core network routing, and a range of associated services such as authentication, access control, mobility management, data transmission, voice and messaging services.

First Generation (1G), the very first generation of wireless communication, marked the advent of mobile telephony and laid the foundation for the later development of wireless networks. Introduced in the early 1980s, 1G systems revolutionised communication by enabling analogue voice transmission, thereby making mobile connectivity available to the public for the first time. 1G networks were built upon analogue technology. 1G, in contrast to subsequent digital systems, delivered voice conversations using analogue signals. Consequently, the sound was transformed into electrical signals that exhibited continuous variations in both amplitude and frequency.

The advent of the Second Generation (2G) witnessed the introduction of the first completely digital mobile solution, which led to the emergence of the mobile phone as a portable personal device and the popularity of text messaging. The Third Generation (3G) and Fourth Generation (4G) facilitated the integration of multimedia services in mobile devices. They opened the way for the emergence of the iPhone and the entire digital sector and services that depend on smartphones, such as mobile Internet, applications, and marketplaces. The advent of the Fifth Generation (5G) should coincide with the increase of interconnected items and the introduction of new technologies that facilitate augmented reality experiences, offered to both consumer and enterprise markets. The deployment of 5G networks started in 2019, focusing on implementing the radio element of 5G as a new access network. This was followed by the deployment of standalone 5G networks which started in 2023, which also involved implementing a new 5G core network.

It might seem strange to start working on the Sixth Generation (6G) of mobile

communication networks when 5G is just beginning to be used worldwide. The big difference between what people thought 5G networks could do and what the first 5G products and solutions could actually do is the reason for this. Moreover, 5G sets itself apart from previous versions of mobile networks by its technological progress, complex structure, and extensive array of uses, such as energy-efficient expansive Internet of Things (IoT), high-speed multimedia, and low-latency communication. Although 5G provides significant performance enhancements compared to previous generations, it has not yet met the necessary criteria for the highly anticipated IoT. In addition, some applications anticipated for the 2030s necessitate a further 1000-fold rise in data speeds and latency's of less than 0.1 milliseconds.

Multiple variables, including enormous IoT, smart cities, and new Artificial Intelligence (AI)/Machine Learning (ML) based distributed applications, are driving the development of the new wireless generations and highlights the importance of this technology. The advent of 6G technology is poised to bring a transformative era characterised by the proliferation of interconnected entities, including humans, vehicles, robots, and drones. This interconnectedness will result in the generation of vast amounts of digital data, reaching the scale of Zettabytes [5, 6]. Additionally, establishing new Key Performance Indicators (KPIs) is necessary to utilise the groundbreaking technologies emerging in the coming decade effectively. These new applications and use cases necessitate meeting many KPIs simultaneously, and the trade-offs acceptable in prior generations may no longer be satisfactory [7, 8]. Therefore, it is reasonable to anticipate a comprehensive transformation of the current wireless networks for the 6G, surpassing the incremental enhancements seen in the current 5G systems, as discussed in Chapter 2.

The 6G wireless systems are expected to seamlessly support various use cases, including, but not limited to, super-smart cities, holographic communication, wireless brain-computer interactions, tactile/haptic-based communications, chip-to-chip communications, five-sensor information transfer, precision agriculture, connected autonomous vehicles, the Internet of Everything (IoE), and telesurgery.

The potential benefits of 6G are extensive and diverse. 6G will support applications that demand high accuracy and dependability, ranging from enhanced mobile broadband to Ultra Reliable and Low Latency Communication (URLLC). These encompass self-driving cars, surgery performed from a distance, and fully immersive experiences using Augmented Reality (AR)/Virtual Reality (VR). Furthermore, 6G seeks to expedite the progress of smart cities, intelligent transportation systems, and enhanced healthcare solutions.

In addition to the previously established requirements like data throughput, latency, reliability, and connectivity, 6G applications are anticipated to have demanding standards for energy efficiency, because enhancing energy efficiency has typically been associated with using energy conservatively, leading to compromising other perfor-

mance measures such as throughput, reliability, coverage, and so on. However, 6G still aims to find solutions that can ensure the energy-efficient functioning of devices and applications while simultaneously meeting other performance objectives.

There are many methods, algorithms and techniques that could be implemented to develop the current wireless generation 5G and moving towards 6G, which have been discussed in detail in Chapter 2, Section 2.4, Section 2.5 and Section 2.6. In this study, new methods, algorithms and techniques based on channel coding/decoding, AI/DL, reconfigurable materials, signal redirection and beamforming are chosen to develop wireless systems that aligns with 6G KPIs. The chosen approaches as indicated in Chapter 2 Section 2.4 are utulised to answer the following questions:

- What are the potential benefits and challenges of incorporating sophisticated channel coding algorithms into 6G networks?
- How can ML algorithms improve decoding in 6G communication systems?
- What novel channel coding techniques can be developed to support URLLC in 6G?
- What are the beneficial effects of new channel coding algorithms with Non Orthogonal Multiple Access (NOMA) strategies in 6G?
- How might AI and ML be implemented into 6G networks to improve performance and efficiency?
- What new technologies and techniques are required to utilise the Terahertz (THz) frequency effectively?
- To what extent the current generation approaches can be modified to comply with 6G KPIs?
- How can 6G networks provide URLLC while allowing massive Machine Type Communication (mMTC)?
- What developments are required in Reconfigurable Intelligent Surfaces (RIS) to improve signal control and coverage?
- How can 6G networks be designed to be both sustainable and energy efficient?

1.1 Research Motivations

With the rapid growth in traffic demand and the ongoing development of 5G new radio networks, experts from industry and academia are now focusing on the future wireless network to be known as "sixth-generation (6G)". The primary objective of this upcoming cellular network is to achieve universal and uninterrupted connectivity for all devices "Connecting the unconnected" in response to the anticipated rapid expansion of the IoE over the next ten years. The introduction of 6G is anticipated to greatly improve current technologies and architectures or create new ones at the infrastructure, spectrum, and protocol/algorithmic levels. This will result in improved services and

complete coverage connections. Significant research initiatives are currently underway worldwide to shape and build the vision of 6G, including but not limited to Smart Networks and Services Joint Undertaking (SNS JU) , Nokia, SK Telecom, NTT, and DOCOMO, 6G Hubs, 6G Flagship. To facilitate various IoT scenarios and meet the demands of emerging applications, 6G must be capable of supporting a significantly higher density of connectivity (estimated at 10^6 devices per Km^2). It should also provide 5 to 10 and 10 to 100 times greater spectral and energy efficiency, respectively, compared to what is achievable with 5G. Additionally, it should offer a reliability of 0.9999999 and support latency in the range of microseconds.

Therefore, in order to accomplish the aforementioned stringent goals, one of the most fundamental issues is to design an enhanced **coding and decoding** techniques to ensure higher reliability and throughput, along with relaxing the orthogonality limitations used in previous generations as a **multiple access** techniques. Digital inclusion and global service coverage are closely connected to reliability. The 6G architecture will facilitate the provision of network coverage in remote locations, such as rural areas, and enable communication over long distances, including over seas and large land masses. This will open up opportunities for new services and enterprises, leading to economic growth by bringing together diverse communication methods that were previously separate. Providing the unlimited coverage and addressing problems as "zero coverage spots", is a breaking system advancement that should be addressed, however this advancement should not overload the current infrastructure in terms of cost and dependability, using approaches that have the ability to **reconfigure** and redirect the signals towards users effectively is a promising approach to achieve such goal.

6G is as likely to be a self-contained ecosystem of AI. The evolution will gradually shift from a focus on humans to a focus on both humans and machines. The implementation of 6G technology will provide instantaneous and unfettered wireless communication. 6G will enable convergence in connectivity, robotics, cloud, and safe and trustworthy commerce, leading to a new landscape for organisations. This will fundamentally transform the way enterprises function. The main characteristics of 6G will encompass intelligent, interconnected management and control capabilities, programmability, integrated sensing and communication, energy efficiency, reliable infrastructure, scalability, and cost-effectiveness.

The architecture of 6G must possess ample flexibility and efficiency to facilitate seamless integration of various components, such as networks, collaborative communication and sensing, non-terrestrial networks, and terrestrial communication. This integration should encompass innovative AI driven facilitators and local and distributed computing capabilities. The notion of "AI everywhere" will be implemented in the network to optimise performance and offer AI as a service in a federated network. AI and ML will ensure the cost-effectiveness of advanced 6G services. These services include seamless

interaction between humans, digital systems, the physical world, and the Internet of Senses. AI and ML will automate **decision making** processes to some extent and enable a zero touch approach.

1.2 Aim and Objectives

The main aim of this study is to **create effective and dependable techniques that can establish a communication system with superior reliability, higher data rate, higher spectral and energy efficiency, elevated user density, unlimited coverage, less delay, and lower energy consumption**. These advancements are intended to meet the requirements of the next wireless generation, 6G. This can be achieved by proposing new channel coding approaches, automated fast decoding methods, adaptive transmission algorithms, and programmable efficient signal redirection, for fair and efficient utilisation and enabling wireless communication flexibility management with high Energy Efficiency (EE), and Spectral Efficiency (SE).

The research aim is accomplished by achieving the following objectives:

1. **Comprehensive Analysis of Emerging Technologies:** Conduct an in-depth examination of current programmable approaches, algorithms, and methodologies across previous wireless generations to identify the essential KPIs defining 6G. This involves assessing the capabilities and limitations of existing technologies and evaluating the emerging techniques expected to transform wireless communication by 2030.
2. **Design of Novel Channel Coding Methods:** Develop new channel coding strategies specifically tailored to the requirements of 6G systems, aiming to enhance data rate, reliability, and overall system performance. The proposed designs will be evaluated in conjunction with advanced multiple access schemes to ensure compatibility with the expected high user density of 6G networks.
3. **Artificial Intelligence–Driven Decoding and Signal Optimisation:** Design and implement an artificial intelligence–based decoding mechanism to reduce decoding latency and overall transmission time, thereby improving energy efficiency and throughput while maintaining high system reliability in dense network environments.
4. **Reconfigurable Intelligent Surfaces (RIS) Assisted Communication for Coverage and Efficiency Enhancement:** Develop a Reconfigurable Intelligent Surfaces (RIS) assisted communication framework capable of optimising spectral and energy efficiency, minimising power loss, and ensuring seamless connectivity across all coverage zones, including traditionally hard-to-reach or zero-coverage areas.
5. **Real-Time Terahertz (THz) Transmission and Intelligent Signal Redirection:** Implement and evaluate a real-time wireless transmission system operating within

the Terahertz (THz) frequency band, capable of simultaneously supporting a large number of users. The system will employ advanced signal redirection and intelligent beamforming techniques to achieve equitable resource distribution, reduced latency, and enhanced spectral efficiency thereby demonstrating the practical realisation of 6G performance metrics.

1.3 Novel Contributions to Science

This thesis explores several facets of the emerging 6G wireless generation, focusing on the integration of novel channel coding, AI, and RIS. The contributions to knowledge consist of four components, whereas the outcomes in the form of new solutions, algorithms, and protocol modifications are outlined below:

1. **Systematic Classification and Evaluation of 6G Technologies:** Provides a comprehensive taxonomy and critical assessment of existing and emerging methodologies relevant to 6G. This contribution identifies and analyses the KPIs, capabilities, and technological limitations defining the transition from previous generations, thereby establishing a clear foundation for subsequent developments within this research (addressing Objective **one** in Section 1.2).
2. **Development and Integration of Novel Channel Coding Schemes with Non Orthogonal Multiple Access (NOMA):** Two new channel coding frameworks Polar Convolutional Serial Code (PCSC) and Polar Convolutional Parallel Code (PCPC) are developed using concatenated serial and parallel architectures. These codes are designed to meet the reliability and throughput requirements of THz based multiuser 6G environments. Their integration with the Non Orthogonal Multiple Access (NOMA) technique demonstrates improved system reliability, fairness, and data rate under high user density conditions. Collectively, these outcomes validate the potential of the proposed codes as efficient solutions for 6G communication systems (addressing Objectives **two**, **three** and **five** in Section 1.2).
3. **Artificial Intelligence (AI) Enabled Fast Decoding Framework:** Develops an Artificial Intelligence (AI) driven decoding architecture for the proposed PCPC scheme, significantly reducing decoding and transmission times while enhancing data rate and energy efficiency. This contribution illustrates the potential of AI to accelerate signal processing and enable adaptive, self-optimising 6G communication systems (addressing Objective **two** and **three** in Section 1.2).
4. **Design of ARIS Decision Making Algorithm (ARIS-DMA):** A novel Adaptive RIS (ARIS) assisted wireless communication framework, termed the ARIS Decision Making Algorithm (ARIS-DMA), is developed to optimise beam redirection and power utilisation. The algorithm employs user-location awareness to ensure complete coverage, including previously unreachable zones, while reducing signal

power loss by approximately 70% and lowering transmission delay. This contribution demonstrates substantial improvements in energy and spectral efficiency (addressing Objective **four** and **five** in Section 1.2).

5. **Artificial Intelligence (AI) Deep Reinforcement Learning–Based Beamforming:** Building upon ARIS-DMA, this research introduces the Deep Q Network ARISDMA (DQN-ARISDMA) framework, which incorporates deep reinforcement learning to enable adaptive and intelligent beamforming. The results indicate significant improvements in spectral efficiency reaching up to 20 Tbps/Hz alongside reduced convergence time and enhanced network responsiveness, establishing the feasibility of real-time, AI empowered 6G beamforming (addressing Objectives **three**, **four** and **five** in Section 1.2).

1.4 In the Next Chapters

The following chapters will discuss this study in detail.

Chapter 1 establishes the context and framework for the entire thesis. It provides an overview of the motivations, aim, and objectives of the research and emphasises the unique and original contributions that this research brings to the field of 6G communication networks. This chapter also provides a concise summary of the organisation of the thesis and enumerates the publications that have emerged from this research.

Chapter 2 comprehensively analyses the most recent literature about 6G communication networks. The discussion commences with the initial steps and progresses from 5G to 6G, focusing on the essential KPIs required for 6G networks. The assessment discusses evolutionary enabling technologies and other breakthrough technologies anticipated to be widespread by 2030. The chapter ends by examining the gaps noted in the existing body of literature, which this research intends to overcome.

Chapter 3 explores different forms of concatenated channel coding, specifically serial and parallel concatenated codes. This chapter also covers integrating Non Orthogonal Multiple Access (NOMA) with novel channel coding identified as Polar Convolutional Serial Code (PCSC) and Polar Convolutional Parallel Code (PCPC). The performance analysis starts by examining performance metrics such as Bit Error Rate (BER) and throughput, followed by a comprehensive evaluation and performance discussion.

Chapter 4 examines the use of Deep Learning (DL) in channel decoding. This chapter introduces Deep Learning PCPC (DL-PCPC) and comprehensively explains the deep network decoding architecture and the sequential processes of data generation, preparation, and validation for the system. The chapter discusses the training procedure and performance measures, including the minimum decoding error and data rate. The chapter ends with a thorough examination of performance and a discourse on the outcomes.

Chapter 5 explores the core principles of ARIS Decision Making Algorithm (ARIS-DMA). It provides a comprehensive explanation of Simultaneously Transmitting and Reflection RIS (STAR-RIS) organisation, categories, and capabilities and the system modelling approach used for ARIS-DMA. It also examines different implementation scenarios and analyses performance indicators, including power loss, delay, user coverage, and Packet Error Rate (PER). The chapter ends with a thorough performance evaluation and a subsequent discussion.

Chapter 6 explores basic beamforming approaches for ARIS-DMA and the system concept for Deep Q Network (DQN) to introduce Deep Q Network ARISDMA (DQN-ARISDMA) beamforming. The chapter covers the system model, channel model, signal model, problem formulation, and the network's architecture and training for DQN-ARISDMA. Performance measures such as fairness, spectrum efficiency, convergence time, and latency are analysed, followed by a thorough examination and discussion of the performance.

Finally, **Chapter 7** presents a concise overview of the research discoveries, derives logical inferences from the study, and proposes potential avenues for future investigation. Additionally, it examines the prospective influence of this research on industrial procedures, highlighting the practical implementations and advantages of the created technologies.

2

Literature Review

In this chapter, we thoroughly explain the different fields of this study. In Section 2.1, we explain the preliminaries of the new wireless generation. Then, we delve into the discussion of the expectations of the transition from 5G to 6G in Section 2.2. Section 2.3 explains the key performance indicators that specify the working era for 6G. In the next section, Section 2.4, we explain the key enabling technologies we use and target for 6G in this research. Section 2.5 will provide a review of other enabling technologies that researchers could use for 6G wireless communication. In Section 2.6, we will review other methods and tools that researchers could have used for this study.

2.1 Preliminaries

The evolutionary history of mobile communication systems [9] can be traced back to the 1980s when the First Generation (1G) analogue cellular system emerged. This initial system, which relied on analogue technology, was eventually replaced in 1990 by the Second Generation (2G) [10] digital network, commonly referred to as the Global System for Mobile communications (GSM). This upgraded system introduced essential features such as voice communication and text messaging, revolutionising the way people communicated with one another. However, despite these advancements, the 2G network still had limitations in data transmission speeds, prompting the development of the Third Generation (3G) in 2001.

The introduction of 3G technology [11] marked a significant milestone in the evolution of mobile communication systems. Unlike its predecessors, 3G offered significantly higher data rates, enabling users to access the internet and other data-intensive services more efficiently. This paved the way for the widespread adoption of the mobile internet and the emergence of various applications and services that rely on high-speed data transmission.

The Fourth Generation (4G), Long Term Evolution (LTE) networks were introduced as technology advanced in 2009 [12]. The advent of 4G networks brought about a

paradigm shift in the mobile communication landscape. With the inclusion of new technologies such as Multiple Input Multiple Output (MIMO) and Orthogonal Frequency Division Multiplexing (OFDM), 4G networks were able to deliver faster and more reliable connections. This, in turn, led to a significant increase in subscribers for various services, particularly internet-based services. The enhanced capabilities of 4G networks improved the user experience and opened new possibilities for industries and businesses to leverage mobile technology for their operations.

Building upon the success of 4G networks, the Fifth Generation (5G) was introduced in 2019 [13]. This latest version of mobile communication systems represents a significant leap forward, as it extends the reach of mobile services beyond just humans to include various devices and objects in industries. With 5G, the Internet of Things (IoT) becomes a reality, enabling seamless connectivity and communication between multiple devices. This transformative capability has the potential to revolutionise industries and make the world a more interconnected and efficient global village, Table 2.1 summarises the differences between the different wireless generations.

The evolution of mobile communication systems has been a continuous process of innovation and improvement. From the early days of analogue systems to the current era of 5G networks, each generation has brought about new capabilities and expanded the possibilities of mobile technology. As we look towards the future, it is clear that mobile communication will continue to play a pivotal role in connecting people, devices, and industries, driving further advancements and shaping how we live and interact [14].

Figure 2.1: 6G wireless communication service targets

Sixth Generation (6G), the forthcoming mobile network generation, will be instrumental in addressing the challenges ahead for us in 2030 and beyond and accomplishing the goals shown in Figure 2.1. As we witness the ever-increasing pervasiveness of mobile communications, it becomes evident that they will assume an even more prominent role in our day-to-day lives, surpassing their current significance.

Table 2.1: Comparison of the different wireless communication generations

KPI [a]	1G	2G	3G	4G	5G
Start/Development	1970/1984	1980/1999	1990/2002	2000/2010	2010/2015
Technology	AMPS, NMT, TACS	GSM	WCDMA	LTE, WiMax	MIMO, mm Waves
Frequency	30 KHz	1.8 GHz	1.6-2 GHz	2-8 GHz	3-30 GHz
Access System	FDMA	TDMA, CDMA	CDMA	OFDMA, SC-FDMA	OFDMA/BDMA
Core Network	PSTN	PSTN	Packet Network	Internet	Internet
Transmission Speed	≈10 Kbps	≈64 Kbps	≈14.4 Mbps	≈1 Gbps	≈20 Gbps
Encoding	Analog	Digital	Digital	Digital	Digital
Supported Services	Voice	Voice Text	Voice Internet	High Speed Internet HD video	UH Speed Broadband VR/AR Self-Driving cars Smart Factories

[a] Key Performance Indicators (KPIs)

Consequently, 6G will accomplish many objectives beyond swift mobile Internet access. These objectives can be summarised as follows [15]:

1. **Convergence**: the integration of physical, human, and digital realms in the context of 6G will necessitate the provision of assistance for digital twinning, immersive communication, cognition, and intelligence connection.
2. **Programmable**: in order to, provide a high degree of flexibility, programming capabilities must be positioned as a fundamental aspect of the upcoming 6G technology.
3. **Deterministic**: 6G must provide support for predictable end-to-end services.
4. **Sensible**: the integration of sensing and communication is a crucial requirement for 6G, since it will facilitate the provision of services such as high-precision localisation and high-resolution sensing.
5. **Sustainable**: the implementation of 6G technology is expected to significantly contribute to sustainability efforts by minimising its impact on energy consumption, resource utilisation, and emissions. Furthermore, it is anticipated to enhance sustainability across various sectors of society and industry.
6. **Reliable**: establishing a reliable and dependable 6G infrastructure is vital to serve as the foundational framework for future societies.
7. **Inclusive**: in order to, promote global inclusivity, it is imperative that the development of 6G technology prioritises scalability and affordability.
8. **Expandable**: to meet the demands of 6G, it is necessary to substantially enhance the KPIs currently achievable with 5G technology.

Standardisation efforts for the development of 6G are anticipated to commence in the year 2030. However, it is worth noting that even in 2020, the ITU-T Focus Group on Technologies for Network 2030 [16] had already released a series of forward-thinking and visionary documents. Moreover, within the European Union, several associations are working towards formulating a comprehensive understanding of what 6G truly entails. One such association is NetworldEurope (ETP) [17], which has released a Strategic and Innovation Research Agenda (SRIA) with a steadfast focus on the forthcoming 6G era, akin to their efforts during the nascent stages of 5G [18]. This document serves as the technological foundation for the objectives that will be implemented through the Smart Networks and Services (SNS) Partnership [19], an alliance between the European Commission (EC) and private entities within the European Union.

While the standardisation efforts for 6G are not projected to commence until 2030, numerous organisations and associations across the globe, including those within the European Union, United States, China, Japan, and South Korea, have already embarked on their respective endeavours to conceptualise and shape the future landscape of 6G. These initiatives encompass strategic research agendas, research projects, private

sector-led alliances, and substantial investments in research and development. Despite this global momentum, it is essential to recognise that certain regions have yet to disclose their comprehensive roadmaps for 6G. Nevertheless, the collective efforts and collaborations forged within these diverse regions will undoubtedly contribute to realising a genuinely transformative and groundbreaking 6G network.

2.2 5G to 6G transition

In the past ten years, there has been an annual increase of 50% to 100% in the volume of mobile data traffic. Empirical evidence suggests that the rise of mobile data will remain the same in the forthcoming decade. There is anticipated to be a sustained growth in interconnected devices, encompassing sensors, linked autos, home gadgets, body cameras, and other similar technologies. This growth will be accompanied by escalating requirements from emerging applications and services [20]. This growth suggests that the forthcoming 6G technology must accommodate a significantly greater mobile data traffic flow, ranging from 100 to 1000 times larger than the current 5G technology.

It should be noted that the increase in mobile data traffic volume does not necessarily lead to a proportional increase in energy usage. To maintain energy consumption levels between 6G and 5G, reducing the overall energy usage per user, base station, and network node is imperative. Additionally, there is a need to enhance the Energy Efficiency (EE) per performed and processed data, aligning with the increasing volume of mobile data traffic [21].

One of the most significant prospects for the forthcoming decade is the potential for immersive communication, holographic telepresence, and augmented reality/virtual reality (AR/VR) to become the prevailing mode of interpersonal interaction. There is a widespread consensus that achieving an optimal level of quality for immersive experiences necessitates a video resolution of 8k per eye [22].

It is anticipated that 6G networks will need to provide end users with data speeds of up to 10 Gbits/s, ensuring a satisfactory user experience to facilitate the new required functionalities. The proliferation of mobile devices does not necessarily correspond to an increase in mobile device density. However, it is anticipated that 6G networks would employ smaller cellular structures, enabling a greater concentration of devices within each cell.

6G expected to support peak densities up to 10 devices per m^2. Moreover, as the mobile data traffic for each device escalates, the capacity will have corresponding augmentation. When individuals utilise AR glasses at a stadium or workstations, it will be essential to accommodate the capabilities of 150 ($Tpbs/km^2$). This capacity demand is approximately ten times greater than that of 5G technology.

2.3 6G Key Performance Indicators (KPIs)

Based on the overarching vision and the ambitious pursuit of a universal smart Mobile Sphere, the forthcoming 6G technology will undergo substantial enhancements and expansions, thereby facilitating a remarkable 10 to 100-fold surge in data throughput while simultaneously bolstering system capacity, broadening coverage to encompass wider and deeper geographical extents, optimizing resource utilization to unprecedented levels, elevating spectrum efficiency, accommodating higher moving speeds effortlessly, significantly reducing latency, and unequivocally propelling the seamless progression of a fully-fledged universal smart Mobile Sphere.

As shown in Figure 2.2 6G is envisioned to be an all-encompassing and extensively interconnected system that boasts broader and more extensive coverage compared to its predecessors. This advanced network will incorporate a multitude of cutting-edge capabilities, including terrestrial communication over short distances between devices, as well as satellite communication, among other functionalities. 6G will have the ability to operate seamlessly in various scenarios, encompassing the realms of airspace, land, and sea. The result will be the establishment of a truly universal mobile broadband communication system that leaves no corner untouched by its pervasive influence [23].

In order to achieve a significantly wider bandwidth, 6G is anticipated to operate at higher frequencies compared to its predecessor, 5G. These frequencies may range from 300 to 800 Terahertz (THz), corresponding to the visible light spectrum. Additionally, 6G will utilize higher frequency radio bands spanning from 24GHz to 40GHz, also known as millimeter wave (mmWave). Moreover, frequencies in the range of 100 GHz to 10 THz will be harnessed by 6G for its operations. These higher frequencies, coupled with innovative technologies, will enable 6G to achieve data rates that are up to 100 times faster than those of 5G, empowering it to attain peak data rates of Tbps and user data rates of 10 Gbps. Furthermore, 6G will make diligent use of the reconfigurable frequency sharing technique, thereby further enhancing the efficiency of frequency reuse [24].

2.3.1 Data rate

Since the inception of wireless communication, there has been an increase in users' demands for data rates. In the 1G era, data speeds were limited to a small number of kilobits per second (Kbps), which then grew to 10^6 bits per second (bps) in the 5G era. However, these data rates have proven to be insufficient for various applications. To address this issue, the development of 6G aims to provide higher bandwidth by operating at higher frequencies. By doing so, 6G has the potential to enhance data rates by 10 to 100 times compared to 5G, enabling peak data rates of Tbps [25].

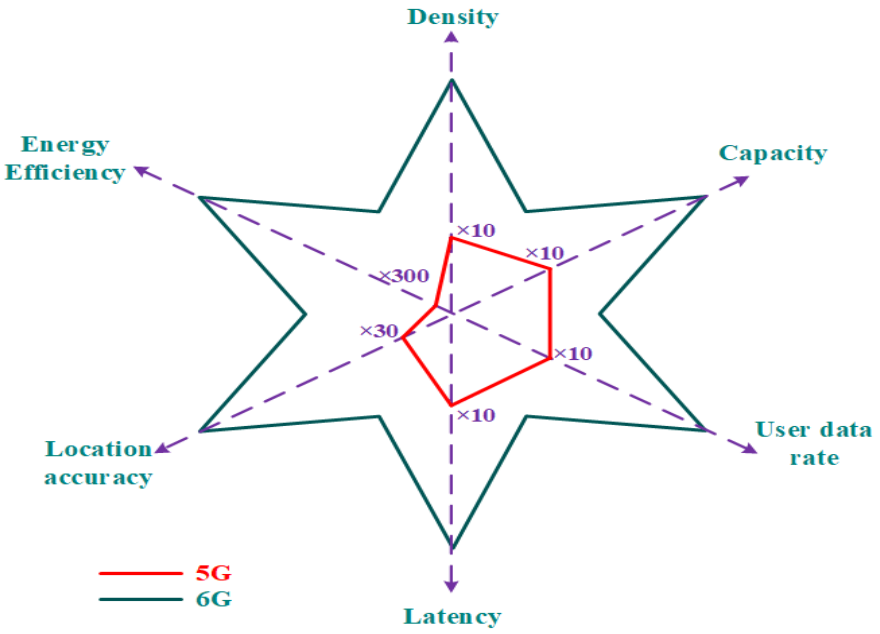

Figure 2.2: 6G wireless communication KPIs goals

It is widely believed that in future smart cities, data rates will need to reach 1 Tbps to enable the autonomous management of numerous operations. Furthermore, individual data rates in upcoming 6G systems are predicted to increase from 1 Gbps in 5G to a minimum of 10 Gbps for each user and up to 100 Gbps. Moreover, 6G can leverage flexible frequency sharing technologies to improve frequency reuse efficiency further, potentially allowing for downloading high-definition videos in a matter of seconds [26].

2.3.2 Spectral Efficiency

The measure of how effectively the assigned frequency spectrum is utilised by wireless systems, specifically 5G or 6G, is commonly referred to as "spectral efficiency". This term denotes the extent to which spectral resources are optimally employed and can be enhanced through various physical layer parameters such as modulation schemes, MIMO, access techniques, and others. Spectral efficiency is quantified as the ratio of the net data rate (in bits per second) to the channel bandwidth (in Hertz) and is typically expressed as b/s/Hz. Notably, 6G wireless technology exhibits a spectral efficiency of 5-10 times greater than 5G wireless [27].

On the other hand, smart buildings will be utilised in the context of 6G to introduce additional freedom to wireless networks, enabling them to deliver unprecedented capacity. On a large scale, buildings will have intelligent surfaces that can reflect signals. These surfaces which is known as RIS will effectively expand the antenna aperture, allowing for collecting more previously inaccessible radio signals; this, in turn, will result in improved energy and spectrum efficiency [28].

2.3.3 Latency or Delay

The term "low latency" pertains to communication that is expeditious and efficient; our objective is to transmit packets within a short duration, minimizing processing delay. In the context of 6G, a maximum latency of 10 μsec is permitted. The forthcoming network of intelligent mobile devices and robotics will necessitate high reliability and ultra-low latency. Future cities will encompass intelligent automobiles, residences, educational institutions, industrial facilities, as well, as transportation systems such as bullet trains, ships, aeroplanes, and Unmanned Aerial Vehicles (UAV), where the integration of self-driving cars is essential to ensure safety and avoid accidents [29]. Sectors such as defence, healthcare, surveillance, and monitoring will demand ultra-reliable and low-latency connections; online gaming services also necessitate high reliability and minimal latency. The Extremely high Reliability and Low Latency Communication with Security (ERLLCS) feature in the 6G wireless system will be integrated with the mMTC and URLLC of 5G, surpassing a reliability standard of 99.99% [30, 31].

2.3.4 Mobility

A diverse range of radios with different characteristics will be supported in the upcoming 6G devices. Rather than being connected to a single cell, users will be connected to the network, enabling multi-connectivity techniques to expand the boundaries of the cells. This seamless transition between various heterogeneous links, including sub 6 GHz, millimetre wave, THz, and Visible Light Communication (VLC), will finally be possible without manual intervention or configuration [32]. Moreover, these devices will ensure the QoS guarantees that fulfil the most demanding mobility requirements anticipated by 6G, such as low latency even in ultra-high mobility scenarios, with speeds of up to 1000 km/h [33].

2.3.5 Massive Connectivity/ Connection Density

Another application scenario for the next generation of wireless communication is mMTC; this use case revolves around integrating Internet of Things (IoT) devices, where communication occurs solely between machines and human involvement is absent. These machines engage in calls, messages, and commands with one another, completely devoid of human intervention. Consequently, it is the machines themselves that interact and communicate with each other. Cooperatively, sensor networks and IoT devices will be interconnected with multiple Base Station (BS). This collaborative connection will facilitate seamless communication between various devices and applications, including wearables, control and monitoring devices, self-driving cars, smart grids,

industrial automation and control devices, and medical and health-related devices. The communication between these devices can be either peer-to-peer or cooperative multi-hop relay transmission.

In this essence, 6G, should support up to 10^7 devices per square kilometre to accommodate this increased connectivity [34]. Given the diverse range of applications and devices, in which each requiring its specific network infrastructure design for content-driven applications or networks, a comprehensive and distinct approach to planning and optimisation is imperative for 6G. Therefore, it is crucial to consider all these requirements when devising strategies for the future of wireless communication.

2.3.6 Area traffic capacity

With the proliferation of connected devices per unit area, there has been a corresponding surge in the demand for higher-capacity channels. An extensively deployed network of sensors generates excess terabytes (TB) of data daily. To accommodate this substantial data production, a backhaul channel with high capacity is required.

In previous wireless generations 1G-5G, wireless protocols were tailored to specific applications. However, with the emergence of massive IoT or mMTC, there is a need for power-efficient and cost-efficient approaches. This expansion of IoTs necessitates the development of vehicular communication, such as Vehicle to infrastructure (V2X), for autonomous driving. The vehicle must interact with other vehicles, pedestrians, and numerous sensors within the vehicle. All these forms of communication must exhibit exceptional reliability, low latency, and security. Another scenario that exemplifies the need for reliable communication is industrial automation, where many sensors communicate and generate vast amounts of data. The minimum area traffic capacity limit for 6G is 1000 $Mbps/m^2$ [31].

2.3.7 Reliability

Incorporating high dependability is crucial for integrating mission-critical and safety-critical applications in the use cases of 6G technology. The advent of 6G technology represents a substantial advancement compared to its predecessor, 5G. The beginning of 6G technology enables the seamless integration of enhanced features into the former 5G technology infrastructure. Introducing intelligence in all network segments, including the core network, access network, and user equipment or connected IoT objects, is expected to enhance performance objectives. The services offered by 6G technology encompass a range of advanced features such as holographic communications, artificial intelligence, high-precision manufacturing, and novel applications utilising VLC.

Reliability performance measurement in real-time applications is quantified with Bit Error Rate (BER), Packet Error Rate (PER), Frame Error Rate (FER), and Symbol

Error Rate (SER). It is anticipated that 6G will surpass its predecessor, 5G, in terms of performance. Notably, 5G is known to approach the reliability upper limit of 1×10^{-5}. It is anticipated that 6G technology will surpass this limitation [35].

In order to quantify the reliability of a communication system, different metrics are used as measures of the accuracy or reliability of a communication system. Still, these metrics operate at different layers of the communication system and capture various aspects of errors. The metric selection to utilise, is contingent upon the particular context and the network layer in the communication system. In the context of analogue or digital signal processing, BER is usually used, PER is commonly used in wireless communication and networking, and FER is specific to the data link layer, SER is often used in digital modulation systems, where the information is stored into symbols, and the symbols are modulated to send the information.

2.3.8 Coverage

The primary objective of 6G networks is to effectively tackle the pragmatic obstacles encountered by traditional networks. The primary objective of 6G communication system is to enhance the connection and expand network capabilities to accommodate the growing demand for data-intensive applications. Universal coverage eliminating zero coverage spots in distant and isolated places can be obtained by the enhancement of network coverage [36]. To meet the needs for connectivity and achieve comprehensive coverage, it is necessary to implement solutions that are both practicable and cost-efficient.

To accomplish these objectives, the development of 6G networks is envisioned to follow a decentralised approach, incorporating the integration of diverse networks, including terrestrial, airborne (aerial), marine, and undersea communications, as well as satellite systems. This facilitates the creation of effective communication access platforms and offers globally encompassing networks with exceptional precision and reliability [22]. The integration of heterogeneous networks is a crucial factor in enhancing network capacity and coverage [37].

2.3.9 Energy Efficiency

EE is an essential metric in the planning and execution of advanced wireless networks 6G, and serves as a vital KPIs. With the advancement of technology, there is an increasing focus on developing communication systems that are both sustainable and energy-efficient. A key objective is to develop 6G networks that prioritise environmental sustainability and optimise energy use [38]. Green communication strategies strive to decrease the ecological footprint of network operations. This may entail utilising sustainable energy sources, energy-efficient equipment, and sophisticated power

management tactics. To attain EE in the context of 6G, promoting the advancement and implementation of devices with high EE is crucial. This can be accomplished by improving the design of devices, using components that consume less power, and using energy-efficient communication protocols. Low-power modes, energy harvesting, and optimisation of device power usage are key factors in attaining this goal.

Moreover, it is necessary to optimise the design and operation of network infrastructure to minimise energy usage. This encompasses base stations, data centres, and additional components of the network. One can utilise strategies such as dynamic resource allocation, sleep modes for idle components, and network virtualisation to minimise energy usage. Likewise, it is crucial to effectively distribute network resources according to demand, traffic patterns, and user specifications [39]. Adapting resource allocation in real-time ensures that the network's capacity aligns with the current demand, preventing wasteful energy usage during periods of low demand. Dynamic resource allocation is facilitated by adaptive modulation and coding, dynamic spectrum allocation, and load balancing.

Furthermore, it is imperative to create communication protocols specifically designed to maximise EE. This encompasses procedures for identifying devices, establishing connections, and transmitting data. Efficiently implementing Medium Access Control (MAC) protocols, adaptive transmission methods, and low-overhead signalling protocols are key factors in achieving optimal communication.

It is necessary to optimise signal processing techniques to minimise computing complexity and energy usage [40, 41]. These activities, including Massive MIMO, improved beamforming, and RIS, are particularly important for processing-intensive operations in 6G networks. Energy-efficient signal processing is achieved using advanced algorithms, machine learning for efficient processing, and hardware acceleration approaches. Also, investigating incorporating energy harvesting devices into 6G networks to harness electricity from the surrounding environment. This feature can be especially advantageous for devices situated in remote or inaccessible areas. Devices and infrastructure can incorporate solar cells, kinetic energy harvesting, and other renewable energy sources.

EE in 6G encompasses various key performance indicators, including the optimisation of devices, network infrastructure, communication protocols, and resource management systems. Significant EE helps save operational expenses and supports worldwide endeavours to establish sustainable and environmentally aware communication networks.

2.4 6G Chosen Evolutionary Enabling Technologies and Related Work

This section and the following one examine the emerging technologies as facilitators of the use cases and associated KPIs of the 6G network, as outlined in Section 2.3. Several of these technologies have been evaluated for use in 5G networks. However, they are not now accessible for commercial use in 5G networks due to either technology constraints or market limitations. Breakthroughs in 6G can occur across several layers, such as Physical Layer (PHY), network architecture, communication protocols, and network intelligence. This section focuses on the evolutionary technologies of 6G. Evolutionary solutions in the context of 6G networks involve utilising already established or implemented technology, such as MIMO. On the other hand, revolutionary solutions strive to use new and innovative technologies, such as THz communications, to cater to the needs of 6G. The revolutionary technologies will substantially change various cellular network layers, such as the PHY layer, compared to the 5G networks. It should be noted that numerous parts of the ground-breaking technologies are still in the stage of scientific inquiry.

The progression of cellular networks from 1G to 6G is an ongoing process [42]; there are now five distinct generations of mobile communication systems, each of which adheres to a separate standard and comes equipped with a unique set of strategies and capabilities. It is important to note that a new generation of mobile communications networks has been developed approximately once every ten years.

The criteria for 6G can be met by utilising new, more advanced, and more intelligent communication methods. For instance, RIS, extra-large MIMO, novel spectrum, holographic radio communications, full-duplex wireless communications, multiple access, and modulation are crucial for maximising the data rates. In addition, methods such as energy harvesting and communication via backscatter are beneficial and necessary for improving EE. Ways that effectively increase connection and provide full coverage include cell-free massive MIMO systems and the combination of terrestrial and non-terrestrial communications. Quantum communication and blockchain technology are two powerful strategies that can strengthen communication security, secrecy, and privacy. Techniques such as holographic teleportation (also known as telepresence), as well as edge computing, can be of great assistance in the pursuit of URLLC communication. Moreover, AI and ML are crucial tools for developing intelligence into wireless generations.

The goal of 6G is to create an integration of many wireless networks that is transparent to the user. This involves the integration of wireless networks that are both terrestrial and non-terrestrial, such as those that are airborne, underwater, and those that utilise satellite communications systems [24]. The seamless integration of networks enables

a usable communication platform and provides high-speed broadband connectivity with complete coverage. Tactile Internet, holographic teleportation, Internet of Smart Things (IoST), which includes smart cities, smart radio environments, smart healthcare, smart grid, smart transportation, smart factories, smart farming, and smart homes, and multi-sensory Extended Reality (XR), which includes AR, Mixed Reality (MR), and VR, are some examples of delay-sensitive applications that are anticipated to be supported by 6G wireless communications networks more than previous wireless generations [43].

Research in 6G communication is a dynamic and multifaceted topic that involves a wide spectrum of technological improvements and novel ideas. It is also a field that is now experiencing rapid growth. The research into 6G, the successor to 5G, is motivated by the ambition of offering connections and capabilities that have never been seen before, thereby determining the future of wireless communication. The development of 6G technologies presents a wide variety of benefits as well as obstacles, which has resulted in the emergence of several important research fields.

A significant focus of current research is on developing methods to achieve extremely high data rates. To allow data rates of one terabit per second and uncover potentially game-changing possibilities for high-bandwidth applications and services, researchers are investigating new modulation algorithms, sophisticated antenna technology, and effective spectrum utilisation.

Another essential area of concentration is URLLC [44]. It is important for applications such as driver less vehicles, industrial automation, and real-time mission-critical services that 6G can deliver near-instantaneous communication with minimal latency. This is the goal of 6G. There is still a great amount of difficulty in ensuring high reliability in dynamic and diverse contexts.

The exponential increase in the number of connected devices in the IoT is something that the idea of mMTC seeks to address. Researchers are looking at scalable and efficient network architectures to support many simultaneous connections. They emphasise the role that 6G will play in realising the potential of industrial IoT and smart cities.

There has been a recent increase in interest in integrated satellite communication because 6G intends to combine terrestrial and satellite networks without any noticeable break in service. This line of study intends to give worldwide coverage, improve connectivity in remote places, and enable continuous communication in various settings. When it comes to improving the performance of 6G networks, AI and ML play a vital role [45]. Researchers are investigating AI-driven potential solutions for intelligent resource allocation, network management, and predictive maintenance. AI technology integration is necessary to adapt to complex and ever-changing network conditions successfully. The development of communication at THz frequencies is a new horizon for 6G research. THz frequencies are required to accomplish exceptionally high-speed communication and enable applications such as extremely rapid wireless networks

and high-resolution imaging. This is accomplished by leveraging these frequencies, a primary focus is finding solutions to the technological issues associated with THz propagation and device development [46].

Although higher carrier frequencies offer a wider bandwidth, the total sequential accessible bandwidth for mmWave systems is still limited to less than 10 GHz, which makes achieving Tbps data rates challenging [47]. THz band communication can provide ultra-high-speed data rates of up to 1 Tbps and support bandwidth-intensive applications. This makes it a promising enabler for 6G technology [36]. The THz band spans from 0.3 THz to 10 THz [48] and is situated between the mmWave and Infrared (IR) bands. It exhibits certain characteristics that are common to both of these bands. The THz band, called sub-millimeter radiation, encompasses wavelengths starting at 1 mm and extending to shorter wavelengths [49]. The frequency range of 275 GHz to 300 GHz is classified as the mmWave band, while the range from 300 GHz to 3 THz falls within the far IR spectrum band [39]. The (300 GHz - 3 THz) band, although in the optical spectrum, shares similarities with the Radio Frequency (RF) band regarding its electrical characteristics. This behaviour can be attributed to THz radiation occupying the region between the RF and optical frequency bands, as depicted in Figure 2.3 [50].

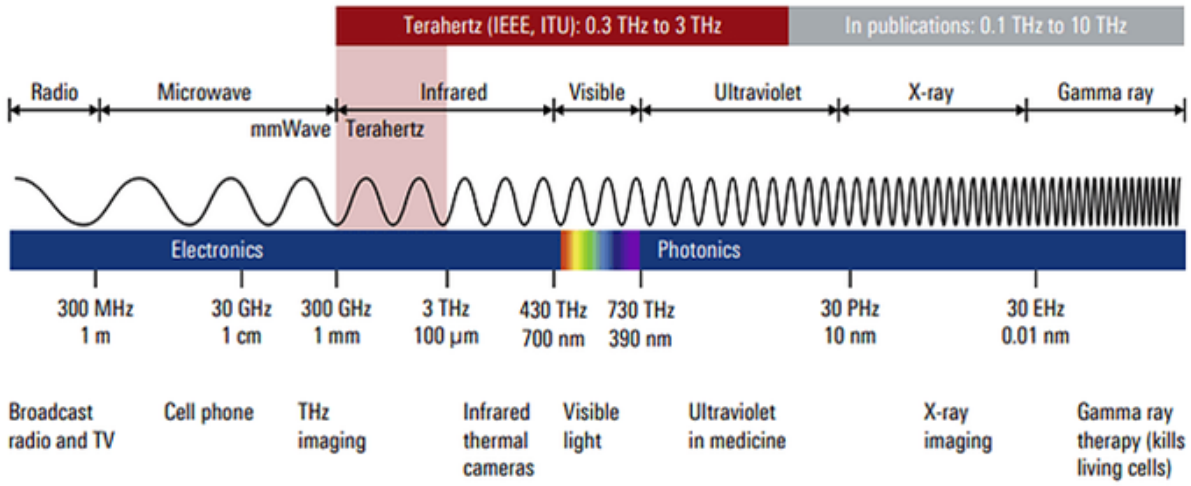

Figure 2.3: The electromagnetic spectrum and its diverse applications based on frequency[25]

The absence of feasible and small-scale methods for generating and detecting THz signals has impeded the feasibility of utilising THz band communication for a significant duration [51]. The inefficiency of semiconductor devices in converting electrical energy into electromagnetic energy at THz frequencies has been a longstanding barrier for THz communication [52]. Nevertheless, during the past 10 years, the disparity in THz technology has been considerably diminished as a result of major progress in semiconductor technologies and the introduction of novel materials that present increased possibilities for THz band communication [53].

Standardisation efforts for THz wireless communications started back in 2008 when the IEEE established an Interest Group on THz communications (IGTHz) under the IEEE 802.15 standard [54]. After that, in 2014, the foundation for the IEEE Task Group on 100G Wireless (TG100G, IEEE 802.15.3d) was founded. As a result, in 2017, IEEE Std. 802.15.3d was issued as the first wireless communication standard in the 300 GHz band to support 100 Gbps and above wireless point-to-point links. The development of IEEE Std. 802.15.3d- 2017 has been based on the 2016 version of the International Telecommunication Union (ITU) radio regulations which include an allocation of the bands from (252 - 275) GHz for the use by land mobile and fixed service on a co-primary basis [55–57].

The 6G network is expected to function over a broad spectrum of frequency bands, with each band providing a distinct purpose to fulfil various communication requirements. While there is considerable discussion over the utilisation of THz frequency bands for 6G, it is important to note that this will merely constitute a portion of the overall solution. 6G will function across many frequency spectrums, but the main expected band is the high-frequency bands as seen in Figure 2.4.

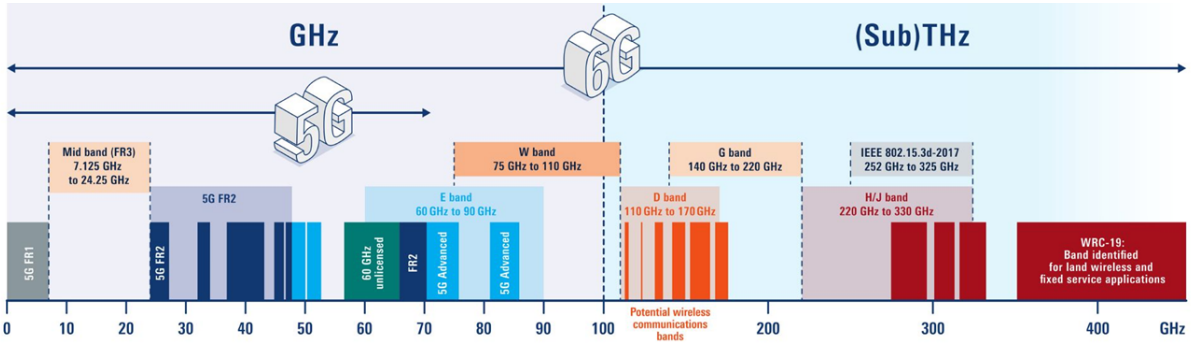

Figure 2.4: The spectrum of frequency bands available for 6G wireless communications[48]

Above 100 GHz (High-Frequency Bands), pushing the boundaries of the spectrum, high-frequency bands hold the promise of ultra-fast data speeds and extremely low latency. This range includes the W-band (above 75 to 110 GHz), D-band (110 to 175 GHz), bands between 275 and 300 GHz, and the THz range (0.3 to 10 THz). The W and D bands are interesting for 6G access. However, they come with challenges, such as shorter range and susceptibility to signal attenuation. These bands are critical for applications that demand instantaneous communication, such as autonomous vehicles and mission-critical systems.

2.4.1 Channel Coding

The 6G network is anticipated to establish a comprehensive and uninterrupted network infrastructure throughout all regions. It will operate at a data throughput of 100 Gbps, utilising a higher frequency band in the THz range, surpassing the 275 GHz band. Additionally, the channel bandwidth will be in the GHz range. The circumstances present novel obstacles for fundamental channel coding and multiple access techniques. The objective of channel coding is to mitigate transmission mistakes, hence ensuring a high level of reliability. Nevertheless, it is one of the most intricate baseband processing components. Due to their exceptional performance characteristics, modern channel coding methods, such as Turbo, Low Density Parity Code (LDPC), and Polar codes, are widely adopted in various communication protocols, including 2G, 3G, 4G, and 5G [58]. As an example, the 5G uses polar codes and can provide user experience with maximum throughput of 20 Gbps and exhibiting a high level of reliability of 1×10^{-5}. The upcoming 6G KPIs and use cases necessitate the development of new code designs to meet the higher reliability and throughput. This entails researching advanced channel coding approaching the Shannon limit [59]. The objective is to achieve exceptionally high throughput, reliability, power efficiency, and low encoding/decoding latency. Examples of these requirements include the development of a Tbps throughput channel coding and decoding techniques that eliminate shaping loss [60].

ElJabri and Moussaoui in their study [61], present an EE model for channel coding in the THz band. Additionally, they explored channel modelling techniques utilising capacity and EE as evaluation metrics. The authors present a channel coding strategy known as Low Weight Coding (LWC) and Minimum Energy Code (MEC) to enhance the EE of THz communication networks. The approaches suggested in the research aim to enhance THz communications, including data rate, channel capacity, EE, spectral energy, and the complexity of nanodevice design. The study examines the significant obstacles posed by range limitation, molecular absorption, and attenuation in terahertz transmission, which are crucial considerations for the advancement of nanoelectronics in the future. However, the scalability or applicability of the offered methodologies in real-world scenarios or realistic implementations needs to be applied [62].

The authors in [63] present two Joint Source Channel Coding (JSCC) schemes, namely the double LDPC and double polar codes. They introduce a Joint Source-Channel Decoding (JSCD) algorithm for double polar DPolar codes, specifically the Turbo Turbo Like Belief Propagation (TLBP) decoder, to be applied to 6G networks. The TLBP decoder is constructed by leveraging the Belief Propagation (BP) decoders used in polar codes. However, the computational complexity, resource requirements, channel variations, latency, EE, and system performance of the proposed JSCC schemes are not considered. Additional investigation can be undertaken to examine, enhance the efficacy, and tackling

various challenges to meet the requirements of forthcoming wireless communication systems 6G. The exploration of incorporating JSCC with other cutting-edge technologies, such as ML and AI, may be examined to enhance the effectiveness and productivity of 6G communications.

The authors in [64] examined and analysed various candidate decoding techniques for URLLC in relation to their error-rate performance and computational complexity. This study examines the utilisation of Ordered Statistics Decoding (OSD), Guessing Random Additive Noise Decoding (GRAND), Successive Cancellation List (SCL), and their respective modifications as the primary candidate decoding strategies for URLLC in 6G. The authors provide evidence to support the efficiency of universal decoders such as OSD and GRAND in achieving near ML decoding for both structured Bose, Chaudhuri, and Hocquenghem (BCH) codes and unstructured random codes while maintaining a comparable level of complexity. The SCL based sequential decoder has been identified as optimal for the trade-off between performance and complexity. The enhanced OSD decoder has the potential to be utilised in conjunction with binary linear short codes such as 128 Cyclic Redundancy Check (CRC) polars to attain error correction capability that is nearly optimal for URLLC. However, additional enhancements in terms of complexity are still required. Also, Sequential Decoding (SQ) demonstrates an exceptional trade-off for decoding short block codes.

The authors in [65] propose a JSCC scheme that utilises Quasi Cyclic LDPC (QCLDPC) codes. This scheme is designed to achieve performance close to the capacity limit while ensuring low complexity. In their research, they address the viability of employing a semantic encoder/decoder that understands Unequal Error Protection (UEP), thereby improving the safeguarding of semantic data within the JSCC system. The effectiveness of the proposed system is assessed by conducting BER measurements, which provide a fair evaluation of its performance regarding 6G communication and the framework of future communication. However, the potential influence of channel conditions, noise levels, scalability, and adaptability on the efficacy of the JSCC system needs further analysis of various communication scenarios and network configurations.

The authors in [66] provide the idea of space-time exchanging theory, which proposes that channel coding can be conducted in the spatial domain, yielding an equivalent coding rate to that achieved in the time domain. Consequently, this approach significantly reduces latency, rendering it a feasible strategy for the design of 6G URLLC. This aligns with the objectives outlined by the third-generation partnership project (3GPP) to minimise latency and guarantee low packet error rates. However, the authors have yet to consider the practical considerations or challenges that may arise when implementing the theoretical notions presented in their research to real-world 6G URLLC systems [67]. Additional studies are required to examine the constraints and practicality of incorporating channel coding with finite block length in the domain of 6G URLLC.

In their study, Zhu and We, [68] investigated the encoding and decoding techniques employed in 6G with Convolutional Code LDPC (CC-LDPC), block code LDPC (BC-LDPC), and polar code. The authors compared these approaches in terms of their error performance, decoding complexity, and latency. The research findings indicate that CC-LDPC demonstrates notable benefits in terms of high reliability, low complexity, and low latency when compared to BC-LDPC and polar code. Despite the promising potential of CC-LDPC, numerous unresolved issues warrant additional investigation. A main issue that arises is the suboptimal performance of the existing CC-LDPC codes when employed for code lengths that are relatively short to moderate. It is postulated that CC-LDPC codes exhibit more sensitivity to the minimum distance when compared to BC-LDPC codes. It is necessary to suggest a specialised building approach to optimise the minimal space of coding structured base matrices for code lengths that are short to moderate. Alternatively, one may consider modifying the coupling structure to mitigate sensitivity.

In their study, Agarwal and Mehta [69] integrated polar coding with convolution coding in the context of MIMO systems, employing OFDM as a multiple access technique. While their results demonstrated improved BER performance compared to other coding schemes such as CC, Reed Solomon (RS) with CC, CC-LDPC, and turbo CC, they did not address the issues of throughput and latency in the context of future communication generations, specifically in the transition from OFDM to Non Orthogonal Multiple Access (NOMA).

In their study, authors in [70] conducted a comparison between concatenated polar codes and outer BCH codes, as well as concatenated LDPC codes and concatenated Turbo codes. The researchers applied random and blind interleaving schemes to assess the BER performance of the concatenated codes. The results indicated that the concatenated codes using blind interleaving outperformed those using random interleaving. Additionally, the concatenation of polar codes with BCH codes demonstrated superior performance. Nevertheless, a drawback of the used approach is the escalating decoding complexity with larger packet sizes. However, to overcome that the decrease in the decoding speed of their coding approach while raising the CRC length and keeping the packet size constant, might be attributed to the reduction in code rate.

In [71] the authors introduced a hash-polar concatenated code as an alternative to the concatenation of CRC polar codes. Their proposed code performs comparably to CRC polar codes while outperforming parity check polar codes regarding FER. Moreover, the proposed channel coding scheme considers the requirements beyond 5G communication and potential future advancements in communication technology.

Li and He [72] introduced a novel coding and decoding approach for CRC concatenated polar codes in their work. This technique aims to maintain the proper paths while promptly eliminating mistakes. Consequently, it enhances the block error rate

performance without significantly escalating the complexity. The results obtained from the simulation demonstrate that the suggested system is capable of considerably improving the performance of the block error rate. Furthermore, it is seen that the system has a more pronounced impact on code lengths that are shorter or medium length compared to the currently available schemes.

As CRC polar concatenated codes are promising approach for the new wireless generation 6G an improvement for the decoding process is presented by the authors in [73]. The proposed CRC polar belief propagation decoding algorithm uses concatenated factor graphs of polar codes and CRC to transfer extrinsic information between the two-factor graphs. The proposed decoding algorithm significantly improves error correction performance compared to a conventional belief propagation decoder. The decoding method also assigns trainable weights to the edges of the CRC polar concatenated factor graph. This improves the decoding algorithm's error probability by giving the graph's edges trainable weights. The suggested proposal shows a small advancement in terms of reliability with no latency overhead.

The authors in [74], introduces a spatiotemporal 2-D channel coding technique for achieving highly reliable MIMO transmission with minimal latency. Computational models have proven the superiority of this approach in terms of performance, latency, and flexibility compared to existing methods. The proposed coding system exhibits excellent adaptability and holds great potential for a wide range of applications. Subsequent efforts will be focused on hardware implementations and systematic applications.

2.4.2 Non Orthogonal Multiple Access Technique

Regardless of the complexity and depth of communication technology, its fundamental purpose remains the transmission of symbols one-to-one manner. The determination of sign information often relies on the pulse level of the rectangular, square wave that corresponds to the Sinc function [75]. To ensure efficient transmission of symbols within the atmosphere, wireless signals must possess the ability to withstand interference caused by signal noise. Additionally, they should be capable of transmitting data at high speeds, even in situations characterised by fading channels and multipath propagation. OFDM has extensive cellular mobile communications and WiFi technology applications. The Cyclic Prefix OFDM (CP-OFDM) waveform has been widely implemented in several communication systems, such as, Wi-Fi, 4G, and 5G. To preserve orthogonality, CP-OFDM necessitates the implementation of stringent synchronisation measures [76].

Nevertheless, the utilisation of OFDM in mobile communication fails to overcome several constraints imposed by the new wireless generation. The square wave employed in OFDM has significant side lobes and is highly susceptible to carrier frequency drift. Additionally, mitigating the baseband waveform's peak-to-average ratio is challenging,

the synchronisation between a discontinuous spectrum and a carrier is not considered suitable. In which the adaptability of OFDM technology to the forthcoming generation of mobile communications is highly challenging [77].

The utilisation of non-orthogonal wireless communication technology has proven to be a highly efficient, effective approach for achieving optimal spectrum efficiency and favourable time-frequency domain features in mobile communication. An illustration of this may be seen in using Filter Bank based Multi Carrier (FBMC) and NOMA technologies within the context of 5G/6G [78]. These technologies effectively integrate various non-orthogonal transmissions and data across sub-carriers. Moreover, implementing a filtering mechanism for user data has the potential to address numerous challenges arising from the current orthogonal technology successfully. Using Rate Splitting Multiple Access (RSMA) [79] technique can lead to increas achievable rates and offer mechanisms for access without the need for explicit grants.

NOMA, is anticipated to emerge as the predominant access technique for the forthcoming 6G mobile communication systems as it allows for the sharing of a single resource among several different subscribers [80]. Integrating polarisation coding technology into NOMA and optimising the channel polarisation decomposition scheme based on generalised polarisation principles are crucial in advancing 5G/6G development. Implementing the 6G network will facilitate developing and refining the polarisation multiple access system's architecture and optimisation.

To build and optimise the polarisation coding communication mechanism, it is necessary to enhance the overall architecture and essential technologies of NOMA, which is based on the idea of multiuser communication. NOMA offers concurrent services for numerous users, simultaneously operating on several frequencies, codes, and spatial domains. At the recipient's side, technologies such as Successive Interference Cancellation (SIC) or Multiuser Detection (MUD) have the capability to eliminate interference, decode user signals, enhance network capacity, minimise communication delays, and augment the number of connections. The technology known as NOMA encompasses two primary domains: power domain NOMA and code domain NOMA [81] (a complete description is provided in Section 3.3).

While the fundamental NOMA design may provide satisfactory performance for many applications, modifying the basic NOMA structure might offer several extra capabilities, especially concerning interference cancellation. Several proposed revisions to NOMA specifically target signal design. In these techniques, the data symbols of the users are altered before superposition to improve the interference cancellation process. Such modifications include coordinate interleaving, phase rotation, asynchronous superposition, and waveform domain NOMA. Various other alterations have primarily concentrated on the practical elements of NOMA. For instance, in reference [82], dynamic NOMA is introduced, wherein the power is adjusted based on the sent data. Additional

enhancements were suggested in [83], in which they encompassed the refinement of the user pairing procedure, the implementation of opportunistic techniques, and the integration of cognitive NOMA.

A novel NOMA configuration, partial NOMA, was introduced in [84]. In this configuration, the spectrum overlap can be reduced to a portion of the full spectrum. The results demonstrate that partial NOMA can significantly enhance the sum rate compared to the scenario when there is complete overlap. Another study proposed a two-user paradigm for NOMA [85]. The researchers conducted link- and system-level simulations to evaluate the performance of the NOMA downlink system. The findings demonstrate that NOMA outperforms Orthogonal Multiple Access (OMA) in terms of both the overall system throughput and the individual user throughput.

To assess the impact of user pairing in the two-user model of the NOMA system, the authors utilised statistically allocated transmit powers among NOMA users [86]. Furthermore, the authors suggested both predetermined and spontaneous user pairing methods. The authors in [87] examine the impact of power allocation on fairness. The fairness index should approach a value of 1 to guarantee an equitable distribution of system resources. The authors proposed a power allocation strategy to uphold the fairness index. The authors in [88] employed the notion of user pairing to establish a cooperative NOMA system. This involved matching users with strong and weak channel conditions while considering imperfect Channel State Information (CSI) and perfect CSI feedback. In their publication [89], the authors introduced NOMA aided precoded spatial modulation NOMA-Precoded Spatial Modulation (PSM), a technique that integrates NOMA with MIMO technology. The researchers in [90] examined the static powers of multiple users and identified that a user may experience an outage if the necessary data rate is not properly selected. In this study, the authors introduced an adaptive power regulation technique for the uplink Power Domain NOMA (PD-NOMA) system, which lets users dynamically modify their transmit power level to improve their throughput or payoffs. The receiver utilises SIC for signal detection. In 2018, the 3rd Generation Partnership Project (3GPP) recognised NOMA as a research icon and issued instructions to assist NOMA, comparing it to OMA [91] taking into account the importance of bit level calculations in the evolving 6G considering new channel coding and modulation approaches.

The authors in [92], introduced a way to enhance noise reduction in polar channel coding used in 5G by implementing a straightforward adjustment utilising polar codes. This alteration involves sorting the reliability of OFDM subcarriers in the physical channel. The suggested method of adapting signals with polar codes to the channel state exhibits superior efficiency compared to traditional solutions. It does not increase the computing complexity of signal processing and decoding. The utilisation of the adaption approach greatly decreases the BER, resulting in channel gain between 3dB and

5dB. However, it introduces modulation and packet size limitations without considering the increasing number of users that 6G planned to support. The proposed methodology in [93] is a NOMA communication paradigm that aims to achieve highly efficient, reliable, and secure multi-user communications by utilising overlaid auxiliary signals and precoded matrices approach. This approach enables higher data rates with lower power ratios. In [94] the authors introduced the NOMA-LDPC model, showcasing improved throughput and reduced BER compared to the NOMA-turbo system across various Signal to Noise Ratio (SNR) ranges. The NOMA-LDPC system has a slightly better throughput of 0.39 Mbps than the turbo system. Their solution accommodates a larger user base, around 20-50 more than the conventional system, without compromising performance. However, while utilising LDPC in conjunction with NOMA may be a more optimal solution for 6G applications, it has limited potential without considering other crucial KPIs for the emerging wireless generation.

Sarieddeen and his co-authors [95] suggested spatial tuning strategies to improve channel conditions in THz-NOMA for multiuser systems. They introduced a set of data detectors based on non-linear MIMO detectors named QR decomposition (QRD) and WR decomposition (WRD) in which these detectors depend on low-complexity channel matrix puncturing to retrieve overlapped data at the receiver side. These detectors dynamically create more complex detectors by combining simpler component detectors. Multiuser NOMA involves the grouping of randomly distributed users into small cell sectors. These users are then assigned varying power levels based on the distance between the user and the BS. While the employed technique effectively decreases the BER at high SNR levels in typical THz settings, the applicability of these results to diverse THz environments or real-life situations remains uncertain. Moreover, considering various KPIs is crucial in 6G, as achieving a higher data rate is a significant KPIs.

> In the last few years, a family of non-linear subset-stream MIMO detectors based on QR decomposition (QRD) has been proposed. The least-complex member of this family is the nulling-and-cancelation (NC) detector, and after that the chase detector (CD) and the layered orthogonal lattice detector (LORD), were introduced respectively. Furthermore, a less complex alternative of subspace detectors decomposes the channel using a punctured QRD, namely, WR decomposition (WRD). These detectors provide a range of performance and complexity trade-offs suitable for THz-NOMA scenarios.

Different research directions for 6G NOMA with channel coding were presented by the authors in [96], the authors suggest utilising Grant Free Access with NOMA (GFNOMA) transmission techniques to achieve 6G IoT connection. The authors introduced a complex framework for energy-efficient communications in GFNOMA, which tackles the problem of resource allocation and allows for compatibility with other

methods. The team utilised BCH and Reed-Muller codes throughout their research, demonstrating improved data reliability. However, they should have considered the anticipated increase in the number of users accommodated in 6G networks. This emphasises the necessity for self-adaptive coding techniques at the PHY to enhance reliability and performance in GFNOMA systems. This can result in enhanced performance and optimised network administration for facilitating extensive connectivity in 6G IoT frameworks. The authors of [97], showed that employing coded NOMA with LDPC code can enhance the BER performance by up to 3dB channel gain compared to uncoded NOMA. Although their findings are not directly applicable to the new wireless generation, they indicate the potential of coded NOMA to offer increased data reliability and throughput, leading to reduced energy and time consumption. The authors of [98] suggest a new linear receiver that utilises the limitations of the Forward Error Correcting (FEC) codes to reduce the error propagation caused by imperfect CSI at the receiver. The channel frequency response is estimated by interpolating the responses of the pilot subcarriers. The innovative receiver can be used for symbol and codeword level SIC. The system is specifically developed to support a MIMO two user uplink NOMA scheme. It operates based on the lowest output energy requirement and can handle modest channel estimate errors. The consideration is focused on transmitting diversity and capacity-achieving LDPC codes. An iterative receiver enhances performance by recovering the Reed-Solomon coded data concatenated in series with an LDPC code.

The authors of reference [99] suggest utilising probabilistic shaping in conjunction with Quadrature Amplitude Modulation (QAM) for multiple NOMA users in Rayleigh fading channels to enhance the SER. Probabilistic shaping is a technique that assigns varied probability to constellation points, ensuring they are equidistantly spaced. Using a constant composition distribution matcher approach, the source can output information symbols with non-uniform probabilities. To maximise the ergodic restricted capacity, a multi-step optimisation process is carried out to determine each user's ideal probability mass function. The optimisation order follows the inverse of the SIC order. The receiver employs a Maximum Posteriori (MAP) based codeword level SIC technique, where the large-scale path loss determines the cancellation order. In contrast to symbol level SIC, codeword level SIC can effectively eliminate inter-user interference induced by previously decoded signals. This is achieved by employing robust FEC codes and a sophisticated soft channel decoder. Meanwhile, the remaining inter-user interference is presumed to follow a Gaussian distribution. To assess the dependability of the suggested approach, precise closed-form formulas for the average probability of error performance are constructed. In addition, a design example integrates the proposed system with the practical LDPC codes to analyse and assess the SER and BER performance.

The authors of [100] suggest a Transmission Control Mechanism (TCM) for two-user downlink NOMA, where the symbols of each user are individually modulated and

combined in the power domain. The detection is carried out simultaneously using the Viterbi method, using the TCMNOMA as a conventional TCM with a trellis structure produced by the tensor product. Choosing suitable power coefficients can guarantee optimal decoding performance. The power coefficients that maximise the tensor product trellis' free distance are determined to get better performance at high SNR. The authors of [101] suggest utilising polar codes for the two-user binary Gaussian multiple access channel. This approach creates two blocks of polar codes for each user, with different power levels. Optimal performance is achieved concurrently by optimising code creation and power and rate allocation. A proposal is made to ensure fairness by implementing a system of alternating power allocation between the two blocks. A hard-decision SIC technique is proposed at the receiver side, which utilises adaptive list size for cancellation. Block Error Rate (BLER) equations for the upper limit are obtained for the regime of finite block length, assuming Binary Phase Shift Keying (BPSK) modulation.

The researchers in [102] developed a detector for two-user downlink NOMA that does not require SIC. The detector employs turbo codes. The suggested detector utilises log-likelihood ratios (LLRs) to analyse each bit of the NOMA symbol. The LLRs are calculated analytically, considering Quadratic Phase Shift Keying (QPSK) modulation for both users. The symbol level and codeword level SIC detectors serve as the standard against which other detectors are measured. The authors of reference [103] provide a simplified and organised coding technique for a two-user downlink NOMA system using BPSK. The coding technique utilises repetition coding and parity check. In this scheme, the symbol of the far user is repeated twice, while the 0 and 1 bits of the near user are mapped to [0,1] and [1,0] correspondingly. This system takes advantage of constructive interference to benefit the user who is far away while also getting rid of the interference caused by the nearby user.

Integrating NOMA with other benchmark technologies holds promising future use for 6G wireless generation. The authors of [104] allocate QPSK and BPSK to the near- and far-users, respectively. The end-to-end channel's Probability Density Function (PDF), which encompasses the BS-RIS and RIS user links, is obtained by applying the central limit theorem to approximate the sum of independent double Rayleigh random variables. Nevertheless, this estimation is reliable when considering a substantial quantity of metasurface components. Reference [105] tested the same performance for Nakagami-fading channels. Bariah et al. [106] provide precise estimations for the BER of both a single metasurface element and many metasurface elements (more than 10). They construct the end-to-end channel's PDF, which is based on Rayleigh fading and includes the BSRIS and RIS user connections.

The researchers [107] investigated a multiuser system that uses RIS with NOMA for the downlink transmission. The suggested method, quadrature NOMA, optimises the diversity order by having the BS multiplex the odd users using the in-phase component.

In contrast, the even users are multiplexed using the quadrature-phase components. The researchers in [108] investigate using RIS-NOMA for indoor applications, the results indicate that increasing the number of reflectors in RIS will improve the overall user experience and QoS in terms of BER, SER, BLER. An analysis of the BER performance of a network using Simultaneously Transmitting and Reflection RIS (STAR-RIS) in a NOMA system has been conducted in reference [109]. A mode-switching protocol enables the communication between a BS and numerous NOMA users situated on both sides, and their research indicates that the farthest user is more sensitive to changes in the power allocation over the change of numbers of RIS elements with overall BER enhancement. Rito and Li [110] utilise alignment approaches for RIS based downlink NOMA systems. The suggested interference cancellation technique improves the signal quality for one user while maintaining the channel quality for the other user. In contrast, the proposed interference alignment technique enables the occurrence of constructive interference in the channel.

2.4.3 Reconfigurable Intelligent Surface Signal Utulisation

The radio building technology massive MIMO (mMIMO) has been established and extensively investigated within 5G wireless communication systems. The notion of mMIMO and ultra mMIMO (um-MIMO) has emerged primarily for higher frequencies [111]. This is because the shorter wavelength allows more antennas to be densely packed within a limited area. Additionally, mMIMO technology can be used at both the BS and User Equipment (UE) levels, resulting in what is known as mMIMO double. An additional method for enhancing wireless communication involves modifying the propagation properties of wireless channels [112]. The existing strategy, which prioritises cells and networks, can be transformed into a user centric approach. In this approach, the cluster responsible for supporting a certain UE in which it can be dynamically chosen by selecting a subset of Access Point (AP) nearby. Integrating distributed mMIMO activities results in a concept known as cell-free mMIMO. This idea enables the collaborative operation of AP in serving UE without any limitations imposed by cellular boundaries. It allows for coherent transmission and reception, providing nearly consistent services throughout the network. To effectively implement distributed MIMO systems, it is imperative to tackle the challenges associated with beam management, viable methodologies for non-coherent operation in higher frequency bands, and the utilisation of full digital beamsteering techniques [113]. The deployment of several antennas over a substantial area, such as the exterior of a building, gives rise to the notion of extremely large mMIMO. However, numerous obstacles persist in this field, including the need to develop accurate channel models, establish effective methods for feeding and controlling each antenna element, implement real-time estimation and

feedback for a significant number of channel elements, ensure synchronisation, devise scheduling strategies for a large number of terminals, explore various architecture and functional split options, integrate access, backhaul, and fronthaul in mesh configurations [114].

5G enables the provision of services such as Enhanced Mobile Broadband (eMBB), mMTC, URLLC, and their respective KPIs. Nevertheless, 6G networks are anticipated to handle more demanding applications, such as holographic telepresence, and fulfil significantly stricter criteria, including Terabits per second (Tbps) data throughput, sub-ms latency to the networking layer, exceptionally high reliability with a packet error rate as low as 10^{-8}, increased device density, extreme energy efficiency/ultra-low energy consumption, very high security, and cm-level accuracy localization. Utilising more of the electromagnetic spectrum in the THz, subTHz, infrared, and visible light bands could effectively address some of these difficulties. In addition, the millimetre and centimetre spectrum now being used for 5G and other legacy systems need to be re-farmed and exploited efficiently, and concerns of co-existence between mobile and non-mobile systems must be properly addressed. It will be necessary to examine waveform and modulation, radio channel characterisation, beamforming, and the practicality of hardware together to design economically feasible 6GTHz communication systems [115].

To fulfil the demanding specifications of the 6G standard, the radio building blocks (waveform, modulation and coding, NOMA, full-duplex, and mMIMO need to undergo more research and development). It is necessary to conduct research on a variety of topics, including, but not limited to, RIS integrated location, sensing, and communications (for purposes such as enabling broad use of robotics in industrial applications), random access for enormous connections, wireless edge caching, and other similar topics. In regards to spectrum reutilisation, 5G commonly employs "low-bands" (bands with a frequency below 2 GHz) and "mid-bands" (bands with a frequency between 2-8 GHz) for eMBB, mMTC, URLLC. "High-bands" (bands with a frequency above 24 GHz Milimeter Wave (mmWave)) are utilised foreMBB and URLLC applications in specific high-density urban areas where the limited coverage range is less of a concern. One of the most important elements that influence the system's capacity is the amount of frequency spectrum that has been allocated and is available for each wireless generation [116].

When considering the comparison between mmWave communication and low- and mid-bands, it is evident that mmWave offers a significantly larger accessible bandwidth. This attribute has great value in the context of 6G technology. The utilisation of mmWave frequencies, specifically those below 50 GHz, has been under consideration for implementing 5G technology. Further, mmWave bands, such as those over 100 GHz, would be required to develop 6G networks. mmWave technology offers a viable alternative for establishing backhaul, fronthaul, and access networks [117]. Due to its

ability to facilitate high data transmission rates, mmWave technology finds practical application in various domains, such as autonomous driving and smart factories. Additional obstacles must be addressed in meeting the needs of 6G networks. These include the development of effective designs for transmitting and receiving beamforming, as well as the implementation of modulation coding schemes that are characterised by low power consumption, affordability, and high data transfer rates. Lower frequency bands are highly valued and governed by strict rules. To meet the high bandwidth requirements of impending 6G systems, it is essential to effectively reutilise the existing low-, mid-, and high-band spectrum resources (for example, by simultaneously utilising licenced and unlicensed airwaves, utilising solutions such as cognitive radio-based technologies) [118], only then will it be possible to satisfy these requirements. To fulfil these challenges, there is a need to enhance wireless communication by the deployment of passive reflecting devices, such as metamaterials and very large-scale antennas. Multi-antenna technology, particularly the use of very large-scale antennas, is crucial for enhancing the spectrum efficiency of wireless mobile communication systems. A high-gain antenna is a vital tool for improving the spectral efficiency of the communication system. Very Large-Scale Antenna (VLSA), also known as Large Intelligent Surfaces (LIS) or Intelligent Reflecting Surfaces (IRS) or RIS, is indeed one of the emerging technologies that researchers are exploring as a potential enabling technology for 6G. These large surfaces consist of numerous low-cost and low-power reflecting elements that can intelligently adjust the phase and amplitude of incoming signals to enhance wireless communication. RIS is a form of metamaterials, (full description is provided in Chapter 5) in which it can improve wireless communication through enhanced coverage and connectivity. Strategic deployment of RIS can enhance wireless communication and meet different 6G KPIs in demanding settings, such as densely built urban areas or isolated locales through different areas:

(a) **Coverage**: Through the strategic configuration of the parts of the RIS, it is feasible to manipulate the direction, phase, and amplitude of the signals, enabling the customisation of the wireless communication environment. This feature can be utilised to overcome barriers, reduce interference, and improve signal intensity orientations. RIS can improve coverage by employing signal focusing. This means that RIS may concentrate signals in specific directions, directing coverage to the areas that want it the most. This can facilitate the expansion of wireless networks. RIS can aid in surmounting impediments such as buildings or other barriers that may obstruct or attenuate wireless signals. By manipulating signals using the RIS's reflective parts, it becomes feasible to reroute and enhance the signal to bypass obstacles. Interference mitigation can be achieved by utilising RIS to manipulate the phase and amplitude of the signal. This can be especially advantageous in densely populated urban areas where many signals may potentially disrupt one

another. RIS can adjust and modify its operations in response to fluctuations in environmental circumstances and user demands, hence optimising the extent of coverage according to real-time necessities.

(b) **Energy & Spectral Efficiency**: RIS can enhance energy efficiency by minimising power usage in communication equipment by optimising signal routes. Spectral efficiency can be improved by using RIS, as it helps reduce interference and optimise signal quality. This can result in a more optimal utilisation of the available frequency spectrum.

(c) **Customisation and Adaptability**: RIS have the capability to adapt dynamically in response to changes in network conditions. This flexibility allows for improved customization of the communication environment, supporting the specific needs of users and applications.

(d) **Security**: RIS can reinforce the security of wireless communications by controlling signal propagation and mitigating the possibility of eavesdropping.

(e) **Low Latency**: RIS can optimise signal routes and minimise communication delays in applications with low latency, such as real-time communication for AR or autonomous vehicles.

Authors in [119] proposed a hybrid relay RIS architecture in which several elements serve as active relays. In contrast, the remaining parts merely reflect the incident signals. Increasing the overall system coverage is one of the primary goals of 6G communication networks. Conversely, this objective must be accomplished without increasing RIS elements complexity. In [120] the authors used sub wavelength unit cells to gain continuous or quasi-continuous apertures, which they claimed enabled holographic communication and reaping the benefit of the diffracted signal by RIS, by combining it with the reflected signal to implement a THz MIMO system. While this looks promising, using the same reflective RIS as a mirror to combine the diffracted signals will increase system interference and signal power loss. Reference [121] suggested a reconfigurable holographic surface multi-user communication system embedded into the BS, providing a holographic beamforming scheme that optimises digital signal transmission. Even though this looks good from a 6G point of view, there needs to be more real time testing in the THz frequency range. A hybrid beamforming approach to improve THz-band coverage in multi-hop RIS assisted networks is presented in [122]. Multiple passive and reflective controllable RISs are installed to aid BS and single-antenna user broadcasts. Simulations suggest their proposed technique improves THz communications with several hops by 50%. Practical phase-shift model that collects the phase-dependent amplitude variation in the element-wise reflection coefficient for RIS to maximise its achievable rate by jointly optimising the transmission and reflection beams is proposed in [123]; while the authors achieved data rate improvement of 33%, system limitations remain within a distance that did not meet 6G aspirations.

A realistic assessment of how RIS technology can fill in coverage gaps is addressed in [124] specific varactor diodes that let them change how they respond depending on what is needed. Even though the performance of the work shown is promising, the system is rearranged with a center frequency of 3.5 GHz, which is not a 6G perspective. One form of hybrid RISs is presented in [125] by enabling the passive element to reflect the impinging signal in a controllable manner, while simultaneously sensing another rounded signal. The sensing capability of hybrid RIS makes it possible to facilitate various functions related to network management, including the estimation of channels and localisation. Even though this implementation introduces a new idea for RIS, it will increase interference and power loss for signal reflection in the system without making signal transmission more effective.

Reference [126] presented a reflecting meta-surface with integrated sensing capabilities by changing the meta-surface tunable atoms to a couple of tiny segments of the incident wave to an array of sensor waveguides. As an illustrative example, they used the sampled incident wave to detect its angle of arrival. Since the basic principle of RIS is to detect the incident signal and its angle, change the signal phase and send it to the intended user, adding sensors to the system, will increase complexity and cost. In [127] a new approach for beamforming design assisted by RIS for Integrated Sensing and Communication (ISAC) systems is considered. This approach combines both active and passive beamforming techniques. The main objective is to enhance the SNR at the UE while ensuring a minimum level of detection probability. The proposed design seeks to optimise the ability to identify targets by calculating the probability of detecting a target and introducing the idea of Ultimate Detection Resolution (UDR). The proposed strategy utilises a bisection search method to get users location and redirect the signals.

In reference [27] an assisted hybridRIS communication with index modulation using space shift keying and spatial modulation to improve overall spectral efficiency and reduce error rate is suggested. In contrast, the hybrid formulation of RIS should refer to the functionality of the RIS itself, not the added system specifications. Two hybrid transmission schemes combining a passive RIS with decode-and-forward relaying are introduced in [128]. Their results, as expected, showed an enhancement in the achievable error rate performance due to the use of relays, which adds another design complexity to the communication system. Reference [129] investigated a beam training strategy for RIS joint beamforming in THz communication, enhancing indoor coverage within a limited distance. Conversely, whilst the process they followed looks promising for indoor applications, it still requires increasing the transmission power to improve the coverage, which is not a feasible real-time solution for outdoor 6G applications. The researchers in [130] proposed a RIS assisted wireless network to facilitate communication between multiple RISs, with multiple single antenna users, a multi-antenna AP, and a finite number of phase shifts being deployed at each element. Their goal was

to minimise transmission power at the AP by jointly optimising the APs continuous transmit precoding and the RISs signal reflection. The simulation results showed that using RISs in a communication system improves the Signal to Interference Noise Ratio (SINR) between AP and RIS regardless of the THz system frequencies.

In [131], the authors present a transmitter RIS architecture that enables efficient communication with low power consumption and high-rate multi-streams. Their proposed approach uses a joint optimisation technique that effectively combines difference-of-convex programming and sequential convex approximation to address the non-convex problem. They introduce a framework that examines the balance between EE and Spectral Efficiency (SE) in a cognitive network. The results illustrate the capability of the transmitter RIS architecture to achieve both low power consumption and high-rate multi-stream transmission. Nevertheless, the complete consideration of the scalability of the transmitter design and joint optimisation technique in 6G, especially in managing bigger network sizes or more complex scenarios, needs to be improved. Reference [132], introduced channel models for the near-field and far-field regions of STAR-RIS. It also obtained closed form formulas for the channel gains of users who receive both the transmission and reflection signals. The study in [133] examined the basic coverage characterisation of STAR-RIS aided two user communication networks. Formulations for maximising the coverage range were developed for both NOMA and OMA systems. In a previous study [134], the researchers investigated the difficulties of minimising power consumption in STAR-RIS assisted unicast and multicast systems. They focused on optimising both active and passive beamforming for various operating protocols of STAR-RIS. In a study conducted in [135], the researchers examined the usage of IRS in an indoor multi-user downlink communication system. They constructed an optimisation problem involving analogue and digital beamforming for tiny BS. The objective was to maximise the sum rate of the system. The analysis in [136] focused on optimising the phase shifts of an IRS. To do this, a branch and bound based method was suggested for designing the IRS phase shifts inside a limited set.

In a study published in [137], the authors examined the effectiveness of a 60 GHz reconfigurable surface with 224 reflecting elements for indoor mobile mmWave communications. The study assumed that direct links were prevented, and the authors managed to minimise the outage probability by determining the ideal location of the user from RIS and BS. Furthermore, in [138], the authors examined the optimisation of channel capacity for indoor mmWave communication with the assistance of RIS. They also put forward methods with low complexity to optimise the phase shifts of RIS and the transmit phase precoder. Furthermore, the authors in [139] examined the combined optimisation of transmit beamforming and RIS phase shifts to maximise the received signal power in single and multi RIS assisted systems. Their results indicate a substantial enhancement in average received SNR by utilising RIS, as evidenced by the number of

significant performance improvements in RIS elements. In their study [140], the authors examined the combined optimisation of RIS position, RIS phase shifts, sub-channel allocation, and power regulation to maximise the total data transmission rate in a THz communication system assisted by RIS. The authors suggested a Block Coordinate Searching (BCS) based technique to tackle the non-convex problem for the generalised number of users. In addition, the authors in [141] developed a solution to maximise EE in the RIS assisted THz communication system. They utilised the covariance matrix adaptation evolution strategy to optimise the transmit beamforming,RIS phase shifts, and power allocation.

In [142] authors present a framework for allocating resources in multi-cell NOMA networks with RIS. The framework aims to maximise the sum rate and formulates it as a problem to be solved. To tackle this complex problem involving integers and non-linear functions, their approach is to break the problem into two separate problems: an optimisation problem (P1) with continuous variables and a matching problem (P2) that involves integer variables, and an iterative algorithm are proposed for solving P1. These algorithms include allocating transmit power, designing the reflection matrix, and determining the decoding order. They utilise relaxation methods such as convex upper bound substitution, successive convex approximation, and semidefinite relaxation. Swap matching-based algorithms are presented for P2 to attain a two-sided exchange-stable state among users, BS, and subchannels. Numerical studies demonstrate that the sum rate of the NOMA networks can be improved using the RIS. In this work [143], they investigate a RIS assisted NOMA system, in which a BS transmits aggregated downlink signals to multiple users. The proposed method implements a user ordering system that relies on the combined channel strength approach. In order to optimise the rate performance and ensure equitable treatment of all users, the objective is to maximise the minimum decoding SINR for each user. This is accomplished by optimising the power allocation at the BS and the phase changes at the RIS in a synchronised fashion. The simulation results indicate that the downlink NOMA system, when assisted by RIS, significantly enhances the rate performance compared to traditional NOMA systems without RIS and traditional OMA systems with or without RIS.

In [144], a traditional Block Coordinate Descent (BCD) algorithm was used to solve the sum rate optimisation problem in STAR-RIS aided MIMO networks for both unicast and broadcast communications. The authors in [145] obtained an expression for the coverage probability of a large MIMO system with STAR-RIS assistance, considering correlated fading and phase-shift faults. In addition, [146] introduced strategies for acquiring uplink CSI for the Time Switching (TS) and Energy Splitting (ES) protocols. Multiple investigations have demonstrated that STAR-RIS is well-suited for NOMA to fulfil the demanding future 6G criteria. NOMA enhances the efficiency of transmitting and receiving signals across different frequencies, while STAR-RIS expands the coverage

area and supports the fundamental idea of NOMA. The channel gains can be modified using TS and ES protocols to provide for adaptable decoding orders based on the needs of the transmitter and receiver. The transmission design of a coordinated multi-point system, specifically a STAR-RIS NOMA system, was discussed in [147]. The objective was to remove inter-cell interference and enhance the intended signal simultaneously.

The problem of maximising EE in a STAR-RIS NOMA network was addressed in [148] using ML. The study focused on utilising a deep reinforcement learning technique known as Deep Deterministic Policy Gradient (DDPG). Furthermore, a STAR-RIS NOMA system was suggested to have linked transmitter and receiver phase shifts. The study also computed the outage probability and power scaling law for this system in [132]. This research [149] aims to achieve the advantages of both cascaded and parallel network typologies by implementing a hybrid RIS networking structure. The cascade topology reduces path loss and increases multiplicative gain, whereas the parallel topology enhances scattering signatures in the specific region (cluster). Initially, cascaded grouping is addressed by utilising an optimal routing strategy that considers consecutive channel attributes. Also, they consider a scenario where active and passive beamforming is used on parallel lines clustered together, which shows an increase in the total possible sum rate and examine the impact of receiver mobility on location shift sensitivity.

The research [150] examines a mmWave NOMA system that is assisted by a RIS. Specifically, the research examines a mmWave NOMA downlink system that uses RIS technology and incorporates a hybrid beamforming architecture. A higher rate and higher coverage are the aims while maintaining minimum power consumption. This problem involves joint optimisation of RIS phase shifts, hybrid beamforming, and power allocation. To convey these aims, they have devised an alternating optimisation technique. To be more precise, they convert the aims into non-convex problems and divide them into three subproblems: power allocation, combined phase shifts and analogue beamforming optimisation, and digital beamforming design. Next, they address the power allocation issue by maintaining the phase shifts of the RIS and the hybrid beamforming at a constant value. Finally, the power allocation matrix employs an alternating manifold optimisation approach and a sequential convex approximation method for designing the phase shifts, analogue beamforming, and transmit beamforming.

The study in [151] examined an architectural framework for mmWave um-MIMO systems with RIS assistance. The researchers utilised the sparsity of mmWave channels to develop two highly efficient precoders. In a study conducted by the authors in [152], they examined the hybrid beamforming and phase shift design formmWave systems assisted by RIS. They put forward an iterative approach that is characterised by its low complexity. The challenge of optimising joint transmit beamforming and phase shift for multi RIS aided mmWave systems was investigated in [139]. The manifold optimisation

method addressed the optimisation problem in RIS- aided NOMA systems [153]. In reference [154], the allocation of resources for a multi-channel RIS NOMA system was examined, an algorithm was developed to determine the power allocation, subcarrier assignment, and phase shifts simultaneously. In addition, various other research issues related to RIS aided wireless communications have recently been explored which include the maximisation of data rate in [155–157], channel estimation in [158], and robust optimisation in [159, 160].

2.4.4 Artificial Intelligent

Based on the 5G-Advanced transformative technical development strategy, industry and academia collaborated to focus on evolution in the first five years while creating 6G requirements. The first test platforms can be expected after 2025. Everyone agrees that the new architecture will be entirely software-based and flexible. 6G communications networks will be the first to include native AI. AI will be more than just an application tool; it will be an essential component of infrastructure, network management, and operations. AI technology contributes significantly to solving problems caused by a high degree of complexity in network operation and maintenance, a high level of adaptability, and a wide range of network conditions. Enhanced mobile application performance and flexibility lead to increased network complexity, posing new problems for operation and maintenance. The realisation of deep integration of AI and 5G creates new network structure and unified planning requirements at many levels, including terminal, network element, network management, AI mechanism, and capabilities [161].

ML enables systems to create models from enormous volumes of data. Key functionalities include Deep Learning (DL), Reinforcement Learning (RL), and Federated Learning (FL). In the past decade, DL has made significant progress and is now widely used for training with massive amounts of data. FL is a learning strategy in which numerous clients with local models work with a data centre to integrate and build a global model, subsequently broadcast to all user devices. RL involves a recursive learning process where an agent interacts with its environment and learns how to take action. ML is generally effective when an accurate mathematical model of the system is unavailable. Still, sufficient training data is available, the system changes slowly over time, and numerical analysis is adequate [162–166]. It is important to note that, there is an endless research efforts on AI different approaches, and there use cases in 6G, an analysis on the amount of AI researches in 6G revels that their is an increased amount of research's taken place as shown in Figure 2.5. However, their is only limited researches that integrate AI with channel coding or decoding [167–181] as shown in Figure 2.6. To be more precise, polar code is expected to be an important component of the 6G standard, due to the fact that it has played a significant role in 5G.

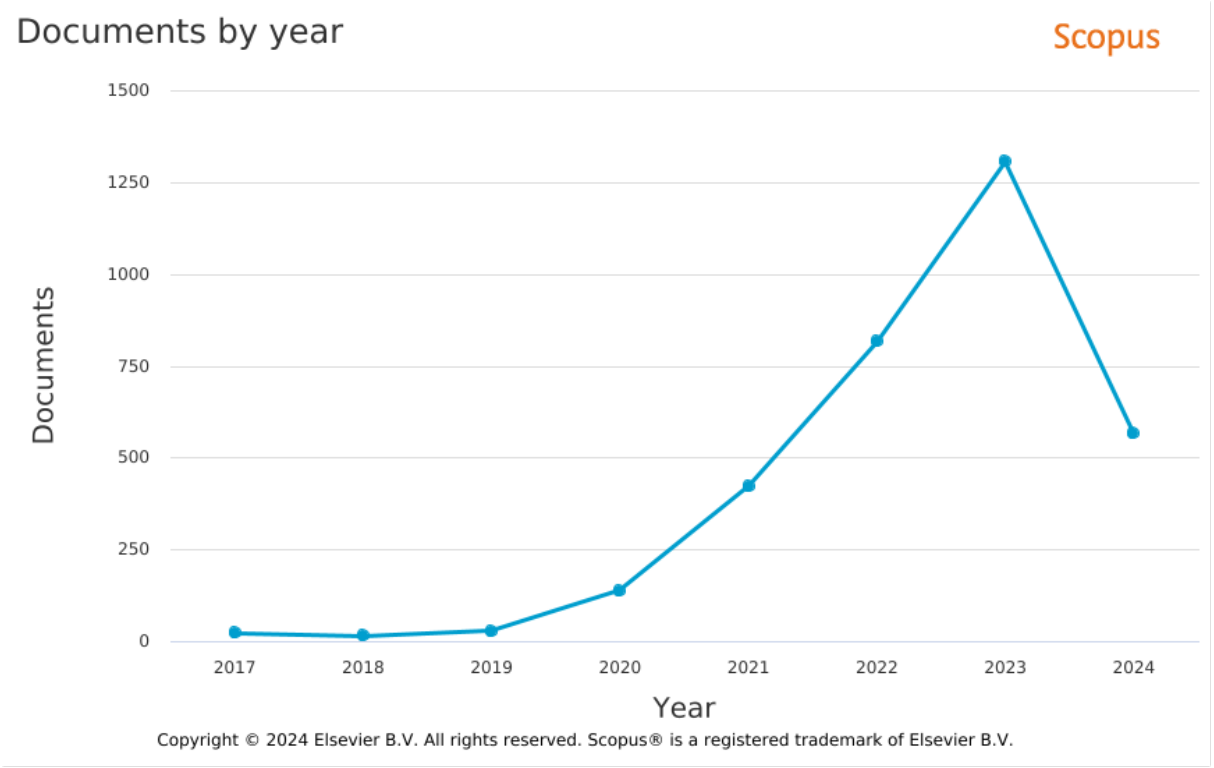

Figure 2.5: Researches that Contribute to the 6G on AI base by year

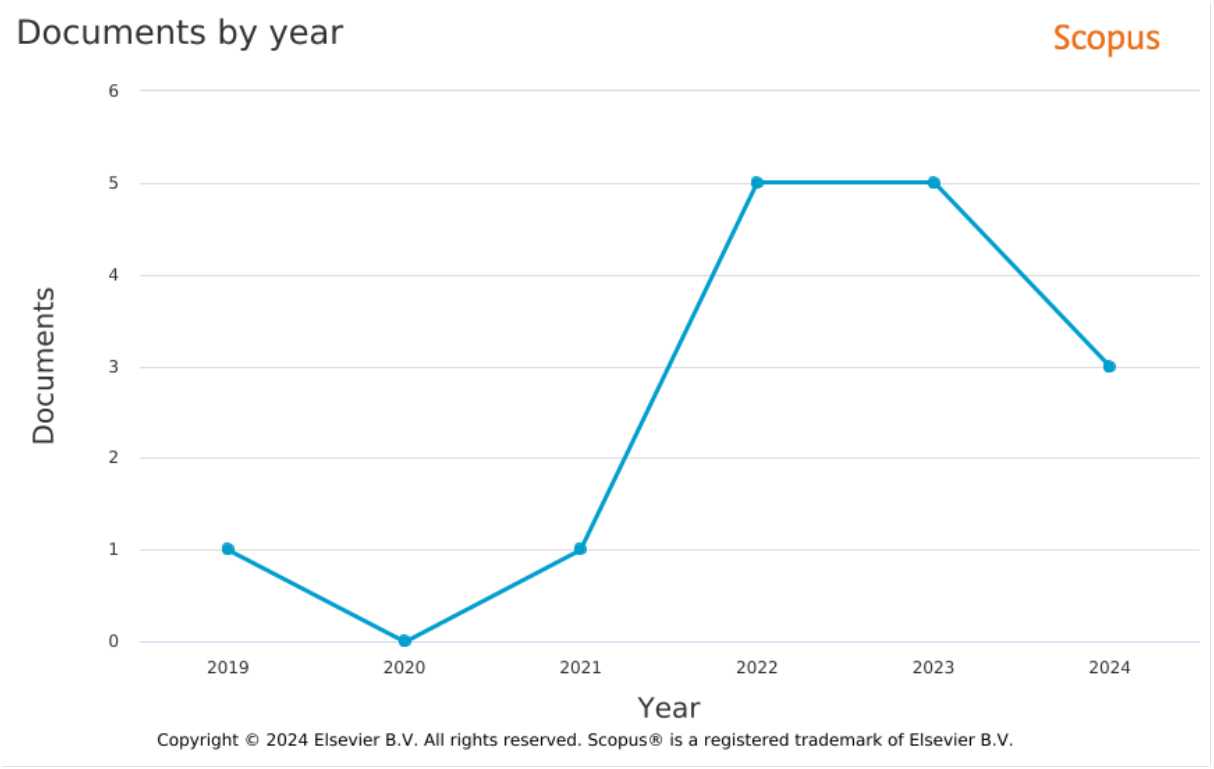

Figure 2.6: Researches that Contribute to the 6G on AI Channel coding/decoding

Additionally, in the earlier generations, the use of LDPC code provide a resilient message transmission techniques that achieve almost ideal error-rate decoding [182]. However, polar codes possess the distinct capability to approach the Shannon capacity as the code length approaches infinity, thanks to the Superposition Coding (SC) decoding algorithm [183], while LDPC is decoded using the BP algorithm.

Ongoing research in both SC and BP decoding is centred on achieving a trade-off between error-rate performance and complexity. This aims to enhance the efficiency and effectiveness of these communication systems. The authors enhanced the BP decoding technique for LDPC codes using DL, as mentioned in [184]. A Tanner graph was employed, and the weights were trained using stochastic gradient descent, resulting in a notable decrease in the BER. In the study cited as [185], a Deep Neural Network (DNN) is employed to calculate the minimum number of iterations required. The study's simulations show that the DNN can accurately forecast the number of iterations needed, particularly in cases with a high SNR. The paper proposes using an iterative BP Convolutional Neural Networks (CNN) decoder to address the issue of correlated noise, as mentioned in reference [186]. This entails incorporating the output of the BP decoder into a feed-forward CNN to determine the associated noise across several channels. Another approach involves using neural networks as a direct replacement for the decoder.

A study [187] utilises a neural network decoder to decode unstructured LDPC and structured polar codes. The simulations demonstrated that the neural network decoder can achieve MAP performance for structured and unstructured codes, even with low block lengths. Expanding on the discoveries of [187], a subsequent study, [188], advanced the topic even further. The researchers in this paper devised a technique to decompose a lengthy polar code with a large block length into smaller, more manageable sub-blocks. Subsequently, each of these smaller components is deciphered using a condensed neural network decoder, enhancing the training procedure's practicality. The outcomes derived by the neural network decoder are then sent using a conventional BP framework.

On the other hand, Figure 2.7 shows the main research approaches related to the application of ML in RIS assisted wireless systems. The most reported frameworks are based on beamforming, channel estimation, signal detection, and federate learning applications. In Table 2.2 we show the latest research conducted to deploy ML in RIS aided communication systems.

Figure 2.7: ML Research Approaches for RIS

Table 2.2: ML approaches on RIS aided communications

Reference	Contribution
[189]	DL dual CNN-based architecture for CSI estimation
[190]	Combined DL and compressive sensing to estimate the CSI utilising only the RIS's active reflective parts
[191]	A DL approach for CSI estimation and symbol detection in RIS wireless systems from the received signals

[192]	DL based estimation of channels from UE to RIS that operates at varying SNR levels and number of multipaths. The model can achieve a high normalisedMSE performance by activating a limited number of elements during the training phase
[193]	Two DL architectures are proposed to estimate CSI by leveraging channel low-rank sparsity. The proposal's efficacy can be enhanced by increasing the density of sensing devices
[194]	It proposed channel estimation as an image noise reduction problem based on CNN architecture. As numerical results show, the proposed model's performance is comparable when the system possesses complete channel knowledge
[195]	Distributed ML based technique for CSI estimation in which the BS and users train together is presented. The idea can improve estimation accuracy when the pilot overhead is lowered to 1/8
[196]	A deep unfolding network was suggested for accurately predicting the downlink channel of a wireless system with RIS. The approach surpasses the least-squares estimator in performance and has a reduced level of complexity, resulting in a lesser training overhead
[197]	The proposed method uses DL to estimate CSI for systems incorporating RIS and massive MIMO technology. The process focuses on extracting the correlation features of subcarriers. The proposal exhibits superior spectrum efficiency while maintaining a reduced signalling burden.
[198]	A DL based approach is used, where the RIS learns the most effective way to interact with the incident signal. Only the channels at the active elements are considered. The approach can obtain data rates that are close to ideal, even without prior knowledge of the geometry of the RIS array
[199]	A DL based method is employed to reconfigure the phase at the RIS by utilising the local propagation environment. The model surpasses the classical least-squares estimator in performance while requiring minimal training time
[200]	An unsupervised DL based method was introduced to predict the phase shift of reflecting elements in a RIS. The model can dynamically adjust its setup in real time while maintaining an acceptable data rate
[201]	The optimisation of beamformers at the BS and reflective coefficients at the RIS is performed using a downlink DL scheme. The suggestion can optimise a rate or minimise a target with a small number of pilots
[202]	A DL based method optimises the active beamforming from the BS to users and the passive beamforming for RIS. The proposed method can attain superior BER performance compared to a traditional system
[202]	The ML technique used optimises the weighted sum-rate in RIS aided system by leveraging the product's characteristics. The suggestion surpasses the performance provided by the block coordinate descent method

[203]	Investigate the joint design of the transmit beamforming matrix at the BS and the phase shift matrix at the RIS, taking advantage of recent breakthroughs in DRL, in which the joint design is obtained through trial-and-error interactions with the environment while monitoring predetermined rewards, all within the framework of continuous state and action
[204]	DRL approach for designing transmit beamforming and phase shifts at the RIS in a multiuser MISO system. The idea addresses hardware limitations for RIS aided wireless systems
[205]	DRL based method for real-time phase control at the RIS, independent of CSI. The proposal outperforms model-free RIS control without sub channel CSI
[206]	DRL approach for jointly designing the phase shift at the RIS and controlling UAV trajectory.The concept enhances the energy efficiency of a RIS assisted UAV system
[207]	A DRL based method for energy harvesting and phase shift control in a RIS-assisted UAV system is proposed. The proposal is efficient and practical, outperforming other options
[208]	DRL technique for optimising a UAV trajectory and active/passive RIS beamforming. The approach improves performance in terms of energy savings and total achived rate

Additionally, in [209], the authors present an AirCom-based FL model that optimises device selection, beamformer aggregation at the BS, and phase shifts at the RIS to maximise the number of devices participating in model aggregation while meeting MSE criteria. In [210], an Offline AirComp improvement of the RIS FL system is proposed. FL is deconstructed using look-ahead data and a Lyapunov framework. A transceiver-decoupled BCD method tunes phase shift. A low-complexity approach based on element-wise successive refinement is used to implement an RIS with a discrete shift constraint. By combining local training with model uploading, [211] proposes an iterative resource allocation approach to reduce energy consumption, where FL applications have been employed in RIS assisted UAV communications. The [212] architecture proposes an FL network using over-the-air communications for high-quality, ubiquitous, privacy and low-latency network coverage. Using UAV power and trajectory, optimise the RIS phase shifts and noise factor for noise suppression to minimise the worst-case MSE.

A RIS assisted system's transmission error and efficiency are improved by optimum signal decoding at the UE device using AI approaches. In [213], the authors proposed demodulating OFDM signals for CNN based RIS MIMO systems. The model trained to produce synthetic channel realisations was tested with BS transmitted data. For Rayleigh fading channels, the Saleh–Vanenzuela model was used. The architecture included a CNN with two hidden layers, Adam optimisation, ReLU activation function.

The output layer outputs were determined by softmax activation. A hybrid CNN-Gated Recurrent Unit (GRU) architecture produced RIS assisted communication system signal detection is presented in [214]. Simulating OFDM data over the channel trained the combined network offline. The CNN architecture included 64 3x3 filters and a pooling layer. The GRU network had four layers, including Tanh activation for hidden levels and sigmoid activation for output layers. The probability of class membership was shown in the output layer. The architecture used cross-entropy loss and Adam optimisation.

The development of tools for simulating RIS assisted communication systems paves the way for researchers to understand better how RIS surfaces interact with networks. For example, open-source channel modelling tools have been developed for indoor/outdoor scenarios, including the physical features of wireless propagation in the presence of an RIS in [215]. The authors of [216] employ ML to construct RIS assisted communication contexts, modelling wireless as a custom interpretable back propagation neural network. The Neural Networks (NN) learns and configures the propagation parameters to allow users to communicate in the vicinity. Each RIS element is configured as a neuron or node, with weight corresponding to the power distribution. The proposed NN reduces the number of tiles necessary for effective communication.

It is important to note that, there is an increased number of researches that summarise the ongoing advancements on merging RIS with AI different approaches [217–257]. In conclusion, the quantity of research undertaken literature surveys on the upcoming wireless generations 6G and AI is summarised in Figure 2.8.

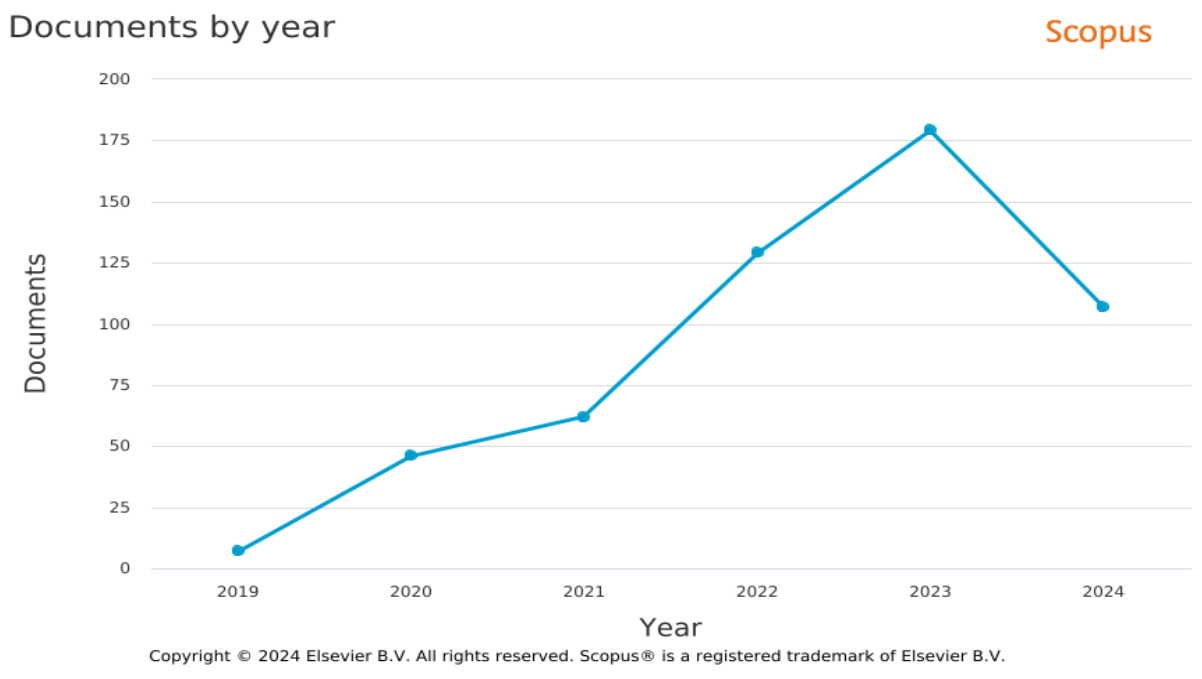

Figure 2.8: The number of Literature Reviews Conducted on AI in regards to 6G

2.5 Other 6G Evolutionary Enabling Techniques

2.5.1 Non-Terrestrial Technologies

The current cellular networks, which rely on outdated land-based technology, have successfully addressed the difficulties of offering widespread wireless coverage in rural regions and the issues of limited availability, reliability, and susceptibility to natural and human-made disasters. To overcome these difficulties, the 6G networks will use non-terrestrial technologies such as UAV assisted wireless communications and satellite connectivity, Figure 2.9 provides a general overview showing the connectivity of non-terrestrial networks. This integration will ensure comprehensive coverage and high-capacity connectivity [258, 259].

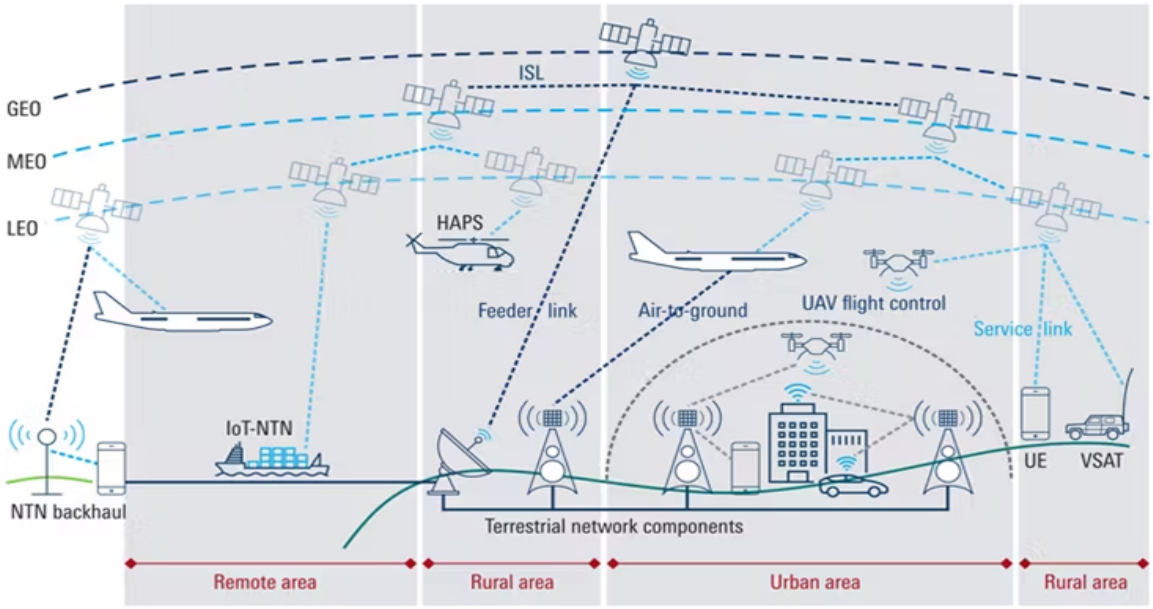

Figure 2.9: Connectivity of non-terrestrial networks[260]

UAV assisted wireless communications involve UAV that can fly at altitudes higher than 100 metres. These UAV have gained significant attention due to their simplicity and cost-effectiveness in providing extensive wireless coverage during emergencies or as relay nodes for terrestrial wireless communications. UAV assisted communications have the potential to be used in 6Genabled IoT networks, which is a promising application. UAV can surpass the geographical and environmental constraints that affect wireless communications. This includes ships in the ocean, sensors deployed in remote or isolated areas, and areas not covered by terrestrial networks.

Two scenarios can be envisioned for integrating UAV into current and upcoming cellular networks [261]. In the initial scenario, UAV can be integrated into the existing cellular network as a type of UE that receives services while in flight, known as Aerial Users (AU). AUs are anticipated to be a mutually beneficial solution for UAV technology

and cellular networks due to their cost-effectiveness. Moreover, AUs can utilise several existing cellular BS without constructing additional essential infrastructures.

In the 6G future, AUs will bring forth numerous novel use cases of UAVs, including urban/road traffic management, search & rescue operations in remote regions, and environmental photography.Additionally, AUs can be a supplementary instrument to enhance the accuracy of positioning systems that rely on cellular networks.

In the second scenario, UAVs can function as aerial BS or relay nodes, assisting with existing terrestrial wireless communications by establishing connectivity from the sky. Non-terrestrial BS/relay nodes offer significant advantages over terrestrial BS/relays at stationary locations [262]. For example, airborne BS or relays can be constructed rapidly if desired. This capability is of utmost importance for use case scenarios, particularly in crises, unforeseen calamities, and search and rescue operations. In addition, aerial BSs/relays have a higher probability of establishing a radio link with terrestrial UEs than terrestrial BSs/relays because they are positioned above the earth. Therefore, they can establish more dependable connections and offer multi-user scheduling and resource allocation for radio access.

Why Not Non-Terrestrial?

UAV based communications present various important challenges. These include the need for different QoS requirements for UAV command/control signals and payload data, the occurrence of severe interference in air-ground communications (uplink/downlink) caused by Line of Sight (LoS) dominant channels, and the difficulties related to the size, weight, and power constraints of UAV [263–266].

(a) **Restricted Payload Capacity**:UAVs often have limited capabilities to carry payloads, which might impose limitations on the communication equipment and antennas they can transport. This constraint could hinder the UAVs capacity to facilitate sophisticated communication technologies in the context of 6G.

(b) **Restricted Duration of Flights**: UAVs frequently face limitations due to their restricted battery life or fuel capacity, leading to brief flight durations. This constraint could impact the duration of UAVs communication services in a 6G network.

(c) **Interference and signal attenuation**: interference and signal attenuation can occur during communication between UAVs and ground stations owing to many factors, such as buildings, vegetation, and atmospheric conditions. In the context of 6G, using high-frequency bands and novel communication technologies may exacerbate these difficulties.

(d) **Regulatory and Legal Challenges**: UAV operations face regulatory and legal challenges due to different legislation and limits. Incorporating UAVs into 6G networks may necessitate resolving legal and regulatory obstacles to airspace administration, privacy apprehensions, and safety mandates.

(e) **Security Risks**: UAVs in communication networks are susceptible to cyber security vulnerabilities, including hacking and jamming. Addressing these challenges becomes crucial for the dependable operation of UAVs in 6G, where there is a greater focus on security and privacy.

(f) **Network slicing complexity**: 6G networks are anticipated to facilitate network slicing, enabling the formation of numerous virtual networks with distinct attributes to fulfil varied demands. Introducing and overseeing network slices for UAVs in the broader 6G infrastructure may bring about intricacies.

(g) **Integration with Pre-existing Infrastructure**: Incorporating UAVs into current communication infrastructure presents difficulties. Achieving smooth communication transitions and compatibility with terrestrial networks may necessitate significant endeavours.

(h) **Cost Considerations**: Deploying and maintaining UAV network can incur significant expenses. It is crucial to thoroughly evaluate the costs of procuring, operating, and upkeeping UAVs for 6G communication services.

2.5.2 Visible Light Commucniaton / Optical Wireless Communication

VLC operates throughout the frequency spectrum ranging from 400 to 800 THz. Unlike RF systems operating in the lower THz range, which use antennas, VLC uses illumination sources, particularly Light Emitting Diodes (LED), image sensors, or photodiode arrays, to establish the transceivers as shown in Figure 2.10 [267]. These transceivers enable a large bandwidth while consuming little power (100 mW for 10 Mbps to 100 Mbps), all while avoiding the production of electromagnetic or radio interference [268].

Because standard LED have a long lifespan (up to ten years), are inexpensive, and have unrestricted access to spectrum, VLC is a desirable option for use cases where battery life and access costs are important considerations. Furthermore, VLC outperforms RF technologies regarding propagation performance in certain non-terrestrial environments, such as aerospace and underwater.

Compared to RF, VLC MIMO gain is weaker, particularly indoors. The high coherence among propagation channels leads to limited spatial diversity. Although spacing LED arrays can reduce coherence [269], VLC MIMO faces receiver design and implementation challenges in which the non-imaging receivers are sensitive to spatial alignments with transmitters, while imaging receivers are too expensive for cost critical use cases [270]. On the other hand, VLC beamforming, unlike RF MIMO beamforming, uses a distinctive optical component called a Spatial Light Modulator (SLM). On the other hand, and like mmWave and THz technologies, VLC likewise depends on LoS channels, as it cannot pass through obstacles or effectively diffract around them [271, 272].

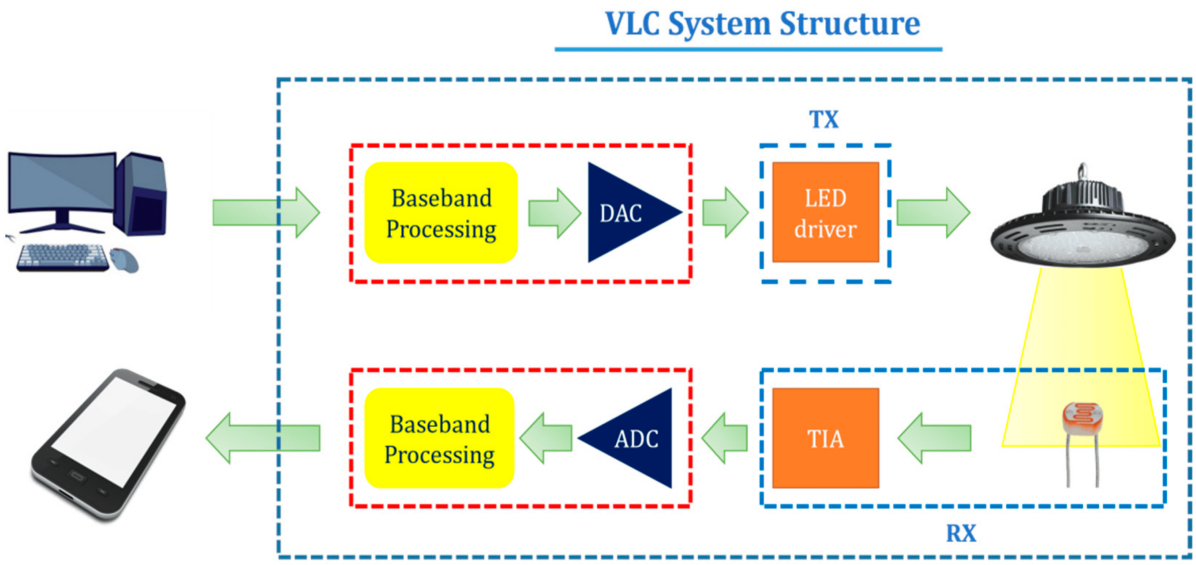

Figure 2.10: A schematic of a VLC System (Tx: Transmitter; Rx: Receiver; DAC/ADC: Digital/Analog converter; TIA: Transimpedance amplifier)[273]

The term Optical Wireless Communication (OWC) refers to wireless communications that utilise IR or UV as transmission. It is a potentially advantageous supplementary technology for conventional wireless communications that operate inside RF bands. The utilisation of OWC in the IR and UV spectrum, has the potential to mitigate challenges and enhance conventional RF communications, particularly in densely populated indoor environments. Additional benefits of OWC include the integration of illumination and data communication, the availability of readily available optical devices, the absence of multipath fading, and the potential to achieve centimetre level positioning in indoor situations, among others [274]. The primary obstacles encompass issues such as light transmission obstruction caused by the proximity of the LoS, the need for interference reduction to enable UE to attain a high SINR, and the development and integration of OWC networks into the 6G of wireless communication technology. Light communication can be utilised to establish connections between the core network using wireline/optical fibre and wireless backhauling, cable TV networks, free-space optical networks, and non-terrestrial networks (such as interconnections based on airborne or spaceborne vehicles) [275].

Why Not Visible Light Communication / Optical Wireless Communication?

VLC systems often need directed antennas with narrow beams to mitigate nearby cell interference and environmental light noise. VLC systems are sensitive to user position and mobility, requiring precise beam tracking. However, this characteristic can be utilised for advantages like improved indoor location accuracy and reduced interference in vehicular communications. VLC systems face a technical challenge due to their unregulated access to the visible light spectrum, which increases security risks and requires stricter security requirements than licensed RF bands [276–282].

(a) **Restricted Range**: VLC generally exhibits a constrained transmission distance compared to alternative wireless technologies. Various elements, such as sunlight, weather conditions, and barriers, influence the range in outdoor environments.

(b) **LoS requirement**: VLC often necessitates an unobstructed path between the transmitter (LED light source) and the receiver (photodetector), known as the line-of-sight requirement. This limitation can restrict its usefulness in situations when direct communication is difficult.

(c) **Interference**: ambient light interference can affect VLC systems, making them vulnerable to disruptions caused by sunlight and artificial lights. Such interference could impact the dependability and efficiency of the communication connection.

(d) **Data Rate**: Data rate challenges arise in VLC because of factors such as modulation's complexity and channel defects, making achieving high data rates reliably in real-world applications difficult.

(e) **Indoor Deployment Limitations**: VLC is typically better appropriate for indoor settings where there is the ability to regulate lighting conditions. Outdoor installations may encounter obstacles due to the fluctuation of ambient light and the issue of sustaining unobstructed visibility.

(f) **Scalability**: Implementing VLC on a big scale may need to be improved in terms of scalability. Managing a network of VLC devices to ensure extensive coverage and smooth transitions between devices could be complicated.

(g) **Security Considerations**: VLC communications are more secure than radio frequency transmissions due to their confinement inside physical boundaries, which reduces the risk of eavesdropping. Nevertheless, the need to guarantee the security of VLC transmission by avoiding unauthorised access and interference remains a crucial factor to consider.

(h) **Energy Consumption**: although VLC devices may exhibit reduced power consumption compared to certain wireless technologies, it is still important to prioritise energy efficiency for both the light sources and the receivers, particularly in battery powered devices.

(i) **Integration with Existing Infrastructure**: incorporating VLC into preexisting communication infrastructure may necessitate substantial modifications and enhancements. It is important to consider the compatibility with different communication technologies and devices.

(j) **Deployment Costs**: setting up VLC infrastructure, which includes installing LEDs and related communication devices, may require an initial investment. The cost-effectiveness of VLC solutions with other wireless technologies is a crucial factor to consider.

2.5.3 Extended Reality / Holographic Communication

XR is a developing technology that combines physical and virtual worlds through wearables and computers to create interactions between humans and machines [283, 284] as indicated in Figure 2.11 [285]. The emerging technologies, AR, VR, and MR employ distinct sensors to gather precise information about the position, alignment, and speed.

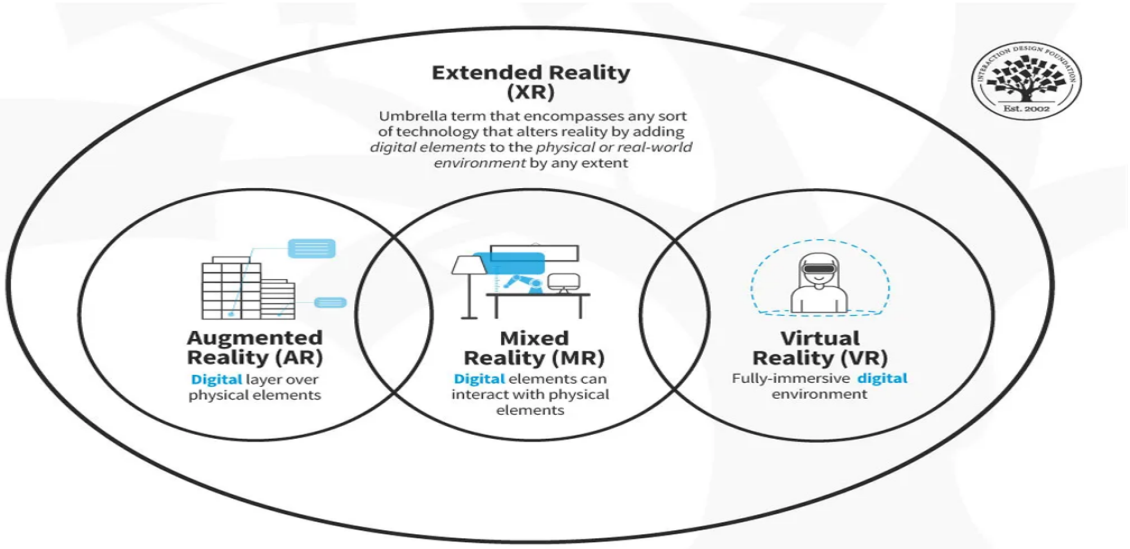

Figure 2.11: XR concept[286]

As AR, VR, and MR are crucial components of 5G technology. The primary determinants influencing the evolution of AR, VR, and MR technology and its applications are the mobility and autonomy of users, meaning that users will not be constrained by their physical location. The evolution of XR will eventually lead to the implementation of holographic communication systems and, ultimately, wireless holographic communication. Users can experience the advancements of holographic communication and holographic displays at any time and in any location. XR technology will have the capability to activate and engage the senses of sight, hearing, touch, smell, taste, and even emotions. Users can partake in education, games, sports, artwork, concerts, and other immersive holographic activities without any restrictions on time or location [37, 287]. Building virtual environments that are realistic and interactive requires the development of holographic display technologies as well as the optimisation of communication protocols [288]. Another potential direction of investigation is the creation of digital twins of physical items, such as networks and devices [289]. Creating both exact and dynamic digital copies makes it possible to do enhanced monitoring, predictive maintenance, and optimisation on 6G networks, which emphasises faster data rates, lower latency, better security, sustainability, and creative applications that will characterise the next era of wireless connectivity.

Why Not Extended Reality / Holographic Communication?

XR and holographic communication are cutting-edge technologies designed to deliver immersive and interactive experiences. Although 6G is currently in its first phases of advancement, certain overall drawbacks and constraints linked to XR and holographic communication exist that could be pertinent to its integration into 6G [290–294].

(a) **High Bandwidth Requirements**: XR and holographic communication necessitate substantial data rates to convey intricate 3D material and provide a smooth user experience due to their high bandwidth requirements. 6G networks need help providing extensive data throughput to meet these applications.

(b) **Delay Sensitivity**: XR applications, particularly those that involve real-time interactions and holographic communication, exhibit a strong sensitivity to delay. 6G networks must have extremely low latency to guarantee a seamless and prompt user experience.

(c) **Device Compatibility**: XR devices, such as AR glasses or VR headsets, may vary in their characteristics and capabilities. Ensuring interoperability and a uniform user experience across a diverse range of devices may provide a problem for 6G networks.

(d) **Energy Consumption**: XR and holographic applications frequently operate on devices that require significant resources, resulting in elevated energy consumption. When designing 6G networks, it is important to consider the energy efficiency of devices to facilitate extended XR experiences without rapidly depleting device batteries.

(e) **Infrastructure Requirements**: The widespread implementation of XR and holographic communication may necessitate substantial changes to the existing infrastructure. This entails the implementation of sophisticated sensors, cameras, and processing capabilities to facilitate XR applications without disruptions effectively.

(f) **Privacy Concerns**: Using XR and holographic communication may entail collecting and analysing delicate data regarding the user's surroundings. Ensuring user privacy and mitigating security risks are paramount in 6G networks.

(g) **Content Quality and Standardisation**: To ensure the delivery of superior 3D information and holographic experiences, it is essential to establish standardised formats and compression techniques. 6G faces the issue of maintaining content consistency and compatibility across several platforms.

(h) **Interference and Environmental Factors**: XR and holographic communication systems are susceptible to interference and environmental factors, including lighting conditions, impediments, and interference. To ensure a robust and dependable communication environment, 6G networks must consider these characteristics.

(i) **User Acceptance and Behaviour**: User acceptance and behaviour play a crucial

role in determining the success of XR and holographic communication in the context of 6G. Widespread acceptance may be influenced by factors such as social conventions, cultural considerations, and potential discomfort with prolonged XR experiences.

(j) **Regulatory and Ethical Challenges**: With the advancement of XR and holographic communication technology, there may be new regulatory and ethical issues to address. It is crucial to tackle concerns regarding content control, user safety, and ethical utilisation of XR technologies to ensure the effectiveness of 6G networks.

2.5.4 Mobile Edge Computing

The term Mobile Edge Computing's (MECs) refers to a network concept established by the European Telecommunications Standards Institute (ETSI), as shown in Figure 2.12 [295] it involves implementing and operating distributed computing capabilities, content caching, network data analytics, and network decision-making at the network edge [296] (refer to [297] for more standards). MECs will emerge as a key participant in the 6G networks by serving as an intermediary layer that facilitates real-time data analytics at the source of data generation. This paradigm is paramount for services/applications with limited resources [298]. Various developing services, such as AR/VR and Vehicle to infrastructure (V2X), require minimal end to end latency. MECs has the potential to significantly reduce this latency by implementing data processing and analytics methods at the edge.

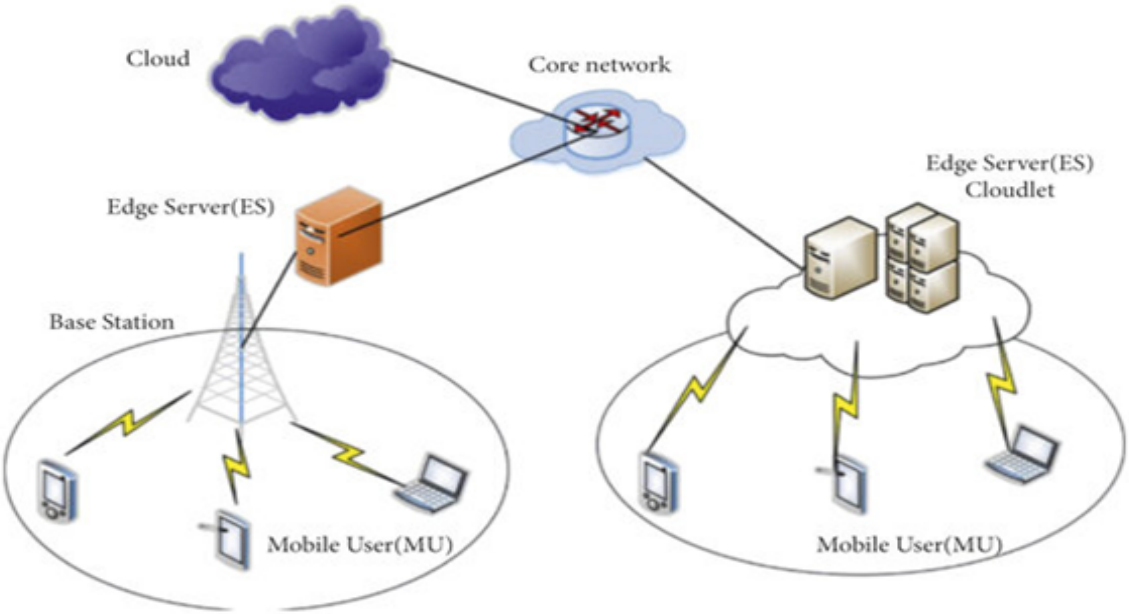

Figure 2.12: Mobile Edge Computing Architecture[295]

In addition, MECs's localised data preparation capabilities can minimise the requirement for transmitting a substantial volume of redundant or superfluous data to the cloud data centres. MECs is anticipated to be utilised to manage network resources, such as computing and communication resources, efficiently [299]. To be more precise, the implementation and functioning of edge servers, also known as MECs servers, at the network's edge can enable semi-centralised resource allocation methods. These methods utilise centralised resource allocation techniques to assign network resources to a group of edge devices, even when limited CSI is available and with minimal complexity. Edge computing technologies will evolve on 5G networks using various computing platform technologies created for open and cloud computing environments. In the real world, this translates into adopting virtualization technologies such as containers and container orchestration and service composition models such as (Software as a Service) and (Function as a Service) [300].

On the other hand, edge computing, particularly far-edge computing, calls for improved management of heterogeneous resource and service instance locations. In addition, constrained resources at the network's edge and the requirement for enhanced energy economy necessitate using lightweight virtualization and more specific orchestration techniques. This indicates that additional enhancements and updates to the existing cloud-specific procedures may be required, and it is not apparent that everything can be brought under the same orchestration efficiently using this evolutionary approach [301]. It is anticipated that computing and networking resources (in-network computing) will eventually combine to form a single computing continuum that will span from user devices and IoT devices to centralised cloud storage. In such a scenario, all services and resources would be naturally managed in a single, integrated manner. This would include not only the application, service, and data plane resources and functions but also the control plane functionalities of the telecommunications system [302, 303].

Why Not Mobile Edge Computing?

Although the benefits mentioned above are significant, several unresolved constraints remain in implementing MECs in 6G mobile networks. Some main challenges include ensuring data consistency across all edge devices, dealing with data scarcity at the edge, addressing the limited adaptability of statically trained models, and addressing concerns regarding data privacy and security, which will impact the effective utilisation of 6G KPIs [304–314].

(a) **Challenging Implementation**: The implementation of MECs in a 6G environment can be complicated, necessitating substantial upgrades and investments in infrastructure. Some networks or organisations may avoid the complexities of deploying and managing edge computing nodes.

(b) **Resource Intensiveness**: Edge computing entails the deployment of computational resources in proximity to the network's edge. Depending on the magnitude and

characteristics of the applications, this can require a significant amount of resources and may only be justifiable in some situations.

(c) **Global Standardisation Challenges**: Attaining worldwide uniformity for MECs can pose difficulties, and complications related to compatibility may emerge. Varied criteria among different regions and vendors may impede the smooth incorporation of MECs within a 6G network.

(d) **Issues regarding security and privacy**: Edge computing gives rise to security and privacy concerns, particularly when handling sensitive data near the data source. Certain organisations may resist adopting MECs due to vulnerabilities in a distributed computing environment.

(e) **Backhaul Limitations**: The efficiency of MECs is frequently contingent on the capacity and dependability of the backhaul network that connects edge nodes to the core network. MECs's advantages may be compromised when the backhaul network is constrained.

(f) **Alternative Architectures**: Certain use cases or industries may adopt alternative architectures that more effectively meet their specific requirements. For instance, a centralised cloud-based approach may be favoured in certain scenarios over a distributed edge computing model.

(g) **Limited Application Relevance**: In specific situations, the advantages of decreased latency and enhanced performance provided by MECs may be insignificant. Applications that do not depend heavily on immediate processing or minimal delay may not experience significant benefits from implementing MECs.

(h) **Cost Considerations**: Implementing and sustaining MECs infrastructure can incur substantial expenses. Organisations can evaluate the advantages and drawbacks and conclude that alternative solutions are more economically efficient.

(i) **Network Congestion**: In networks with a high level of congestion, the benefits of MECs, such as decreased latency and enhanced performance, may be decreased. The efficacy of edge computing solutions can be affected by network congestion.

(j) **Regulatory and Compliance Challenges**: Various geographical areas may impose distinct regulations and compliance obligations concerning the processing and storage of data. Complying with these regulations while implementing MECs worldwide can present difficulties.

(k) **Limited Resources at the Edge**: Edge computing resources, such as processing power and storage capacity, are generally more limited than centralised cloud infrastructure. The restriction could impact the range and intricacy of applications that can be effectively hosted at the edge in 6G.

(l) **Scalability**: Scalability is of utmost importance in 6G as the number of connected devices and the demand for edge services grow. Ensuring that the MECs infrastructure can handle this increased load is imperative. Expanding the capacity of

edge resources to accommodate increasing demand while maintaining optimal performance poses a significant challenge.

(m) **Interoperability**: Ensuring compatibility between different MECs systems and devices from diverse suppliers can be intricate. Seamless interoperability is crucial in the 6G era, as it encompasses a wide range of applications and services, ensuring a unified edge computing ecosystem.

(n) **Latency Variation**: Latency fluctuations may arise in MECs despite its objective of minimising latency through computing proximity to the edge. These fluctuations can be attributed to network conditions and the workload on edge nodes. Meeting stringent latency requirements for specific applications in 6G may be problematic.

(o) **Data transfer overhead**: Depending on the specific demands of the application, it may be necessary to transfer data between the edge and centralised cloud services. Efficiently managing data transfer to minimise latency and optimise resource use is crucial for developing 6G technology.

(p) **Energy Consumption**: Edge devices may possess restricted energy resources, particularly those utilised in mobile settings.

2.5.5 Blockchain

Blockchain is mostly recognised as the technological infrastructure supporting Bitcoin [315]. The fundamental concept behind a blockchain is the distribution of authority and control across multiple nodes, resulting in a decentralised system. Consequently, the database of this system is not centralised but rather spread throughout a network of participants, specifically computers. The decentralised nature of this approach as shown in Figure 2.13 [316] ensures a high level of resilience and security for databases kept on the blockchain, eliminating the risk of a single point of failure. Crucially, the blockchain is accessible to every participant in the network [317]. This is facilitated via a system known as consensus, which consists of rules designed to guarantee unanimous agreement among all participants regarding the state of the blockchain ledger.

A blockchain is a decentralised and transparent digital record shared among all participants, usually in a peer-to-peer network [317–319]. The genesis block is the initial block from which a series of blocks is derived. A new block is added to the chain by generating a hash value based on the information of its parent block. A block generally comprises two components: the block header and transaction data. Specifically, the title mostly includes the following details: the block version, which indicates the validation rule; the hash of the parent block; the timestamp, the number of transactions; and the MerkelRoot, which combines the hash values of all transactions in this block. The blockchain user base expands incrementally as transactions are executed. A miner compiles and organises transactions into a block by resolving a computationally

challenging issue known as proof of work. Once the newly mined block is created, it is disseminated to the whole blockchain network. All nodes in the network participate in the consensus process to verify its authenticity and incorporate the new block into the chain.

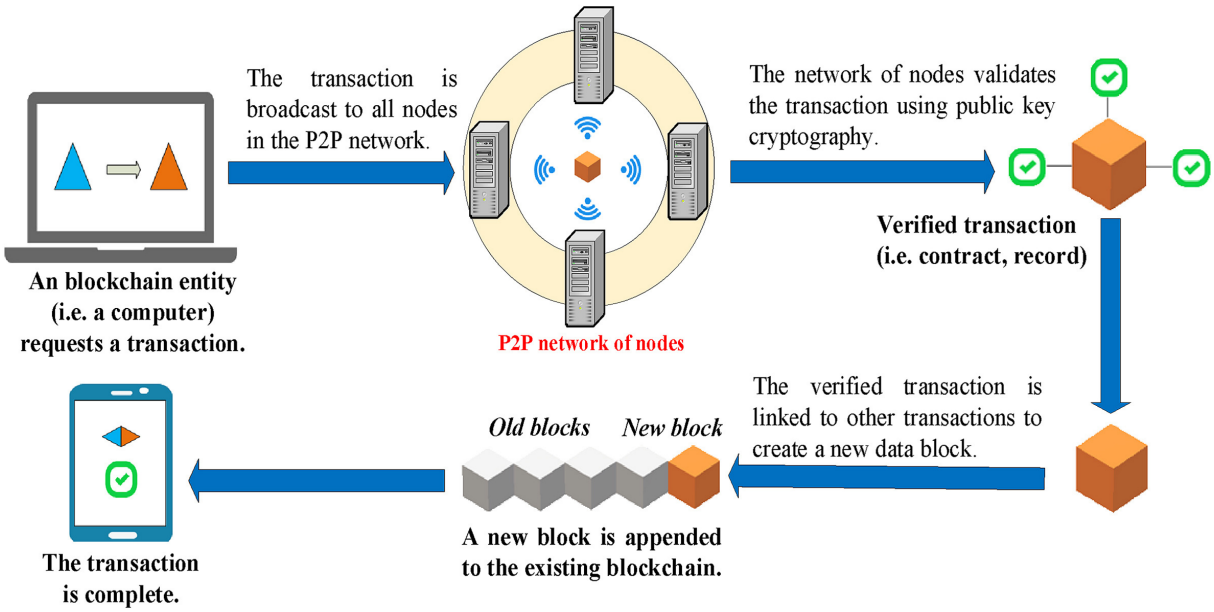

Figure 2.13: The concept of blockchain operation[320]

Why Not Blockchain?

While blockchain technology has various advantages, its limitations and disadvantages in the context of 6G KPIs can be analysed based on the requirements and expectations of 6G networks [311, 321–332]. Here are some considerations regarding blockchain limitations in alignment with 6G KPIs:

(a) **Scalability**: The capacity and throughput of a blockchain network may be affected by scalability difficulties, particularly when the number of transactions grows. This could impede the ability of 6G networks to manage many devices and data transactions effectively.

(b) **Excessive Energy Usage**: The energy-demanding consensus processes employed by certain blockchains, such as Proof of Work, may contradict the energy efficiency objectives of 6G. The increasing importance of energy consumption in developing environmentally friendly and efficient communication networks may give rise to sustainability problems.

(c) **Throughput and Latency**: Blockchain networks may face challenges in meeting the low-latency demands of 6G applications, especially when rapid response times are essential. The consensus methods and block confirmation timings can cause delays. Some blockchain networks may have limitations on their throughput, which refers to the amount of transactions completed within a given time period.

This constraint could hinder the effectiveness of real-time applications and high-frequency transactions.

(d) **Storage and Bandwidth Requirements**: The significant storage and bandwidth requirements of blockchain networks may impede the efficiency of 6G. Managing extensive blockchain data negatively influences network resources and restricts the efficient transmission of data.

(e) **Integration with Legacy Systems**: Integrating blockchain technology with the current 6G network architecture and outdated processes may provide challenges due to its complexity. The compatibility demands of 6G may conflict with the intricacies of incorporating blockchain into long-standing communication.

(f) **Privacy and Security**: Although blockchain technology improves security, the openness of certain blockchains may not meet the privacy needs of 6G networks. Ensuring a harmonious equilibrium between exposure and safeguarding user privacy is paramount, particularly in applications where data confidentiality is essential.

(g) **Smart Contract Vulnerabilities**: Security vulnerabilities in smart contracts can jeopardise the security of 6G networks. Given that 6G encompasses essential apps and services, any weaknesses in smart contracts could be exploited, resulting in a risk to network integrity.

(h) **Development and maintenance expenses**: The expenses related to the creation and upkeep of blockchain networks may hinder the attainment of cost-effectiveness in 6G. The allocation of funds for blockchain infrastructure must be carefully weighed against the cost-effectiveness objectives of 6G networks.

(i) **User Education and Adoption**: The intricate nature of blockchain could potentially hinder user experience and the widespread acceptance of this technology. Streamlining interfaces and improving user education may be necessary to ensure widespread user adoption of blockchain capabilities in 6G applications.

(j) **Regulatory Compliance**: The decentralised nature of blockchain and the difficulties in meeting regulatory compliance may conflict with the legal and regulatory obligations of 6G networks. It is essential to address regulatory obstacles while preserving the decentralised advantages of blockchain technology.

2.6 Revolutionary Technologies to be Conducted by 2030

2.6.1 Quantum Communication

In light of the fast technological progress, there has been a significant surge in the need for highly dependable, fast, energy-efficient, and secure communication. As a result, researchers have shown a strong interest in the developing subject of Quantum

Communication (QC) because of its ability to do complicated computations reliably and efficiently. QCis expected to play a crucial role and have a strong impact in decreasing computing complexities and improving the security of 6G and future communication systems. Researchers are looking into Quantum Key Distribution (QKD) and quantum-safe cryptography algorithms to make communication networks more secure and adaptable to the current network infrastructure [333]. Several research studies addressed different QC objectives like quantum optical communications, quantum optical twin, data quantum communication [334–343].

2.6.2 Digital Twin

Currently, digital technology is primarily utilised to detect common indications and prevent serious diseases by analysing the human body structure within the limits of the existing network capacity. The real time availability and accuracy of the system require enhancement. By harnessing the advancements in 6G technology and integrating several scientific fields, including bioscience, materials science, and bioelectronic medicine, it becomes possible to generate digital replicas of the human body known as digital twins. To create a comprehensive virtual representation of the human world and achieve real-time monitoring of personalised health data, the digital twin replicas of the human body will utilise a multitude of intelligent sensors (more than 100 devices per person). These sensors will accurately and instantaneously reflect the condition of vital organs, the mental system, the respiratory system, the urinary system, the musculoskeletal and emotional state. Moreover, the 6G technology will enable the integration of MRI, CT, colour Doppler ultrasound, blood routines, urine biochemistry, and other specialised images and biochemical examination results. This will allow individuals to receive a precise evaluation of their health status and prompt intervention when necessary. Furthermore, AI can be incorporated into professional medical institutions to offer accurate diagnostics and references for customised surgical treatment [344, 345].

2.6.3 Device to Device Communication

Device to Device (D2D) communication [346] is the direct exchange of information between two or more user devices without relying on an intermediate network infrastructure. This mode of communication facilitates local D2D communication, improving efficiency and enabling diverse applications. Although D2D communication has been present in previous generations of wireless communication, it is anticipated to undergo further development and have a substantial role in 6G technology. D2D communication can offer 6G network infrastructure for various technologies such as NOMA, network slicing, and MECs to achieve this objective. In addition, it is anticipated that fast and low-delay D2D communication will be crucial for 6G networks [136, 277, 347–349].

There are significant challenges in the 5G D2D connection [350–354], that require standardisation to address the restrictions related to the KPIs of the upcoming 6G wireless generation, Table 2.3 illustrates a brief description of the challenges of D2D related to the 5G and their impact over the 6G KPIs.

Table 2.3: D2D challenges and effect of 6G KPIs

KPI restrictions	Challenge	Impact on KPI
Interference and Spectrum Management	large number of devices are communicating in close proximity	spectral efficiency, throughput, and reliability
Security and Confidentiality Issues	difficulties in monitoring and controlling transmission	reliability and credibility
Allocation and management of resources	Optimising resource allocation	network efficiency and dependability
Coordination and synchronisation	high user mobility	latency, diminished reliability, and lower QoS
Energy Consumption	higher energy usage	network's sustainability and efficiency
Integrating with cellular networks	handover mechanisms and coordination	communication disruptions and network reliability

2.6.4 Grant free Transmission

Grant free transmission technology has been identified as a key trend in upcoming mobile networks. Undoubtedly, this technology has been categorised as a crucial medium access control technique for facilitating extensive IoT connectivity across mobile networks; in the context of 5G networks, many grant free transmission strategies have been implemented for mMTC and URLLC services. However, the capacity provided by these techniques still needs to be improved [355, 356]. In light of the continuous expansion in the quantity of smart physical devices and the widespread use of these services, developing more effective grant free transmission solutions for the 6G networks is imperative. The combination of NOMA and grant free transmission, known as GF-NOMA, is a highly promising solution for 6G enabled IoT systems due to NOMA ability to minimise delays [357].

Most typical NOMA solutions employ a centralised scheduling scheme, where IoT devices are already connected and many network parameters, such as spreading sequences and power control, are predetermined. However, the performance of typical NOMA algorithms might be significantly deteriorated due to the special characteristics of mMTC traffic. These characteristics include mass uplink communication, tiny size and periodic data transfer, and diverse QoS requirements. This type of traffic might result in

signalling overhead and increase the delay of the centralised scheduler. To address this difficulty, one possible option is to use grant free transmission. This approach allows devices to communicate their data in an automated way using randomly selected time or frequency resources. This enables low latency access and reduces the signalling overhead associated with scheduling requests.

2.6.5 Sparse Signal Processing

Sparse sampling, sometimes referred to as compressive sensing, is a signal processing approach that makes the best use of signal sparsity to efficiently and accurately reconstruct signals using a reduced number of samples. The applications of this paradigm have been examined in several parts of 5G and beyond 5G networks, such as MIMO random access, embedded security, Cloud Radio Access Network (CRAN), and channel and source network coding based on the compressive paradigm. The utilisation of sparse signal processing algorithms enables the precise and efficient identification of active IoT devices in the grant-free transmission methodology [358–360].

An important obstacle in grant-free transmission, particularly in facilitating extensive IoT connectivity, is identifying the operational IoT devices for data decoding [360]. The utilisation of sparse signal processing is crucial to achieving THz communications in the 6G networks. Compressive sensing techniques can recover sparse channel information in THz channels, which are characterised by low density. The compressive sensing paradigm effectively utilises the sparsity feature to greatly enhance future wireless networks' spectrum and energy efficiency and IoT devices [361].

2.6.6 Holographic MIMO Surfaces

Holographic MIMO surface (HMIMOS) is a crucial technology that enables 6G. mMIMO systems, which consist of BSs equipped with enormous antenna arrays, are employed in 5G networks to meet the high data transfer demands. However, the complete implementation of large MIMO systems is challenging because of factors like energy consumption and the high expenses associated with fabrication and operation. With the impressive progress in programmable metamaterials, RIS have great potential to address the significant challenges of mMIMO systems and achieve the ambitious goal of 6G networks. This is achieved by enabling seamless connectivity and control of the environment in cellular wireless networks through intelligent software. HMIMOS is anticipated to enhance mMIMO technology by changing the wireless network environment into a reconfigurable intelligent entity, resulting in size, cost, weight, and energy usage improvements [362–366]. HMIMOS can fulfil three distinct roles: receiver, transmitter, and reflector, to achieve this objective. The unique attributes of HMIMOS, namely intelligence and reconfigurability, position it as a promising

technology to meet the many demands of 6G, such as low latency, low power, and high-throughput communications. When discussing communications, there are two primary categories of applications for HMIMOS: outdoor and indoor. HMIMOS outdoor applications encompass energy efficient beamforming, establishing connections between users and BS, PHY layer security, and wireless power transfer. On the other hand, indoor applications focus on precise indoor positioning and coverage augmentation within indoor environments.

2.6.7 Three Dimensional Network Architecture

The existing cellular network architectures, both current and past, have been specifically built to provide connectivity between network access points and ground based UEs in a Two Dimensional (2D) manner. On the other hand, it is anticipated that the 6G network will combine terrestrial and non-terrestrial technologies to provide Three Dimensional (3D) network coverage [367, 368]. The 3D strategy is significantly more timely and economically efficient than fixed 2D infrastructures. Telecommunications operators must incur the cost of deploying dense mobile networks to ensure extensive connectivity. This is particularly advantageous when operators aim to rapidly deliver uninterrupted and dependable services in rural areas or during natural disasters. 3D coverage will facilitate the establishment of communication systems for deep sea and high altitude environments. Although the benefits mentioned above are substantial, implementing 3D network architecture will present numerous obstacles before this technology can be effectively utilised in practical cellular networks. These challenges include developing channel models for air-to-ground communications, optimising trajectories, managing resources, and establishing new topologies.

2.6.8 Cell Less Architecture

The cell less communication architecture, sometimes referred to as cell free, has been suggested as a solution to address the decline in performance caused by the handover process in cellular networks [369–372]. In this design, a UE has the ability to establish communication with several BSs or APs using coordinated multipoint transmission and reception protocols rather than being limited to connecting with just one BS. Implementing cell free communications can improve connection and reduce the latency caused by the handover procedure. In the era of 6G, rapidly deploying diverse communication systems and utilising several frequency bands will make cell less communications unavoidable. UEs can seamlessly shift from one network to another without needing a changeover process and will autonomously select the optimal connection among a variety of heterogeneous networks, such as THz, mmWave, and VLC. As a result, the typical handover process concerns, such as data loss and handover

delays/failures, can be relieved and achieve higher QoS. Cellular communications without the need for physical cells will enable mobile devices to move smoothly without any additional burden caused by transferring connections.

2.7 Discussion

In this chapter, the preliminaries of 6G wireless communication along with the important KPIs for the transition from 5G to 6G were discussed. Three types of reviews were presented in the literature background: one for the enabling technologies used in this thesis to achieve the aim and objectives. The second one addresses the other possible techniques along with their limitation regarding the aim and objectives of this work. The last one addresses the revolutionary technologies to be conducted by 2030.

3

Channel Coding

This chapter introduces two new channel coding techniques: serial and parallel concatenation. Section 3.1 comprehensively explains the foundation of concatenated codes. Next, in Section 3.2, the principles of Non Orthogonal Multiple Access (NOMA) are described. The subsequent Section 3.3, presents the serial and parallel concatenated codes with the integration of NOMA. Section 3.4 comprehensively describes the performance indicators that validate the superiority of the novel channel coding techniques. In Section 3.5, the performance evaluation and comparison of the new channel coding for 6G will be discussed in relation to the existing state of the art for 5G.

3.1 Concatenated Channel Coding

In recent years, there has been a notable and substantial expansion in the realm of digital communications, particularly in the realms of cellular, satellite, and computer communication. These domains have experienced significant growth and development. Within the intricate and complex networks of communication that exist within these domains, the information is meticulously and precisely encoded as a series of binary digits, which are the fundamental building blocks of digital communication.

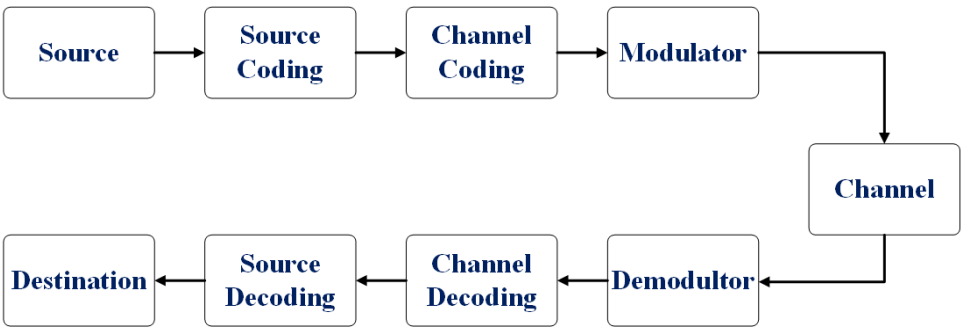

Figure 3.1: Communication System with Coding

The binary digits serve as the foundation upon which the entire communication system is built. They carry and transmit the crucial and vital information across the

various communication channels. As the binary bits are transmitted, they undergo a process of source encoding, channel encoding and modulation, as shown in Figure 3.1, which involves the transformation of these digital signals into analogue signal waveforms. This transformation allows for the effective and efficient transmission of the signals across the communication channel.

However, this transmission process has challenges. The communication channel introduces various forms of noise and interference, which can lead to the corruption and distortion of the transmitted signal. This distortion and corruption can significantly impact the information's accuracy and integrity. At the receiving end of the communication channel, the distorted and corrupted signal is converted back into binary bits through a process known as demodulation. This conversion process aims to recover and reconstruct the original transmitted binary information. However, it is important to note that the binary information received only approximates the original binary data. This approximation is due to the inherent limitations and challenges posed by the transmission process.

The transmission of the binary bits can lead to errors, commonly referred to as bit mistakes. The occurrence and quantity of these bit errors are contingent upon the level of noise and interference present within the communication channel. Channel coding is employed to address and mitigate the impact of noise and interference on the accuracy of the transmitted information, which represents a common technique in digital communication systems. Channel coding serves as a safeguard for digital data, protecting it from the disruptive effects of noise and interference. By strategically adding extra bits to the transmitted information stream, channel coding enhances the resilience and robustness of the communication system. These additional bits are supplementary components that identify and rectify problems within the received data stream. As a result, the transfer of information becomes more dependable and reliable. However, it is important to note that channel coding implementation does come with certain trade-offs. The addition of extra bits to the transmitted information stream leads to a decrease in the overall data rate. This decrease is necessary to ensure the integrity and accuracy of the transmitted information. Additionally, channel coding may also result in an increase in bandwidth requirements. The introduction of extra bits necessitates a greater allocation of resources, such as bandwidth, to accommodate the enhanced communication system. Despite these trade-offs, the implementation of channel coding remains a crucial and effective technique in safeguarding digital information within digital communication systems.

There are two primary classifications of channel codes, specifically block codes and convolutional codes, which exhibit numerous distinctions. Block codes adopt a rigorous approach that relies on finite field arithmetic and abstract algebra. These codes possess the capability to detect or correct errors. Block codes involve the acceptance of a block

comprising k information bits and the generation of a block containing n coded bits. The n coded bits are formed by adding $n - k$ redundant bits r to the original k information bits according to predetermined regulations. These codes are commonly referred to as (n, k) block codes as shown in Figure 3.2. Within this category there is a selection of frequently employed block codes, including Hamming, Golay, BCH, and RS (which utilize nonbinary symbols). The decoding of block codes and the estimation of the k information bits are accomplished through various techniques.

Figure 3.2: Block Coding Structure

On the other hand, convolutional codes are extensively employed as channel codes in practical communication systems. These codes are formulated with a distinct, robust mathematical framework and are primarily utilized for real-time error rectification. Convolutional codes transform the complete data stream into a one stream codeword. The encoded bits are depends not solely upon the present k input bits but also upon preceding input bits as shown in Figure 3.3. The primary decoding approach for convolutional codes is grounded on the widely employed Viterbi algorithm [373].

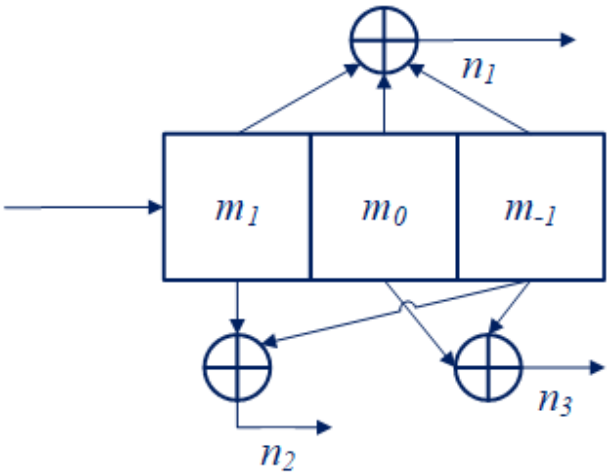

Figure 3.3: Convolutional Coding Structure

Concatenated codes are an effective means of acquiring lengthy and potent codes by utilising uncomplicated constituent codes. The initial category of codes falling under this classification are referred to as product codes. They were initially introduced by Elias in his work [374]. At their most basic level, product codes can be represented as a collection of matrices, where each row within these matrices represents a codeword in

one constituent code, while each column represents a codeword in another constituent code. These codes have played a significant role in establishing numerous theoretical findings within coding theory. The concept of product codes was subsequently expanded upon to form the notion of concatenated codes, as introduced by Forney [375]. Although the minimum distance of product codes is considerably smaller than that of optimal codes of comparable length, the error correction capability of product codes is quite extensive. To demonstrate this aptitude, we examine certain characteristics of product codes. One noteworthy attribute of product codes is their capacity to correct burst errors. All error patterns confined to a number of rows that is less than half the minimum distance of the column code or a number of columns that is less than half the minimum distance of the row code can be rectified.

Concatenated codes can be created by combining two or more codes in a serial or parallel manner. In essence, concatenated codes are highly effective in wireless communication channels due to two primary factors. The initial factor pertains to their possession of comparatively elevated minimum distances, and the other factor is the utilization of interleaving. Interleaving is typically employed to convert burst errors into random ones, allowing for correction via forward error control codes. In contrast, concatenated codes possess the appropriate framework for correcting burst errors without the additional requirement of interleaving.

3.1.1 Serial Concatenated Channel Coding

A serial concatenated error control system, as exemplified in Figure 3.4 consists of two distinct sets of encoders and decoders. A data block of length k is first encoded by an (n_1, k) encoder to produce C_1 codeword as a result of applying the outer code; the resulting vector C_1 is then processed by an interleaver of size C_1. The interleaved data block is then encoded by an (n_2, C_1) encoder, which represents the inner code and produces the final codeword C_2.

Serially concatenated or famously known as turbo codes, represent a powerful class of error-correcting codes that have gained prominence in modern communication systems. Developed in the early 1990s, these codes have mitigated errors during data transmission over unreliable channels. The fundamental concept behind serially concatenated codes involves using two or more constituent codes. In a serial concatenated code, the data stream is first encoded by the first constituent encoder, and the resulting codeword is then interleaved before being fed into the second constituent encoder, creating an iteratively refined and concatenated codeword. This iterative process can be repeated multiple times, enhancing the overall error-correction capabilities of the code.

The interleaving step is crucial in breaking up burst errors, where consecutive bits may be corrupted together due to the nature of the channel. By interleaving the codewords,

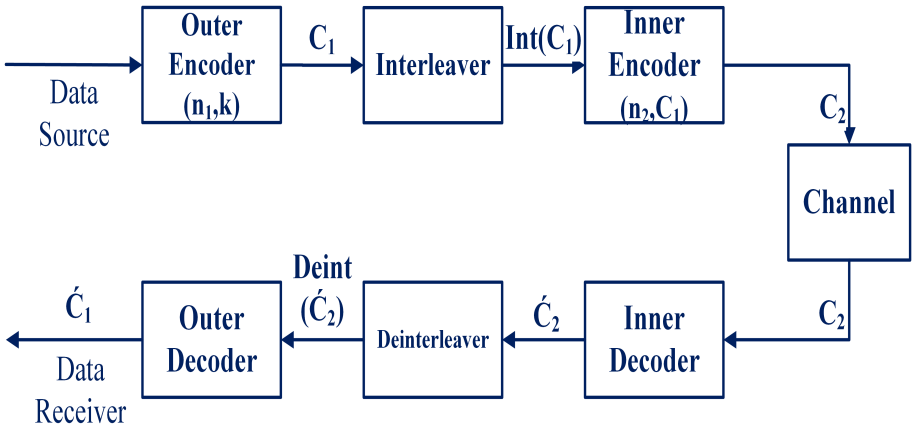

Figure 3.4: Serial Concatenated Code Structure

the errors become distributed across different parts of the codeword, allowing the constituent codes to address and correct them effectively. The iterative decoding process involves exchanging information between the constituent decoders, contributing to the code's remarkable error-correcting performance. Serially concatenated codes are used extensively in various communication systems, including but not limited to satellite communication, wireless communication, and digital storage devices. Their ability to achieve near-Shannon limit performance, which is the maximum theoretical limit for error correction, has made them indispensable in ensuring reliable and robust data transmission in the presence of noisy channels. As technology advances towards 6G, serially concatenated codes play a key tool in pursuing more efficient and resilient communication systems to comply with 6G KPIs.

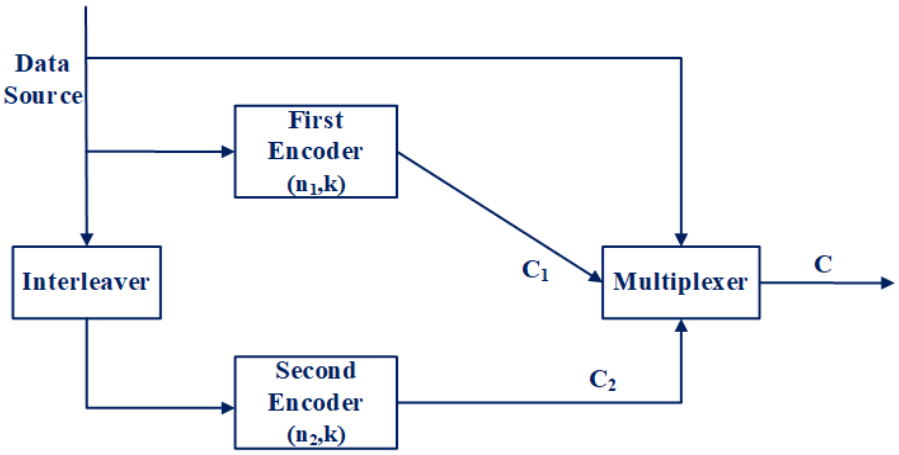

Figure 3.5: Parallel Concatenated Code Structure

3.1.2 Parallel Concatenated Channel Coding

In parallel concatenation as first introduced in [376], the encoders work synergistically in parallel for the same information data set, as illustrated in Figure 3.5. This is in contrast to serial concatenated codes, in which the information bits are fed into the encoders that are employed one after the other. In parallel concatenation, the first encoder is responsible for generating a codeword C_1 from the (n_1, k) first encoder, which is based on an information dataset of size k. In the meantime, the identical information dataset of size k is interleaved and fed into the second encoder (n_2, k) to generate the second codeword C_2. To generate the codeword C, it is necessary to multiplex C_1, C_2, and the initial information dataset; this is considered the final stage in the process of producing the resultant codeword C which will be transmitted across the channel.

3.2 Non-Orthogonal Multiple Access (NOMA)

NOMA has been proposed as a promising option for future wireless networks to enhance network performance by leveraging its potential advantages, such as improved SE, compatibility, fairness, flexibility, and extensive connection. Unlike the traditional OMA scheme, NOMA allows multiple users to be served using the same orthogonal radio resources, such as time and frequency. This is achieved by utilising power domain Superposition Coding (SC) at the transmitter and SIC at the receiver. Specifically, the SC method encodes messages for different users by varying the power levels, a technique known as power domain multiplexing. At the receiver, the SIC approach decodes the signals meant for weaker users before decoding their signals, specifically targeting stronger users. NOMA has been recognised as a feasible technology for enabling the widespread use of IoT devices in future wireless networks, as it provides extensive connectivity. As explicated in Section 2.4.2, numerous researchers have demonstrated the effective utilization of NOMA to meet the data rate requirements of both network and user level regarding 6G technologies.

SC has been recognised as a means to enhance the capacity of broadcast channels and the SE in wireless systems. This enables the transmitter to simultaneously transmit signals from numerous users, in which the SC is employed at the transmitter to effectively combine signals from numerous users. In NOMA system, where two users and one BS is considered, the signal transmitted from the BS to the users is addressed by:

$$x = \sqrt{P_T \alpha_1} s_1 + \sqrt{P_T \alpha_2} s_2 \tag{3.1}$$

where α_1, α_2 are user specific power factor and must satisfy the condition $\alpha_1 + \alpha_2 = 1$, P_T is the total transmit power, and s_1, s_2 denotes the intended users signal.

During the decoding process at the receiver, users near the BS can extract their signal

from other users because of the more favourable channel conditions [377], whilst users farther away from the BS can only extract their signals due to less favourable channel conditions. The fundamental concept of the SIC technique employed at the receiver is to decode distinct user signals sequentially and progressively reduce inter user interference. The incoming signal is first demodulated and decoded to identify the signals intended for individual users. Upon decoding a user signal, the related interference is subtracted from the other received signals. The second multiplexed signal can be demodulated and decoded without interference from the first detected signal. Thus, the received signal for the system is as in Equation 3.2

$$y = h\left(\sqrt{P_T\alpha_1}s_1 + \sqrt{P_T\alpha_2}s_2\right) + noise \tag{3.2}$$

consequently, the received signal at each user can be expressed as follows:

$$\hat{y_1} = h_1\sqrt{P_T\alpha_1}s_1 + noise \tag{3.3}$$

$$\hat{y_2} = h_2\sqrt{P_T\alpha_2}s_2 + h_2\sqrt{P_T\alpha_1}s_1 + noise \tag{3.4}$$

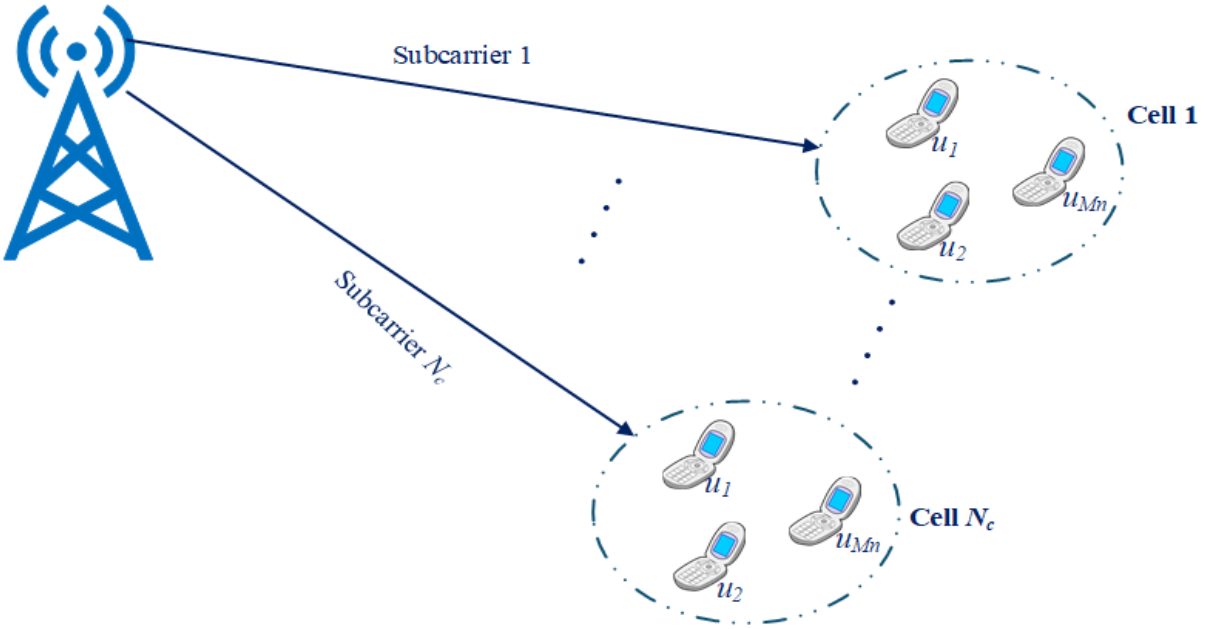

Figure 3.6: Downlink NOMA System

In this thesis, we consider the use of PD-NOMA with the novel concatenated channel coding described in Section 3.3, the layout for the downlink transmission system is shown in Figure 3.6. In our demonstration, we assume that there is one BS and M users randomly distributed in each N_c cell. BS and users are equipped with a single antenna. The total system bandwidth BW_T is equally distributed for the N_c cells as subchannels each has a bandwidth of $BW = BW_T/N_c$. Let's consider the number of users on a

subchannel to be equal to $M_n(n = 1, 2, \ldots, N_c)$,$M = \sum_{n=1}^{N_c} M_n$, the power of the m_{th} user in the n_{th} subchannel is $p_{n,m}(m = 1, 2, \ldots, M_n)$. The BS sends a superposition coded signal on the n_{th} subchannel generlised form of Equation 3.1 as in Equation 3.5, where $x_{n,m}$ is the transmitted signal of the m_{th} user in the n_{th} subchannel.

$$x_n = \sum_{m=1}^{M_n} \sqrt{p_{n,m}} \cdot x_{n,m} \tag{3.5}$$

The received signal at the m_{th} user is affected by the channel coefficient $h_{n,m}$ which represents the link from the BS to the m_{th} user as follows:

$$y_{n,m} = h_{n,m} \cdot x_n + w_{n,m} = h_{n,m} \sum_{i=1}^{M_n} \sqrt{p_{n,i}} \cdot x_{n,i} + w_{n,m} \tag{3.6}$$

where, $w_{n,m}$ denotes the Additive White Gaussian Noise (AWGN) with zero mean and σ_n^2 variance, (i.e. $w_{n,m} \sim CN_c\left(0, \sigma_n^2\right)$). Equation 3.6 can be generalised as in Equation 3.7, where the received signal includes the original user signal and the other user signals which are treated as the interference signals (i.e. $h_{n,m} \sum_{i=1}^{M_n} \sqrt{p_{n,i}} \cdot x_{n,i}$ is the inter user interference signal on the subchannel n).

$$y_{n,m} = h_{n,m}\sqrt{p_{n,m}} \cdot x_{n,m} + h_{n,m} \sum_{i=1, i\neq m}^{M_n} \sqrt{p_{n,i}} \cdot x_{n,i} + w_{n,m} \tag{3.7}$$

In PD-NOMA, users are allocated varying power levels according to their channel conditions. Generally, users experiencing superior channel conditions are assigned less power, whilst those with inferior conditions are assigned increased power, $p_1 < p_2 < \cdots < p_{m_n}$, therefore the m_{th} user can successfully extract their signal and remove the inter-user interference from the other users. The base station emits a composite signal encompassing all users' data. Based on that and using SIC, each user decodes signals in a specific order based on power levels. A strong user first decodes the weaker user's signal (which has higher power) by treating its own signal as noise. Once decoded, the strong user reconstructs and subtracts the weaker user's signal from the received signal. After cancellation, the remaining signal primarily contains the intended lower-power signal, which the strong user can decode easily. A weak user only decodes its own signal directly because the strong user's signal is much weaker (due to lower power allocation). The interference from the strong user's signal is typically minimal and can often be treated as noise, making direct decoding feasible.

It is important to note that SIC operation does not need prior knowledge of other users' exact signals; it only requires knowledge of their power allocation and channel conditions. It relies on the fact that high-power signals are easier to decode, allowing them to be subtracted from the total received signal. As long as the receiver knows

the power levels and modulation schemes assigned to different users, it can iteratively cancel out signals without explicit knowledge of the data content of other users. SIC in PD-NOMA depends on the power difference among users and the ability to iteratively subtract already-decoded signals.

The receiver now processed SIC operation were the rate of the m_{th} user expressed as in Equation 3.8, and the sum rate is expressed as in Equation 3.9, which follows Shannon theorem:

$$R_{n,m} = B \log_2 \left(1 + \frac{|h_{n,m}|^2 p_{n,m}}{|h_{n,m}|^2 \sum_{i=1}^{m-1} p_{n,i} + \sigma_n^2} \right) \tag{3.8}$$

$$R_n = \sum_{m=1}^{M_n} R_{n,m} \tag{3.9}$$

To enhance the precision of the SIC at the receiver and minimise the delay in separating signals, we grouped the users in the cells based on their channel gain. The channel gains of all users are arranged in increasing order based on the user's instantaneous CSI collected by the BS. As M is an even number of users, the process of user grouping includes segregating the users with the greatest disparity in channel gain in one cell. Specifically, the user with the highest channel gain is paired with the user with the lowest gain. In contrast, the user with the second highest channel gain is grouped with the user having the second lowest channel gain, and so forth. In case of an odd number of users, the middle user will be grouped with the user of the highest channel gain since it will have the largest difference in the cell.

3.3 Polar Convolutional Serial Code and Polar Convolutional Parallel Code (PCSC and PCPC)

Two concatenated formulas for channel coding are proposed and compared, and the coding formula is tested with PD-NOMA system transmission in this thesis as a first contribution. As shown in Figure 3.7, a serial concatenation formula for channel coding is proposed using polar code as the outer code and convolutional code as the inner code, in which the code is named as Polar Convolutional Serial Code (PCSC).

The second channel coding formulation proposed is the parallel concatenation of polar code and convolutional code named Polar Convolutional Parallel Code (PCPC). The information data bits are coded first by polar code as the first encoder, and an interleaved version of the data is encoded by convolutional code as the second encoder. The last step to produce the output data stream is to multiplex the output of two encoders and the original data stream as shown in Figure 3.8.

The subsequent sections describe the polar encoder, convolutional encoder, polar decoder, and convolutional decoder, in which they are used directly for PCSC. On the other hand, in PCPC, we deployed the encoders as stated afterwards; meanwhile, the decoding process uses an iterative algorithm that consists of multiple steps ahead of obtaining the decoded data information bits.

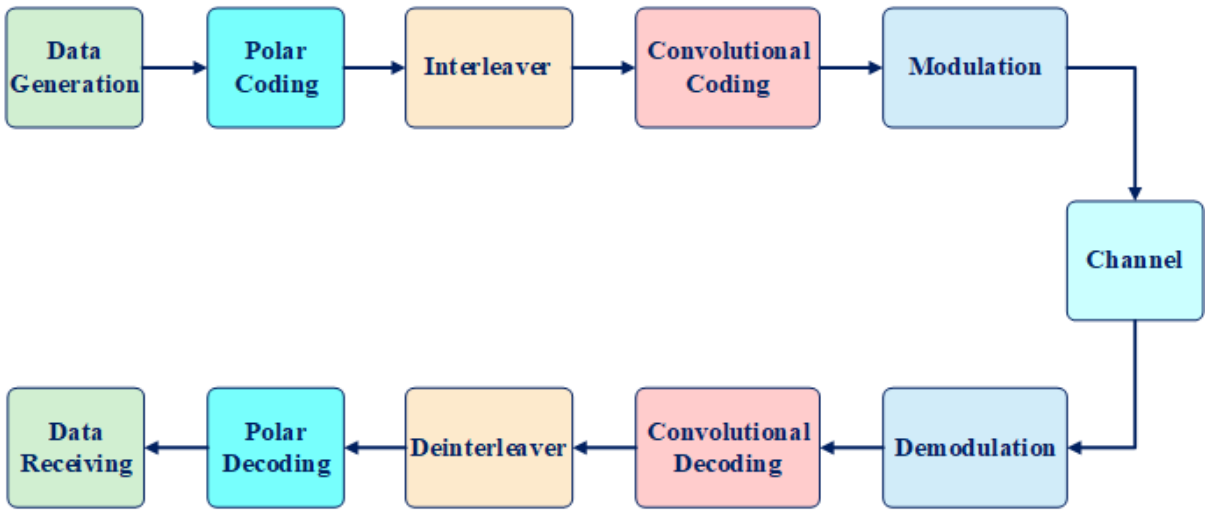

Figure 3.7: PCSC Block Diagram

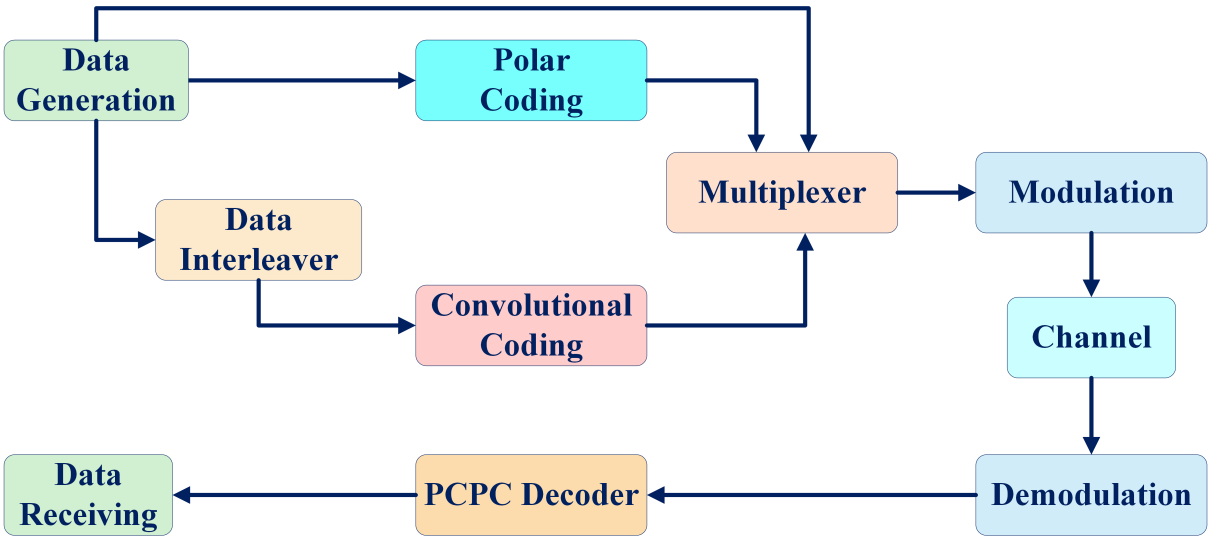

Figure 3.8: PCPC Block Diagram

3.3.1 Polar Encoder

As depicted in Figure 3.7, we used polar code as the outer code and convolutional code as the inner code. Polar codes, which were first introduced by Arikan [183], a type of capacity-achieving linear block code, are built around the channel polarisation. The

polarisation effect describes the phenomena in which certain equivalent bit channels become almost noiseless while others become worthless as the code length approaches infinity. An (N, K) polar code is a block code that takes K information input data bits and produces N output bits.

For polar codes with a length of $N = 2^n$ (i.e. n is a positive number), polar encoded data information can be obtained by having N polarised channels $\{W_N^1, W_N^2, \ldots, W_N^N\}$, when the number of N tends towards infinity; some polarised channel capacities tend to value one to form the reliable channel. These channels typically convey information with an extremely low likelihood of mistake, closely resembling a perfect channel with the capacity value of one.

In contrast, another percentage of channels become practically ineffective for dependable information transfer. The capacity of these channels approaches zero as N approaches infinity, usually known as the frozen bits. From a practical standpoint, these channels have a high susceptibility to errors, rendering them unsuitable for dependable data transfer.

The polar code word construction used is obtained from Equation 3.10, where the used encoding structure for $N = 16$ is shown in Figure 3.9. G is the generator matrix and u is the information data bits $\{u_1, u_2, \ldots, u_i\}$, N is the code word length, the code word X is $\{X_1, X_2, \ldots, X_i\}$, this code has frozen bit of value $N - K$.

$$X = u \times G \tag{3.10}$$

The generator matrix G is designed as in Equation 3.11, where R_N is an $N \times N$ bit reversal permutation matrix and $\otimes$ is the Kronecker product [378], and $G_2 = \begin{bmatrix} 1 & 0 \\ 1 & 1 \end{bmatrix}$.

$$G_N = R_N \times G_2^{\otimes n} \tag{3.11}$$

There are two stages in obtaining the received data: channel combining and splitting. First, in the channel combining process, two copies of the channel W are combined to generate a channel W_2 as follows:

$$W_2(y_1^2|u_1^2) = W(y_1|u_1 + u_2)W(y_2|u_2) \tag{3.12}$$

Then, the combined channel is split into two different channels, which follow the transform as in Equation 3.13 and Equation 3.14, in which $(W, W) \mapsto (W_2^1, W_2^2)$ and $W_2^1 : \{0,1\} \mapsto y^2$, $W_2^2 : \{0,1\} \mapsto \{0,1\} \times y^2$:

$$W_2^1(y_1^2|u_1) = \sum_{u_2} \frac{1}{2} W_2(y_1^2|u_1^2) = \sum_{u_2} \frac{1}{2} W(y_1|u_1 \oplus u_2)W(y_2|u_2) \tag{3.13}$$

$$W_2^2(y_1^2, u_1|u_2) = \frac{1}{2} W_2(y_1^2|u_1^2) = \frac{1}{2} W(y_1|u_1 \oplus u_2)W(y_2|u_2) \tag{3.14}$$

Having that, the combined channel is represented by:

$$W_N(y_1^N, u_1^N) = W_N(y_1^N, u_1^N G_N) \tag{3.15}$$

Now after having the vector channel W^N, the next step is to split W_N back to a set of N binary input as in Equation 3.16, where (y_1^N, u_1^{i-1}) represents the output of W_N^i and u_i is it is input:

$$W_N^i(y_1^N, u_1^{i-1}|u_i) \triangleq \sum_{u_{i+1}^N \in X^{N-i}} \frac{1}{2^{N-1}} W_N(y_1^N|u_1^N) \tag{3.16}$$

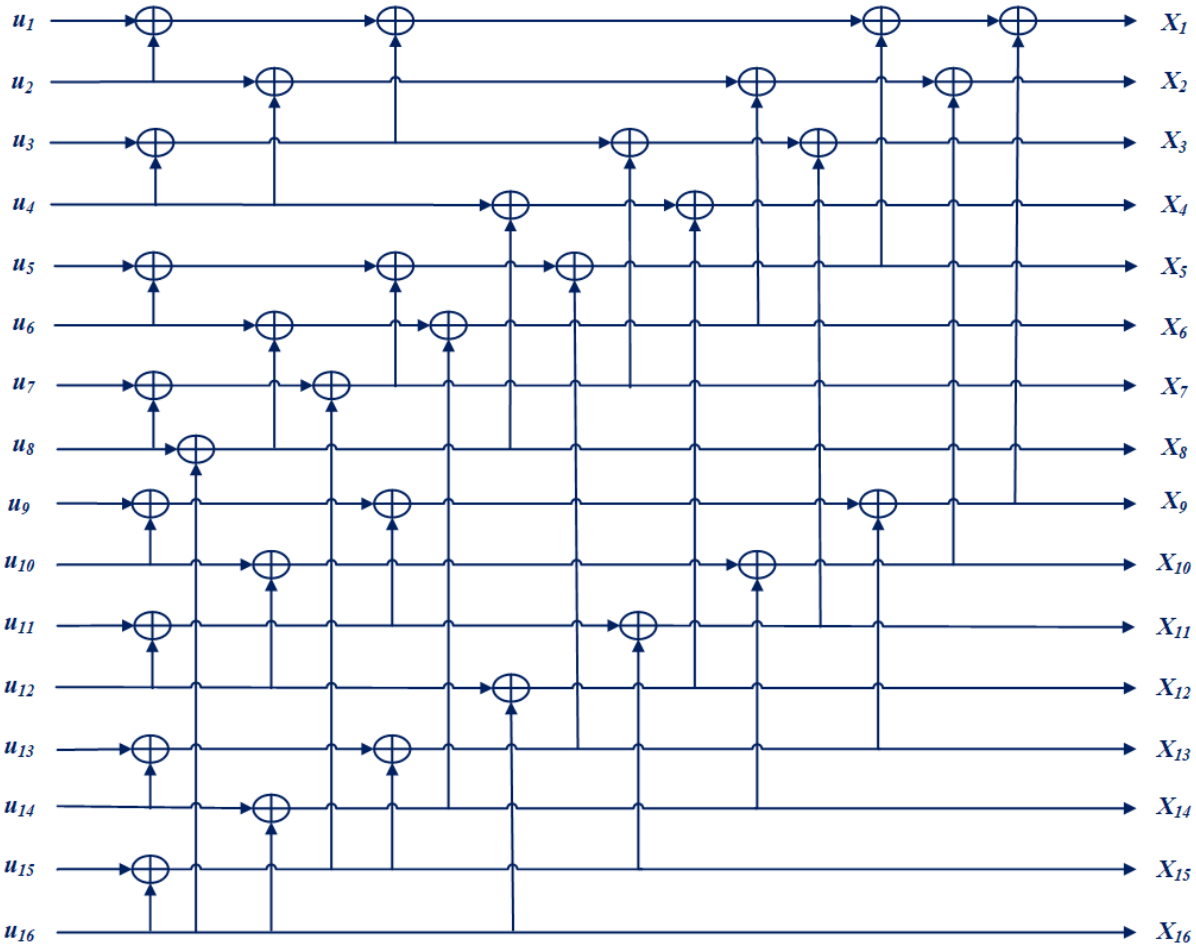

Figure 3.9: Encoding Structure of N=16 Polar Code

3.3.2 Convolutional Encoder

Back in 1955, Elias introduced a new channel coding scheme [379]; the new coding scheme depends not only on the present state of the data information sequence to be encoded but also on previous states of the data information sequence. This means

that convolutional code contains memory elements known as shift registers, and the encoded data information sequence depends on the current input block and previous input blocks.

In our approach, we used a systematic convolutional code. Three parameters are used to define convolutional codes, which are (N, K, D) where N is the output bits, K is the information input data bits, and D is the number of memory stages in the encoder also known as constraint length. Generally, in convolutional codes, it is preferred to select small integers for N and K, while D is preferred to be large to gain lower error probability. As depicted in Figure 3.10, the convolutional encoder has N value of three and K value of one with three shift register D with modulo-2 adders represented by exclusive OR gates for output calculations.

In the field of coding theory, a systematic code refers to an error-correcting code where the input data is directly included in the encoded output. In contrast, a non-systematic code does not include the input symbols in the output.

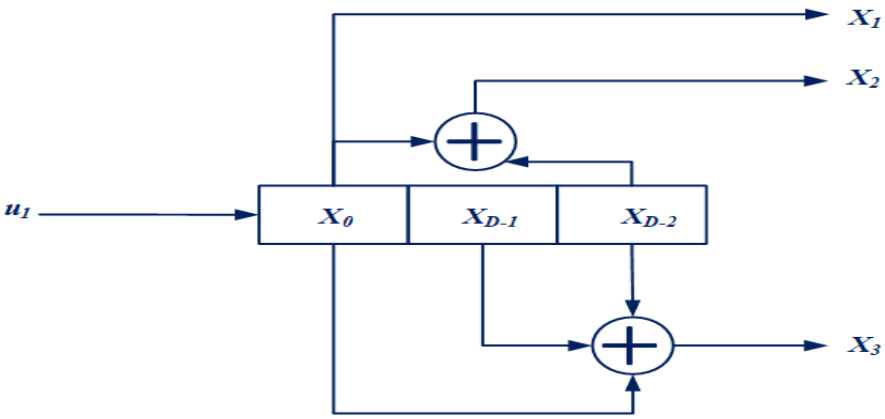

Figure 3.10: Convolutional Code Block Diagram

The code word is obtained by applying the information sequence $u_i = u_1 u_2 \dots u_k$ into several finite shift registers equals D. The codeword vector for each shift register is calculated using Equation 3.17, Equation 3.18, and Equation 3.19 respectively. The final codeword vector is obtained using Equation 3.20.

$$X_1 = X_1^{(1)} X_1^{(2)} \dots X_1^{(K)} \tag{3.17}$$

$$X_2 = X_2^{(1)} X_2^{(2)} \dots X_2^{(K)} \tag{3.18}$$

$$X_3 = X_3^{(1)} X_3^{(2)} \dots X_3^{(K)} \tag{3.19}$$

$$X_N = X_1^{(1)} X_2^{(1)} X_3^{(1)} X_1^{(2)} X_2^{(2)} X_3^{(2)} \dots X_1^{(K)} X_2^{(K)} X_3^{(K)} \tag{3.20}$$

3.3.3 Polar Decoder

The decoding of polar code in PCSC is processed in a recursive manner; this is based on Successive Cancellation Decoding (SCD) [380]. The used algorithm, namely Successive Cancellation List Decoding (SCLD), as we deploy a list of parallel successive decoders. The SCLD is done by aligning two consecutive SCD of $N = 8$. The decoding butterfly diagram is shown in Figure 3.11, the Likelihood Ratios (LRs) is calculated from right side to left side. The decoded data stream is performed by calculating the LRs at each node in the graph. The decoder block diagram for $N = 16$ is shown in Figure 3.12, where we used two decoders in parallel. The calculation of likelihoods is done in a reverse direction of the encoding, in which it is done from right to left; at first the LRs is calculated as follows:

$$L_N^{(i)}(y_1^N, u_1^{i-1}) = \frac{W_N^{(i)}(y_1^N, u_1^{i-1}|u_i = 0)}{W_N^{(i)}(y_1^N, u_1^{i-1}|u_i = 1)} \tag{3.21}$$

At this stage, the decoder has the knowledge of the output from the previous stage u_1^{i-1} in order to decode u_i; additionally, the decoder in advance knows the values of frozen bits $\{u_f, f \in A^c\}$ in which A^c is the frozen bit set. In the decoding process we consider four parameters (N, K, A, u_{A^c}), in which N is the code word length, K is the number of information bits, A is the information set, and u_{A^c} is the frozen bits vector stream. The decoder needs to retrieve the information recursively and generate an estimate of $\hat{u}_1^N$ to obtain u_1^N from Equation 3.21 as the LRs.

At first, the frozen bits are set to 0 then the SCLD is performed by the following steps:

- If $i \in A^c, \hat{u}_i = u_i$
- If $i \in A$, calculate the LRs from Equation 3.22 and Equation 3.23
- make the decision as in Equation 3.24

$$L_N^{(2i-1)}\left(y_1^N, \hat{u}_1^{2i-2}\right) = \frac{L_{N/2}^{(i)}\left(y_1^{N/2}, \hat{u}_{1,0}^{2i-2} \oplus \hat{u}_{1,e}^{2i-2}\right) L_{N/2}^{(i)}\left(y_{N/2+1}^N, \hat{u}_{1,e}^{2i-2}\right) + 1}{L_{N/2}^{(i)}\left(y_1^{N/2}, \hat{u}_{1,0}^{2i-2} \oplus \hat{u}_{1,e}^{2i-2}\right) L_{N/2}^{(i)}\left(y_{N/2+1}^N, \hat{u}_{1,e}^{2i-2}\right)} \tag{3.22}$$

$$L_N^{(2i)}\left(y_1^N, \hat{u}_1^{2i-1}\right) = \left[L_{N/2}^{(i)}\left(y_1^{N/2}, \hat{u}_{1,0}^{2i-2} \oplus \hat{u}_{1,e}^{2i-2}\right)\right]^{1-2\hat{u}_{2i-1}} L_{N/2}^{(i)}\left(y_{N/2+1}^N, \hat{u}_{1,e}^{2i-2}\right) \tag{3.23}$$

$$\hat{u}_i = \begin{cases} 0, \text{if } \mathrm{L_N^{(i)}(y_1^N, u_1^{i-1}) \geq 1} \\ 1, \text{otherwise} \end{cases} \tag{3.24}$$

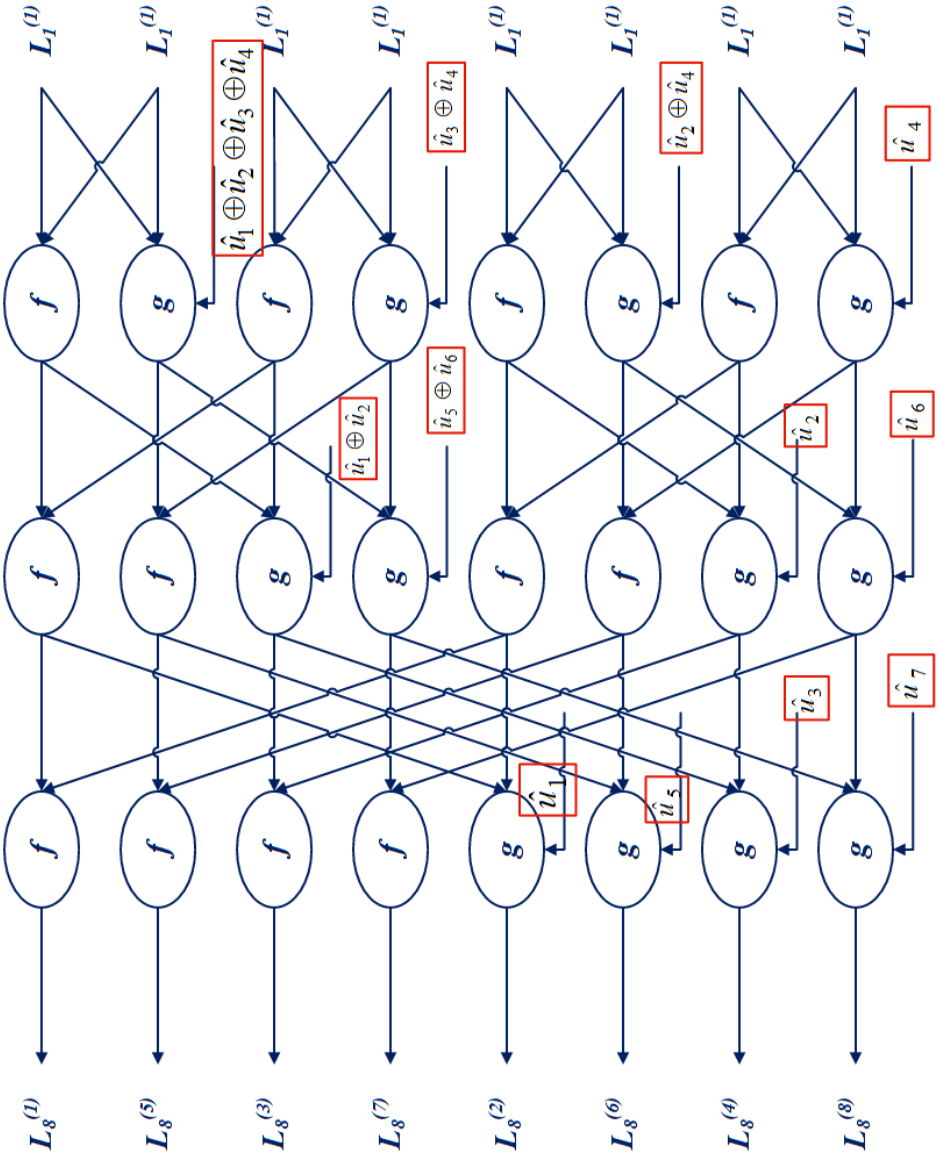

Figure 3.11: Polar Code Decoder for $N = 8$

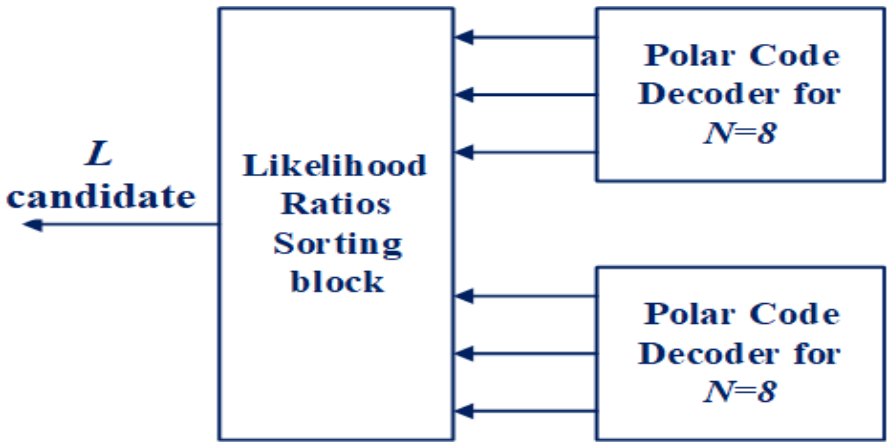

Figure 3.12: Polar Code Decoder for $N = 16$

As mentioned earlier, the value of LRs is calculated recursively and traced back until the code length equals one (i.e. $N = 1$), in which the last LRs value to be calculated is $L_1^{(1)}(y_i) = W(y_i|0)/W(y_i|1) \cdot L_1^{(1)}(y_i)$.

We stated that the LRs values is conducted from right to left in Figure 3.11, where the values of f and g is calculated as in Equation 3.25 and Equation 3.26. The o value represents $L_{N/2}^{(i)}\left(y_1^{N/2}, \hat{u}_{1,0}^{2i-2} \oplus \hat{u}_{1,e}^{2i-2}\right)$, and p value represents $L_{N/2}^{(i)}\left(y_{N/2+1}^{N}, \hat{u}_{1,e}^{2i-2}\right)$

$$f(o, p) = \frac{1 + op}{o + p} \tag{3.25}$$

$$g(o, p, \hat{u}_{sum}) = o^{1-2\hat{u}_{sum}} p \tag{3.26}$$

3.3.4 Convolutional Decoder

The convolutional code is decoded using the Viterbi algorithm [381], a maximum likelihood decoding method. This process utilises a trellis diagram to select the shortest path and recover the original information. The Viterbi method is a decoding technique used for convolutional codes. It aims to discover the path with the highest likelihood by comparing the metrics of all possible paths in a trellis. This comparison is made iteratively, using the path metric entering each state and the received vector y.

In order to conduct the decoded data information stream, the decoding starts by finding the lowest Path Metric (PM) from the trellis representation as in Figure 3.13 by comparing all paths branch metrics at each node in the trellis; the search procedure is done level by level. The PM at every level is calculated and compared with other trellises PMs; the decoder remembers the path with the least metrics value and eliminates all other paths. The remembered paths are called the survivor paths, whereas reaching the end of the transmission sequence, there is only one survivor path, which represents the maximum likelihood path for the codeword.

The trellis figure depicts states using nodes and illustrates transitions between states using arrows. Each arrow contains the annotation of the input bit that triggers the transition and the output bits. Each iteration of the stages displays all potential transitions during a specific processing period, originating from all states at the beginning of that period (arranged in a column on the left side of the stage).

The diagram shows the sequence of states that follows from a sequence of input bits as a path through the trellis. This idea is exploited in the design of the decoder since this operation can be thought of as estimating the path through the trellis given a sequence of received bits. Once the path is known (or estimated), the original sequence of encoded bits is the one that created the path. This decoding idea was formalised in the form of Maximum Likelihood (ML) decoding and efficiently implemented using Viterbi algorithm. The retrieved data bits are obtained by the following steps:

1. **Initialisation:** Initialise each state's PM and surviving path history. Set the PM value to zero for the first state. Construct the trellis diagram in Figure 3.13 to represent the convolutional code.
2. **Transition Metrics:** Compute the transition metrics by analysing the given sequence and comparing it to the predicted transmitted bits.
3. **Survivor Paths:** During the forward pass in survivor paths, the PM is updated, and the survivor paths are chosen based on the transition metrics at each time step. Revise each state's PM by considering the incoming branch metric and the accumulated PM of the previous state.
4. **During the backward pass (decoding):** one should initiate the final time step and retrace the steps through the trellis by following the surviving paths. Select the path with the lowest PM as the decoded path. Retrieve the deciphered binary digits from the trellis diagram.

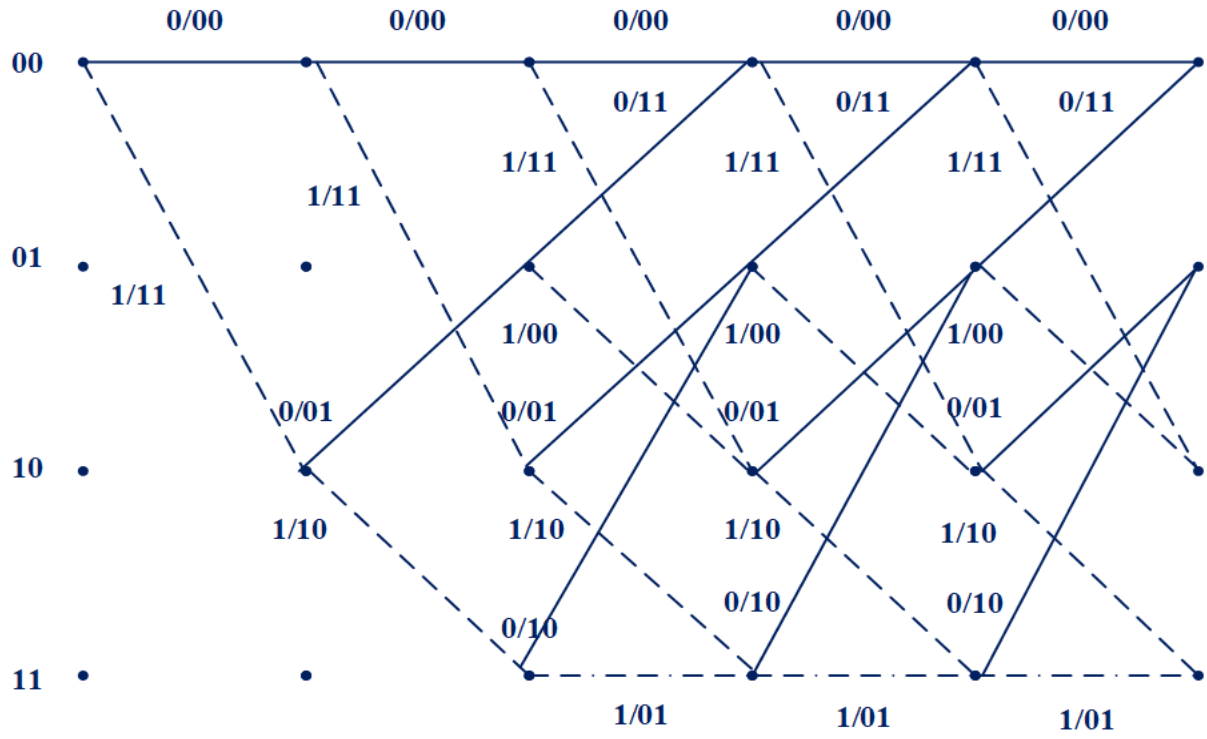

Figure 3.13: Trellis Diagram for Convolutional Decoder

3.3.5 Parallel Concatenation Decoding

The decoding process for PCPC is slightly more complicated than the decoding process of PCSC structure. In order for the received data to be correctly decoded, a more powerful decoding algorithm is suggested based on the Soft Input Soft Output (SISO) segment principle. The decoding is being processed serially, as described in Algorithm 1.

Algorithm 1 Decoding for Parallel Concatenation

$reciveddata \rightarrow rd, data_1 + parity_1 \rightarrow dp_1, parity_2 \rightarrow dp_2, maxiteration \rightarrow I_{Max}$
for i=1:L **do** ▷ L=length of received data bits
  $dp_i = rd_i : rd_{i+1}, dp_{2_i} = rd_{i+2} : rd_{i+3}$
end for
for iteration=1:I_{Max} **do**
  for k=1:K **do** ▷ K=length of information data bits
    for $j = 1 : length(dp_1)$ **do**
      $b_j(x_j) = \sum m_j(x_j)$ ▷ compute a belief
      if $b_j(x_j) = min(b_j(x_j), b_{j+1}(x_{j+1}))ori = Max$ **then**
        $m_j(x_j) = b_j(x_j), databits(n) = m(n)$
      else
        recompute the belief
      end if
    end for
  end for
  $Interleaver(databits(n))$ ▷ Start Interleaver
  $SetM = 4, N = 4, blocksize = 16$
  for $t = 1 : length(databits)$ **do**
    for $i = 1 : blocksize$ **do**
      $databits = reshape(transpose(databits), M, N)$
      $databits = reshape(databits, 1, blocksize)$
    end for
  end for ▷ End Interleaver
  $DB(n) = databits$
  $Multiplexer(DB, dp_2)$ ▷ Start Multiplexer
  $db(1 : 2 : end) = DB, db(2 : 2 : end) = dp_2$ ▷ End Multiplexer
  $Viterbi(db, length(db)$ ▷ Start Viterbi
  $correctpathlength \leftarrow cp_L, startingstate \leftarrow c_m = 0$
  for $j = 1 : length(db)$ **do**
    for $m = 1 : 6$ **do**
      $Findcp_{L_{c_{m+1}}} = min(cp_{L_{c_m}}, cp_{L_{c_{m+1}}})$
      $P_{c_{m+1}} = cp_{L_{c_{m+1}}}$
    end for
  end for ▷ End Viterbi
  $De - Interleaver(db)$ ▷ Start De-Interleaver
  for $t = 1 : length(db)$ **do**
    for $i = 1 : blocksize$ **do**
      $db = reshape(transpose(db), M, N)$
      $db = reshape(db, 1, blocksize)$
    end for
  end for ▷ End De-Interleaver
  if $iteration = Max$ **then**
    $DecodedData = db$
  end if
end for

The first decoder depends on the BP algorithm [382], the factor graph representation of polar codes in Figure 3.11 is used when decoding PCPC. In the decoding process, each node of the factor graph has two probabilities and receives computational results from the left- and right-side nodes to detect their node values.

The BP decoding includes passing the Log Likelihood Ratio (LLR) through the factor graph from right to left and from left to right. Each node in the graph is associated with two values of LLR, one is from left-to-right ($R_{i,j}$) and the other from right-to-left ($L_{i,j}$) in which (i) represents the rows at each stage (j) on the factor graph. The decoding process involves calculating ($R_{i,j}$) and ($L_{i,j}$) as follows:

$$R_{i,j+1} = f(R_{i,j}, R_{i+2^j,j} + L_{i+2^j,j+1}), \tag{3.27}$$

$$R_{i+2^j,j+1} = f(R_{i,j}, L_{i,j+1}) + R_{i+2^j,j}, \tag{3.28}$$

$$L_{i,j} = f(L_{i,j+1}, L_{i+2^j,j+1} + R_{i+2^j,j}), \tag{3.29}$$

$$L_{i+2^j,j} = f(R_{i,j}, L_{i,j+1}) + L_{i+2^j,j+1}, \tag{3.30}$$

f in Equation 3.27,3.28,3.29, and 3.30 is obtained as an approximate as

$$(f(x,y) \approx \tilde{f}(x,y) = \text{sgn(x)sgn(y)min(|x|, |y|)})$$

where (sgn) function returns the sign of the input value; in case the input is a positive number, the function returns (1); if the input value is negative, the function returns (-1); lastly, if the input value is zero the sign function returns (0). Also, the function returns the minimum value between (x,y).

BP algorithm performs the iterative update from right to left and left to right probabilities for maximum iteration of $I_{Max} = 25$, to determine the LLR as in Equation 3.31 and make the output decision using Equation 3.32

$$LLR_N^{(I_{Max})}(u) = \ln\left(\frac{P_{L\to R}^u(1)}{P_{L\to R}^u(0)}\right) + \ln\left(\frac{P_{R\to L}^u(1)}{P_{R\to L}^u(0)}\right) \tag{3.31}$$

$$\hat{u}_{I_{Max}} = \begin{cases} 1, \text{if } \text{LLR}_{\text{N}}^{(\text{I}_{\text{Max}})}(\text{u}_{\text{IMax}}) > 0 \\ 0, \text{otherwise} \end{cases} \tag{3.32}$$

The output decision from BP decoder is the input for the interleaver; the interleaved information data bits are multiplexed with the second encoder parity bits denoted as dp_2. The multiplexed information data bits are next to be decoded using the Viterbi decoder in Section 3.3.4. The resultant information data bits are deinterleaved first before obtaining the received information data bits if the maximum iterative range is met.

3.4 Performance Indicators

As mentioned in Section 2.3, the new wireless generation, 6G, is expected to overcome the limitations of the current generations. In order to comply with 6G and in the channel coding context, performance indicators are measures that are utilised to evaluate the coding scheme's efficiency in enhancing the reliability, data rate, and coverage of communication across a channel.

3.4.1 Bit Error Rate (BER)

Bit Error Rate (BER) is the rate at which errors occur in a data stream due to noise, interference, distortion, or synchronisation problems in a communication channel. It is an essential measure utilised to assess the precision of data transmission. Precision and dependability are crucial in digital communication and data transmission. Ensuring data integrity is essential for tasks such as downloading files, streaming films, and exchanging information over the internet. BER quantifies the ratio of incorrect bits received to the total bits supplied in a data transmission system. It measures the precision of data transport and offers information on the effectiveness of a communication channel or digital link. The sender transmits a predetermined pattern or sequence of bits to the receiver to ascertain the BER. The recipient then contrasts the received bits with the initial broadcast pattern and detects any inconsistencies. BER is calculated as the ratio of the number of bit errors to the total number of transferred bits over a specified time period. BER is commonly quantified as a ratio or percentage that indicates the likelihood of bit errors happening while data is being transmitted.

Understanding BER values relies on the particular application and the expected performance level. Lower BER numbers often signify superior transmission accuracy and greater data integrity. A BER of 10^{-6} indicates that a one-bit mistake happens statistically for every one million bits sent. A BER of 10^{-9} indicates a one-bit error in every billion transmitted bits, representing a highly dependable system. Precision in data transfer is essential in fields including telecommunications, networking, wireless communication, and digital storage. BER is a key measure used to assess the quality and efficiency of communication systems. Engineers and researchers can evaluate the efficiency of error correction systems, modulation schemes, channel coding, and system architecture by analysing the BER. Reducing the BER typically involves higher complexity, greater bandwidth usage, or increased power consumption. Engineers and designers must find an equilibrium among BER, system specifications, and available resources.

Various applications have distinct BER objectives that must be achieved to guarantee dependable data transfer. High-speed optical fibre networks require very low BER

values, usually between (10^{-9} to 10^{-12}). Still, wireless communication systems can handle slightly larger error rates of (10^{-3} to 10^{-6}) due to signal propagation difficulties. Advanced wireless communication systems like cellular networks or Wi-Fi attain BER levels ranging from (10^{-6} to 10^{-9}). These statistics demonstrate a greatly decreased error rate and guarantee more dependable data delivery. As mentioned in Section 2.3.7 6G is anticipated to outperform 5G reliability. Polar code, which is used in 5G have the range of reliability between (10^{-4} and 10^{-6}) in the ideal transmission conditions.

In a noisy channel, the uncoded BER is commonly represented as a function of the normalised carrier-to-noise ratio, known as SNR and calculated as in Equation 3.33, where (E_b) is the average signal energy per data bit and ($N_\circ$) is the single-sided power spectral density of the additive white Gaussian noise, and ($erfc$) is the complementary error function.

$$BER = \frac{1}{2}\text{erfc}\left(\sqrt{\frac{\text{E}_\text{b}}{\text{N}_\circ}}\right) \tag{3.33}$$

In QAM, the energy per data bit (E_b) is related to the signal constellation and the symbol energy (E_s), which is given by:

$$E_s = \frac{A^2}{2} \tag{3.34}$$

where, (A) is the amplitude of each QAM symbol, then the energy per data bit (E_b) is given by Equation 3.35, where (M) is the number of constellation points in the QAM modulation scheme.

$$E_b = \frac{E_s}{\log_2 M} \tag{3.35}$$

Calculating the coded BER on the other hand depends also on the minimum Hamming distance d_{min} [383], total number of information bits associated with the minimum weight codewords $A_{d_{min}}$, number of information bits K, and the overall code rate R_c as in Equation 3.36.

$$BER = \frac{1}{K}A_{d_{min}}Q\left(\sqrt{2d_{min}R_c\frac{E_b}{N_\circ}}\right) \tag{3.36}$$

3.4.2 Throughput

Throughput is the volume of data that can be sent and received during a certain time frame. Throughput is the average speed at which messages reach their intended destination successfully. Throughput offers a practical measurement of actual packet delivery, as opposed to the theoretical measurement provided by packet delivery.

Network throughput provides users with information about the rate at which packets are delivered to their intended destination. Throughput is quantified in bits per second (bps). This term can be used interchangeably with data packets per second, indicating network throughput. Network throughput is typically measured by calculating the average, which is seen as a reliable indicator of the network's overall performance. If a network administrator observes low throughput, it could indicate a packet loss problem.

The general definition for throughput is the ratio of the number of correct received bits (or packets) divided by the interval of the whole transmission. Equation 3.37 represents throughput in terms of bit per second, where ($K_{correct}$) is the total number of correctly received bits, (K_{total}) is the total number of transmitted bits, and (R) is the bit rate. In 6G, the throughput is expected to hit the target of Tbps.

$$Thr = \frac{K_{correct}}{K_{total}} \times R \tag{3.37}$$

3.5 Performance Analysis

In this section, as depicted in Figure 3.14 to Figure 3.21, we characterise the error correction and throughput performance associated with the new channel coding techniques in Section 3.3. As illustrated in Section 2.3, the performance measures must adhere to the requirements of the new wireless generation 6G. The performance evaluation process considers different sets of code lengths, modulation index for a specified number of PD-NOMA users and different numbers of communication cells as illustrated in Table 3.1.

Table 3.1: Performance evaluation parameters

Parameter Name	Parameter Symbol	Value
Number of users	M	10×10^6
Number of cells	N_c	500
Number of BS	BS	1
Message length	k	1 528
Shift registers	D	3
Code length	N	2048 4096 8192
Modulation approach	BPSK QAM	2 16 64 256
Data length	L	$1(Tera)$
Frequency	F	300 GHz

As an initial stage, validating the performance of PCSC and PCPC in accordance with error correction capability BER and data throughput is shown in Figure 3.14 and Figure 3.15. First, the PD-NOMA architecture deployed without any channel coding is analysed to evaluate the efficiency of the suggested concatenated structure within the context of 6G data rate transmission. At the same time, performance evaluation for the same PD-NOMA architecture is compared with Polar Code (PC) as the channel coding approach utilised in 5G with the maximum channel capacity-achieving code. This comparison is made to determine whether the PCSC and PCPC techniques are superior. It is well-established that channel coding is essential for data transmission in any communication system.

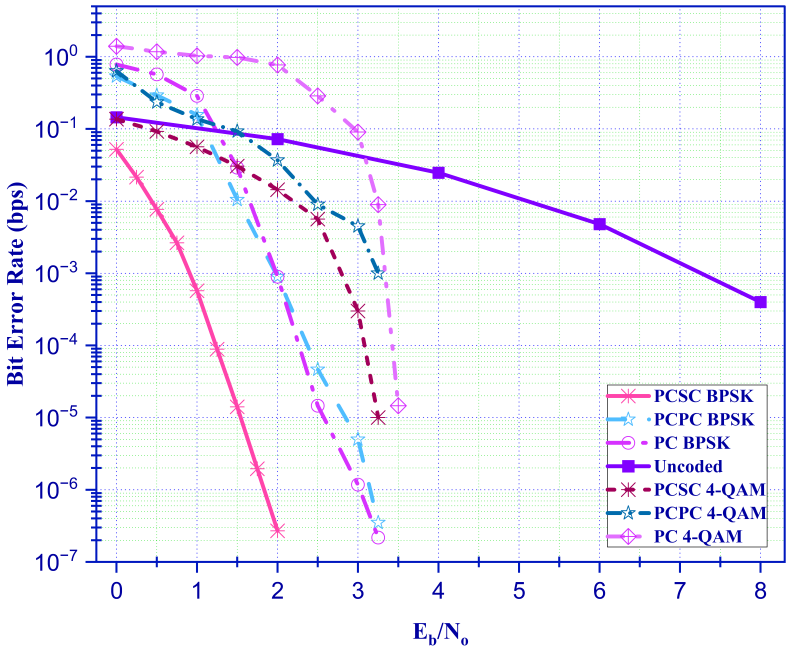

Figure 3.14: BER Performance Comparison, $N = 1024$

Figure 3.14 compares the BER performance of the PCSC and PCPC with PC for BPSK and QAM, employing $N = 1024$, $k = 528$ for polar code, and $N = 3$, $k = 1$, $D = 3$ for convolutional code for both BPSK and QAM, as these parameters are the test-line which is deployed in the current wireless generation 5G. Looking into the results, it can be noticed that the performance of all the tested channel coding techniques outperformed the uncoded transmission system. This is due to the error that can affect the reliability of the transmission, resulting in a very high error range. The channel coding gain can reach 6.5dB achievement between PCSC and the uncoded system transmission and approximately 5dB for PCPC. Additionally, a channel coding gain of approximately 1.4dB with an error rate of 10^{-3} is achieved while deploying PCSC compared to PC using BPSK modulation. While this indicates a better error correction behaviour for

PCSC, the performance of error correction for PCPC is convergent to PC performance. As real-time communication scenarios are working under higher modulation levels, the proposed coding techniques must be tested and validated to serve the same concept. As an initial testing step, PCSC and PCPC are tested with 4 QAM modulation; for the same error rate of 10^{-3} the channel coding gain achieved is 0.75dB for PCSC. In the case of PCPC, when the error rate is moderate from 10^{-1} to 10^{-2}, the channel coding gain ranges from 2dB to 1dB. On the other hand, both PC and PCPC have the same performance only at 10^{-3} error rate.

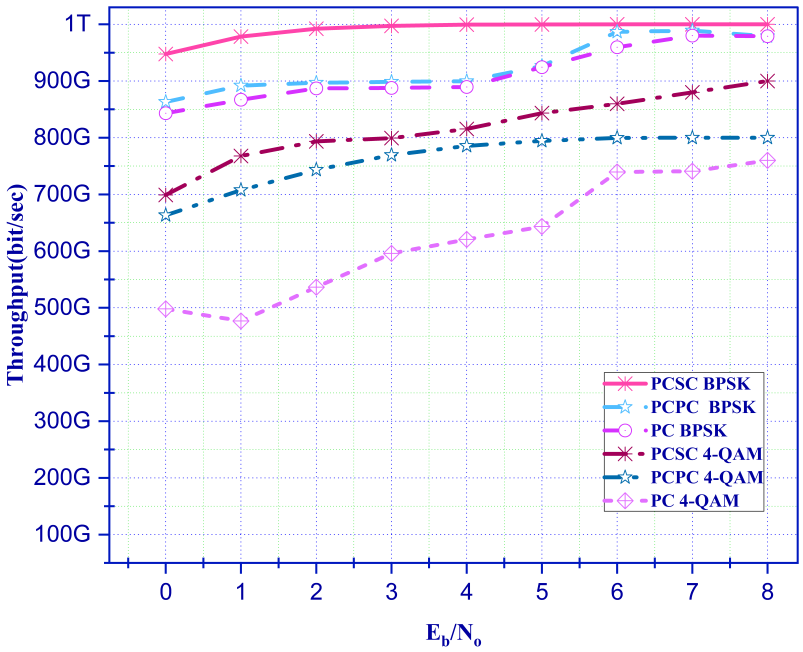

Figure 3.15: Throughput Performance Comparison, $N = 1024$

In order to have a full understanding of the behaviour of the developed channel coding, throughput data transmission is considered in terms of bit per second. The target of 6G is to reach the terahertz data rate throughput. As shown in Figure 3.15, PCSC with BPSK modulation shows very promising results in which it outperforms the 5G coding technique PC and PCPC, at the initial testing stages PCSC achieves 100 Gbps difference against its superiors. As the validation process continues to achieve higher data rates with BPSK, the performance of PCSC with QAM outperforms PC by 200 Gbps for PCSC and 150 Gbps data rate achievement for PCPC. As these promising results are achieved, the need to test PCSC and PCPC for higher codeword length is encouraging.

As the new generation 6G is expected to work with real-time IoT and VR applications, the communication system will require higher data processing and modulation rate starting from 16 QAM to 256 QAM for information exchange between the transmitter and receiver through the communication channel.

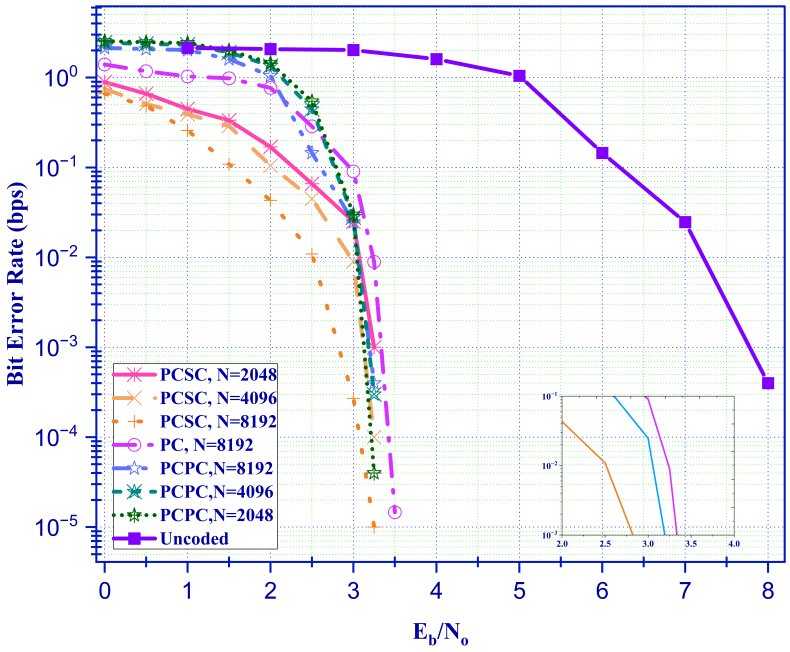

Figure 3.16: BER Performance Comparison for 16 QAM

Figure 3.16 shows the results of PCSC and PCPC with different codeword length ($N = 2048, 4096, 8192$) with 16 QAM modulation. Starting from 10^{-1} error rate and $N = 2024$, the channel coding gain when compared to PC reaches 0.75dB. As the codeword length goes up to $N = 4096$, the channel coding gain shows better performance and reaches 1dB. This performance reaches a 1.5dB channel gain when the codeword length $N = 8192$, PCSC performance with 16 QAM gives a clear indication for the achievement upon PC that has a limited codeword length in 5G. On the other hand, the performance of PCPC with 16 QAM matches the performance of PC with a small amount of channel coding gain enhancement does not go higher than 0.25dB, where the difference between PCSC and PCPC is not more than 0.75dB as shown in the zoomed part of Figure 3.16. This gives us an indication that there is a possibility to enhance the performance of PCPC by developing the encoding part or decoding part as will be described in Chapter 4.

The throughput performance as in Figure 3.17 achieves a higher data rate by 100 Gbps at 8 SNR, it can be noticed that the performance of PCSC where $N = 8192$ shows it is best performance against PC with 400 Gbps data rate at 5 SNR. As noticed again the performance of PCPC matches the performance of PC for some values of SNR 1, 2, 6,and 7, while for the other values of SNR the performance of PCPC achieves less throughput than PC. However, at the highest value of SNR, which equals 8, the minimum data rate achieved using PCPC with the lowest value of $N = 2048$ is 700 Gbps, which motivates this study to further improve this channel coding technique.

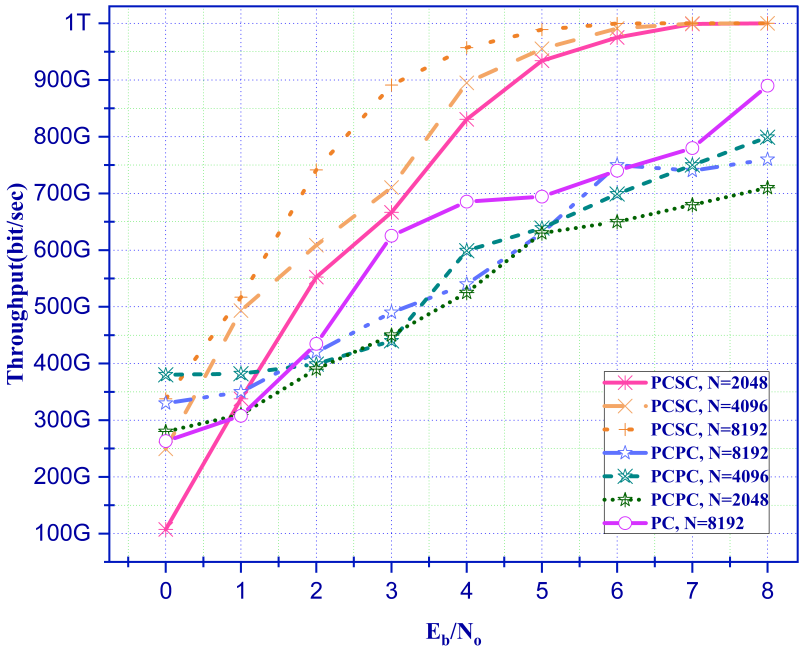

Figure 3.17: Throughput Performance Comparison for 16 QAM

This performance highlights the superiority of PCSC over PC and PCPC in regards to 6G KPIs, and the wide range of the future applications hightailed in Chapter 2 that requires high data rate with lower error rate. As QAM is a digital modulation technique commonly employed in communication systems to send digital information across analogue channels. Increased modulation levels in QAM involve utilising larger constellation sizes, with each symbol representing a greater amount of information. For example, a 16 QAM utilises a constellation consisting of 16 distinct points, each symbolising a specific combination of amplitude and phase. As 5G networks frequently employ advanced QAM techniques like 64 QAM or 256 QAM, which are more complex than those used in previous generations. Utilising higher-order QAM to validate the superiority of PCSC and PCPC is mandatory.

Figure 3.18 depicts PCSC and PCPC BER performance for a higher level of modulation with 64 QAM. As the modulation level goes higher, the performance of PCSC conveys better performance than PC. This performance ranges from 2.5dB to 1.5dB channel coding gain, having compared PCSC with PC used in 5G, PCSC achieves 2.5dB channel coding gain at 10^{-1} error rate and 1.5dB gain at 10^{-3} error rate; this performance can be noticed for the higher level of code word length $N = 8192$. Having said that, it is important to highlight the advantageous performance that PCSC shows over PC even with a lower codeword length. For $N = 4096$ PCSC attains 2dB and 1.25dB channel coding gain for 10^{-1} and 10^{-2} respectively. Using lower level of code word length for PCSC with $N = 2048$ outperform PC with $N = 8192$, PCSC achieves 1.65dB coding

gain for 10^{-1}, 1dB and 0.75dB for 10^{-2} and 10^{-3} respectively. This behaviour gives an indication of how powerful PCSC is in breaking the limitations that previous wireless generations might put on 6G expectations.

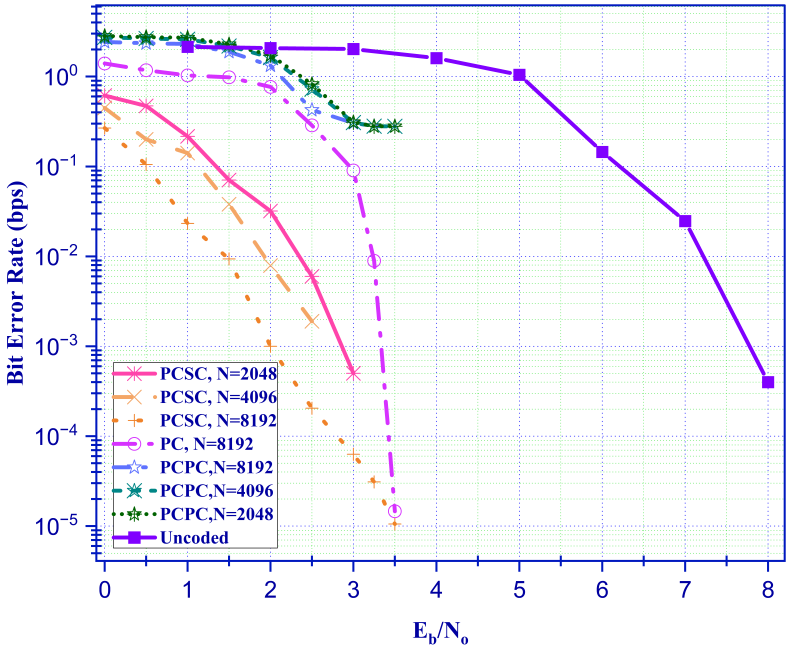

Figure 3.18: BER Performance Comparison for 64 QAM

Unfortunately, PCPC shows different behaviour than PCSC, firstly the performance of PCPC for the different levels of N is identical to each other. The second thing to notice is that PCPC performance is inferior to PC by 0.5dB; we believe that this is due to the time-consuming decoding algorithm which is commonly used for this type of concatenated codes as depicted in Section 3.3.5.

The performance evaluation in Figure 3.19 for PCSC and PCPC in terms of throughput is not different from the BER performance discussed earlier. As the modulation index goes higher, the performance of PCSC shows remarkable behaviour with a 740 Gbps data rate compared to 375 Gbps for 16 QAM. As the new coding technique is suggested as a promising channel coding to be operated with the new wireless generation 6G, it must be validated against 5G channel coding PC. PCSC succeed to achieve Tbps data rate throughput with the low value of SNR equals to 3, where PC manage to deliver only 600 Gbps data rate. PCSC preserves its stable performance as SNR goes higher even with the lowest value of code word length $N = 2048$. On the other hand, PC failed to match PCSC performance in achieving Tbps data rate transmission, where the data rate gradually increases; however, it does not correspond to the high-demand communication service and applications for 6G. PCPC BER performance is reflected in the data rate efficiency; it can be noticed that the amount of successively received data through system

transmission ranges from 400-800 Gbps. As these data rate efficacy sounds promising, however, in the context of 6G it is still under the required performance.

In order to have a practical point of view for the operation system using PCSC and PCPC, the performance must be addressed for higher modulation level where 256 QAM is used. In 5G PC moderate between 64 to 256 QAM depends on the channel conditions, thus PCSC and PCPC effectiveness must be verified with 256 QAM as well.

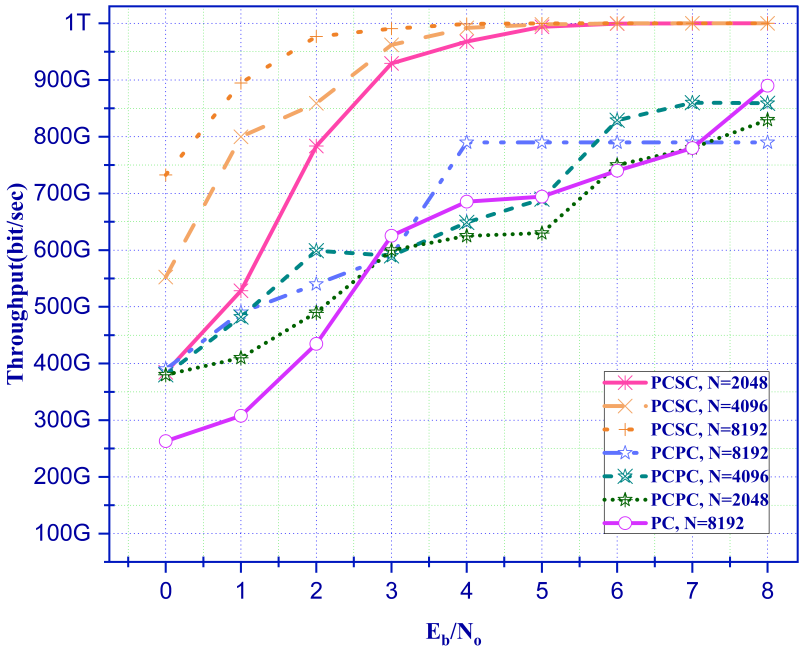

Figure 3.19: Throughput Performance Comparison for 64 QAM

Figure 3.20 and Figure 3.21 shows the performance of PCSC and PCPC BER and throughput respectively. As a start, let us consider the behaviour of PCSC with the range of code word length $N = (8192, 4096, \text{and } 2048)$. Comparing PC with PCSC for different error rates 10^{-1}, 10^{-2}, and 10^{-3}, PCSC achieves 2.75dB, 2dB, and 1.75dB respectively. Moreover, the performance of PCPC is observed as well; there is not much noticeable achievement; in fact, PC performs better than PCPC under the same testing conditions.

As mentioned earlier, the error rate performance is reflected in the data rate achieved from Figure 3.21, 800 Gbps is accomplished at the start of the transmission process where the Tbps data rate is achieved at 2 SNR with a stable performance during the full transmission process. However, as expected from the BER observation, the efficiency of PCPC is not promising to be conducted at its stage for 6G communication system. It is noticed that PCPC conducts better performance than PC at some stages of the transmission, nonetheless fails to deliver Tbps throughput and PC might have better performance at some stages. The varying efficiency gives an indication that one of the stages for conducting PCPC is working as a drawback for the channel coding process,

in which it must be improved in order to be valid and considered as a channel coding technique for the 6G communication system.

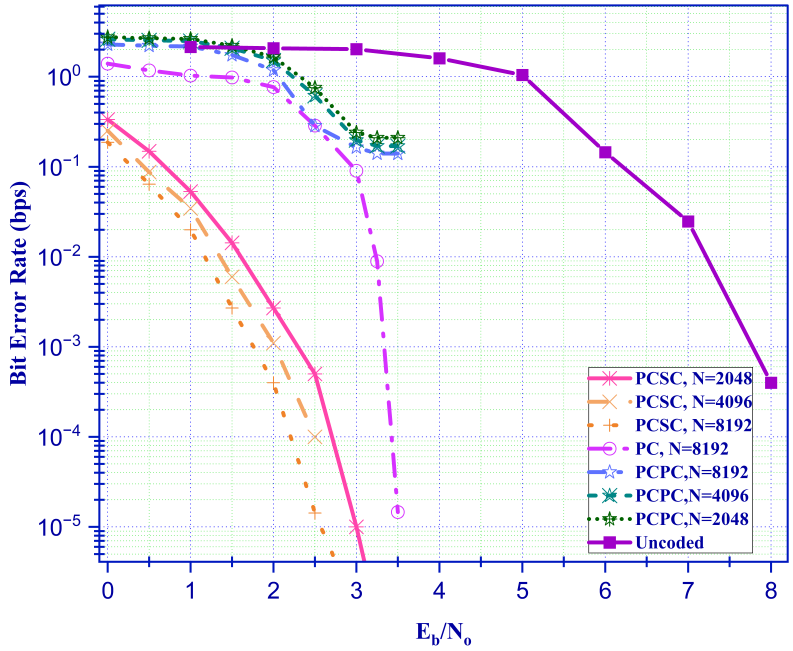

Figure 3.20: BER Performance Comparison for 256 QAM

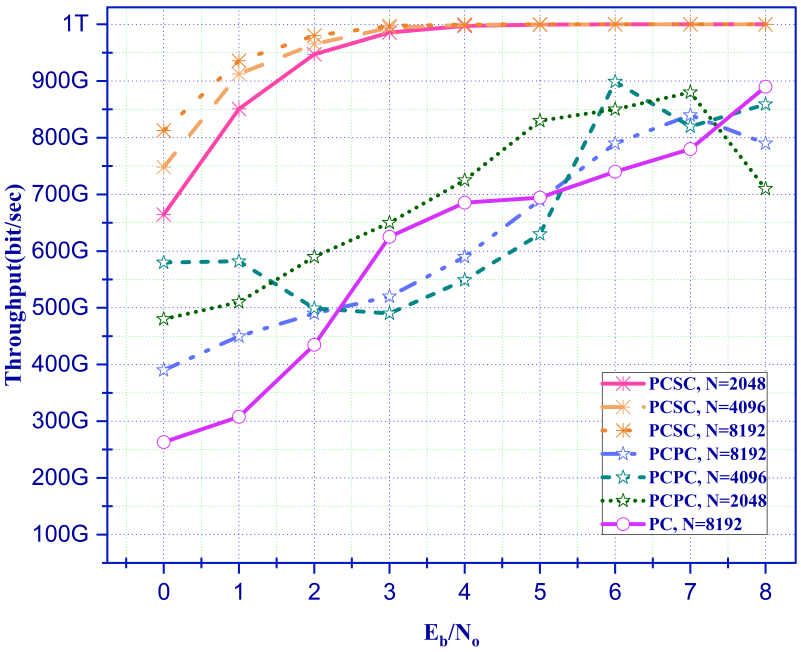

Figure 3.21: Throughput Performance Comparison for 256 QAM

3.6 Discussion

Channel coding is a vital component of communication systems, essential for guaranteeing reliable as well as efficient data transfer. One of the important reasons to have powerful and reliable channel coding within the communication system is the error detection and correction capability to improve the overall reliability of the communication system. Another important factor is the support for higher data rates by compensating the errors that might arise in the next wireless generation 6G. These two important measures allow the communication system to mitigate channel noise and interference, increase communication range, improve signal quality, ensure data integrity, and adapt to channel conditions.

In this chapter two novel channel coding techniques namely PCSC and PCPC are presented to work with 6G communication networks [4]. The substantial achievement of up to 3dB channel coding gain and Tbps data rate is a promising approach to be conducted with the new wireless generation 6G. The presented channel coding efficiency approves its superiority through the different validation processes, with different coding rates, codeword lengths, and modulation approaches.

The validation process considers $1km^2$ area divided into 500 PD-NOMA with 10×10^6 total users, although the network is under high-density level the performance of PCSC proves it is advantageous efficiency in meeting the 6G KPIs. Moreover, PCSC demonstrates stable performance with different testing properties, in which it has the potential to achieve the high demand applications for 6G.

4

Deep Learning for Channel Decoding

This chapter introduces deep learning polar convolutional parallel concatenated (DL-PCPC) decoding. Section 4.1 comprehensively explains the decoding process for PCPC in relation to Chapter 3. Next, in Section 4.2, the methodology and modelling of DL-PCPC are described. The subsequent Section 4.3 comprehensively describes the performance indicators that validate the superiority of the novel DL-PCPC approach. In Section 4.4, the performance evaluation and comparison of DL-PCPC for 6G will be discussed in relation to the existing state of the art for 5G.

4.1 Decoding of Parallel Concatenated Codes

Over the past few years, there has been a rapid expansion in wireless communication technology, which has gained substantial interest from a variety of governments and organisations [384]. The upcoming wireless generation, 6G, is anticipated to provide support for several networking paradigms, such as heterogeneous networks, satellite networks, and carrier networks. This support aims to enhance the strength and dependability of transmissions. Considering that most existing communication channels include support for Wireless Fidelity (Wi-Fi) and cellular technologies with certain restrictions, it is essential to incorporate 6G performance indications to enhance the user experience successfully [385–387].

As discussed in Chapter 3, an essential factor in wireless communication to meet 6G requirements is an error-free transmission with minimum delay and minimum energy consumption. In Chapter 3, we successfully introduced two different channel coding techniques that provide higher data reliability and throughput. It is noticed that PCSC surpasses PCPC in performance for different performance analyses; this is because the long iterative decoding process for PCPC as it is the main drawback noticed during the evaluation of this work. Consequently, integrating AI-based methods with new developed techniques is of the utmost importance in terms of their ability to enhance 6G techniques to achieve 6G KPIs.

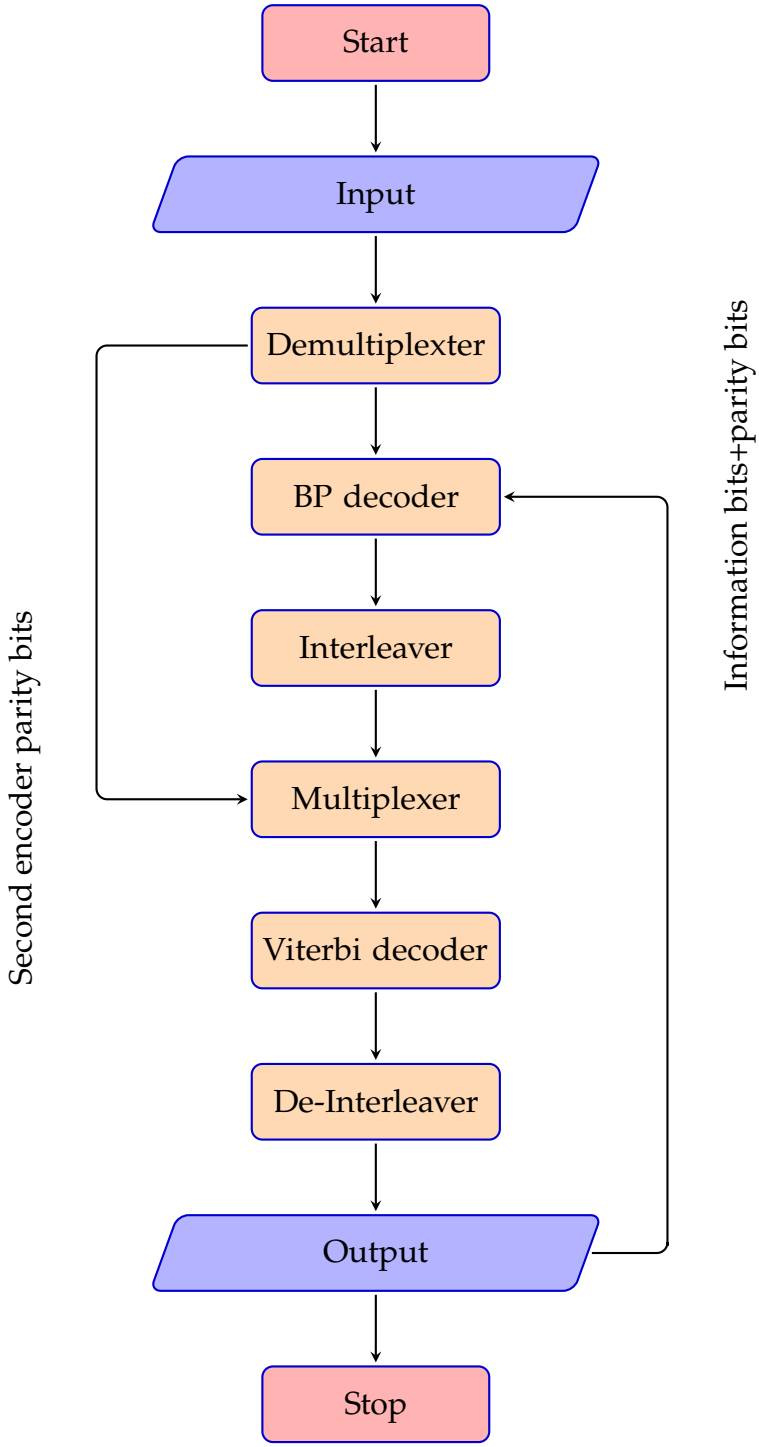

Figure 4.1: Successive Cancellation Decoding (SCD) for PCPC

Deep Learning (DL) is introduced as a subset of ML, which has recently become known as a robust set of methods that can produce impressive results in many research areas. DL is based on the architecture of neural networks and employs multiple layers ("deep") of artificial neurons [184, 388–392].

Deep learning techniques have recently been used to create channel coders and decoders, resulting in outstanding performance across different communication channels. Research has demonstrated that employing feed-forward deep learning can yield to better results compared to channels that use standard techniques spacially for high-interference communication channels [65, 393–397]. Nevertheless, prior studies have demonstrated that the existing wireless generations are unable to deliver the sufficient bandwidth capacity that is anticipated from 6G. However, researchers have specifically concentrated on utilising deep learning techniques for channel coding in earlier wireless generations. The polar code, which is known for its superior performance in the context of deep learning, has been extensively studied [398–402].

As detailed in Section 3.3.5, the decoding process for PCPC is based on SISO segment principle and can be summarised in Figure 4.1, in which this decoding process known as Successive Cancellation Decoding (SCD). In Section 3.5, the performance analysis shows that PCSC outperforms PCPC, after extensive research to differentiate the main reason for the contrast in the results between PCSC and PCPC; and a step by step analysis for the proposed system, we conclude that the decoding process for the parallel concatenation is the distinguishing factor between the two distinctive channel coding presented here.

4.2 Deep Learning PCPC Decoding

In this section, the newly established DL decoding method network model, as well as the training process and the requirements, are discussed. According to the newly developed deep learning method, the coded data blocks are processed as a single block for the total number of network neurons. This approach allows the decoding process to perform a greater number of bps than its iterative counterpart.

4.2.1 Deep Network Decoding Design Architecture

The decoding process maps the received (coded) data, which is (rd) in Algorithm 1, to an original message estimation using the decode function $(F : \hat{c} \rightarrow \hat{m})$. The received signal passes through a series of transposed convolutional layers and Rectified Linear Unit (ReLU) activation function. The decoding function is designed to minimise the average distribution between the original message and the reconstructed (estimated) message by introducing a minimum average function $F_{\omega l}$ as defined in Equation 4.1:

$$Minavg = \arg \mathrm{E}_{p(m_l, \hat{m}_l)} \left[d\left(m_l, \hat{m}_l\right) \right] \tag{4.1}$$

The minimum average function parameters are, $d\left(m_l, \hat{m}_l\right)$ which is the distribution measurement and the probability distribution for the original and the reconstructed messages $p\left(m_l, \hat{m}_l\right)$. In the training process, the decoder will update the minimum average function iteratively and use the received coded signal. The decoding function will perform multiple iterations; each iteration will use the total codeword length into the DL network block parametrised by the weights ω_l, where the network function has 132 weighted neurons. The weighted inputs (output sequent) $q_l = \hat{c}.\omega_l$ are added with a bias b where at the final stage, the result is filtered with a ReLU as in Equation 4.2.

$$\mathrm{Re}LU(q_l) = \max\{0, q_l\} \tag{4.2}$$

As shown in Figure 4.2, the first decoder function $F_{\omega l}$ takes the codeword $\hat{c}_1$, a demultiplexed version of the codeword $\hat{c}_2$, and a prior version of the predicted original message $\hat{m}$; the first iteration initial value of the original message is set to 0. The first decoder output is the sequent q_1, which will be the input for the second decoder block. The last iteration output from the decoder stage will feed into the ReLU function to predict the final message.

> The Rectified Linear Unit (ReLU) or rectifier activation function adds nonlinearity to a DL model and resolves the problem of disappearing gradients. The function interprets the positive component of its input.
> The activation function is highly favoured in the field of deep learning. Within artificial neural networks, the activation function of a node determines the output of that node based on a specific input or combination of inputs. ReLU is the predominant activation function employed in DL models. The function returns 0 for any negative input; for any positive number x, it returns x.

4.2.2 Data Generation and Network Specification

The deep network model is tested and validated to extract the data stream features with a 200,000 binary stream codeword dataset for PCPC decoding. Each code word $\hat{c}$ is processed by decoding blocks F_ω with the parameters $\hat{c}_1$, $\hat{c}_2$ and $\hat{m}$. In other words, we decode $\hat{c}$ for a known coding scheme with the abovementioned initial parameters.

Each block represents one of the predictions in the prediction stream. The average value for each prediction is calculated as in Equation 4.1, and the one with the minimum average distribution is the most accurate prediction.

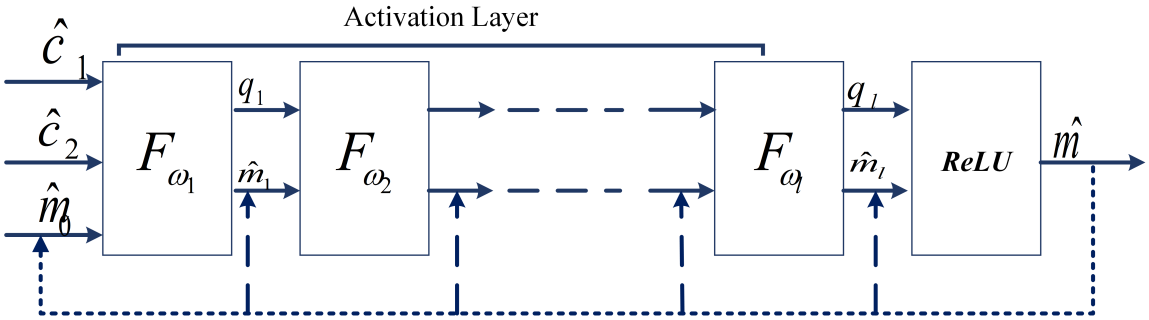

Figure 4.2: Deep Learning Decoding Function

4.2.3 Data Preparation and System Validation

After code word generation is completed, the generated dataset is split into three parts, 20% for validation data, 20% for test data, and 60% as network training data. The decoding data is tested with the 6G terahertz frequency range. The training procedure optimises the weight of the trainable network parameters using back-propagation, and the optimisation technique used is the Nesterov accelerated adaptive moment estimation (Nadam) algorithm [403]. The Nadam algorithm quickens the learning process by combining mini-batch gradient descent with Nesterov momentum [404]. To correspond to our activation function, the weights of the hidden layers are initialised using the lecun normal initialiser [405].

Moreover, we employ Binary Cross Entropy Loss (BCE) as our loss function [406]. BCE is a loss function employed in ML and DL to quantify the discrepancy between projected binary outcomes and actual binary labels. It measures the dissimilarity between probability distributions, which helps in training models by penalising erroneous predictions. It is commonly employed in tasks such as binary classification, which involves categorising data into two types. BCE evaluates the expected probabilities by comparing them to the actual class output, which can only be either 0 or 1. Subsequently, it computes a score that imposes penalties on the probabilities depending on their deviation from the anticipated value. That refers to the proximity or distance from the true value.

$$\text{BCE} = -\frac{1}{N}\sum_{i=1}^{N}\left[y_i \log(p_i) + (1-y_i)\log(1-p_i)\right] \tag{4.3}$$

where, N is the number of data samples (observations), y_i is the actual binary label (the true class) for the i-th observation (0 or 1).

4.2.4 Training Process

The training parameters are configured to operate for a number of epochs, during which the training dataset is randomly shuffled and fed into the model at each epoch. If the minimum average function does not change for a period of at least 25 consecutive epochs, then the training process will be considered complete. The maximum iteration value is similar to the iteration limit that we previously set for the decoding method used in Section 3.3.5. The DL-PCPC network, consists of six layers to form a fully connected Convolutional Neural Networks (CNN). The first five layers are convolutional, fully connected function layers with activation layer. The last layer utilises ReLU as a final activation function and batch normalisation layer, which enhances the system's overall performance and lowers the number of internal multivariable shifts.

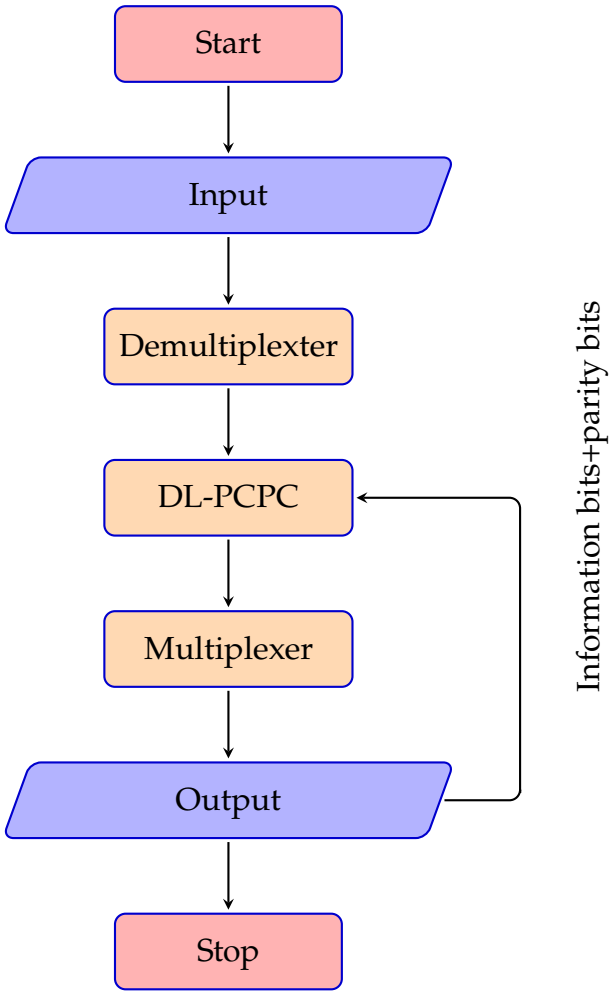

Figure 4.3: DL-PCPC Design Architecture

Figure 4.3 illustrates the DL-PCPC network, where the codeword data is sent through a demultiplexer and then fed into the iterative blocks of the deep learning network, which is shown in Figure 4.2. The output from the deep network will be multiplexed before the final estimation of the original data is determined based on Equation 4.1.

4.3 Performance Indicators

This section illustrates the performance metrics that we utilised to evaluate the differences between the performance of DL-PCPC and SCD.

4.3.1 Minimum Decoding Error

Minimum Decoding Error is commonly known as a criterion utilised in decoding algorithms, particularly in error-correcting codes or the decoding of encoded communications. Error-correcting codes are employed to identify and rectify problems that may arise during the transmission or storage of data.

Decoding algorithms aim to determine the most probable original message or signal based on the received input, which may be distorted. The "Minimum Decoding Error" criterion seeks to decrease the probability of decoding mistakes, guaranteeing that the decoded message closely approximates the original message. The minimum decoding error is calculated for each iteration, where the decoding error is the difference between the original data and received decoded data using the maximum likelihood [407] as in Equation 4.4.

$$\hat{m} = \arg\max_{m} L\left(m \,|r\right) \tag{4.4}$$

4.3.2 Data Rate of Correct Data

The speed at which accurate or mistake-free data is sent via a communication link is known as the data rate of correct data. It measures how quickly and error-free accurate data is delivered. In practice, the transfer rate of correct data is controlled by the communication channel's capacity, the dependability of the transmission medium, the effectiveness of error detection and correction systems, and the quality of the encoding/decoding scheme utilised.

For example, in a digital communication system, if a specific channel has a data rate of 1 Mbps and 99% of the data transmitted over this channel is error-free, the data rate of correct data would be 0.99 Mbps, indicating that 99% of the transmitted data is successfully received without errors. The data rate of correct data is an important metric in assessing the performance and reliability of communication channels, especially in applications where data integrity is critical, such as telecommunications, networking, and data storage.

4.3.3 Energy Efficiency

The energy efficiency of data transmission in high-speed data transmission systems is measured in Terabit per Joule (Tb/J), particularly in the context of communication networks; it represents the amount of data (terabits) that can be transmitted or processed per unit energy (joule) consumed.

The calculation of Tb/J involves dividing the total amount of data transmitted or processed measured in terabits by the total energy consumed measured in joules as in Equation 4.5 [408].

$$Tb/J = \frac{Total\ data\ transmitted\ or\ processed\ (Tb)}{Total\ energy\ consumed\ (J)} \tag{4.5}$$

Systems with higher Tb/J values are considered more energy-efficient because they can transmit or process more data per unit of energy consumed, leading to lower energy costs and reduced environmental impact.

4.3.4 Delay

An important metric in communication is the time required to transmit the entire message or data packet from the sender to the receiver, known as delay. This time includes the time consumed in the decoding process known as the processing delay which is the time it takes to process the entire packet (error check and decoding). In order to prove the superiority of DL-PCPC over SCD without increasing the delay, we calculated the time required by the two decoding algorithms for each iteration for the 25 iterations to decode the received data as shown in Section 4.4.

4.4 Performance Analysis

In this section, as depicted in Figure 4.4 to Figure 4.9, we characterise the minimum decoding error, data rate, energy efficiency, and delay in relation to DL-PCPC and SCD. In order to have a clear view of the performance evaluation of DL-PCPC, the test parameters are implemented in relation to the decoding process parameters used in Section 3.5, which is illustrated in Table 4.1 for 300 and 400 GHz.

Table 4.1: DL-PCPC Performance evaluation parameters

Parameter Name	Parameter Symbol	Value
Number of users	M	10×10^6
Message length	k	528
Code length	N	8192
Modulation approach	QAM	256
Data length	L	$1(Tera)$

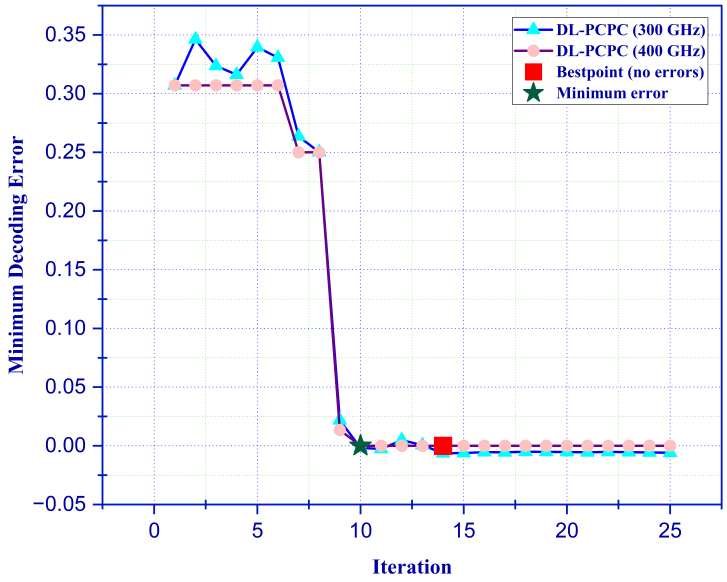

Figure 4.4: Minimum Decoding Error for DL-PCPC

Figure 4.4 and Figure 4.5 shows the performance of DL-PCPC and SCD measuring the minimum decoding error achieved at each iteration. At the simulation's beginning, the recorded decoding error value shows a high error value of 0.35Tbps.

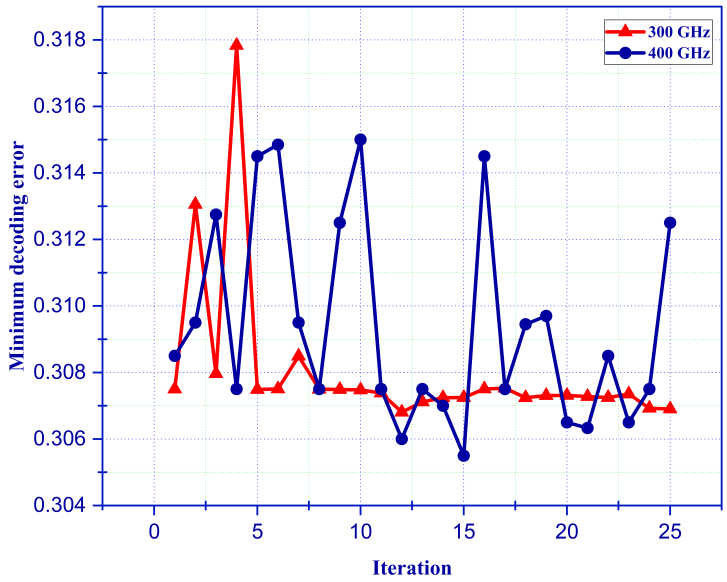

Figure 4.5: Performance of SCD Decoding Error

DL-PCPC in Figure 4.4, shows similar behaviour under the tested frequencies, where the decoding error value starts to drop at iteration six to reach the minimum value

of 0.01Tbps at iteration number ten. With negligible variations in the performance, the stability of the deep learning network starts at iteration number 14, where the minimum decoding error reaches zero value. On the other hand, looking at Figure 4.5 the performance of SCD shows higher decoding error values for both tested frequencies. The minimum decoding error that SCD can achieve is 0.28Tbps at iteration number 15. When the maximum iteration is reached, the minimum decoding error is 0.31Tbps with operation frequency 400GHz, while at the operation frequency 300GHz, the minimum decoding error doesn't go lower than 0.3Tbps.

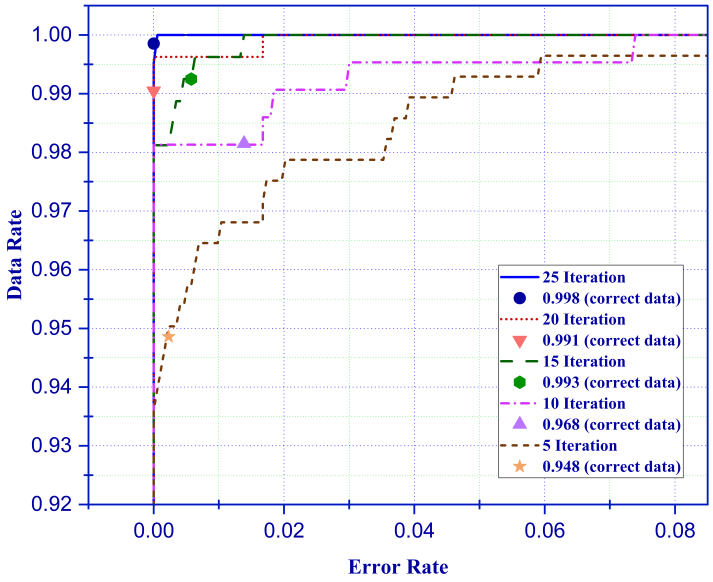

Figure 4.6: DL-PCPC Data Rate of Correct Data

The second important metric is the data rate, as it is a measure of how much data can be transferred over a period of time, which is shown in Figure 4.6, the results are shown for an operating frequency of 400GHz in which at the test time the results of 300 and 400 GHz were identical. The performance results of DL-PCPC show a 95% data rate on the fifth iteration, and as the number of iterations goes higher, a 99% data rate is achieved. Comparing DL-PCPC with SCD in Figure 4.7 shows an overall more than 70% improvement in data rate, which means faster data transmission, which is essential for tasks such as video streaming, VR, XR, VLC and much other application that 6G should support. As discussed in Section 2.3.1 6G is anticipated to enhance the data rate by 10 to 100 times, DL-PCPC proves its superiority to support 1Tbps transmission.

In regards to the performance indicator stated in Section 4.3.3, the EE of DL-PCPC and SCD are shown in Figure 4.8. DL-PCPC manage to reach a 99.948% EE, which means the ability to process higher data rates and reach the 6G rate of Tbps with lower energy consumption.

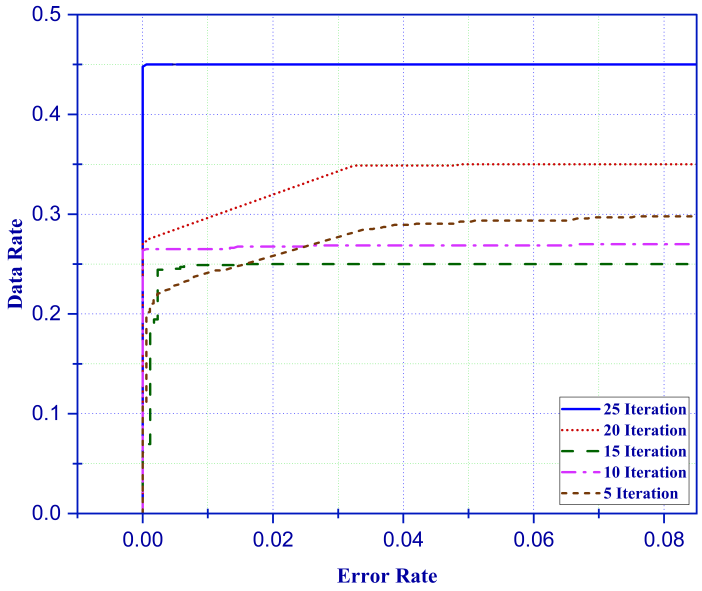

Figure 4.7: SCD Data Rate of Correct Data

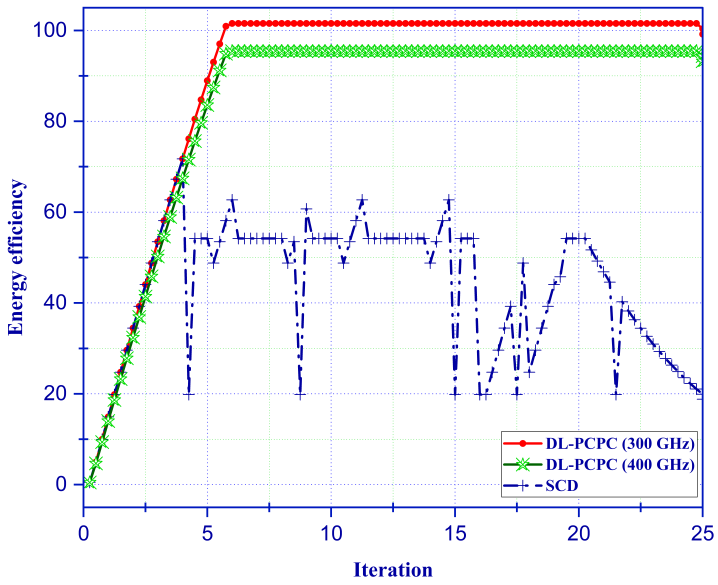

Figure 4.8: Performance of DL-PCPC Energy Efficiency

DL-PCPC at both frequencies outperform SCD by 40%, we can start to notice this behaviour at iteration six after DL-PCPC gradually shows a higher level of EE, where DL-PCPC shows stable performance of 99.9% EE, while the performance of SCD starts to drop gradually with unstable behaviour at some points.

In general SCD fails to show an EE level higher than 60% for the full transmission period. Overall, DL-PCPC shows approximately 60% improvement in EE than the traditional method when decoding parallel concatenated codes which makes DL-PCPC an energy-efficient channel decoding approach for 6G, which is meant to lower the energy consumption by at least three times, as discussed in Section 2.3.

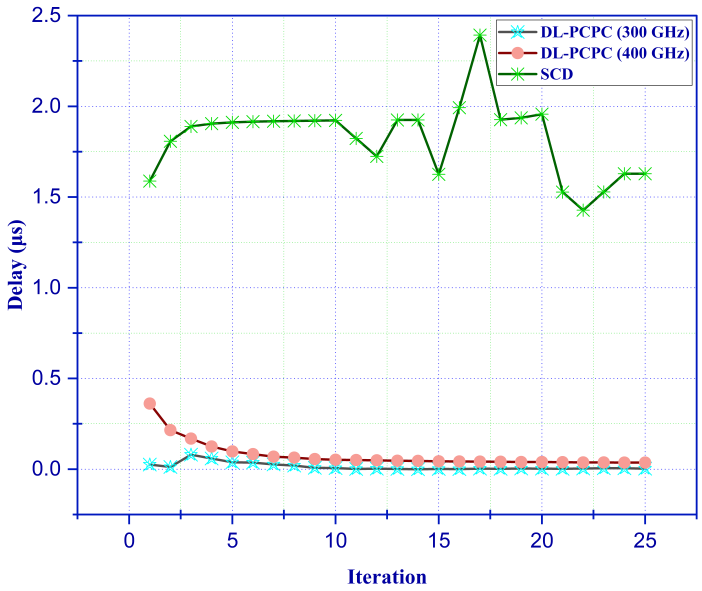

Figure 4.9: System Delay for DL-PCPC and SCD

System delay is a significant performance indicator for validating deep learning design efficiency. Figure 4.9 shows the massive difference in system delay using DL-PCPC compared with SCD. The new deep learning design managed to minimise the system delay to 0.003μs for the overall decoding process at the last iteration. On the opposite of that, SCD, where the delay goes no under 1.45μs for the full decoding time in each iteration. This improvement can be stated as a nearly 100% improvement in the consumed time for the decoding process.

4.5 Discussion

In this chapter, we have developed and suggested a novel channel decoding method for 6G communication, building upon our prior concatenated channel coding approach in Chapter 3.

The effectiveness of DL-PCPC decoding technique, which integrates deep learning into the decoding process, has been demonstrated in the frequency range of the 6G communication system while achieving THz data rates [3]. DL-PCPC achieves maximum EE of 100%, surpassing the commonly employed iterative decoding techniques. The performance indicators demonstrate that DL-PCPC can achieve error-free channel decoding and a system accuracy of 99.8%. The system architecture ensures the highest achievable data rate while minimising the workload and requiring only 14 iterations to achieve that.

Furthermore, the system delay remains at a low level compared to the often employed iterative decoding SCD. Moreover, system delay maintains to remain at a deficient level compared with frequently used iterative decoding.

Nevertheless, the outcomes are anticipated to enhance as the data block's length rises; moreover, this can only be verified once it is tried on the system. Additionally, neural-assisted codes must be taught how to use memory throughout encoding and decoding to achieve superior performance for extended data block lengths. We provide evidence showing how deep learning can improve the decoding process for the performed code word data length, which is expected to deliver the same promising performance for greater code word lengths.

5

Adaptive Reconfigurable Intelligent Surface

This chapter introduces Adaptive RIS (ARIS), which is implemented for THz 6G communication system to enhance the reliability, coverage, latency, and minimise power loss. Section 5.1 comprehensively explains the fundamentals of RIS in communication system. Next, in Section 5.2 the novel ARIS modelling methodology is described. The subsequent Section 5.3 thoroughly describes the ARIS Decision Making Algorithm (ARIS-DMA). In Section 5.4, the implementation scenarios used to test ARIS-DMA in accordance with 6G KPIs are described. Section 5.5 comprehensively clarifies the performance indicators that validate the superiority of ARIS-DMA. Next, in Section 5.6, the performance evaluation and comparison of ARIS-DMA for 6G is discussed in relation to the existing state of the art.

5.1 Reconfigurable Intelligent Surface Fundamentals

RIS, or reconfigurable intelligent surface, is a two-dimensional structure that can be programmed to have specific electromagnetic properties using metamaterial technology. Metamaterials are synthetic materials designed with unique structures and characteristics that enable the exact regulation and manipulation of electromagnetic waves. In addition, metamaterials typically comprise minuscule structural components with diameters significantly smaller than the wavelength of electromagnetic waves. Metamaterials can achieve exact control over electromagnetic wave refraction, reflection, and transmission by carefully engineering their constituent elements' geometric configuration, spatial organisation, and material characteristics. As a result, they exhibit unique characteristics that are not naturally present in materials, such as negative refraction, perfect lensing effects, and cloaking ability [409].

Metasurface technology has developed alongside the generalised Snell's law, enabling precise customisation of interface phase distributions to regulate electromagnetic

waves. Metasurfaces can be systematically designed with specific capabilities like focusing, polarisation conversion, and absorption using the generalised Snell's law. The fundamental principles of refraction and reflection, known as Snell's laws, can be stated as follows:

$$\begin{cases} \sin(\theta_t)\, n_t - \sin(\theta_i)\, n_i = \left(\frac{\lambda}{2\pi}\right)\left(\frac{\Delta\phi}{\Delta x}\right) \\ \sin(\theta_r) - \sin(\theta_i) = \left(\frac{\lambda}{2\pi n_i}\right)\left(\frac{\Delta\phi}{\Delta x}\right) \end{cases} \tag{5.1}$$

where the refractive indices of two signals are denoted as n_i and n_t. θ_t, θ_r, and θ_i represent the angle of refraction, the angle of reflection, and the angle of incidence signal. ϕ and $\Delta\phi$ denote the phase-discontinuity points of the two paths at the interface of the medium in Equation 5.1. The variable Δx denotes the distance between the intersecting points, and λ represents the wavelength of the electromagnetic wave. Equation 5.1 shows that we can manipulate the design of the reflection and refraction of the electromagnetic waves on the metasurface by varying the parameter $\frac{\Delta\phi}{\Delta x}$ [410]. In Equation 5.1, n_i, n_t, and λ are constants. In RIS, the value of θ_t and θ_r is controlled to determine the direction of the reflected and refracted waves by adjusting $\frac{\Delta\phi}{\Delta x}$.

5.1.1 RIS Structure

RIS is usually built comprising three different layers, as shown in Figure 5.1, to facilitate the control of the propagation environment.

1. **First layer:** consists of a two-dimensional array of RIS elements that interact directly with incident signals.
2. **Second layer:** is a copper plate that is capable of preventing the signal energy from escaping.
3. **Third layer:** is a printed circuit linked to the RIS controller and capable of controlling the phase shifts of the RIS elements.

RIS, as stated earlier, is a two-dimensional artificial surface made up of numerous sub-wavelength elements. It can be used to cover various surfaces such as walls, ceilings, buildings, and even traffic tools. The RIS can control and program the parameters of the electromagnetic waves that come into contact with it. Thus, it can be inferred that the key characteristics of RIS are reconfigurability, programmability, and discretisation, with reconfigurability being the dominant feature. Initially, RIS is considered as a 1-bit digital coding meta-surface. RIS consists of $M \times N$ elements, where each element is encoded as either '0' or '1' with a phase difference of π. It is possible to control the states of elements in real time by using tunable devices such as diodes.

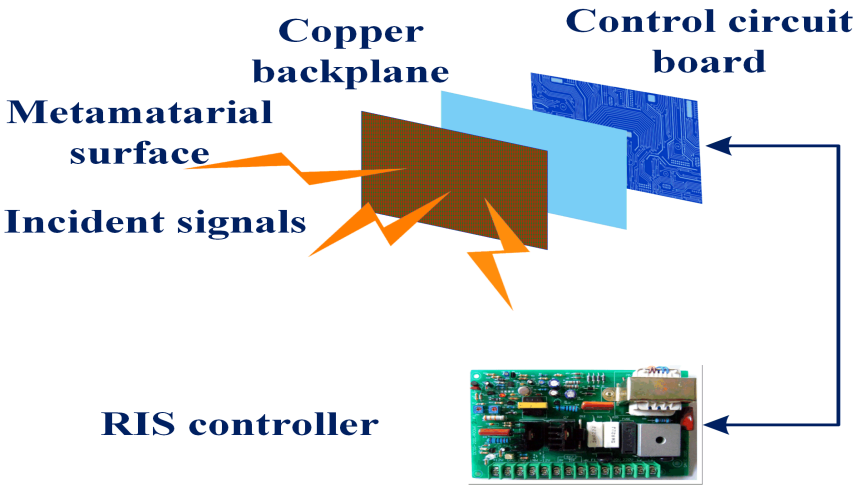

Figure 5.1: Components of an RIS

RIS comprises multiple passive reflective elements that can reflect the signal to the user. These RIS elements are made up of Positive Intrinsic Negative (PIN) diode, which have ON and OFF states that can control the direction of the incidence signal. The ON and OFF states are controlled by changing the biasing voltage through a small gap (hole), resulting in a different ElectroMagnatic (EM) field for the outgoing signal in the direction of the desired user; this in fact is affected by how permeable (μ) and permissive (ε) the RIS elements are.

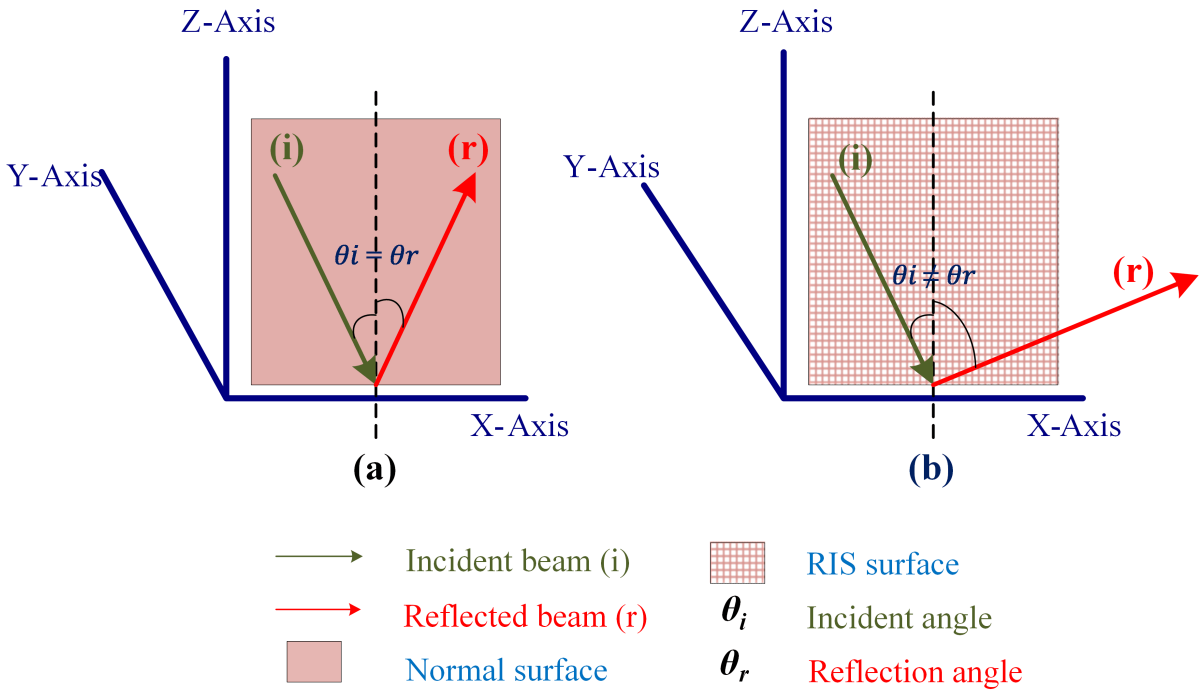

Figure 5.2: RIS Working Principle

Applying Snell's law of signal reflection emphasises that whenever a wave packet reaches an interface, it bounces back in the same direction it originated. The distinctive

features of RIS are due to its design characteristics. In the normal state without using RIS, the angle between the unit vector that hits any surface and the unit vector that bounces back in the same direction as the impact vector stays the same for both incoming and outgoing beams, as shown in Figure 5.2a. So that $\theta_i = \theta_r$, where i and r stand for the incoming and outgoing signal phase shift, respectively. In contrast, applying Snell's law to the RIS will reflect the incident signal in the desired direction for the user, thus resulting in different incoming and outgoing beams, which means $\theta_i \neq \theta_r$, as shown in Figure 5.2b.

5.1.2 RIS types and Functionality

Dividing RIS into many categories enables a more accurate and efficient selection process that can be customised to meet different communication needs and situations. Categorisation facilitates tailored applications to optimise system performance and achieve a more efficient balance between cost-effectiveness and resource utilisation.

Passive RIS and Active RIS

Passive RIS is composed of EM metamaterials, artificially created materials with distinct structures and properties to enable the exact regulation and manipulation of EM waves. They typically comprise minuscule structural components with diameters far smaller than the wavelength of EM waves. Metamaterials may exert remarkable control over EM waves refraction, reflection, and transmission by accurately manipulating their structural units' shape, arrangement, and material properties.

Passive RIS is more environmentally sustainable than standard communication relay systems since it uses reflective elements to change the input signal without power amplifiers. In addition, passive RIS is used just for signal reflection, giving it the properties of simultaneous two-way communication and transmission across the whole spectrum. The passive RIS element also consists of a phase-shift circuit that does not require direct-current power. However, despite offering an extra means of communication, passive RIS has limited capacity improvements because of the influence of double fading or multiplicative fading effects [411].

On the other hand, the active RIS incorporates an amplifier circuit that uses more power [412]. The Active RIS can increase the intensity of the incoming signal for each reflection component, hence improving the receiver's SNR. Active RIS has a greater system power consumption and a more complex hardware structure than passive RIS. This is because active RIS integrates power amplification components. Although active RIS has some disadvantages, its potential for application remains optimistic. Researchers have suggested active RIS [413–416] as a potential way to mitigate the negative impact of multiplicative fading effects and solve the issue of limited capacity in passive RIS.

Reflective RIS, Transmissive RIS and STAR-RIS

Three operating modes of RIS: transmissive RIS, reflective RIS, and STAR-RIS, have been extensively studied to accommodate different wireless communication systems and applications. This section examines how well RIS works in these three operating modes and compares and contrasts their advantages and disadvantages [417–420].

The reflective RIS has been subject to the most comprehensive research among the three options [125, 421–434]. By strategically deploying reflective RIS in an optimal site, we may create an extra line-of-sight connection that can intelligently reorganise the electromagnetic surroundings, enhance signal integrity, boost system capacity, and reduce energy usage. Moreover, implementing the reflective RIS can effectively increase the disparity in channel quality between authorised users and potential eavesdroppers, enhancing the system's overall security performance. Nevertheless, the reflective RIS is only operational when both the BS and the user are positioned on the same side; consequently, its working range angle is restricted to 180 degrees.

When the communication link between the BS and the user is obstructed, such as in an outdoor to indoor communication setting, and high-frequency transmissions encounter obstructions; relying alone on reflective RIS cannot provide an effective communication environment. To overcome this restriction, the concept of transmissive RIS has been introduced and has garnered significant interest [435–448]. In communication scenarios from outdoor to indoor in the millimetre-wave frequency band, the signal attenuation via walls is substantial, and the utilisation of reflective RIS is inadequate to redirect signals around obstacles [449, 450].

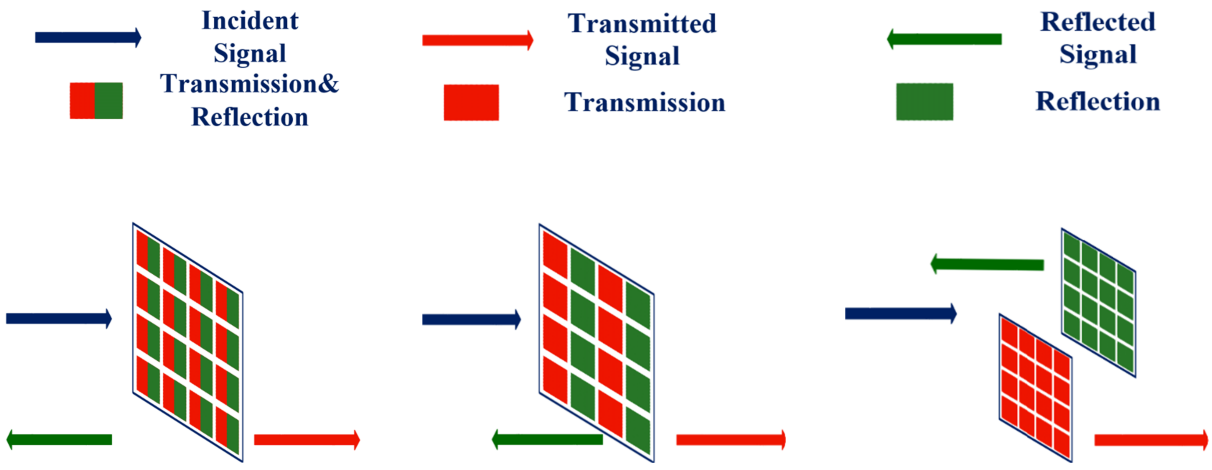

(a) Energy Splitting (ES) (b) Mode Switching (MS) (c) Time Switching (TS)

Figure 5.3: Three Practical Protocols for Operating STAR-RIS

In real-life communication, users are commonly positioned on both ends of the RIS. Relying solely on either reflective RIS or transmissive RIS is inadequate in such instances. As a result, researchers have proposed the concept of STAR-RIS to overcome

this constraint [451–467]. STAR-RIS possesses distinctive attributes that provide a comprehensive 360-degree coverage range, giving it more flexibility than traditional RIS in modifying the electromagnetic environment. STAR-RIS functions in three unique modes: Energy Splitting (ES), Time Switching (TS), Mode Switching (MS), as demonstrated in Figure 5.3.

In the ES mode, all components of STAR-RIS are expected to function simultaneously in both transmission and reflection modes, providing significant design adaptability with modifiable coefficients for each component. Nevertheless, the abundance of components in this arrangement leads to higher expenses. For ES, as shown in Figure 5.3a, all elements of the STAR-RIS are assumed to operate in the transmission and reflection mode, where the energy of the signal incident on each element is generally split into the energies of the transmitted and reflected signals with an energy splitting ratio of $\beta_m^t : \beta_m^r$, where $\beta_m^t, \beta_m^r \in [0, 1]$ and $\beta_m^t + \beta_m^r = 1$. ES RIS technology, although showing potential in various areas, still exhibits limitations and drawbacks. Here are a few possible disadvantages:

1. **Complexity and Cost:** Implementing ES RIS systems can be complex and costly due to the requirement for multiple energy sources, such as solar panels or power grids, to supply energy for each component. The system's complexity can lead to higher implementation and maintenance expenses, thereby limiting its suitability for specific applications or settings.
2. **Energy Efficiency:** Although ES RIS has the ability to adapt its configuration to enhance signal propagation, the energy splitting process may generate inefficiencies, resulting in energy loss. This can diminish the system's overall EE, particularly in situations where energy resources are limited or expensive to sustain.
3. **Limited Flexibility:** ES RIS depends on ES techniques to generate power for certain components, which could restrict its adaptability in some scenarios. In dynamic systems characterised by fluctuating or unexpected energy availability, ES may face challenges in maintaining optimal performance due to limitations on energy allocation.
4. **Reliability and Robustness:** Using many energy sources and intricate ES techniques in ES RIS systems can create possible vulnerabilities and diminish their reliability and resilience. In situations where continuous communication is of utmost importance, such as emergency response or operations that are crucial to the mission, these weaknesses may present substantial difficulties.
5. **Environmental Effect:** The choice of energy sources for ES RIS elements may have significant environmental implications that need to be considered. For example, if non-renewable energy sources like fossil fuels or grid electricity are used, the environmental consequences of ES RIS implementation may be greater when compared to other options.

6. **Regulations and Standardisation:** ES RIS deployment may encounter regulatory obstacles concerning energy use, spectrum allocation, and compliance with environmental rules. Overcoming these regulatory obstacles can be a lengthy process and may restrict the extensive implementation of ES RIS technology in specific geographical areas or sectors.

Within the MS mode, STAR-RIS is again classified into two distinct modes: transmission mode and reflection mode. For MS, as shown in Figure 5.3b, all elements of the STAR-RIS are divided into two groups. Specifically, one group contains M^t elements that operate in the transmission mode, while the other group contains M^r elements operating in the reflection mode, where $M^t + M^r = M$. The MS mode is a fusion of standard RISs that only carry out reflection or transmission. This mode achieves its functionality by optimising the selection of modes and phase shift coefficients for both transmission and reflection on an element-wise basis. Nevertheless, the MS mode only employs a limited number of elements for transmission and reflection, preventing it from attaining the same gain level as the ES mode.

The MS RIS technology has notable benefits in wireless communication systems but has several downsides and restrictions. Here are a few possible drawbacks:

1. **Switching Time and Latency:** MS RIS effectively adjusts to varying communication conditions by using mode switching or configuration changes. Nevertheless, transitioning between modes might cause latency, resulting in delays in data transfer. Delays in time-sensitive applications, such as real-time communication or high-frequency trading, can negatively impact performance.
2. **Complexity and Overhead:** Integrating MS RIS systems can introduce complexity and overhead to communication networks. The requirement for advanced control algorithms and coordination methods to handle mode switching raises the system's complexity and computing overhead. This complexity can affect the system's ability to handle an increased workload and efficiently use resources, especially when the technology is deployed on a broad scale.
3. **Limited Spatial Resolution:** MS RIS functions by regulating the phase and amplitude of reflected signals to modify the way signals propagate through the environment. However, MS and RIS elements may not be able to resolve very well in terms of space, especially when there are a lot of multipath environments or complicated propagation channels. This constraint can impact the precision and efficiency of beamforming and signal handling.
4. **Sensitivity to Channel Variability:** Changes in the communication channel, such as signal weakening, fading, and interference, can affect MS and RIS performance. Variations in channel conditions can influence the effectiveness of MS decisions and reduce the system's overall performance. Adapting MS and RIS to dynamic and unpredictable channel environments might present considerable difficulties.

5. **Energy Consumption:** Although MS and RIS have the potential to increase EE through signal propagation optimisation, the gains made might outweigh the higher energy required for mode switching and control operations. The continuous transition between modes and the fine-tuning of parameters requires energy, especially in active MS and RIS setups. Ensuring the sustainability of MS and RIS systems requires a careful balance between energy usage and performance optimisation.
6. **Deployment and Integration Challenges:** Implementation and integration problems may arise when implementing MS and RIS in real-world settings because of issues with integrating them into existing infrastructure, ensuring compliance with regulations, and managing the logistics of implementation. Managing MS and RIS deployment across several nodes or locations while ensuring compatibility with legacy systems and regulatory requirements may be a complex and time-consuming task.
7. **Cost:** Implementing and deploying MS and RIS technology may require substantial initial expenses, such as acquiring hardware, installing it, and maintaining it. Furthermore, continuous operational costs such as power usage, system monitoring, and optimisation may add to the total cost of ownership.

Unlike the MS and ES modes, the TS mode entails the cyclic transition of all elements between transmission and reflection modes. Different from ES and MS, the TS STAR-RIS exploits the time domain and periodically switches all elements between the transmission mode and the reflection mode in different orthogonal time slots, where the transmission and reflection period must follow $\Lambda^t + \Lambda^r = 1$, as in Figure 5.3c. This method streamlines modifying coefficients using temporal intervals to determine reflection and transmission coefficients. However, frequent switching between modes requires expensive and high specifications hardware capable of perfect time synchronisation. The TS RIS technology brings new and innovative features to wireless communication systems but also has certain limitations and drawbacks. Here are a few possible disadvantages:

1. **Complexity and Implementation Challenges:** Implementing TS RIS systems can be complex because accurate synchronisation and coordination of time-switching activities across numerous surface elements are required. The level of complexity rises as the deployment size and the number of components increases, presenting difficulties in system architecture, synchronisation protocols, and hardware integration.
2. **Limited Adaptability:** TS RIS uses TS methods to dynamically modify the phase and amplitude of reflected signals. Nevertheless, TS RIS versatility might be constrained compared to alternative reconfigurable surfaces like phase-shifting or hybrid surfaces. TS procedures can be limited in adapting to changing communication conditions due to fixed or predefined setups.

3. **Sensitivity to Time Variability:** Time variations, such as signal propagation delays, synchronisation faults, and fluctuations in communication channels, can affect TS RIS systems' performance. Time variability can negatively impact the precision and efficiency of TS processes, resulting in inefficient signal processing and decreased system performance.
4. **Time Resolution:** TS RIS functions by utilising TS schedules to regulate the characteristics of signal reflection across time. Nevertheless, the ability to switch between different time intervals in TS activities may be restricted due to limitations in hardware capabilities, the accuracy of synchronisation, and the delay in processing. A sufficient time resolution can impact the level of control and the capacity to adjust to rapidly changing communication settings.
5. **Energy Consumption:** While TS RIS has the potential to optimise signal propagation and improve EE, TS operations may consume additional energy resources. Continuous switching between different time slots or configurations and associated control and synchronisation overhead can increase overall energy consumption. Balancing EE with performance optimisation is crucial for sustainable TS RIS deployment.

5.2 System Modelling Methodology

Instead of relying on the standard STAR-RIS feature to split the system resources between the reflected and transmitted signal, in this thesis we implemented a novel decision-making algorithm that optimises the signal power to redirect the signal towards their intended user. The merging of ARIS Decision Making Algorithm (ARIS-DMA) in the wireless network system to target users in zero coverage spots, remarkably increasing area coverage and density. On the other hand, using STAR-RIS will not increase network coverage or density because zero coverage spots will remain without coverage, as will be validated.

5.2.1 Adaptive Reconfigurable Intelligent Surface Decision Making Algorithm (ARIS-DMA) Mutual Design Parameters

Figure 5.4 shows an illustration of the collaborative transmission system similar to that used in this thesis with the aid of the ARIS Decision Making Algorithm (ARIS-DMA). In this network, we consider an ARIS-DMA-aided downlink communication system operating over a THz frequency, where the p^{th} antenna of BS_1 communicates with multiple single-antenna users with the aid of an ARIS-DMA that consists of M elements. In this thesis, we assume that obstacles block the direct links between the BS and the users, as this is the most challenging scenario in conventional communication systems.

To ensure simplicity of presentation and reveal the fundamental design properties, in accordance with the network shown in Figure 5.4, first we demonstrate the network system that considers four blocked users UE_n, one BS, and one ARIS-DMA located on top of building number one B_1, all users are blocked from the BS by obstacles.

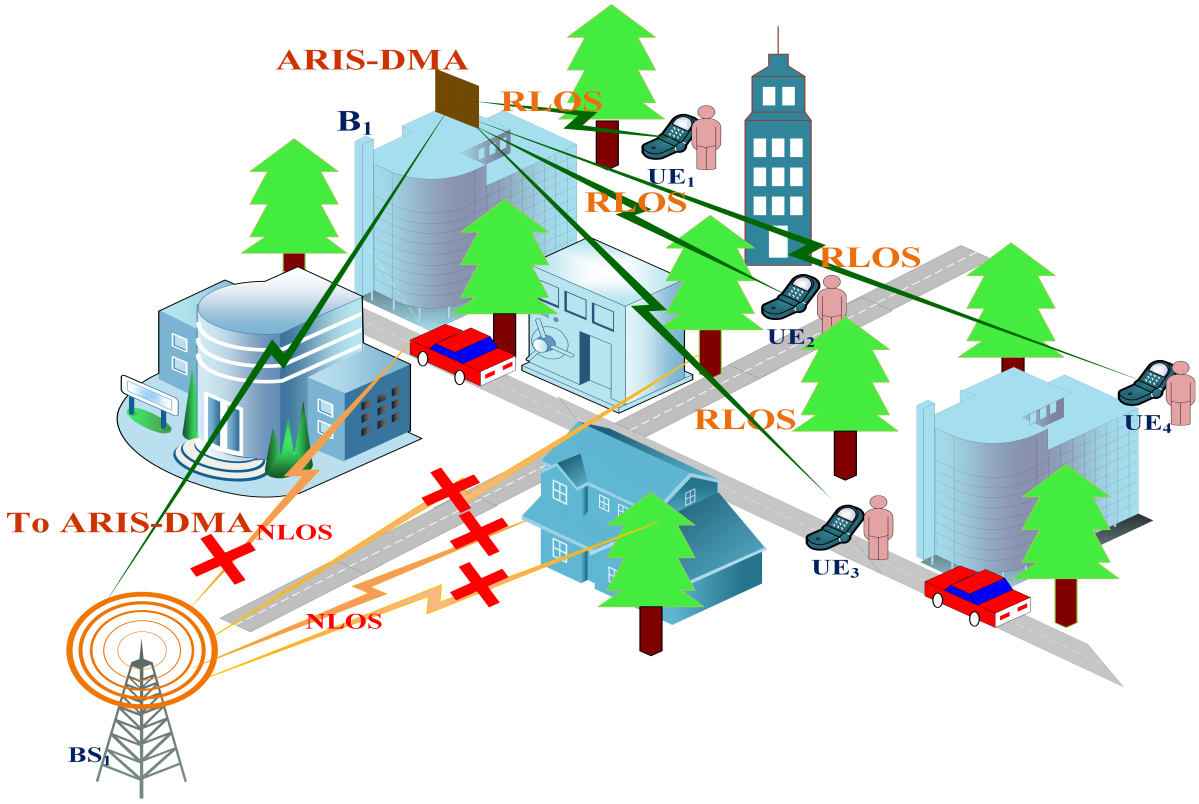

Figure 5.4: Illustration of an ARIS-DMA Aided Downlink Communication System

In Figure 5.4 LOS –> line of sight, RLOS –> redirected line of sight, NLOS –> no line of sight

As a start, we perform an initial test to check the signal redirection in means of transmission and reflection with full power for different angles, indicating different users' locations using MATLAB2024b. As demonstrated in Figure 5.5, where the signal transmission has full signal power with a full beam directed towards the user in the transmission area with different angles and different user locations. Instead of relying on the STAR-RIS feature that splits the system resources between the reflected and transmitted signal, the implemented novel ARIS-DMA directs the signal power in one way towards the intended user. This process allows ARIS-DMA to target users in zero coverage spots, remarkably increasing area coverage and density. On the other hand, using STAR-RIS will not increase network coverage or density because zero coverage spots will remain without coverage as will be seen in Section 5.6.

The new signal redirection, as shown in Figure 5.5, keeps the signal power focused in one direction towards the intended user and does not split the system resources between the transmitted and reflected signal as in the case of STAR-RIS. In order to focus on the maximum performance improvement offered by ARIS-DMA, it is anticipated that the BS will have access to the instantaneous and statistical channel state information $\text{CSI}_{ints,stat}$ for all channels.

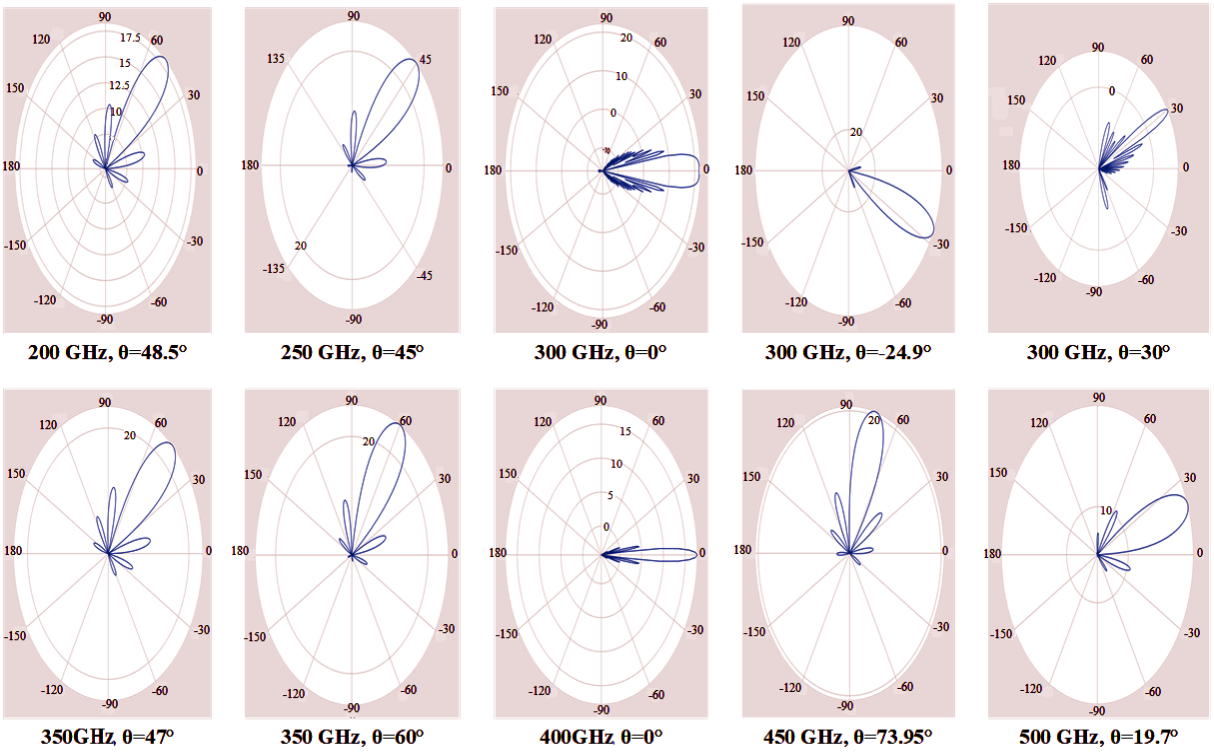

Figure 5.5: Redirecting User Signal with Focused Beamforming

The next step is to optimise the ARIS-DMA, which is designed and controlled by an ARIS-DMA controller to transmit or reflect the incident signals simultaneously based on user location in the network system.

The network in Figure 5.4 shows that the ARIS-DMA is located on top of B_1, and it is designed with M patches, each of which has a $100cm^2$ patch size, with $0.01mm$ of air space between them. Additionally, the mutual ARIS-DMA design parameters which are fixed through the testing process are: the ARIS-DMA element response, $|\Gamma_m| = 0.9$; signal power, $P_s = 45$dBm; wavelength, $\lambda = 0.001$m; ARIS-DMA antenna gain, $G_{ARIS} = 1$; and power radiation parameters, $\varepsilon_r = \varepsilon_t = 0.99$.

All the parameters that are not defined inside the text are identified in Table 5.1, which illustrates the mutual design parameters.

Table 5.1: Mutual model design parameters

Parameter	Definition
M=15	Number of ARIS elements
l_M	$10cm$
N_θ	Number of phase shifts, where $N_\theta = \{0, \ldots, 2n\pi/N_\theta, \ldots, 2(N_\theta-1)\pi/N_\theta\}, 1 \leq n \leq N_\theta - 1$
U^n_{AG}	User antenna gain
S	Power density
Z_{air}	Air impedance
E_r	Electric field
A_e	Effective aperture
A_{ARIS}	ARIS-DMA effective aperture
P_s	Signal power
l^U_{ARIS}	Distance between ARIS-DMA and user
l^{BS}_{ARIS}	Distance between ARIS-DMA and BS
NP^{BS}	BS normalised power radiation
NP^U	User normalised power radiation
$NP^{ARIS,BS}$	ARIS-DMA normalised power radiation from BS
$NP^{ARIS,U}$	ARIS-DMA normalised power radiation to the user
$A_{r,t}$	Signal amplitude response
CSI_{inst}	Instantaneous channel state information
CSI_{stat}	Statistical channel state information
$I_{response}$	Impulse response
DF	Digital filter
FD	Fading distribution
CH_{gain}	Channel gain
R_M	Reflection/transmission coefficient, which equals $\lvert R_M \rvert exp(-j\phi_M) exp(-j\frac{2\pi}{\lambda}(l^{BS}_{ARIS} + l^U_{ARIS}))$

5.2.2 Signal Model

To elaborate on the concept of STAR-RIS, Figure 5.6 shows that the wireless signal incident on the STAR-RIS is divided into transmitted and reflected signals. To characterise the ARIS-DMA features, let S_m denote the signal incident on the m^{th} element of the ARIS-DMA, where $m \in M \triangleq 1, 2, \ldots, M$. The signals transmitted and reflected by the m^{th} element is modelled in Equation 5.2 and Equation 5.3, where $\sqrt{\beta^t_m} \in [0, 1]$, $\theta^t_m \in [0, 2\pi]$ and $\sqrt{\beta^r_m} \in [0, 1]$, $\theta^r_m \in [0, 2\pi]$ are the amplitude and phase shift response of the m^{th} element's transmission and reflection coefficients, respectively. In the practical scenario, the phase shifts (i.e.,θ^t_m and θ^r_m) can be chosen independently of each other.

$$x^t_m = (\sqrt{\beta^t_m} e^{j\theta^t_m}) S_m \tag{5.2}$$

$$x^r_m = (\sqrt{\beta^r_m} e^{j\theta^r_m}) S_m \tag{5.3}$$

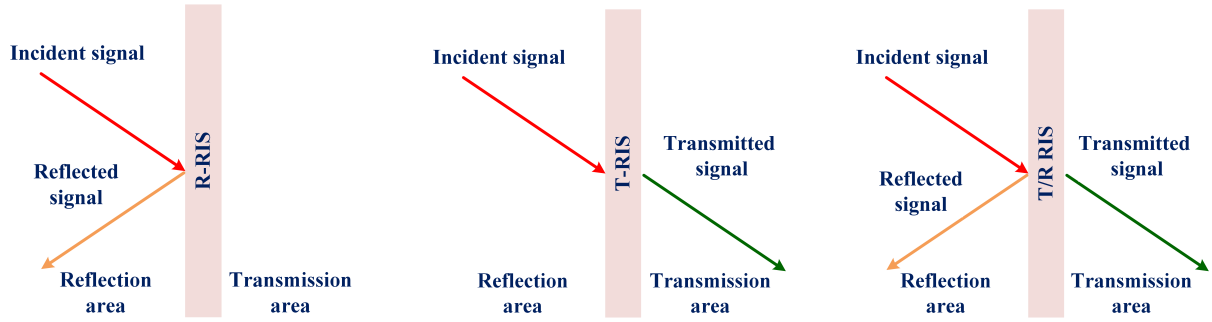

(a) Reflective RIS (b) Transsmisive RIS (c) STAR-RIS

Figure 5.6: Reflection and Transmission Areas

On the other hand, the adjustments for the amplitude coefficient (i.e.,$\sqrt{\beta_m^t}$ and $\sqrt{\beta_m^r}$) for STAR-RIS are coupled. Thus, the sum of the transmitted and reflected signal powers must be equal to the power of the incident signal, which should satisfy each element's condition in Equation 5.4.

$$\beta_m^t + \beta_m^r = 1, \quad \forall m \in \mathcal{M} \tag{5.4}$$

Accordingly, the conventional operating protocol for a STAR-RIS splits the power of the incident signal between the transmitted and reflected signals, with a splitting ratio of $\beta_m^t : \beta_m^r$. In this case, the transmission and reflection coefficient matrices are given as in Equation 5.5 and Equation 5.6, respectively, in which $\beta_m^t, \beta_m^r \in [0,1]$, and $\theta_m^t, \theta_m^r \in [0, 2\pi], \forall m \in \mathcal{M}$. As can be noticed, both coefficients can be optimised, resulting in a higher degree of flexibility in the communication system's design. However, the conventional protocol wastes half of the signal power, resulting in less coverage and higher power loss.

$$\mathbf{\Theta}_t^{\mathrm{ES}} = \mathrm{diag}\left(\sqrt{\beta_1^t}e^{j\theta_1^t}, \sqrt{\beta_2^t}e^{j\theta_2^t}, \ldots, \sqrt{\beta_M^t}e^{j\theta_M^t}\right) \tag{5.5}$$

$$\mathbf{\Theta}_r^{\mathrm{ES}} = \mathrm{diag}\left(\sqrt{\beta_1^r}e^{j\theta_1^r}, \sqrt{\beta_2^r}e^{j\theta_2^r}, \ldots, \sqrt{\beta_M^r}e^{j\theta_M^r}\right) \tag{5.6}$$

5.2.3 Channel Model

As mentioned in Section 5.2.1 and illustrated in Figure 5.6, the utilisation of the standard STAR-RIS in its present state inevitably leads to a 50% loss in signal power, reducing the coverage area during transmission. This is in contrast to the ARIS-DMA technique presented in this thesis. To provide a clear and concise explanation of the new ARIS-DMA, the channel model must be clarified first. This channel model adjustment is crucial for assessing the effectiveness ARIS-DMA network.

Let H be the channel matrix between the BS and the users, and $[H]_{n,p} \triangleq h^{(n,p)}$ be the gain from the BS p^{th} antenna to the user n. Path loss, fast fading, and ARIS-DMA responses are considered when modelling the channel. Then, the single channel model between the m^{th} ARIS-DMA element and the BS p^{th} antenna and user n is given by:

$$\hat{h}_m^{(n,p)} = \sqrt{\alpha_m^{(n,p)}} g_m^{(n,p)} \Gamma_m^n \tag{5.7}$$

where $\alpha_m^{(n,p)}$ represents path loss, $g_m^{(n,p)}$ is the fading coefficient with zero mean and independent unit variance for different ARIS-DMA channels, and Γ_m^n represents the ARIS-DMA element response.

The path loss $\alpha_m^{(n,p)}$, on the other hand, is modelled as in Equation 5.8, where λ is the wavelength, G represents BS antenna gain, γ is the path loss exponent, F_m^p is the radiation power at the m^{th} ARIS-DMA element which is received from the p^{th} BS antenna, F_m^n is the signal power radiation from the m^{th} ARIS-DMA element to the user n, G_{ARIS} is the ARIS-DMA antenna gain, and D_m^p is the distance between the BS and ARIS-DMA, and D_m^n is the distance between the ARIS-DMA and user.

$$\alpha_m^{(n,p)} = \frac{\lambda^2 G {l_M}^2}{M} \frac{G_{ARIS} F_m^p F_m^n}{(D_m^p D_m^n)^\gamma} \tag{5.8}$$

The effect of user location and angle with respect to the BS and ARIS-DMA is elucidated by modelling and measuring the signal power radiation as in Equation 5.9 and Equation 5.10, respectively. In Equation 5.10, determining the ε value depends on the user's location in the transmission or reflection area.

$$F_m^p = \cos^2 \theta_m^p G_{ARIS} \tag{5.9}$$

$$F_m^n = \cos^2 \theta_m^n \varepsilon_{(t,r)} \tag{5.10}$$

Accordingly, by aggregating the effect of all M ARIS elements we can separate the average path loss as a common factor from the channel effects, thus, Equation 5.7 can be expressed as in Equation 5.11, with an average value of path loss and summation of the channel effects.

$$h^{(n,p)} = \sum_{m=1}^{M} \hat{h}_m^{(n,p)} = \sqrt{\hat{\alpha}^n} \sum_{m=1}^{M} g_m^{(n,p)} \Gamma_m^n \tag{5.11}$$

5.3 Adaptive Reconfigurable Intelligent Surface Decision Making Algorithm (ARIS-DMA)

In this section, we describe the decision-making algorithm introduced into the ARIS-DMA controller to enable the adaptive ability of ARIS elements to transmit and reflect the incident signal simultaneously. This algorithm models the incident signal moving towards the intended user without wasting 50% of signal power. The details of the developed algorithm are summarised in Algorithm 2, where the user location d_{ue} from the BS is the main factor determining the allocated power of transmission or reflection in this thesis. Accordingly, this decision will be affected by the user's location according to the ARIS-DMA, defined as $D_{p(trans,ref)}$. As the targeted validation specification for network communication in this thesis is to provide a higher coverage area, including the zero coverage spots users. Referring to the network in Figure 5.4, it can be noticed that the communication link between U_1, U_3, U_4, and BS_1 is obstructed by different types of obstacles.

Algorithm 2 Proposed ARIS-DMA function decision making

Determine CSI_{inst} and CSI_{stat} for the network between BS_n and U
$CSI_{inst} = vec(I_{response}, DF, d_{ue})$
$CSI_{stat} = vec(FD, CH_{gain}, d_{ue}, LoS)$
if U in reflection area **then**
  while $D_{pref} = 1 \& D_{ptrans} = 0$ **do**
calculate $P_{opposite}$
Ensure: $P = P_r$
    $x_r = P_r A_r . \eta_{ARIS} e^{j\theta_r} x_n$
  end while
else$U$ in transmission area
  while $D_{pref} = 0 \& D_{ptrans} = 1$ **do**
calculate $P_{opposite}$
Ensure: $P = P_t$
    $x_t = P_t A_t . \eta_{ARIS} e^{j\theta_t} x_n$
  end while
end if

At first, CSI_{ints} and CSI_{stat} are shared between the BS and ARIS-DMA controller, in which the CSI_{ints}, contains the exact user location in regard to the continuous movement from the BS and ARIS-DMA. In the communication system network, the BS and ARIS-DMA are always fixed, resulting in direct calculation of the user exact location in reference to the ARIS-DMA at the ARIS-DMA controller (i.e.,$D_{p(trans,ref)}$).

On the other hand, CSI_{stat}, known as the long-term CSI, will always share information with the ARIS-DMA controller about the possibility of the existence of an LoS with the ARIS-DMA in order to update the decision process.

Based on the information shared between the BS and the ARIS-DMA controller and the user location data obtained from both, the signals received by the user can be written as in Equation 5.12 and Equation 5.13, in which they depend on the user being in the transmission or reflection area, respectively.

$$x_t = 2PA_t\eta_{ARIS}e^{j\theta_t}x_n \tag{5.12}$$

$$x_r = 2PA_r\eta_{ARIS}e^{j\theta_r}x_n \tag{5.13}$$

The x_n represents the intended signal for the user n, where, for simplicity of clarification, $n = 1:4$, referring to the network in Figure 5.4.

The characteristics of the redirected signal for transmission and reflection are modelled in accordance with ARIS-DMA space wave impedance η_{ARIS} and the user location from the BS d_{ue} as in Equation 5.14, where θ_i, $\theta_{r,t}$ are the incident and reflected or transmitted signal phase shifts, respectively, and η_0 is the space wave impedance constant.

$$\eta_{ARIS} = j\frac{\eta_0}{\cos\theta_i}\cot\left(\frac{(\sin\theta_i - \sin\theta_{r,t})}{2}\right).d_{ue} \tag{5.14}$$

As indicated in Equation 5.12 and Equation 5.13, the signal delivered to the user is associated with the power value P; modelling this value is the most important part of the ARIS-DMA's functionality. As in the conventional STAR-RIS, the power term is divided into two parts, one for transmission and the other for reflection, and as stated in Equation 5.4, this means P can be rewritten as in Equation 5.15.

$$P = P_t + P_r \tag{5.15}$$

To model the signal power in an adaptive manner, the location of the user in regard to the ARIS-DMA is considered in the power calculation; thus, Equation 5.15 is recalculated as in Equation 5.16, where the value of the factors $D_{p(trans,ref)}$, depends on the user location derived from the ARIS-DMA, will set one of the equation parts to zero. Substituting these values in Equation 5.15 and Equation 5.16 and extracting the second term power signal on the opposite side to $P_{opposite}$, which equals (SA_eA_t) in the case of reflection and (SA_eA_r) in the case of transmission.

$$P = (S \times \mathrm{A}_e \times D_{ptrans} \times A_t) + (S \times \mathrm{A}_e \times D_{pref} \times A_r) \tag{5.16}$$

$$P_t = (S \times \mathrm{A}_e \times D_{ptrans} \times A_t) + P_{opposite} \tag{5.17}$$

$$P_r = (S \times \mathrm{A}_e \times D_{pref} \times A_r) + P_{opposite} \tag{5.18}$$

As a result of remodelling the signal power using the suggested power allocation, the power for transmission and reflection will follow Equation 5.17, and Equation 5.18, in which the full signal power will be allocated for either the transmitted or reflected signal simultaneously, keeping in mind the fact that the transmitted and reflected signals are calculated in accordance to Equation 5.12 and Equation 5.13 respectively, will direct the signal for the intended user depending on θ_t and θ_r, where $S = \frac{|E_r|}{2Z_{air}}^2$, and $A_e = U_{AG}\frac{\lambda^2}{4\pi}$, in which the signal electric field E_r and the normalised radiation power NP are calculated in Equation 5.19 and Equation 5.20, respectively.

$$E_r = NPR_M\sqrt{2Z_{air}P_sU_{AG}^n A_{ARIS}G_{ARIS}} \tag{5.19}$$

$$NP = \frac{\sqrt{NP^{BS}NP^{ARIS,BS}NP^{ARIS,U}NP^{U}}}{4\pi l_{ARIS}^{BS} l_{ARIS}^{U}} \tag{5.20}$$

5.4 Implementation Scenarios

For ease of explanation, the downlink communication network in Figure 5.4 is explained first for three performance evaluation scenarios:

1. **zero to a few obstacles**
2. **few to moderate obstacles**
3. **moderate to many obstacles**

The communication network consists of four users referred to as U_1, U_2, U_3, and U_4, one BS referred to as BS_1, and one ARIS-DMA located on top of a building referred to as B_1. As the network experiences different obstacle densities, users' locations are set in accordance to represent the three scenarios; U_3 is considered as the first scenario, U_4 is considered as the second scenario, and U_1 and U_2 are considered as the third scenario.

It is important to note that the actual performance test results used Table 5.2 parameters and are compared against STAR-RIS and BS handover in this thesis, as it is demonstrated in Section 5.6.

5.4.1 Zero to a Few Obstacles

In this scenario, there exists a LoS between BS_1 and U_3 but with few obstacles; in the case of fast movement or high winds, the network will suffer from high interference

and attenuation of the downlink signal. Although the BS's signal provide high signal quality and minimal latency, optimising the signal routes through the ARIS-DMA on top of B_1 will increase communication reliability with respect to higher interference and attenuation. However, using the STAR-RIS will provide the user with the signal but at the cost of signal quality and latency overhead. This is because STAR-RIS can only serve one user at a time to transmit or reflect the signal efficiently. In the current example, there is only one user, but in the case of multiple users, this will result in a higher delay time. On the other hand, using the current BS handover mechanism will generate 10% higher delay as discussed in Section 5.6.

5.4.2 Few to Moderate Obstacles

The effect on downlink communication becomes more noticeable when moving to locations with more obstacles or obstacles of intermediate height. Barriers such as buildings or trees cause signal reflections, diffraction, and partial obstructions. In this scenario, U_4 is located in a zero-coverage spot, where there is NLoS with respect to BS_1. The first solution comes to the mind in order to provide U_4 with coverage is to use BS handover to do that. While adopting BS handover will provide the user with their intended signal providing coverage, the transmission delay will be extremely high; this is because finding a different BS with a LoS with U_4 will cause extra overload in the network in terms of time, power loss, and signal error rate .

On the other hand, using the STAR-RIS holds the possibility to provide U_4 with their intended signal. However, there is a high level of power loss with moderate coverage, due to the fact that STAR-RIS as shown in Figure 5.3 is operating in either of the three protocols, which as a result will cause higher resources degradation in time and energy. Additionally, the long distance between the user and the STAR-RIS is causing a higher concern about signal degradation because signal diffraction and scattering. Alternatively, the continues movement of the user will make it harder for the STAR-RIS to adopt the synchronisation in a proper way to provide the user with their intended signal; as a result, this will affect the coverage area and reduce it.

During such situations, the ARIS-DMA adapts its surface configuration in real-time to minimise the impact of obstacles, optimising the transmission routes and compensating for any signal degradation. The new decision making protocol will enable the ARIS-DMA to transmit and reflect the incident signal simultaneously without any power loss.

Notably, the ARIS-DMA successfully remodels the signal power and phase and then redirects the signal to U_4 while the user is in the transmission area. It can be noticed here that the main focus is on the transmission area because the current state-of-the-art system splits the signal power in the STAR-RIS, which is the main drawback. The ARIS-DMA solves this drawback effectively and surpasses the STAR-RIS, especially in

accordance with the new wireless communication generation, 6G KPIs. Notwithstanding the difficulties, the system consistently sustains dependable downlink transmission, utilising the ARIS-DMA adaptability to improve the signal's strength and overcome insignificant obstacles.

5.4.3 Moderate to Many Obstacles

The last and most realistic wireless communication system scenario is an area with a high density of obstacles; downlink communication faces increased complexities in environments characterised by dense obstacles, such as urban areas with tall buildings or densely wooded regions featuring reflections, shadowing, and multipath fading impeding the signal propagation.

In accordance with the described area in Figure 5.4, U_1 and U_2 are located in highly obstacle-dense area with NLoS between users and BS_1. In the downlink scenario, BS_1 fails to send the signals to their intended users; instead, BS_1 sends the signals to the ARIS-DMA element on top of B_1; the ARIS-DMA controller will analyse the incident signals using Algorithm 2 and redirect the signals towards U_1 and U_2 with full transmission power, resulting in a 100% coverage area.

The ARIS-DMA employs the novel iterative algorithm to actively and simultaneously reconfigure the incident signal, creating focused signal paths and minimising the impact of obstacles on signal strength. By adopting the ARIS-DMA, the downlink communication remains robust, ensuring effective data delivery to the user devices despite the challenges posed by the obstacle-dense environment. As the stated examples mention only four users, the real-time test and performance analysis, which are shown in Section 5.6, prove the superiority of the proposed ARIS-DMA approach using the performance evaluation test parameters in Table 5.2, with higher and different density levels and a varied range of THz frequencies, making it a promising approach for deployment in 6G networks with THz applications.

5.5 Performance Indicators

This section provides an illustration of the performance metrics that we utilised in order to evaluate the differences between the performance of ARIS-DMA, BS handover, and STAR-RIS.

5.5.1 Power Loss

In communication networks, power loss refers to the reduction in signal power as it propagates through the network components, such as cables, connectors, splitters, amplifiers, and other devices. The power loss is quantified in (dBm) which represents

power levels relative to one milliwatt (mW) and can occur due to various factors including attenuation, dispersion, impedance mismatches, scattering, and packet loss. To calculate power loss in a communication network, we need to know the, total power P, the initial power for the transmitted signal P_{ts}, and the power for the received signal P_{rs} at the user. First, we calculate the power loss in dB as follows:

$$PL\,(dB) = 10 \times \log\left(\frac{P_{ts}}{P_{rs}}\right) \tag{5.21}$$

then the power loss in dBm is calculated in respect to power loss in dB as in Equation 5.22.

$$PL\,(dBm) = PL\,(dB) + Reference\ Power\ level\,(dBm) \tag{5.22}$$

given that the reference power level for dBm is 0 dBm, Equation 5.22 is rewritten as in Equation 5.23.

$$PL\,(dBm) = PL\,(dB) \tag{5.23}$$

5.5.2 Delay

Delay in communication network systems refers to the duration required for data packets to travel from a source node to a destination node. This measure is crucial and significantly impacts the performance and user experience of several network applications, such as real-time communication, multimedia streaming, and data transfer.

In order to calculate the total delay in the communication network system there are four types of delay that must be taking into consideration.

1. **Queuing Delay (Q_D):** Queueing Delay depends on factors such as network congestion, packet arrival rate, and queue management policies and is measured empirically using network simulation.
2. **Processing Delay (Pr_D):** Processing Delay depends on the processing capabilities of network devices and the complexity of packet processing tasks. It is typically measured in microseconds or milliseconds
3. **Transmission Delay (T_D):** $T_D = \frac{Packet\ Size}{Transmission\ Rate}$
4. **Propagation Delay (P_D):**$P_D = \frac{Distance}{Propagation\ Speed}$

Thus the overall system delay is calculated as follows:

$$D = Q_D + Pr_D + T_D + P_D \tag{5.24}$$

5.5.3 User Coverage

User coverage in a communication network corresponds to the degree to which users inside the network area possess dependable access to the network services or resources. Network connectivity success rate is a metric that quantifies the percentage of users who are able to establish a connection to the network and have adequate communication performance. Calculating user coverage involves assessing the spatial distribution of users within the network coverage area and determining whether each user can establish a connection with sufficient signal strength, quality, and no packet loss.

The user coverage is calculated as in Equation 5.25

$$User\ Coverage\,(\%) = \left(\frac{Number\ of\ Users\ with\ Reliable\ Connection}{Total\ number\ of\ Users}\right) \times 100 \quad (5.25)$$

5.5.4 Failed Signal Rate (FSR)

FSR is a quantitative metric employed to assess the dependability of a communication system, specifically in signal-switched networks. It denotes the likelihood that a transmitted signals would be received with errors or lost during the process of transmission. In this thesis our main focuses is to calculate the FSR in regards to the lost signal during the transmission process.

To calculate the FSR, we typically need to know two main parameters: the number of transmitted signals N and the number of lost signals E, so the FSR is calculates as in Equation 5.26.

$$FSR = \frac{E}{N} \quad (5.26)$$

5.5.5 System Efficiency

In order to conduct the ARIS-DMA efficiency in this thesis we conduct a set of replicated tests with identical operating settings and features to assess the accuracy of the ARIS-DMA results.

5.6 Performance Analysis

In this section, as depicted in Figure 5.7 to Figure 5.12, we characterise the FSR, power loss, user coverage, delay, and system efficiency associated with the new ARIS-DMA in Section 5.3. As illustrated in Section 2.3 the performance measures must adhere to the requirements of the new wireless generation 6G. The performance analysis process

considers the implantation scenarios in Section 5.4 with the validation parameters as illustrated in Table 5.2.

Table 5.2: Performance evaluation test parameters

Parameter Name	Value
User density (km^2)	3×10^6 9×10^6 16×10^6
THz frequency (GHz)	300 400 500

We initially analysed the performance of cooperative STAR-RIS and BS-BS handover systems before investigating the performance of the ARIS-DMA and comparing the three. The performance analysis considers a highly dense user area, with 80% of the users having NLoS with respect to the BS.

As one of the objectives in this thesis is to provide a convenient solution for the power loss problem caused by the STAR-RIS in the previous wireless generation 5G. In order to comply with the KPIs in Section 2.3, we characterised the THz frequency band (300-500) GHz for the evaluation process, because 6G is anticipated to work with this range of frequencies as shown in Figure 2.3.

First, lets examine the amount of signal power loss with 300 GHz and variation of user density with of 16×10^6. As shown in Figure 5.7. It can be seen that as the number of users goes higher, ARIS-DMA shows a stable performance with a maximum loss of 1.71 dBm at 7×10^6 user density while at the same density level the power loss in STAR-RIS equales to 16 dBm, a result that fits perfectly with the objective in this thesis. To be more precise, ARIS-DMA performs better than the STAR-RIS as the tested area becomes denser, when the simulation reaches the maximum user density, the ARIS-DMA shows only 0.33 dBm signal power loss. On the contrary, using the STAR-RIS shows 10.95 dBm power loss. On the other hand, BS-BS handover performance shows relatively better results than the STAR-RIS at first, since the handover process does not split the signal power between two signals. However, as the user density gets higher the power loss can reach 24 dBm when the user density is approximately 9×10^6. The BS-BS handover shows an incremental power loss performance. The power loss in BS approach can result from degradation, scattering, diffraction, and signal reflections. Table 5.3 summarises a comparison of power loss for different user density levels with 300 GHz.

As the frequency goes to higher level of 400 GHz and 500 GHz, the ARIS-DMA approach exhibits a consistently low power loss across all user densities and frequency bands. Even at increased user densities 16×10^6 users, power loss stays under 5 dBm, indicating exceptional energy efficiency. As can be noticed, the STAR-RIS exhibits power loss variations between 5 dBm and 25 dBm at 300 GHz as user density increases.

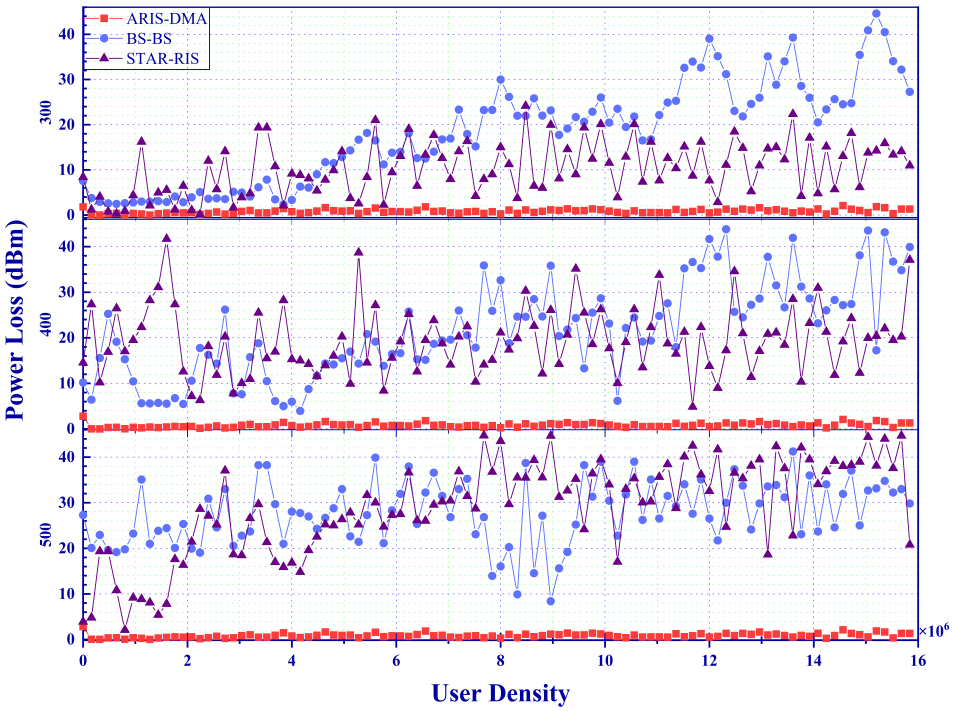

Figure 5.7: Power loss comparison levels

At 400 GHz, power loss exceeds to an average of 37 dBm in high-density conditions. This performance stays consistent, at 500 GHz the power loss ranges between 5 dBm to 30 dBm at lower densities, but escalates significantly to 44 dBm with high user density.

Additionally, BS-BS direct transmission has the lowest efficiency. The BS-BS approach demonstrates the most power loss of the three approaches. At 300 GHz, power loss ranges from 5 dBm to 45 dBm, while BS-BS approach shows better performance with lower user density the power loss escalates with higher user density. At 400 GHz and 500 GHz, power loss often exceeds 40 dBm in areas with high user density, where the losses are inconsistent, ranging from 20 dBm to 45 dBm, rendering it the least power-efficient alternative.

Table 5.3: Power loss comparison in (dBm)

Density	ARIS-DMA	STAR-RIS	BS-BS
3×10^6	0.13	3.94	5.14
6×10^6	0.76	9.45	14
9×10^6	0.64	8.1	23.5
16×10^6	0.33	10.95	27.26

The second performance metric used in this thesis is the delay, an important factor that affects the communication system very badly when introducing new approaches. In any communication system the newly introduced approach should not put an extra burden than the current used approaches.

Figure 5.8 shows a comparison between the ARIS-DMA presented in this thesis, STAR-RIS and BS-BS handover transmission approaches. The conducted results is for the maximum user density of 16×10^6 with the three set of frequencies 300 GHz, 400 GHz, and 500 GHz for maximum of 100 transmissions.

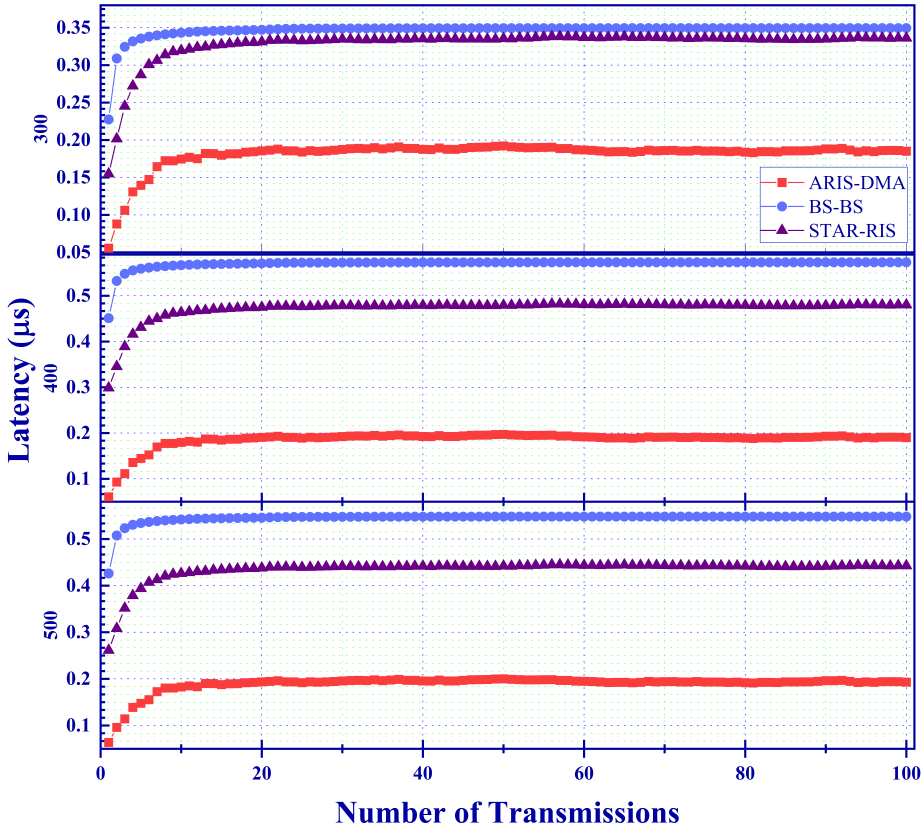

Figure 5.8: System delay comparison

As noticed, all three tested approaches shows steady performance for time usage, however there is a remarkable performance difference achieved by ARIS-DMA. ARIS-DMA minimised the latency by 45% compared to STAR-RIS and 47% for BS-BS handover, respectively for 300 GHz. While STAR-RIS and BS handover can provide relatively low delay level working with 6G wireless communication, ARIS-DMA outperform this level by $0.16\mu s$ in case of BS handover, and $0.15\mu s$ in STAR-RIS case.

Another objective in this thesis as illustrated in Section 1.3 is to solve the current problem of zero coverage spots that all wireless generations still affected by them, which as a result still causing limited coverage services. Figure 5.9 shows a comparison in terms of the coverage area between ARIS-DMA, STAR-RIS, and BS handover for three different THz frequencies as the tested area experiencing different user density levels.

If we took the chance first to stop over the performance of ARIS-DMA at the frequency of 300 GHz. It is noticed that ARIS-DMA successfully provide 100% coverage, it is important to remark that all the users were randomly distributed and 80% of the users

have NLoS with the BS. ARIS-DMA analysis the user location and redirect the signal towards the user, this will provide users with NLoS with full coverage. Comparing the obtained results from ARIS-DMA with the results obtained from BS handover, there is an enhancement in coverage area by 26%. Defiantly the BS handover can provide high level of coverage, however this approach can only provide a maximum 74% coverage in highly dense area. As we were observing the test we noticed that signal congestion in this case is high which as a result leads to high level of diffraction and signal fading.

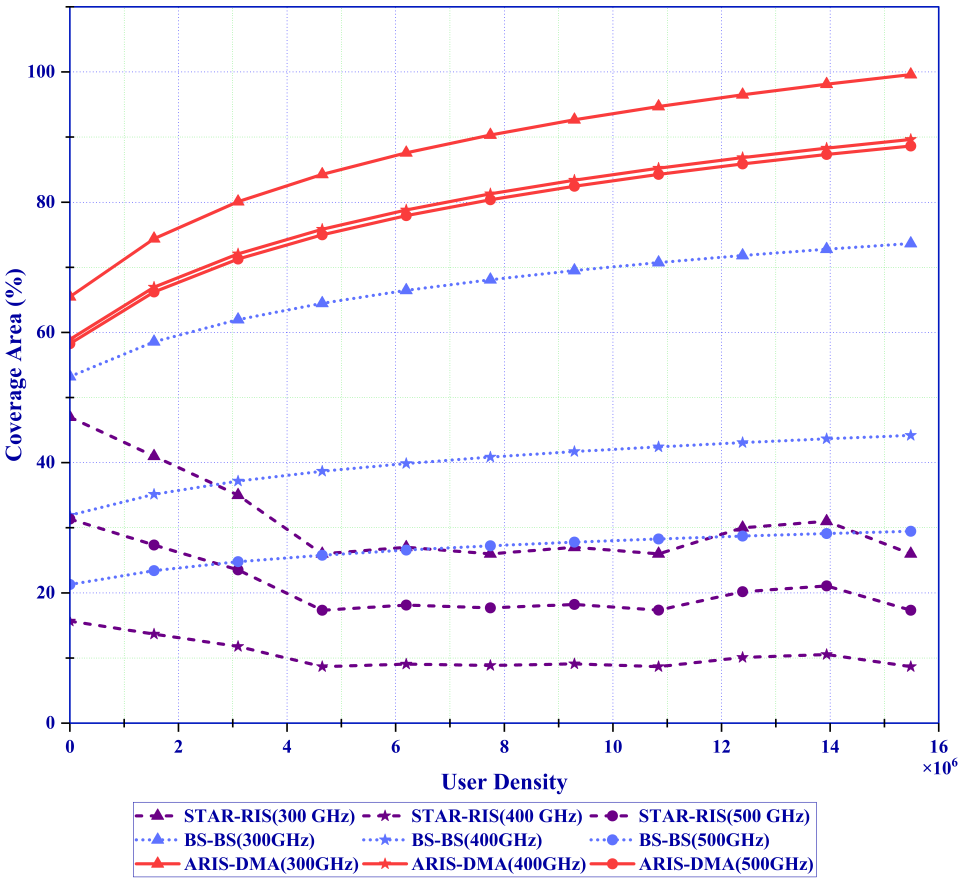

Figure 5.9: Comparative analysis of coverage area

Moving to the STAR-RIS performance for the same operating frequency, it is evident that the maximum coverage area that STAR-RIS can provide is only 26%. However, at the beginning of the simulation test the coverage area provided was approximately 50%, this performance starts to degrade as the number of users increase. This degradation is due to the fact that if the users are in a zero coverage spot area, and the distance between users and STAR-RIS is relatively long, the power associated with the signal will fade before reaching the intended user because STAR-RIS transmit the signal with half of the power as the STAR-RIS divides the signal in order for the signal to be transmitted to the user located in the transmission area.

On the contrary, the ARIS-DMA successfully managed to provide approximately 100% coverage with exactly 99.5% coverage under the same conditions. This superiority

highlights the importance of ARIS-DMA whether the user is located in the transmission or reflection area. Also, it can be noticed that the BS-BS handover performance is moderate between the ARIS-DMA and the STAR-RIS, with exactly 74% coverage; this, on the other hand, proves that the ARIS-DMA successfully outperformed the current state-of-the-art transmission approaches. As we analysed the performance of ARIS-DMA for higher THz frequencies,Table 5.4 summarises the simulation results for the different frequencies used with different user densities.

Table 5.4: User coverage comparison

Frequency (GHz)	ARIS-DMA	STAR-RIS	BS-BS
300	80%	35%	61.9%
400	72%	11.7%	37%
500	71%	23.5%	24.7%

(a) User Density=3×10^6

Frequency (GHz)	ARIS-DMA	STAR-RIS	BS-BS
300	92.6%	27%	69.5%
400	83.3%	9%	41.7%
500	82.4%	18.2%	27.8%

(b) User Density=9×10^6

Frequency (GHz)	ARIS-DMA	STAR-RIS	BS-BS
300	99.5%	26%	73.6%
400	89.6%	8.6%	44%
500	88.6%	17%	29%

(c) User Density=16×10^6

Furthermore, as the communication system being tested operates in places with a high number of users and obstacles, we calculated FSR, which computes the total number of undelivered signals to users in regard to the total number of signals that were meant to be delivered to users. In order to calculate the FSR we used PCSC channel code presented in Section 3.3. The results of FSR indicate that the ARIS-DMA outperformed the STAR-RIS and BS approaches, as shown in Figure 5.10 and Figure 5.11, for different user densities and THz frequencies.

First, we measured the FSR for different user densities in order to gain a clear idea of the ARIS-DMA performance stability. As shown in Figure 5.10, using the ARIS-DMA in the network with a user density of 3×10^6 under 300 GHz operating frequency gives a 12dB channel gain compared to the STAR-RIS and BS-BS handover. Moreover, the performance of the STAR-RIS relatively matches the performance of BS handover at the lowest density tested.

Moving to the next density level of 9×10^6 users, the ARIS-DMA and BS-BS handover approximately show the same performance, with only 1dB channel gain achieved by the ARIS-DMA; oppositely, the channel gain achieved by the ARIS-DMA reaches 13dB compared to STAR-RIS.

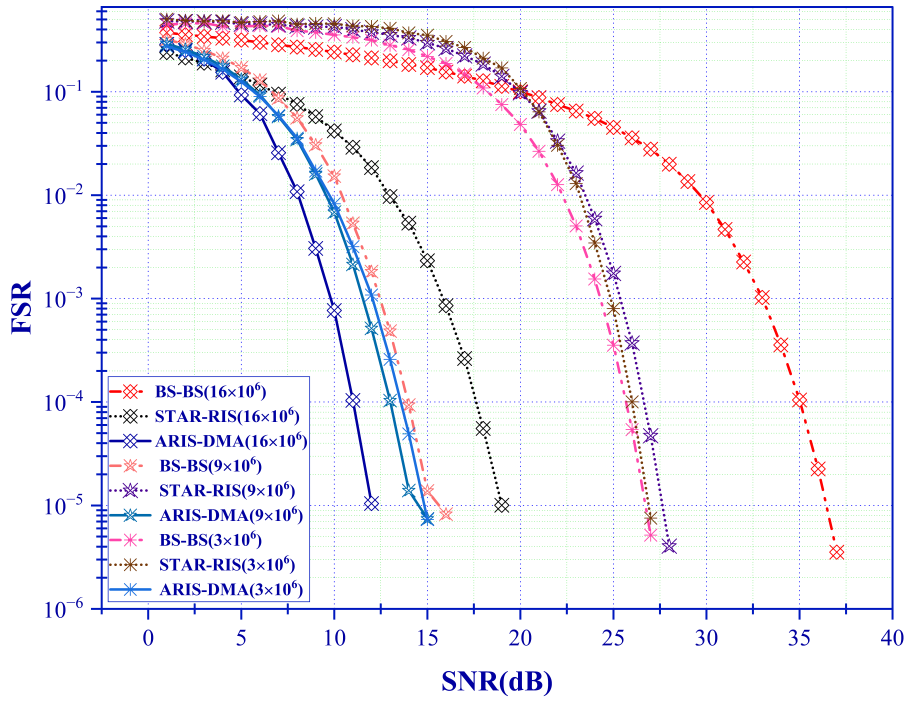

Figure 5.10: FSR comparison for different user densities and 300 GHz

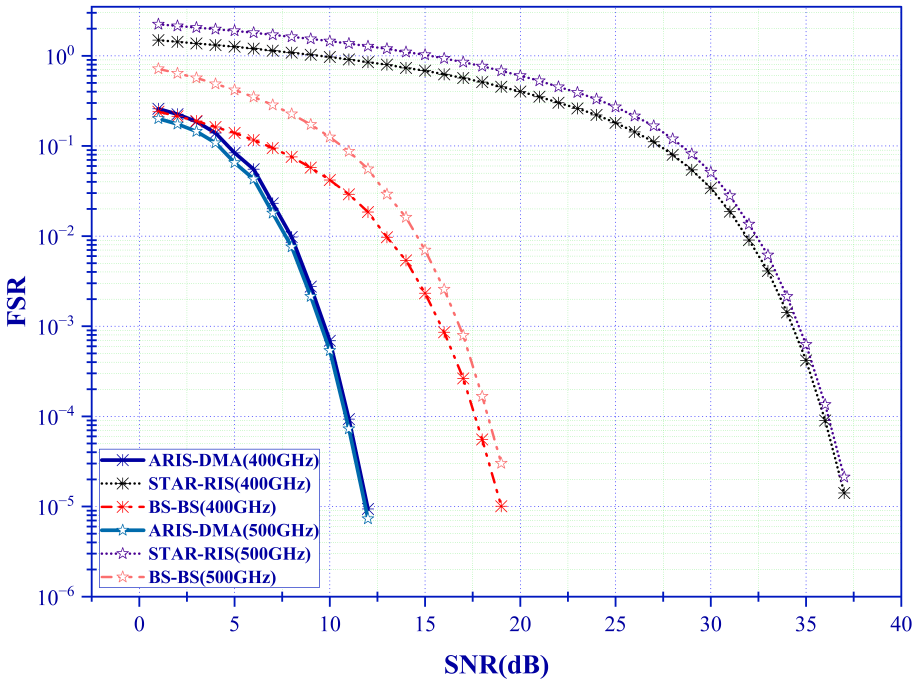

Figure 5.11: FSR comparison 16×10^6 users density

As the ARIS-DMA performance should satisfy the requirement of 6G wireless generation, a higher density level must be taken into consideration, with 16×10^6 user. In Figure 5.10, as the density increased, the performance of both STAR-RIS and BS-BS handover dropped. In this regard, the achieved channel gain for ARIS-DMA reaches 25dB compared to BS-BS and 10dB compared to STAR-RIS. These promising results motivate the analysis of the ARIS-DMA performance for 400 and 500 GHz, which is shown in Figure 5.11. It is evident from Figure 5.11 that the ARIS-DMA has stable excellent performance compared to STAR-RIS and BS-BS handover, achieving 26dB and 8dB channel gain, respectively.

Achieving stable ideal performance in wireless communication is crucial to ensure a consistent and satisfactory user experience. So far in this Section 5.6, the reliability, coverage area, energy efficiency objectives stated in Section 1.3 is addressed using ARIS-DMA and PCSC.

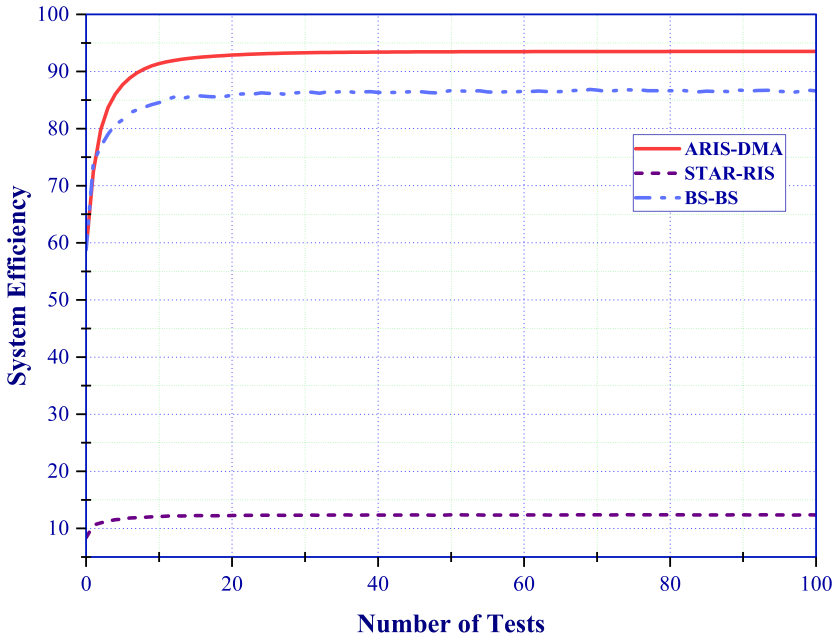

Figure 5.12: Overall system efficiency

Additionally, in this thesis we conducted an additional performance evaluation analysis to validate the efficiency of the ARIS-DMA aided wireless communication system. To confirm the consistent and dependable performance of the ARIS-DMA, taking into account the aforementioned validation metrics, we conducted 100 repeated tests with identical operating settings and features to assess the accuracy of the results. As depicted in Figure 5.12, the ARIS-DMA exhibits system dependability and stability of 95%, whereas STAR-RIS only maintained system reliability of 11% during these tests. Implementing the ARIS-DMA in the wireless communication system led to a significant increase in wireless communication efficiency of 84%. It is important to note measuring the system efficiency is based on conducting the same results with (±0.5) uncertainty.

5.7 Discussion

In this chapter, we have developed an aided wireless communications system with ARIS-DMA for 6G communication, in order to provide a reliable, unlimited coverage, minimal power loss communication system. The effectiveness of ARIS-DMA, which integrates low cost and effective RIS with the modification of transmission and reflection properties to provide the maximum user coverage especially in the transmission area and the user in zero coverage spots.

ARIS-DMA, has been demonstrated in the frequency range of the 6G communication system while achieving THz data rates. ARIS-DMA achieves maximum coverage of 100%, surpassing the current state of art approaches STAR-RIS and BS handover. The performance indicators demonstrate that ARIS-DMA can achieve lower power loss reaches 80% and high coverage area of 100%. Moreover, ARIS-DMA achieves lower delay by 50% and maximum reliability of 25dB channel gain. This has been achieved with system efficiency reaches 95%.

The novel idea of a ARIS-DMA is to eliminate the signal power loss and limited coverage area of the conventional STAR-RIS and the high delay of BS handover. ARIS-DMA use the exact user location to provide the user with the coverage with maximum power. The aforementioned results highlight the potential and effectiveness of using ARIS-DMA for 6G and its diverse range of applications.

6

Deep Learning for enhanced aris beamforming

This chapter introduces deep learning Q network introduced as Deep Q Network ARISDMA (DQN-ARISDMA). Section 6.1 showcase the beamforming techniques used in wireless aided STAR-RIS system in relation to Chapter 5. Next, in Section 6.2, interpretation of the system model are described. The subsequent Section 6.3 comprehensively describes the performance indicators that validate the superiority of the DQN-ARISDMA. In Section 6.4, the performance evaluation and comparison of DQN-ARISDMA for 6G will be discussed in relation to the existing state of the art.

6.1 Fundamental Beamforming Techniques for RIS

The fundamental aspect of RIS groundbreaking technology revolves around signal redirection and beamforming. Beamforming is a crucial technique in wireless communication that improves the SNR of received signals, eliminates unwanted interference, and directs transmitted information to specific places [468].

Conventional Semi Definite Relaxation (SDR), Maximum Ratio Transmission (MRT), and Minimum Mean Square Error (MMSE), are well-established approaches in the field of beamforming [469]. SDR, known for its inherent simplicity, aims to reduce interference, which refers to the disruption of a signal by other signals, by using transmission signals that are orthogonal to each other. The MRT approach, on the other hand, employs the principle of maximising the SNR, which is a measure of the strength of a signal relative to the background noise, at the receiver, hence providing robustness in situations characterised by elevated levels of noise [470]. The MMSE technique is a complex method that seeks to decrease the average squared difference between the desired and received signals. This methodology offers superior reliability in comparison to alternative methods and is commonly used in array processing applications, which involve the manipulation of signals in an array of sensors [471].

The effectiveness of these traditional methods has been impressive in previous generations of wireless communication. However, the unique challenges presented by 6G require a reconsideration of their viability. It is crucial to implement an updated beamforming approach to satisfy the demands of 6G, which include increased data throughput, reduced latency, and adaptability to changing network conditions.

In recent years, ML has demonstrated superior capabilities in resolving irregular network communication problems and expediting computational processes compared to traditional iterative methods. Advanced ML techniques, including Deep Deterministic Policy Gradient (DDPG), Proximal Policy Optimisation (PPO), and Convolutional Neural Networks (CNN), are the most essential in optimising the control and configuration used with ARIS for improved wireless communication performance in the context of beamforming. While these methods in its current form offer significant advantages for beamforming with ARIS, they also have certain disadvantages. For example but not limited to, sample inefficiency, parameter sensitivity, stability issues, high computational cost, implementation complexity, overfitting, high latency.

Still the use of Deep Q Network (DQN) if done properly has the potential to revolutionise beamforming in 6G communication by learning from past experiences and dynamically optimising resource allocation in real-time situations [472, 473].

Currently, there have been several works investigating the use of DQN with STAR-RIS, but these works are not limited to the ones mentioned in this thesis, [122, 472, 474–488].

6.2 System Model and Interpretation

6.2.1 System Model

As shown in Figure 6.1, a RIS assisted multi-user downlink network is considered, where the RIS equipped is the developed ARIS-DMA in Chapter 5, with (M) horizontal and (L) vertical patches, in which they form (H) ARIS-DMA surface, and one BS with (A) antennas provides services to (N) users. The locations of BS, ARIS-DMA are fixed, and users are randomly distributed and moving over Rician channel. The received signal at the (N_{th}) user is a result of a superposition between the signal from BS to ARIS-DMA and the signal from ARIS-DMA to the user, which is expressed in Equation 6.1.

$$Y_n = b_n^H \Theta G_A^H X + w_n \tag{6.1}$$

The complex space vector in this chapter is denoted as (S), in Equation 6.1, $b_n^H \in S^{H\times 1}$ denotes the beamforming link between the ARIS-DMA and the (n_{th}) user, while $G_A^H \in S^{H\times A}$ is the link between ARIS-DMA and BS, $X = O_n s_n$ is the transmitted signal, $O_n \in S^{A\times 1}$ is the beamforming vector, s_n is the information symbol for the n_{th} user, w_n is the noise.

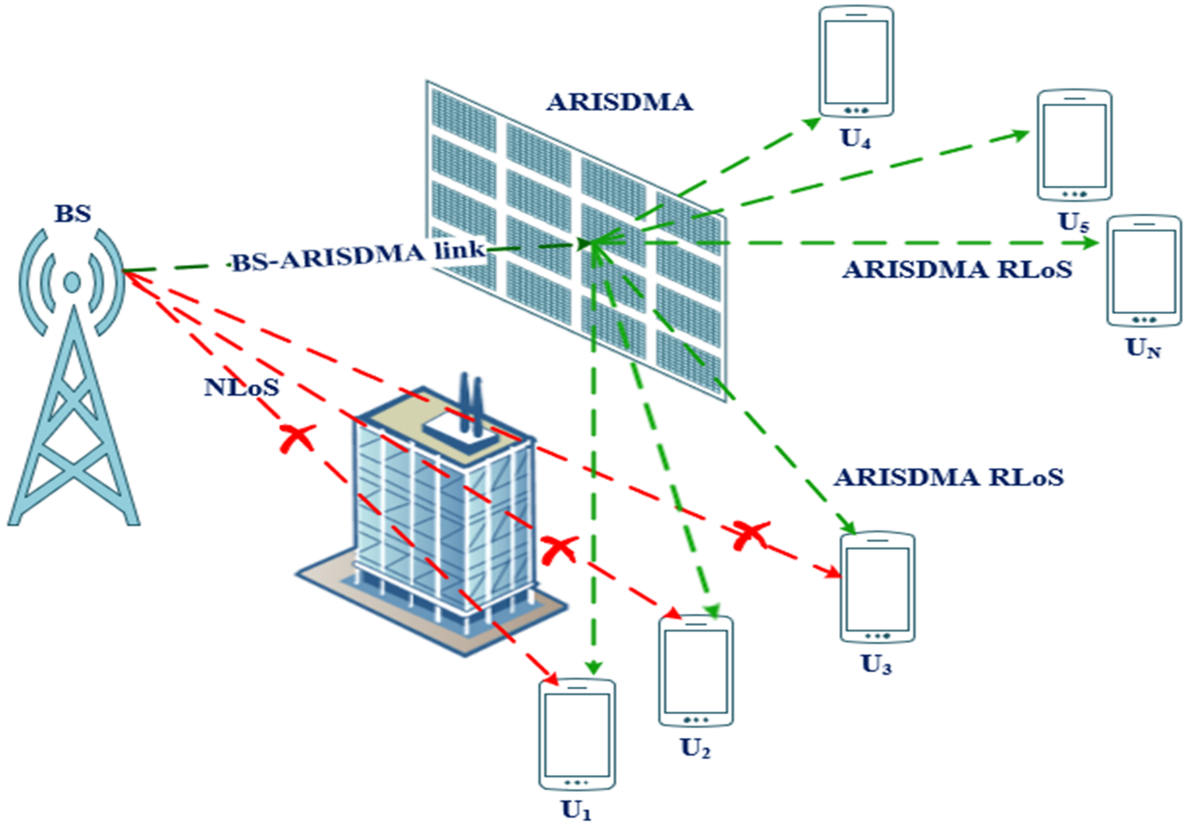

Figure 6.1: Schematic of the ARISDMA multi-user downlink communication system

The ARIS-DMA transmission and reflection matrix is denoted by:

$$\Theta = diag\left(\left[e^{j\theta_1}, e^{j\theta_2}, \ldots, e^{j\theta_H}\right]\right) \tag{6.2}$$

where $\theta_H \in [0, 2\pi)$ denotes the phase shift of the H_{th} element. In this chapter, the values of θ_H are assumed to be continuous in the interval $[0, 2\pi)$.

Since the scope of this research is not channel estimation, CSI knowledge is assumed to be known as in Chapter 5.

6.2.2 Channel Model

Let $h_{bs,n} \in C^{1\times1}$ and $h_{bs,H} \in C^{H\times1}$ is corresponding to the BS-user n and the BS-ARIS-DMA channels. Correspondingly, the channel between the ARIS-DMA and the user n is denoted by $h_{H,n} \in C^{H\times1}$. As mentioned earlier the BS and ARIS-DMA positions are known and the distance between them in also known. The users are randomly moving, and the distance between them and ARIS-DMA are continuously changing. Thus, the channels can be modeled as in Equation 6.3 to Equation 6.5:

$$h_{bs,n} = \sqrt{pl\left(d_{bs,n}\right)} h_{bs,n}^{NLoS} \tag{6.3}$$

$$h_{bs,H} = \sqrt{pl\left(d_{bs,H}\right)} \left(\sqrt{\frac{K_{bs,H}}{K_{bs,H}+1}} h_{bs,H}^{LoS} + \sqrt{\frac{1}{K_{bs,H}+1}} h_{bs,H}^{NLoS} \right) \tag{6.4}$$

$$h_{H,n} = \sqrt{pl\left(d_{H,n}\right)} \left(\sqrt{\frac{K_{H,n}}{K_{H,n}+1}} h_{H,n}^{LoS} + \sqrt{\frac{1}{K_{H,n}+1}} h_{H,n}^{NLoS} \right) \tag{6.5}$$

where $d_{bs,n}, d_{bs,H}, d_{H,n}$, are the BS-user link, the BS-ARIS-DMA link, and the ARIS-DMA-user links respectively. The propagation path loss for all channels is modeled as $pl\left(d\right) = \rho_0 \left(\frac{d}{d_0}\right)^{-\alpha}$, where ρ_0 is the path loss at the reference distance in which d denotes the distance between the transmitter and the receiver, α represents the path loss exponent, and $K_{bs,H}$,$K_{H,n}$ is the Rician factors [489, 490].

$h_{bs,H}^{LoS}$, and $h_{H,n}^{LoS}$ are the deterministic LoS components, which is calculated as:

$$h_{bs,H}^{LoS} = \left[1, \ldots, e^{j(h-1)\pi \sin\left(d_{bs,H}\right)} \ldots, e^{j(H-1)\pi \sin\left(d_{bs,H}\right)}\right] \tag{6.6}$$

$$h_{H,n}^{LoS} = \left[1, \ldots, e^{j(h-1)\pi \sin\left(d_{H,n}\right)} \ldots, e^{j(H-1)\pi \sin\left(d_{H,n}\right)}\right] \tag{6.7}$$

$h_{bs,H}^{NLoS}$, and $h_{H,n}^{NLoS}$ are the NLoS components, as a result, the combined channel power gain from the BS to the user n with the aid of ARIS-DMA is given by:

$$h_n = \left| h_{bs,n} + h_{H,n} \Theta h_{bs,H} \right|^2 \tag{6.8}$$

6.2.3 Signal Model and Problem Formulation

In order to determine the n_{th} user received SNR, the vector of beamforming weights O_n for all users is denoted as $O = [o_1, \ldots, o_n]$. The channel matrix for all users is defined as $B_n^H = \left[b_1^H, b_2^H, \ldots, b_n^H\right]$ and $B = B^H \Theta G_A^H \in S^{N \times A}$, is the overall channel matrix, thus the SNR for each user is defined as in Equation 6.9, in which $(.)^T$ denotes the conjugate transpose of any matrix and I_n is the total interference and noise at user n.

$$SNR_n = \frac{\left(o_n B_n\right)^T \left(o_n B_n\right)}{\mathrm{I}_n}, n = 1, 2, \ldots, N \tag{6.9}$$

This chapter aims to comply with thesis objectives to maximise the data rate and efficiency, as well as minimise the delay. Within the intricate realm of wireless communication systems, the task of 'maximising the sum rate' is a crucial one. It involves striving to achieve the highest overall data transmission rate across all users in a multi-user communication setting. Within a wireless network, the task of maximising the

total rate involves understanding each user's distinct channel circumstances, interference levels, and data rate needs. Maximising the sum rate requires optimising multiple parameters, including (channel constraints, power constraints, phase shift constraints, beamforming, ARIS-DMA phase shift matrix). Thus, the long term joint optimisation problem can be formulated as:

$$\max_{\{\Theta,O,B\}} = \sum_{n=1}^{N} R_n, \tag{6.10a}$$

$$\text{s.t.} \quad SNR_n = \frac{\left|\left(h_n^H O_n\right)^2\right|}{\sum_{m\neq n}\left(h_n^H O_m\right)^2 + K_{H,n}} \geq SNR_{\min}, \quad \forall n, \tag{6.10b}$$

$$\sum_{n=1}^{N} \|\mathrm{O}_n\|^2 \leq P_{\max}, \quad \forall n, \phi \in \Phi, \tag{6.10c}$$

Maximising the transmit power with the total data rate of users is considering two important constraint, at first the total transmit power of all users should not exceeds a maximum value of P_{max} as in Equation 6.10c, where the second constraint states that the phase shift values should stay between 0 and 2π. Maximising data rate has a direct relation with beamforming and phase shift matrices. This means that both matrices must have an optimal design to maximise the sum rate. The maximisation involves dividing the main maximisation approach into sub approaches and optimizing them iteratively, the sub approaches are then applied through randomisation and normalization.

6.2.4 Deep Q Network Adaptive Reconfigurable Intelligent Surface Decision Making Algorithm (DQN-ARISDMA)

A Deep Q Network ARISDMA (DQN-ARISDMA) is proposed in this section, where a DQN is employed to map the phase shift along with the power optimisation presented in Chapter 5. The motivation for proposing DQN-ARISDMA is that the conventional DL algorithms require diverse training data, which are challenging to obtain for communication scenarios. On the contrary, different from the conventional DL, the DQN-ARISDMA interacts with a dynamic environment, thus the algorithm learns from its own experience, which is stored in a dataset, to obtain the best decision results, based on the Markov decision process. As shown in Figure 6.2, the DQN-ARISDMA contains three stages, state, action and reward explained as follows:

1. **State Representation (S_n):** The state represents the environment's current configuration for user n, including the CSI, user locations, and possibly historical information. It could be represented as:

$$S_n = [h_1, h_2, \ldots h_H, u_1, u_2, \ldots u_N]$$

where h_H represents the channel gain from the transmitter to the ARIS-DMA element, and u_N represents the statues of the N^{th} user.

2. **Action Space (A_n):** The action stage corresponds to the beamforming weights applied to the ARIS-DMA elements. In a digital beamforming scenario, the action space is discrete, representing different beamforming directions or combinations as:

$$A_n = [O_1, O_2, \ldots O_N]$$

3. **Reward Function (R_n):** The reward R_n reflects the quality of the system's performance after taking action A_n in state S_n.

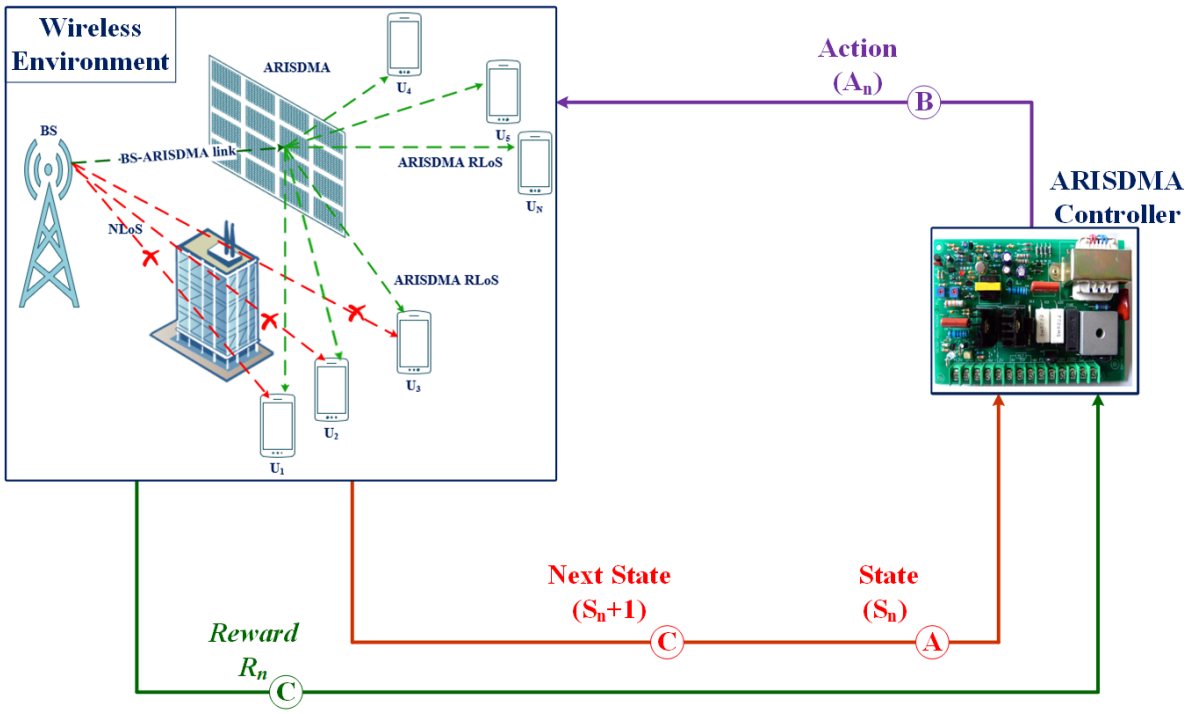

Figure 6.2: DQN-ARISDMA system model

Instead of relying solely on the BS or user channels, combining the two is utilised to establish unique characteristics for each element of the ARIS-DMA. Thus, using B_n^H and G_A^H as a two-dimensional feature vector allows more streamlined processing and data analysis, in contrast to utilising each vector separately. This combination as a result will lead to enhanced efficiency, to be more precise, the new combined feature for i^{th} ARIS-DMA element is rewritten in Equation 6.11, where $V \in S^{N \times A}$.

$$V_i = B_n^H G_A^H \tag{6.11}$$

The main target in this section is to find the best transmit beamforming matrix, depending on the effective channel. In wireless communication systems, the effective

channel considers the environment's effects, such as scattering and reflections, between the transmitter and the receiver. An optimal transmit beamforming matrix modifies the transmitted signals' phase and amplitude to increase the strength of the received signal at the receiver. DQN-ARISDMA seeks to find the best course of action by choosing the highest Q-value while accounting for the crucial elements related to Q-learning. It is intended to determine the greatest value to calculate the Q-value for each observation iteratively. Thanks to this procedure, the algorithm can make well-informed, effective and tuned decisions for peak performance.

Algorithm 3 DQN-ARISDMA algorithm

Initialise the environment, the DQN-ARISDMA size, and the training batch size Z, training rate, and simulation parameters
Initialise the DQN-ARISDMA with random weights O parameters
for each episode **do**
  Reset the environment and initial state
  for each user $0 \leq n \leq N$ **do**
    Input the current phase shifts $\Theta[n]$ and the CSI$h_{bs,H}[n]$, $h_{H,n}[n]$, $h_{bs,n}[n]$ to the DQN-ARISDMA
    DQN-ARISDMA predict and output the phase shifts according to Equation 6.13
    Calculate the data rate and feed into loos function
    Train DQN-ARISDMA O_n with the loss in Equation 6.14 and Equation 6.15 for each episode
    $[n] \leftarrow [n+1]$
  end for
end for

Algorithm 3 illustrates the steps processed by DQN-ARISDMA to obtain the predicted phase shifts for the optimum beamforming. The DQN-ARISDMA is trained by the interaction with the environment and converges the phase shift. Another advantage of the proposed DQN-ARISDMA algorithm is that it has higher data rate, fairness level, spectral efficiency, and lower convergence time, delay, and packet error rate as will be discussed in Section 6.4. The designed DQN-ARISDMA depends on three main stages as illustrated in Figure 6.2, in the state stage indicated as (A) the network observes and collects information of BS channel and user channel which is identified as a collection of the wireless environment characteristics; where S_n, is the combined BS and user channel characteristics for each user n, and send these information to the DQN-ARISDMA controller. The next stage (B) is where the DQN-ARISDMA controller takes the decision S_{n+1} that is made based on the current channel characteristics S_n. The last stage (C) is known as the wireless environment reward R_n which is updated based on the taken decision, in which the DQN-ARISDMA reinforce good behaviour and discourage bad behaviour based on the highest Q-value achieved as in Equation 6.12 and Equation 6.13.

$$Q\left(S_n, S_{n+1}\right) \leftarrow Q\left(S_n, S_{n+1}\right) + \alpha Q^*\left(S_n, S_{n+1}\right) \tag{6.12}$$

$$Q\left(S_n, S_{n+1}\right) \leftarrow Q\left(S_n, S_{n+1}\right) + \alpha \left\{ r + \gamma \max_{S'_{n+1}} Q^*\left(S'_n, S'_{n+1}\right) - Q\left(S_n, S_{n+1}\right) \right\} \tag{6.13}$$

where, r is the immediate decision obtained by the DQN-ARISDMA controller, α is the learning rate, which determines the extent to which new information overrides old information, Q^* is the optimal Q-value for the next (S_n, S_{n+1}) pair, and γ is the buffer used to reduce the correlation between the training data and enhance the stability of convergence, which determines the importance of future decisions in the update in a range of $[0, 1]$.

6.2.5 Loss Function

The loss function is a crucial metric that determines the performance of a given model concerning its training data. It serves as an indicator of the disparity between the predicted values and the actual values. Minimising the loss function is imperative to improve a model's accuracy since this implies that the model's predictions align more with the target values. We calculated the loss function for single beamforming for DQN-ARISDMA as in Equation 6.14.

$$Loss = \left(Q\left(S_n, S_{n+1}\right) - \left(r + \gamma \max_{S'_{n+1}} Q^*\left(S'_n, S'_{n+1}\right) \right) \right)^2 \tag{6.14}$$

Given the anticipated expansion of wireless communication in the 6G new generation, which will ultimately support ten times the number of users compared to the current generation, it becomes imperative to establish a comprehensive characterization of the loss function for this particular goal. The overall loss function for DQN-ARISDMA is expressed in Equation 6.15.

$$Loss = \frac{\left(Q\left(S_n, S_{n+1}\right) - \left(r + \gamma \max_{S'_{n+1}} Q^*\left(S'_n, S'_{n+1}\right) \right) \right)^2}{Z} \tag{6.15}$$

6.2.6 Network Architecture and Training

The adopted network architecture as illustrated in Figure 6.3 consists of one convolutional layer (CV) followed by six fully connected layers (FC). Each FC layer neurons are proportional to the number of reflecting elements H to ensure that the DQN-ARISDMA

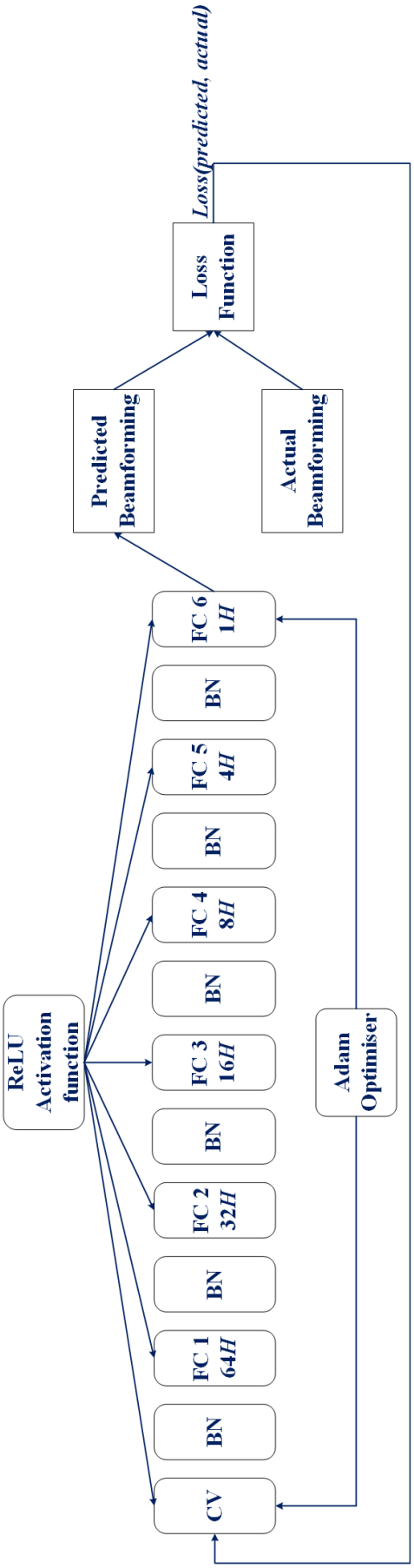

Figure 6.3: DQN-ARISDMA Network Architecture

network has enough capacity to learn from larger datasets as the wireless system scales up. Therefor the fully connected layers (FC) layers are made up of $64H$, $32H$, $16H$, $8H$, $4H$ and H neurons respectively.

To prevent network overfitting and improve training process Batch Normalization (BN) layer is placed between each FC layers and after the first CV layer. All FC layers use ReLU as an activation function to prevent the vanishing gradient problem. Adam optimiser is used to train the network with an initial training rate of 0.0001, as the number of maximum batch size Z is set to 6000, 80% of the generated data samples are used for training and the remaining 20% are used for validation.

6.2.7 Simulation Parameters

The ARIS-DMA used in this chapter follows the design in Chapter 5, which is designed to transmit and reflect the incident signal to their intended users at the same time, 200 adaptive reflection and transmission elements H is applied in which their element response equals 0.9, transmission power 1000 mW, wavelength λ of 0.1, ARIS-DMA antenna gain is 1 and power radiation parameters are 0.99.

The tested and configured area experiences high user density of (3×10^6, 6×10^6, 9×10^6, 12×10^6, and 16×10^6) $user/km^2$ in which they are randomly distributed, with one BS which has eight transmitting antennas A, in which wireless communication system with high user density indicates higher transmission data rates.

To elucidate the performance of DQN-ARISDMA, considering system stability, training efficiency, and testing performance, we generate 12×10^6 samples for training, 10×10^6 samples for validation, and 8×10^6 samples for testing.

As the DQN-ARISDMA is designed to support the latest wireless communication generation 6G. The operating frequencies for THz transmission which are used to test DQN-ARISDMA performance are 300, 400, and 500 GHz.

6.3 Performance Indicators

This section provides an illustration of the performance metrics that we utilised in order to evaluate the differences between the performance of DQN-ARISDMA with DDPG, PPO and CNN in the context of beamforming. The following subsections illustrates the performance indicators used to compare DQN-ARISDMA with the current state of art techniques.

6.3.1 Fairness

The fairness index known as (Jain's Fairness Index) is a quantitative measure employed to assess the equity of resource distribution across numerous users inside

a communication system. The metric offers a singular numerical representation that indicates the level of fairness in the distribution of resources across users, with larger values denoting more equity. Jain's Fairness Index is a mathematical measure that quantifies the fairness of resource allocation among individual users. It is calculated by dividing the total of squared individual user throughput's by the square of the sum of the individual user throughput's, where it ranges from 0 to 1. Mathematically, it is represented in Equation 6.16, where T_i represents the throughput of user n, N is the total number of users:

$$J = \frac{\left(\sum_{n=1}^{N} T_n\right)^2}{N \sum_{n=1}^{N} T_n^2} \tag{6.16}$$

6.3.2 Spectral Efficiency

Spectral efficiency, quantifies the effectiveness of a communication system in using its available bandwidth to transfer data. It is commonly quantified as the ratio of bits per second to hertz (bps/Hz), representing the quantity of data that can be sent over a particular bandwidth during a specified duration. Spectral efficiency is a crucial performance measure in wireless communication systems since it directly determines the system's capacity to accommodate high data rates within a restricted frequency band. It is mathematically defined as in Equation 6.17, where, R is the data rate or throughput, and B is the bandwidth.

$$SE = \frac{R}{B} \tag{6.17}$$

6.3.3 Convergance Time

In DL, convergence time refers to the duration it takes for an algorithm to reach a stable or optimal solution during the training process. In the context of beamforming with wireless system, convergence time is a crucial consideration when deploying DL algorithms to optimize beamforming weights and phase shifts. As a convergence criterion we specifies the throughput, and determined the threshold value or target performance level that indicates satisfactory convergence, when the average throughput across all users reaches 95% of the maximum achievable throughput.

6.3.4 Delay

In this indicator we calculate the time required by DQN-ARISDMA and its comparatives to determine the optimal beamforming solution.

6.3.5 Data Rate

Data rate, which is also known as bit rate, is the rate at which data is transferred from the sender to the receiver within a communication system. It is typically measured in bits per second in this chapter it is measuerd in Tbps.

6.3.6 Packet Error Rate

In the case of DQN-ARISDMA, the packet error rate is defined as the rate at which the DQN-ARISDMA agent makes incorrect decisions or fails to achieve the desired objectives in the task it is designed to solve. This is evaluated through the simulation experiments, where the performance of the DQN-ARISDMA agent is compared against DDPG, PPO and CNN, in terms of its ability to achieve the desired outcomes with minimal errors.

6.4 Performance Analysis

In this section, as depicted in Figure 6.4 to Figure 6.13, we characterise the fairness, SE, convergence time, delay, data rate and PER associated with the new DQN-ARISDMA in Section 6.2. As illustrated in Section 6.3 the performance measures must adhere to the requirements of the new wireless generation 6G. It is worth mentioning that DQN-ARISDMA is previously compared with SDR, MRT, and MMSE in [1].

The bar charts in Figure 6.4 to Figure 6.6 depicts the fairness level for the different beamforming methods analysed at a frequency of 300, 400 and 500 GHz, considering different levels of user density. As indicated in Section 6.3.1, fairness is a metric that quantifies the degree to which the beamforming capabilities are allocated evenly across users. For the three different frequencies, DQN-ARISDMA consistently shows the highest fairness across all user densities. This indicates that DQN-ARISDMA is particularly effective at maintaining an equitable distribution of resources among users, even as the number of users increases.

DDPG, PPO, and CNN exhibit varying levels of fairness, generally maintaining mid-to-high fairness levels. However, their performance fluctuates more than DQN-ARISDMA, suggesting that these techniques may be more sensitive to changes in user density and frequencies indicating that these techniques may struggle to evenly distribute resources effectively, particularly at higher user densities.

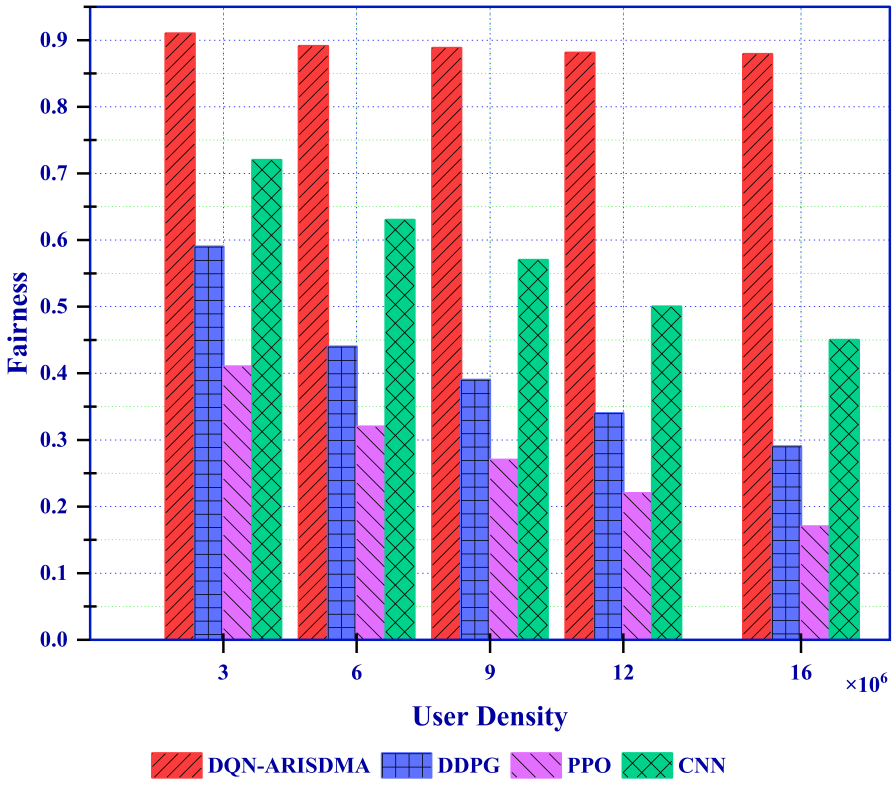

Figure 6.4: Fairness Comparison for 300 GHz

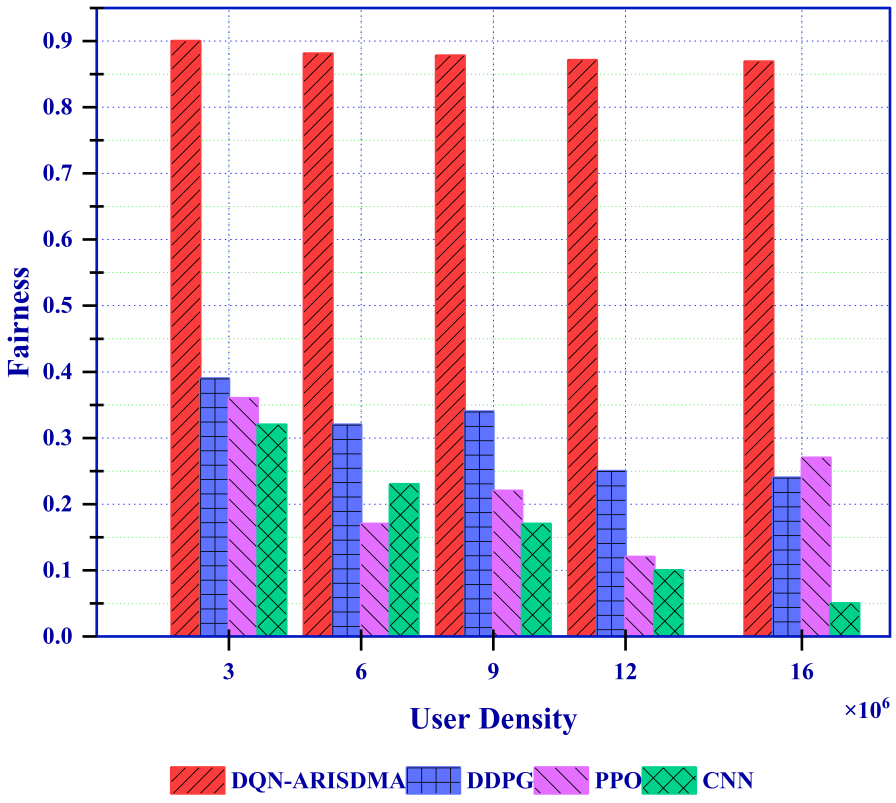

Figure 6.5: Fairness Comparison for 400 GHz

DQN-ARISDMA achieves the highest fairness (approximately 0.9), for the three different frequencies followed by CNN with mid-level fairness for 300 GHz and 500 GHz. DDPG on the other hand has the lowest performance at 500 GHz. At 400 GHz DDPG and PPO shows slightly same performance while CNN shows the lowest performance. The findings demonstrate the exceptional effectiveness of DQN-ARISDMA in ensuring fairness among users with varying densities and different frequency. This implies that DQN-ARISDMA is more resilient and has the ability to allocate beamforming resources fairly, making it a preferable option in situations with a high number of users.

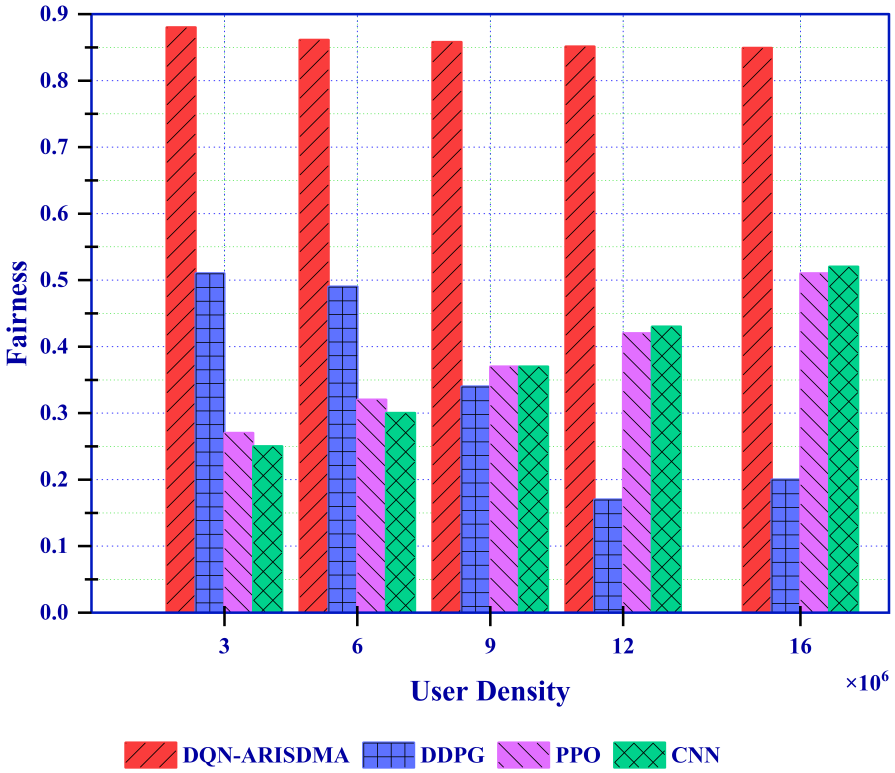

Figure 6.6: Fairness Comparison for 500 GHz

The other important performance indicator is SE, as shown in Figure 6.7 to Figure 6.9. When examining the spectral efficiency of frequencies at 300, 400, and 500 GHz under different SNR levels, it is evident that there is a similar performance pattern across various beamforming approaches. DQN-ARISDMA consistently delivers the best SE across all frequencies and SNR levels, surpassing DDPG, PPO, and CNN by a wide margin. At low SNR levels, namely -20dB, DQN-ARISDMA retains a significant advantage over other approaches. It achieves SE of around 4 Tbps/Hz at 300 GHz, 4.5 Tbps/Hz at 400 GHz, and 6.5 Tbps/Hz at 500 GHz. In contrast, the other techniques do not exceed 1 Tbps/Hz. As the SNR climbs to 0dB and beyond, the performance of DQN-ARISDMA improves significantly. At 300 GHz it achieves a throughput of around 11 Tbps/Hz and reaches its highest values of 16 Tbps/Hz, when the SNR is 20dB. DDPG, PPO, and CNN demonstrate notably reduced SE at all SNR levels.

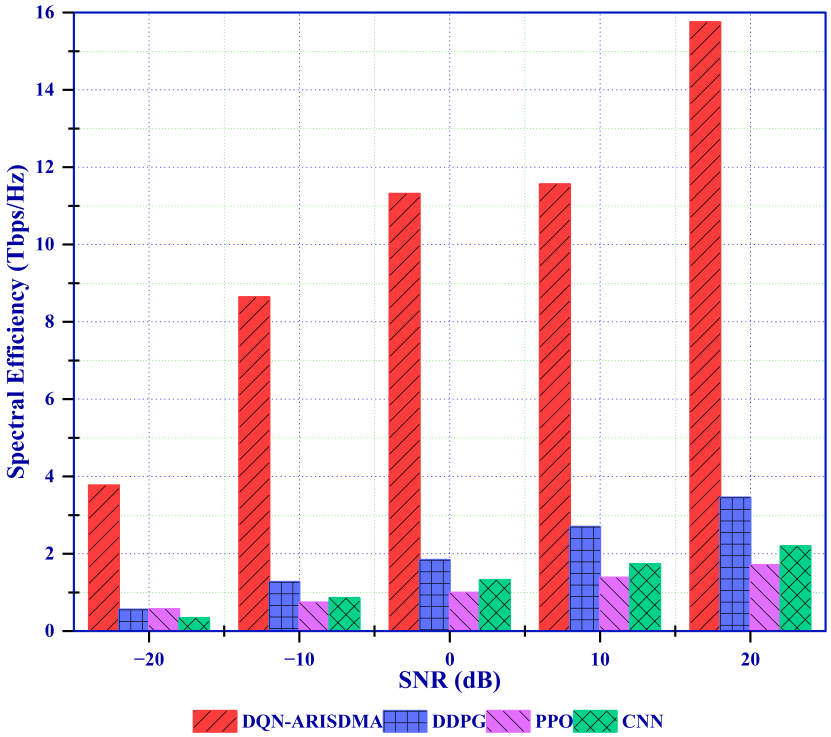

Figure 6.7: Spectral Efficiency Comparison for 300 GHz

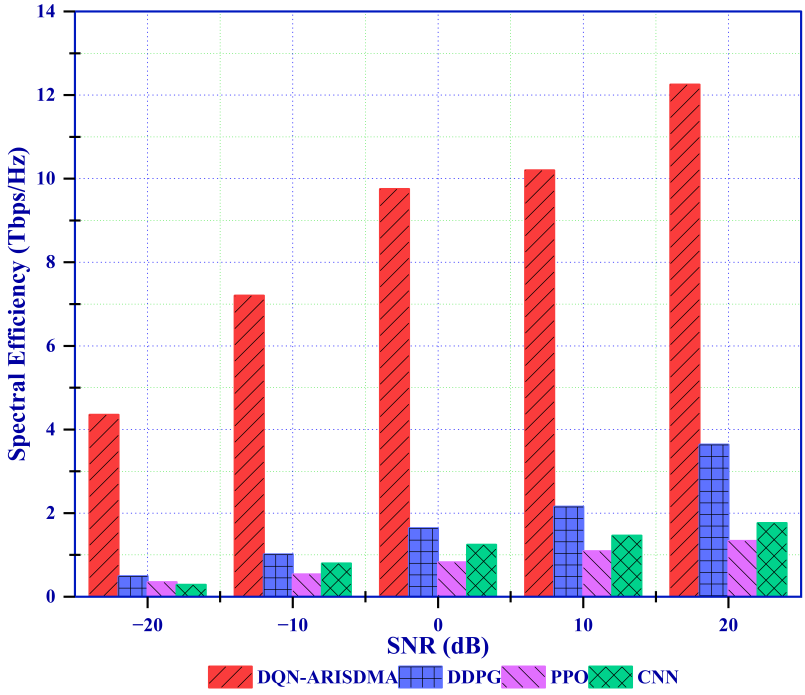

Figure 6.8: Spectral Efficiency Comparison for 400 GHz

DDPG shows marginal enhancements at higher SNR, but it still does not match the performance of DQN-ARISDMA. The consistent superiority of DQN-ARISDMA demonstrates its resilience and effectiveness in handling high-frequency spectrum resources, making it an efficient solution for next-generation THz communication systems. This is particularly important as maximising SE is crucial in meeting the growing need for high data rates.

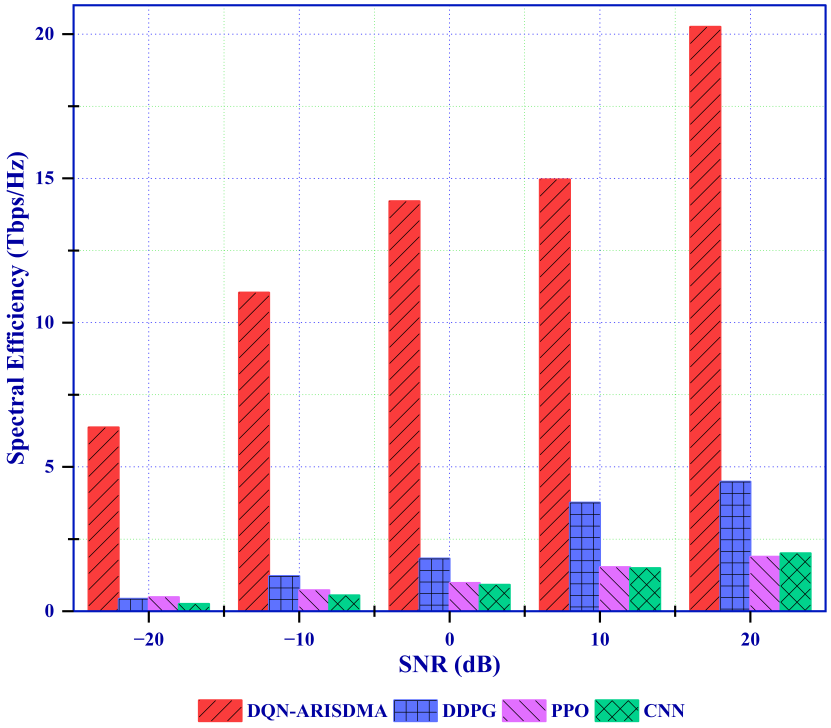

Figure 6.9: Spectral Efficiency Comparison for 500 GHz

The performance for higher frequency range is illustrated in Figure 6.8 and Figure 6.9, the performance clearly indicates the superiority of DQN-ARISDMA over the other approaches for both 400 and 500 GHz. In Figure 6.8, at an SNR of -20dB, the DQN-ARISDMA attains roughly 4.5 Tbps/Hz, while DDPG, PPO, and CNN only surpass 0.5 Tbps/Hz marginally. With an increase in SNR to -10dB, the SE of DQN-ARISDMA rises to approximately 7.5 Tbps/Hz, markedly exceeding that of DDPG (around 1 Tbps/Hz), PPO (approximately 0.7 Tbps/Hz), and CNN (about 1 Tbps/Hz). At 0dB SNR, the SE of DQN-ARISDMA is approximately 9.5 Tbps/Hz, which is roughly five times greater than that of the nearest competing method, DDPG, at around 2 Tbps/Hz. The performance gap becomes increasingly pronounced at higher SNR values. At an SNR of 10dB, the SE of DQN-ARISDMA surpasses 10 Tbps/Hz, while the alternative methods remain under 3 Tbps/Hz. At an SNR of 20dB, the SE of DQN-ARISDMA exceeds 12 Tbps/Hz, whereas DDPG attains roughly 3.5 Tbps/Hz, and both PPO and CNN are approximately 2 Tbps/Hz. Figure 6.9 demonstrates similar trends, though with enhanced SE performance. At an SNR of 20dB, DQN-ARISDMA attains approximately

20 Tbps/Hz, nearly sixfold the performance of DDPG, which is around 4 Tbps/Hz. The persistent dominance of DQN-ARISDMA at all SNR levels illustrates its effectiveness in enhancing SE for high-capacity 6G networks.

The other performance indicator considered is convergence time as shown in Figure 6.10. The speed at which convergence occurs is crucial in wireless communication and DL solutions since it directly affects the network's responsiveness and efficiency.

The results illustrated in this section emphasise the remarkable effectiveness of DQN-ARISDMA in decreasing the time it takes to reach convergence as the number of users grows. With a user count of 16×10^6, DQN-ARISDMA achieves the ideal solution in less than 6 μs. In contrast, the competing techniques face a continual increase in convergence time, taking 50% time higher than DQN-ARISDMA with 500 GHz. DQN-ARISDMA consistently maintains this level of performance across the other frequencies in the 6G spectrum 300 and 400 GHz, exhibiting a significant difference of up to 75% compared to DDPG, PPO, and CNN. This achievement is crucial for DQN-ARISDMA, as it demonstrates it's ability to adapt and learn to manage changing network circumstances effectively.

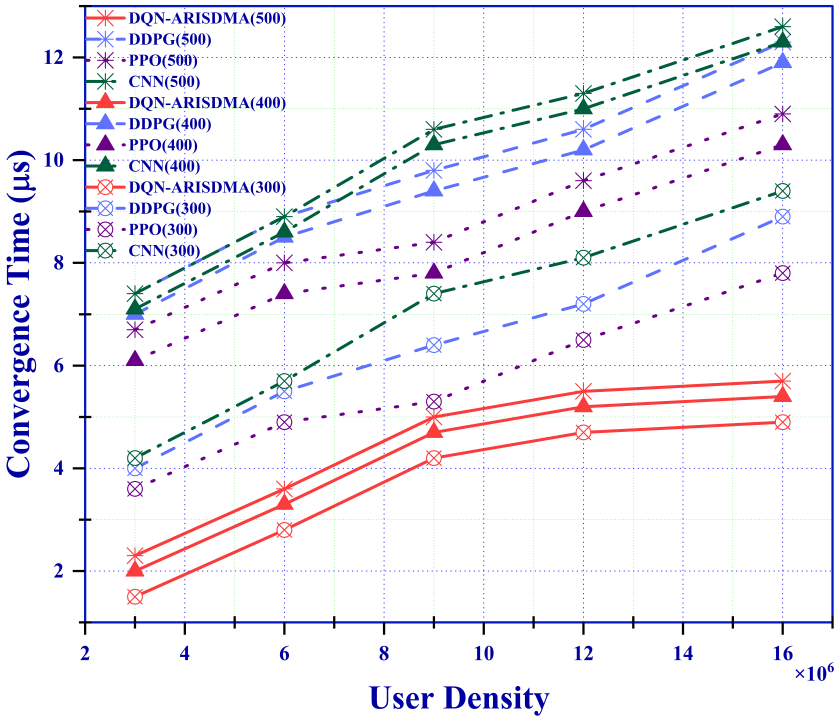

Figure 6.10: Convergence Time Comparison for different frequencies

The conventional beamforming techniques DDPG, PPO, and CNN used in 5G, failed to maintain good performance as the number of users increase. These approaches depend on static resource allocation algorithms, which are less effective in dynamic situations. As users increase, the time it takes for conventional approaches to converge also increases, leading to higher delays in network adaptation, as in Figure 6.11.

The delay encountered by users during communication is significantly affected by the user density in the tested network, as seen in Figure 6.11. Each method exhibits relatively lower latency on the network with moderate density of 3×10^6 users. However, a distinct and discernible shift in the pattern becomes apparent when the density grows, DQN-ARISDMA surpasses the other beamforming approaches in terms of delay reduction. The DQN-ARISDMA system is able to efficiently allocate resources and make decisions based on learning, allowing it to swiftly adjust to changing conditions and priorities for fast communication with minimal delay. DQN-ARISDMA, as compared to DDPG, PPO, and CNN, demonstrates a notable benefit in reducing communication time. With many users, namely 12×10^6 and 16×10^6 users, DQN-ARISDMA experiences much-reduced delay. The other methods need more time to effectively handle network resources, resulting in increased delays as the number of users increases. DQN-ARISDMA, on the other hand, has exceptional performance in minimising delay, even in situations with high network congestion.

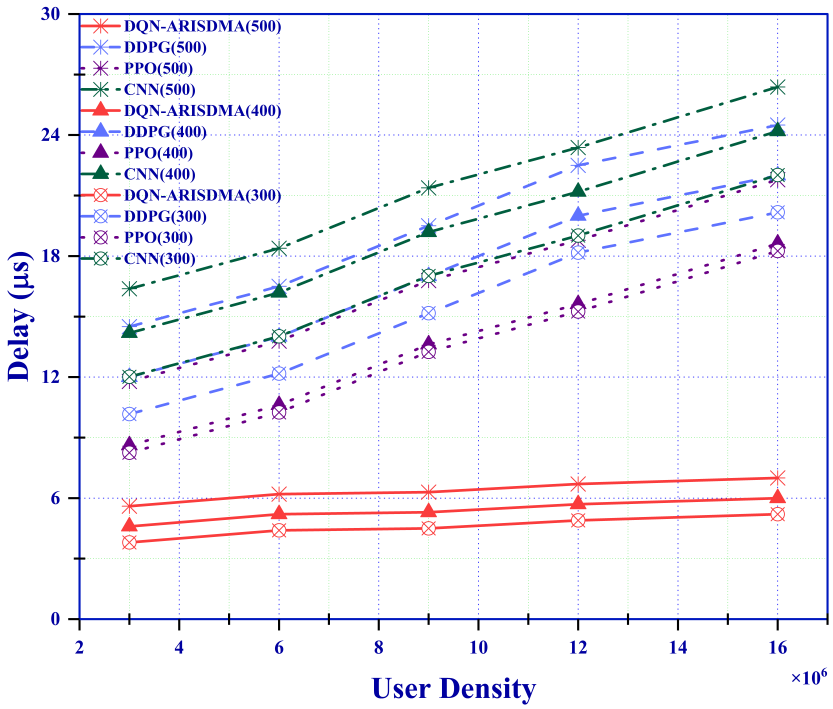

Figure 6.11: Delay Comparison for different frequencies

In wireless communication data rate performance is important. Figure 6.12, shows the data rate performance for (300, 400, and 500) GHz at different SNR levels, where distinct patterns and variations in performance is noticed. At 300 GHz, the data rates gradually and consistently increase as SNR increases. However, the data rate remains comparatively low compared to higher frequencies. More precisely, the three methods DDPG, PPO, and CNN exhibit incremental improvements; however, their data transmission speeds reach a maximum of less than 0.4 Tbps at a SNR of 20dB.

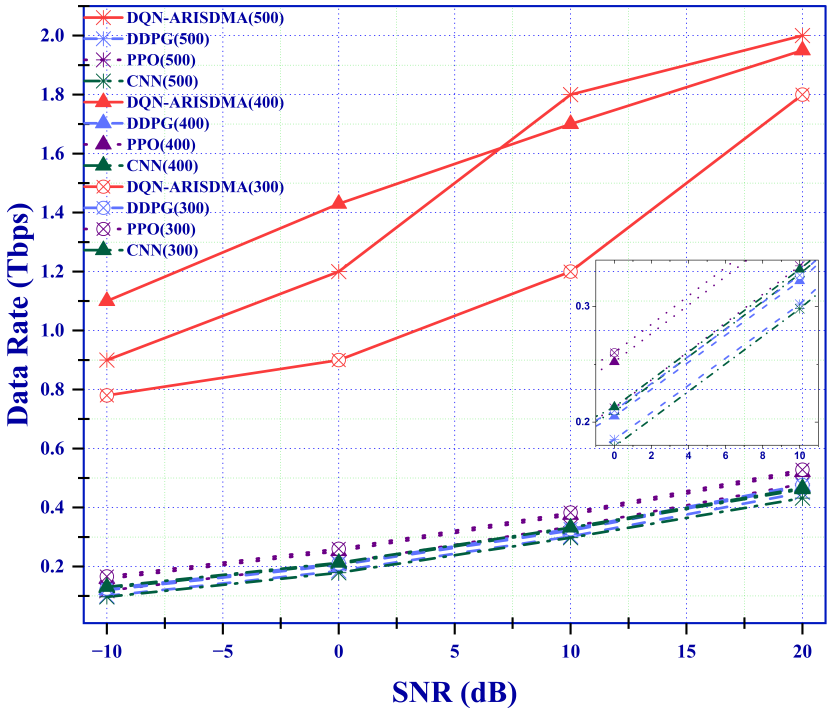

Figure 6.12: Data Rate Comparison for different frequencies and 16×10^6

On the other hand, the 400 GHz frequency exhibits a significant increase in data rates as the SNR increases. This is especially true for the DQN-ARISDMA approach, which achieve data transmission speeds above 1 Tbps at higher SNR levels. This highlights the expanded data transmission potential of the 400 GHz frequency. The 500 GHz frequency is superior to the other two frequencies, as it results in a large increase in data rates with a higher SNR. Specifically, the DQN-ARISDMA approach achieve data rates exceeding 2 Tbps at 20dB SNR. This emphasises the exceptional capacity of the 500 GHz frequency range for high-speed data applications. Nevertheless, the 500 GHz band exhibits heightened susceptibility to SNR fluctuations, underscoring the need for sophisticated signal processing techniques and methods to harness its potential effectively which highlights the significance of choosing suitable methods to optimise data transmission in high-frequency communication systems.

DQN-ARISDMA maintains higher data rates, reaching a 100% higher data rate than the other approaches under 300 GHz, 400 GHz, and 500 GHz. The adaptability of DQN-ARISDMA to excel in low SNR conditions, where error resilience is paramount, and in high SNR conditions, where maximizing data rates is critical, is an important achievement in regards to the objectives to meet the 6G KPIs.

The last performance indicator is PER, the examination of PER at frequencies of 300, 400, and 500 GHz at different SNR, as seen in Figure 6.13, provides valuable information on the dependability and effectiveness of DQN-ARISDMA for 6G high-frequency band. At a frequency of 500 GHz, the PER stays relatively high when the SNR is low.

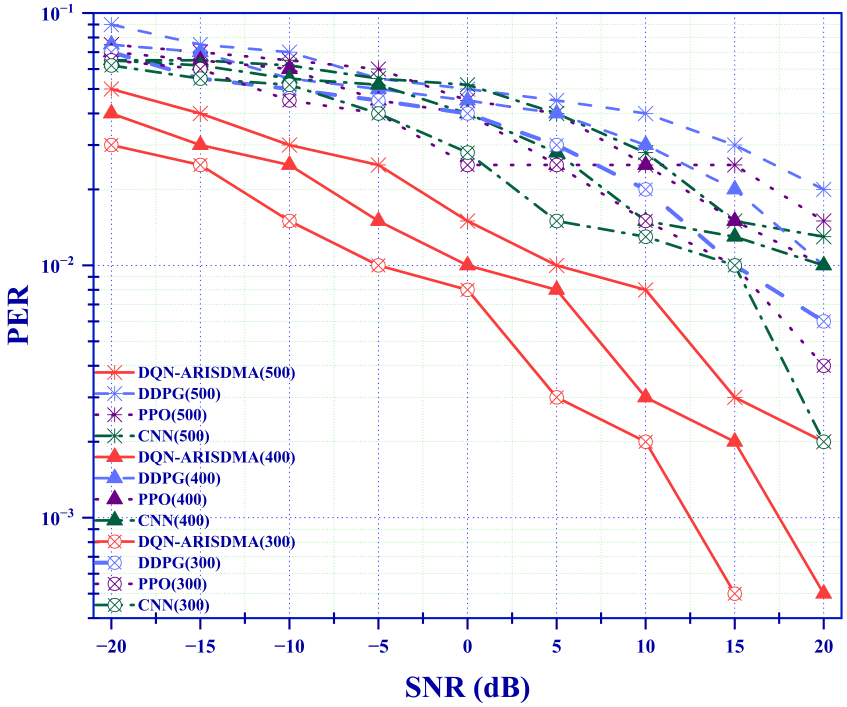

Figure 6.13: PER Comparison for different frequencies and 16×10^6

However, as the SNR increases, the PER consistently decreases. The DQN-ARISDMA demonstrate superior performance and achieve PER close to 10^{-2} at higher SNR equals to 5dB. Increasing the SNR leads to moderate gains in dependability.

At a frequency of 400 GHz, the PER decreases significantly as the SNR increases. This decline is especially noticeable for the DQN-ARISDMA, which attain PER below 10^{-2} faster than 500 GHz level. This implies that a frequency of 400 GHz can provide much-improved error performance under situations of a moderate SNR.

Among the three frequencies, the 300 GHz band has the lowest PER, where, DQN-ARISDMA achieves PER as low as 10^{-2} with channel gain of 5dB and 10dB compared to 400 GHz and 500 GHz respectively, Table 6.1 summarise the PER values of DQN-ARISDMA compared with DDPG, PPO, and CNN.

Table 6.1: PER comparison

SNR	DQN-ARISDMA	DDPG	PPO	CNN
-20	0.03	0.07	0.065	0.062
-15	0.025	0.055	0.06	0.055
-5	0.01	0.045	0.04	0.04
0	0.008	0.04	0.025	0.028
5	0.003	0.03	0.025	0.015
15	0.0005	0.01	0.01	0.01
20	0	0.006	0.004	0.002

(a) 300 GHz

SNR	DQN-ARISDMA	DDPG	PPO	CNN
-20	0.04	0.075	0.07	0.065
-15	0.03	0.07	0.065	0.062
-5	0.015	0.05	0.045	0.052
0	0.01	0.045	0.04	0.04
5	0.008	0.04	0.025	0.028
15	0.002	0.02	0.015	0.013
20	0.0005	0.01	0.01	0.01

(b) 400 GHz

SNR	DQN-ARISDMA	DDPG	PPO	CNN
-20	0.05	0.09	0.075	0.065
-15	0.04	0.075	0.07	0.065
-5	0.025	0.055	0.06	0.055
0	0.015	0.05	0.045	0.052
5	0.01	0.045	0.04	0.04
15	0.003	0.03	0.025	0.015
20	0.002	0.02	0.015	0.013

(c) 500 GHz

6.5 Discussion

In this chapter, we have developed a beamforming solution for ARIS-DMA developed in Chapter 5, this new beamforming depends on deep Q network which is refereed to as DQN-ARISDMA.

The effectiveness of DQN-ARISDMA beamforming presented in this chapter, which integrates deep Q learning into the beamforming process, has been demonstrated in the frequency range of the 6G communication system while achieving THz data rates. DQN-ARISDMA mange to support high level of user density with the highest fairness approximately 1 compared with DDPG, PPO, and CNN. Moreover, DQN-ARISDMA achieves higher SE reaches up to 20 Tbps/Hz, the pursuit of high SE is a fundamental objective in the development and implementation of contemporary wireless communication systems. It facilitates faster transmission speeds, optimised use of frequency bands, reduced expenses, enhanced network capability, and improved service quality.

The SE achievement is reflected directly on DQN-ARISDMA data rate and PER performance, high data rate in a communication system refers to the ability to transfer a substantial volume of data within a specific time frame, with greater rates indicating faster connection and the capacity to handle more data intensive applications. High data rates are crucial for modern communication systems as they enable faster, more efficient, and reliable data transmission.

On the other hand , low PER is a key indicator of a high-quality and reliable communication system. Achieving low PER enhances the quality of service, reduces latency, and improves the overall user experience, making it essential for a wide range of applications from real-time communication to critical data transmission especially for the upcoming wireless generation 6G.

In order for DL approaches to be efficient in learning and provide high performance it should require low convergence time and delay. A network with low convergence time can rapidly learn the optimal policy, resulting in effective resource utilization and adaptability to surroundings changes. Minimal latency guarantees prompt decision-making and responsiveness, which is vital for applications necessitating instant feedback and actions. DQN-ARISDMA shows an extraordinary level of minimising both the convergence time and delay by more than 50% which complies with 6G targets to minimise the time required for transmission to lower level of that of the previous generations.

7

Conclusions and Future Works

This chapter provides a concise overview of the study and presents the findings and conclusions of the thesis. Subsequently, several recommendations for future endeavours and progress are given to indicate how the findings of this study can be utilised.

7.1 Summery

> When wireless is perfectly applied the whole earth will be converted into a huge brain, which in fact it is, all things being particles of a real and rhythmic whole

Nikola Tesla, in 1926 at an interview with Collier's magazine predicted the future of communications and precisely the wireless communications. However, he did not expect the high user demands and the growing network size. In order for Tesla prediction to be applied, number of organisations had to be initiated and standardisation's had to be introduced resulting in five generations of wireless communication with the latest known as 5G currently used. According to that, new approaches and techniques were continuously introduced by researchers for each generation to overcome any limitations or restrictions, in order for each wireless generation to achieve it is desired requirements and KPIs.

The emergence of 6G wireless technology began to attract interest in the mid-2010s, with notable conversations and initial proposals surfacing in academic and commercial domains. Nevertheless, the concept of 6G as the subsequent advancement following 5G gained traction and underwent thorough examination during the latter part of the 2010s. In the period from 2017 to 2018, a number of academic papers and first research proposals began to appear, exploring the potential advancements and technologies that could shape the development of 6G. In 2018, the University of Oulu in Finland initiated

the 6G Flagship program, which is the first research program in the world dedicated to investigate the technological advancements and necessities for 6G networks. In 2019, the ITU initiated the process of defining the future of 6G, with a specific emphasis on the innovations and applications that will follow 5G.

Notwithstanding that there is unlimited research to develop new approaches and techniques to comply with 6G KPIs, there is still found limitations in adhering the most important measures in each wireless generations. This thesis focuses on developing a new channel coding approach integrated with a ARIS for THz 6G communication networks. This study seeks to meet the increasing need for faster data rates, better use of available frequencies, and increased dependability in the next 6G networks.

The objectives of 6G communications are ambitious and seek to greatly improve the capabilities and performance of wireless networks beyond the current capabilities of 5G. The objectives are motivated by the necessity to facilitate a diverse array of sophisticated applications and services, encompassing those that necessitate extremely fast data transmission, little delay, exceptional dependability, and extensive connectivity. The 6G targets are to accomplish ultra high data rates, extremely low latency, massive connectivity, high reliability and availability, enhanced spectral and energy efficiency, expanded coverage, advanced sensing and communication integration, programmability and flexibility, sustainability and cost effectiveness, AI and ML integration, and holographic and extended reality communications.

In order to adhere the requirements of the new wireless generation, in this thesis two novel channel coding approach has been developed in Chapter 3 named Polar Convolutional Serial Code (PCSC) and Polar Convolutional Parallel Code (PCPC), specifically for efficient operation in the THz range, offering improved data transmission rates and enhanced dependability. The coding approach aims to overcome the difficulties associated with molecule absorption and signal attenuation that are inherent in THz frequencies. Moreover, in order to elaborate more on the performance of the channel coding in regards to 6G, the conducted channel coding techniques utilise the use of Non Orthogonal Multiple Access (NOMA) as resource allocation to replace the current orthogonal resource allocation used in the previous generations. The comparative analysis showcases the superiority of the new methods in terms of both BER and throughput, which satisfies the ultra high data rates, high reliability and availability requirements.

As the conducted results shows better performance for PCSC more development is carried out on the decoding process of PCPC in Chapter 4, as Deep Learning PCPC (DL-PCPC) . Integrating DL into the decoding process demonstrates higher data rate, higher reliability, higher EE, and lower delay.

Expanding the coverage area while providing massive connectivity is addressed in Chapter 5, by introducing adaptive reconfigurable intelligent surface into a wireless

communication system. In this thesis a ARIS Decision Making Algorithm (ARIS-DMA) is developed which simultaneously transmit and reflect the incident signal offering significant benefits in terms of signal quality, coverage, spectral and energy efficiency, capacity, reliability, and cost-effectiveness. Unlike the traditional STAR-RIS where the system resources usually split between the users in the transmission and reflection areas, in this thesis using the ARIS-DMA enables the dynamic control and optimization of the wireless environment, which plays a critical role in meeting the ambitious performance targets of 6G and supporting the diverse and demanding applications of the future.

After successfully elaborating on the use of STAR-RIS and developing an adaptive form of it, namely ARIS-DMA, in Chapter 5, Chapter 6 presents an enhanced version of ARIS-DMA by integrating DL. The Deep Q Network ARISDMA (DQN-ARISDMA) integrates reinforcement learning in the means of DQN to enable an intelligent beamforming approach for the network. Leveraging DL, particularly DQN is designed to dynamically adapt to the change in network conditions, optimise the resource allocation and improve the spectral efficiency which demonstrates how effective the adoption of DQN-ARISDMA to reduce the convergence time and delay, which is crucial for real-time applications in 6G networks.

7.2 Conclusions

In this study, simulation-based solutions were introduced to develop new technologies that meet the 6G performance requirements, by aligning with user expectations and minimising the need for extensive modifications to the existing communications infrastructure, the implementation of the new generation of communications can be expedited, offering significant advantages over the current generation.

In order to accomplish this task, a set of performance indicators must be addressed and met. Coverage, delay, data rate, reliability, system efficiency, energy efficiency, are the most important metrics to evaluate the newly adopted techniques in any wireless communication system.

In Chapter 3, we have created and assessed innovative methods for encoding data in communication channels. These methods involve combining serial and parallel concatenated codes with NOMA technology, which will be used in future 6G communication systems. Our goal was to overcome the constraints of the current 5G technologies by improving the reliability, data throughput, through unique channel coding schemes.

This study is based on concatenated channel coding, combining numerous techniques to improve error correction capabilities. Using serial and parallel concatenation techniques, we have created two novel coding methods, namely PCSC and PCPC. These techniques combine polar codes and convolutional codes to produce better performance in terms of BER and data throughput. We conducted a thorough assessment of the per-

formance of PCSC and PCPC, utilising a range of measures, including BER, throughput, and the influence of different modulation schemes and codeword lengths.

The comparative analysis of BER performance between PCSC and PCPC codes, in comparison to established 5G coding approach PC, indicate that PCSC consistently performs better than PC across various modulation schemes (BPSK,QAM) and codeword lengths. For example, when using 64 QAM and a codeword length of $N = 8192$, PCSC coding yields a channel coding gain of 2.5dB at an error rate of 10^{-1}. The notable enhancement in BER highlights the capability of PCSC to increase the accuracy and dependability of data in 6G networks.

The practical feasibility of PCSC and PCPC for 6G was also assessed by evaluating the throughput, a crucial metric for measuring the data transmission rate. PCSC outperforms PC in terms of throughput, particularly in high modulation circumstances. As an illustration, PCSC can attain a data rate of 740 Gbps using 64 QAM modulation. PCSC's capacity to maintain high data rates even in difficult circumstances positions it as a strong contender for future 6G applications.

The emergence of PCSC and PCPC represents notable progress in channel coding for 6G, we have developed resilient coding methods capable of effectively managing the higher data rates and dependability requirements of upcoming wireless networks. The performance evaluations indicate that PCSC in particular, exhibits significant enhancements compared to current coding techniques, positioning it as a highly viable choice for integration into 6G systems.

As shown in Table 7.1 and Table 7.2, PCSC's improved error correction capabilities provide greater data integrity, which is vital for applications that demand dependable communication, such as autonomous driving and telemedicine. Its capacity to sustain a low BER across different modulation methods and codeword lengths is evidence of its resilience. Furthermore, generating data speeds of Tbps is a crucial objective for 6G, and PCSC's performance in this area shows promise.

Table 7.1: Performance evaluation of PCSC with different codeword length

Codeword length	Throughput (%)	Coding gain (dB)
2048	83.85	4.5
4096	66.65	5.75
8192	58.45	6.25

The substantial increase in data transfer rate, particularly in situations with advanced signal modulation, demonstrates that PCSC can efficiently accommodate the data-intensive applications expected in 6G networks. PCSC's ability to adjust to diverse codeword lengths and modulation methods guarantees its scalability across a wide range of 6G applications.

In Chapter 4, we focuses on developing and assessing Deep Learning PCPC (DL-

Table 7.2: Performance evaluation of different coding schemes for 6G

SNR	PCSC (BPSK)	PCPC	PC (BPSK)	PCSC (QAM)	PC (QAM)	Un-coded NOMA
0	0.052	0.536	0.780	0.136	1.398	0.1449
0.5	0.007	0.292	0.569	0.092	1.176	0.131
1	0.00057	0.156	0.286	0.056	1.028	0.11
1.5	1.4e-05	0.010	0.029	0.030	0.980	0.09
2	2.6e-07	0.00089	0.00089	0.014	0.769	0.0722

PCPC) channel decoding algorithms for 6G communication systems. Our objective was to improve the decoding procedure by using DL, specifically emphasising reaching high data rates in the THz range, optimising energy usage, and minimising system delay. The findings we obtained emphasise the notable enhancements in decoding performance, data throughput, EE, and system delay. This highlights the promise of DL-PCPC for future wireless communication networks.

DL-PCPC consistently surpasses SCD in performance, reaching a minimum decoding error of 0.01 Tbps by the tenth iteration, whilst SCD struggles to achieve anything below 0.28 Tbps. The substantial decrease in decoding error highlights the efficacy of the DL-PCPC method in guaranteeing precise data delivery. DL-PCPC outperforms SCD by achieving a data rate of 99% with greater repetitions. The DL-PCPC's ability to enhance data rate by 70% demonstrates its capacity to handle data-heavy tasks, including video streaming, VR, and XR, which are expected to be prevalent in 6G networks.

The capability to attain data speeds of up to 1 Tbps establishes DL-PCPC as a viable solution for forthcoming 6G networks. This feature is crucial for meeting the growing need for high-bandwidth applications, guaranteeing that 6G can fulfil its commitment to greatly improve data transmission speeds. Also, DL-PCPC demonstrates a perfect EE of 100%, surpassing SCD by a margin of 40%. This improvement indicates that DL-PCPC can handle larger data rates while consuming less energy, which aligns with the objective of 6G to decrease energy consumption by at least threefold compared to earlier generations. Moreover, DL-PCPC greatly decreases system latency to 0.003 μs, representing an over 100% enhancement compared to SCD, which has a latency of 1.45 μs. The significant decrease in delay guarantees that DL-PCPC can accommodate low-latency applications, which is necessary for 6G.

The technological advancement made by DL-PCPC has significant ramifications for the future of wireless communication. DL-PCPC enables the implementation of advanced communication technologies that may support many applications, such as immersive media and critical infrastructure monitoring while satisfying the demanding performance standards of 6G. DL-PCPC's adaptability to varied codeword lengths and modulation methods guarantees its scalability across a wide range of 6G use cases.

It is a highly adaptable technology that can effectively meet the varied requirements of upcoming communication networks. Although DL-PCPC has shown remarkable performance, additional research is required to thoroughly investigate its full potential. Furthermore, investigating the utilisation of DL-PCPC across various frequency ranges and network setups would yield more profound understanding of its potential.

In addition to the achievements gained by adopting novel channel coding and decoding techniques into 6G system, we have implemented the ARIS in THz 6G communication systems to improve reliability, coverage, latency, and power efficiency. Our objective was to enhance the efficiency of signal power distribution to target users, particularly those in areas with little coverage, by utilising the ARIS Decision Making Algorithm (ARIS-DMA) in Chapter 5. This novel strategy was evaluated using 6G KPIs and compared to cutting-edge techniques such as STAR-RIS and conventional BS handover.

ARIS-DMA showed a noteworthy decrease in power loss compared to STAR-RIS and BS handover, particularly in user-dense situations. When the user density reached 16×10^6, ARIS-DMA experienced a power loss of only 0.33 dBm, while STAR-RIS had a power loss of 27.26 dBm. This suggests that ARIS-DMA is much improved in preserving signal strength. As reducing system latency is essential for real-time applications in 6G networks. ARIS-DMA achieved a latency reduction of 42% compared to STAR-RIS and 44% compared to BS handover, resulting in a delay of only 0.15 µs. This enhancement guarantees accelerated data transmission and a highly responsive communication network. One of the main objectives of ARIS-DMA was to target areas with no network coverage. According to the performance evaluation, ARIS-DMA achieved almost complete coverage, surpassing STAR-RIS 26% and BS handover 73.6% at a frequency of 300 GHz and a user density of 16×10^6. This outcome emphasises the efficacy of ARIS-DMA in guaranteeing extensive network coverage.

In addition to that, in high-density settings, ARIS-DMA demonstrated a significant channel gain of up to 25dB compared to STAR-RIS, suggesting a decreased FSR. The performance of ARIS-DMA remained consistent across several frequencies (300, 400, and 500 GHz), demonstrating its resilience in ensuring dependable communication even under difficult circumstances. The total system efficiency of ARIS-DMA was confirmed by multiple tests. ARIS-DMA had a system dependability of 95%, which was notably superior to the 11% attained by STAR-RIS. The practical feasibility of ARIS-DMA in real-world 6G installations is highlighted by its great efficiency.

The ARIS-DMA system can potentially improve network reliability and efficiency by greatly reducing power loss and system latency while offering almost complete coverage. These enhancements are essential for facilitating the high data transmission speeds and minimal delay necessary for 6G applications. Furthermore, the ARIS-DMA's capacity to adjust to different user densities and environmental circumstances makes it

a scalable option for many deployment scenarios. ARIS-DMA can efficiently optimise signal delivery, whether in densely populated urban regions or sparsely covered rural areas. Although ARIS-DMA has demonstrated impressive performance, future studies could investigate the incorporation of more sophisticated DL methods and real-time adaptive algorithms to augment its potential further. Furthermore, conducting real implementation and field testing in various scenarios is crucial to confirm the theoretical conclusions and guarantee smooth integration into the current infrastructure.

Building on that, we have developed a new beamforming solution called Deep Q Network ARISDMA (DQN-ARISDMA) in Chapter 6. This solution uses deep Q networks to improve the beamforming process for ARIS-DMA. This novel methodology tackles the distinct obstacles faced by 6G communication systems to attain THz data rates while accommodating high user densities and delivering exceptional fairness, SE, data rates, and PER performance.

Attaining a high SE is essential in order to satisfy the increasing need for high data rates in the context of 6G. The capability of DQN-ARISDMA to optimise SE results in increased data rates and decreased PER, which is crucial for various applications including real-time communication and important data transmission. Additionally, for DL techniques to be effective, it is crucial to have efficient learning and quick adaptation. The low convergence time and delay of DQN-ARISDMA provide quick decision-making and responsiveness, which is crucial for applications that demand immediate input and actions. Moreover, ensuring a high level of fairness guarantees an equal distribution of resources, which improves both the user experience and the network's performance. Also, the PER achieved by the DQN-ARISDMA suggests a high level of reliability, which is essential for ensuring the quality of service in 6G networks. The practical implications of these findings indicate that DQN-ARISDMA is highly suitable for deployment in 6G networks, as it offers substantial enhancements in performance and efficiency. The method's capacity to manage high-frequency spectrum resources and adjust to changing network conditions renders it a resilient solution for forthcoming wireless communication systems.

The DQN-ARISDMA beamforming solution seamlessly combines deep learning and beamforming techniques for ARIS-DMA in 6G communication networks. DQN-ARISDMA successfully fulfils the ambitious performance goals of 6G by attaining outstanding fairness, SE, data speeds, low PER, and reduced convergence time and latency. The findings illustrate the capacity of DL to transform beamforming techniques, opening up possibilities for fast, dependable, and efficient wireless communication in future network generations. This complete strategy for beamforming guarantees that 6G networks can effectively handle the high requirements of future applications and services, establishing a strong basis for continuous progress in wireless technology.

7.3 Future Research Directions

Although this thesis has made significant contributions to 6G wireless communication, some ongoing research issues are still predicted to evolve alongside the advancements in THz communications. To further improve the research area, new and innovative contributions are necessary to address these new issues. This section outlines current research areas and potential future directions in this context.

The proposed channel coding techniques PCSC and PCPC can be extended to consider the development of adaptive modulation and coding techniques that automatically alter the coding and modulation parameters in response to real-time channel conditions to optimise performance. Furthermore and due to the emergence of quantum computing, the development of quantum-resistant channel coding algorithms is crucial for ensuring secure communication in 6G. This could be done by exploring the integration of quantum key distribution with the developed channel coding in this thesis. Another open research field is the integration of digital twin, it is highly promising to make use of digital twin technology to generate live simulations of 6G networks, facilitating the examination and enhancement of channel coding techniques in various network scenarios. Additionally, leverage digital twins for proactive maintenance of communication networks and optimization of network resources to guarantee dependable and efficient performance.

To increase the performance of DL-PCPC, further research should be conducted with an emphasis on constructing more advanced neural network architectures. This entails investigating many categories of neural networks, such as Recurrent Neural Networks (RNNs) and transformer models, which have the potential to deliver superior performance for sequential data and long-range dependencies. In addition, sophisticated data augmentation approaches should be researched to boost the training process and improve the model's capacity to generalise to unfamiliar data. Furthermore, it investigates the application of post-quantum cryptography techniques in the DL decoding framework to bolster security and adapt DL based decoding methods to meet the special demands of IoT and edge computing settings, particularly emphasising energy efficient and resource limited devices.

While this study offers potential strategies and research contributions for ARIS-DMA assisted wireless communication, it does have several limitations in regards to the implementation of ARIS-DMA. The first limitation is that the assumption that complete CSI is accessible, this assumption is improbable to be incorporated into practical communication systems. Nevertheless, we could not further study these difficulties due to the constraints of the research topic. The second important thing is that certain aspects of power consumption and overhead should be fully considered, such as pilot overhead and robots' energy overhead in ARIS-DMA. The overheads in the physical

world are inevitable. Therefore, conducting further research on ARIS-DMA overheads is worthwhile to enhance the standardisation and implementation of ARIS-DMA. The last limitation that this study faced that it needs more experimental validation for the proposed algorithms. Despite making considerable effort to acquire a ARIS-DMA prototype for conducting tests, the author failed to get the opportunity to deploy the simulation based algorithms on hardware due to fund constraints. Also, expanding the utilisation of ARIS-DMA to difficult settings such as underwater and remote rural locations and the implementation of ARIS-DMA on UAV to enhance network coverage and minimise communication delays in these areas is a promising open research problem that could be addressed with the presence of ARIS-DMA.

Applying the DQN algorithm to the ARIS-DMA in the form of DQN-ARISDMA has yielded encouraging outcomes. However, there is potential for additional enhancements. For instance, employing multi-step learning to update the Q values, which is based on considering numerous future steps instead of just one, can lead to more informative updates and enhance the stability of the learning process. In addition, two learning methodologies can be employed as well. The first one is transfer learning, which involves utilising pre-trained models from analogous tasks or contexts. This strategy enables the DQN to acquire knowledge rapidly and efficiently in novel or changing environments. Another approach is to employ curriculum learning, which involves training the agent on increasingly challenging tasks. This can enhance the DQN's ability to acquire intricate policies more efficiently.

7.4 This Research's Effect on Industrial Practice

This study contributions in new channel coding, deep learning based channel decoding, adaptive reconfigurable intelligent surfaces, and deep Q networks with adaptive reconfigurable intelligent surfaces, will have a major impact on industrial practice, specifically in the advancement and implementation of advanced communication systems such as 6G. The following are the primary effects for each contribution separately:

1. **Channel Coding (PCSC, PCPC)**
    - **Improved Data Throughput:** Implementing new channel coding methods allows for increased data rates, which are crucial for applications that need a significant amount of bandwidth, such as streaming high-definition videos and providing immersive VR/AR experiences.
    - **Improved Error Rates:** Increased error correction capabilities result in decreased mistake rates, improving communication systems' dependability. This is particularly important for industrial automation, autonomous vehicles, and remote healthcare applications.

- **Energy Efficiency:** Optimising channel coding minimises the necessity for retransmissions, resulting in energy conservation and prolonged battery longevity for mobile and IoT devices.
- **Scalability:** Advanced channel coding algorithms facilitate handling the many linked devices anticipated in IoT, smart cities, and industrial IoT deployments.

2. **DL-Based Channel Decoding (DL-PCPC)**
    - **Adaptive Performance:** Deep learning-based decoding can adjust to changing channel circumstances in real time, ensuring constant performance in diverse situations. This is particularly important for mobile and wireless communications in dynamic industrial settings.
    - **Reduced Latency:** Enhanced decoding procedures that are quicker and more effective minimise communication delays, a crucial factor for time-critical tasks like autonomous driving and real-time industrial control systems.
    - **Enhanced Security:** Proficiency in managing intricate decoding tasks is advantageous for creating highly secure communication protocols and safeguarding industrial data from interception and modification.
    - **Cost Reduction:** Implementing deep learning algorithms to automate decoding procedures might decrease the intricate hardware requirement, reducing the expenses associated with building and managing communication infrastructure.
3. **Adaptive Reconfigurable Intelligent Surfaces (ARIS-DMA)**
    - **Improved Coverage and Capacity:** ARIS-DMA can adapt and improve signal strength and quality, greatly improving coverage and capacity in urban areas and indoor locations where traditional infrastructure may have difficulties.
    - **Energy Efficiency:** ARIS-DMA optimises signal routing to minimise energy usage, resulting in more sustainable and cost-effective communication networks.
4. **Deep Q Networks (DQN-ARISDMA)**
    - **Autonomous Network Management:** DQN-ARISDMA facilitates automated network management, minimising the requirement for human involvement and enabling more prompt and adaptable network operations.
    - **Enhanced QoS:** DQN-ARISDMA facilitates automated network management, minimising the requirement for human involvement and enabling more prompt and adaptable network operations.
    - **Scalability and Flexibility:** DQN-ARISDMA can manage intricate decision-making procedures, rendering it capable of scaling and adjusting to various network scenarios and demands in industrial applications.

As an advanced system, the integration of these advanced technologies have synergistic benefits:

1. **End-to-End Optimization:**
   (a) **Improved Performance Across the Network:** By integrating innovative channel coding techniques with DL-based decoding, the overall error rates can be substantially diminished, resulting in enhanced data transmission reliability. Integrating these components with DQN-ARISDMA enhances the communication network's efficiency and resilience.
   (b) **Holistic Approach:** Every technique focuses on distinct areas of communication issues, such as error correction, adaptive decoding, signal optimisation, and resource management. Collectively, they generate a cohesive and enhanced communication encounter.
2. **Enhanced Reliability and Performance:**
   (a) **Error Reduction and Robust Decoding:** The combination of advanced channel coding with DL based decoding guarantees minimum mistakes, even in demanding situations. ARIS-DMA can enhance the quality and range of signals. When effectively controlled by DQN-ARISDMA, it ensures consistent reliability and real-time performance.
   (b) **Consistent QoS:** The integrated technologies can adjust to different conditions to uphold a consistent QoS, which is essential for applications such as autonomous driving or industrial automation.
3. **Cost Efficiency:**
   (a) **Resource Optimization:** The DQN-ARISDMA algorithm may allocate resources, such as bandwidth and power, by utilising real-time data. This leads to a reduction in waste and an enhancement in overall efficiency. This enhances the energy conservation obtained through ARIS-DMA and the decreased retransmissions resulting from improved channel coding and decoding.
   (b) **Reduced Infrastructure Costs:** ARIS-DMA can be implemented on current systems, reducing additional infrastructure requirements. Also, advanced coding and decoding techniques result in increased efficiency, leading to a decrease in operational costs.
4. **Rapid Deployment and Adaptation:**
   (a) **Scalable Solutions:** The presented techniques can scale in proportion to rising requirements, such as an increasing number of consumers or faster data speeds, without the need for significant human modifications or upgrades.

Practical Synergies in Industrial Applications:

1. **Smart Manufacturing:** Effective and dependable communication is essential for a smart factory's Machine to Machine (M2M) connectivity. Advanced PCSC and PCPC channel coding and DL-PCPC decoding techniques guarantee the accuracy and reliability of data. The ARIS-DMA system efficiently optimises the signal pathways within the factory, and the DQN-ARISDMA algorithm dynamically controls the network resources to prevent congestion.
2. **Autonomous Vehicles:** Autonomous cars require low latency and excellent reliability. By integrating these technologies, we can establish reliable communication channels with minimal latency, allowing for vehicles' safe and efficient operation.
3. **Remote Healthcare:** Reliable high-speed connectivity is crucial in the field of telemedicine. The combined impacts of these technologies guarantee the preservation of high-quality video and data streams, hence improving patient care.

These proposals provide a starting point for more study and practical applications in the field of wireless communication modelling for 6G. However, the methodology employed in this thesis has the potential to be applied in domains beyond those that have been mentioned.

fin.

Bibliography

[1] A. K. Ahmed and H. S. Al-Raweshidy, "Performance evaluation of deep q networks for hybrid reconfigurable intelligent surface in 6g networks," in *2024 International Conference on Computer, Information and Telecommunication Systems (CITS)*, 2024, pp. 1–8. DOI: 10.1109/CITS61189.2024.10608029.

[2] A. K. Ahmed and H. S. Al-Raweshidy, "Highly efficient hybrid reconfigurable intelligent surface approach for power loss reduction and coverage area enhancement in 6g networks," *Applied Sciences*, vol. 14, no. 15-6457, 2024, ISSN: 2076-3417. DOI: 10.3390/app14156457.

[3] A. K. Ahmed and H. S. Al-Raweshidy, "Deep learning polar convolutional parallel concatenated (dl-pcpc) channel decoding for 6g communications," in *2023 International Conference on Computer, Information and Telecommunication Systems (CITS)*, 2023, pp. 01–05. DOI: 10.1109/CITS58301.2023.10188712.

[4] A. K. Ahmed and H. S. Al-Raweshidy, "Performance evaluation of serial and parallel concatenated channel coding scheme with non-orthogonal multiple access for 6g networks," *IEEE Access*, vol. 10, pp. 39 681–39 690, 2022. DOI: 10.1109/ACCESS.2022.3166943.

[5] W. Saad, M. Bennis, and M. Chen, "A vision of 6g wireless systems: Applications, trends, technologies, and open research problems," *IEEE Network*, vol. 34, no. 3, pp. 134–142, 2020. DOI: 10.1109/MNET.001.1900287.

[6] S. Dang, O. Amin, B. Shihada, and M.-S. Alouini, "What should 6g be?" *Nature Electronics*, vol. 3, no. 1, pp. 20–29, Jan. 2020, ISSN: 2520-1131. DOI: 10.1038/s41928-019-0355-6.

[7] I. F. Akyildiz, A. Kak, and S. Nie, "6g and beyond: The future of wireless communications systems," *IEEE Access*, vol. 8, pp. 133 995–134 030, 2020. DOI: 10.1109/ACCESS.2020.3010896.

[8] N. Rajatheva *et al.*, "White paper on broadband connectivity in 6g," *arXiv: Signal Processing*, 2020.

[9] M. Z. Asghar, S. A. Memon, and J. Hämäläinen, "Evolution of wireless communication to 6g: Potential applications and research directions," *Sustainability (Switzerland)*, vol. 14, no. 10, pp. 1–26, 2022, ISSN: 20711050. DOI: 10.3390/su14106356.

[10] R. A. Meyers and P. H. Waters, "Synthesiser review for pan-european digital cellular radio," *IEE Colloquium on VLSI Implementations for Second Generation Digital Cordless and Mobile Telecommunication Systems*, pp. 8/1–810, 1990.

[11] B. Barani and B. A. D. Ikonomou J. S. Dasilva, "European third-generation mobile systems," *IEEE Communications Magazine*, vol. vol. 34, n, pp. 68–79, October 1996. DOI: 10.1109/35.544325.

[12] I. G. L. M. Dramitinos, "A bandwidth allocation mechanism for 4g," in *Proceedings of the 2nd European Wireless Technology Conference*, 2009, pp. 96–99.

[13] E. Summary, "5g ppp progress monitoring report – 2019," pp. 1–68, August 2020.

[14] A. Osseiran, J. F. Monserrat, and P. Marsch, "5g mobile and wireless communications technology," *5G Mobile and Wireless Communications Technology*, pp. 1–406, 2016. DOI: 10.1017/CBO9781316417744.

[15] S. A. A. Hakeem, H. H. Hussein, and H. Kim, "Vision and research directions of 6g technologies and applications," 2022. DOI: 10.1016/j.jksuci.2022.03.019.

[16] L. Richard, "Network 2030 a blueprint of technology, applications and market drivers towards the year 2030 and beyond," *Focus Group on Technologies for Network 2030*, 2020.

[17] NetworldEurope, "Strategic research and innovation agenda."

[18] NetworldEurope, "White paper on 5g: 5g: Challenges, research priorities, and recommendations," 2014.

[19] E. Partnership and H. Europe, "European partnership under horizon europe clean aviation," pp. 1–141, June 2020.

[20] C. D. Lima *et al.*, "Convergent communication, sensing and localization in 6g systems: An overview of technologies, opportunities and challenges," *IEEE Access*, vol. 9, pp. 26 902–26 925, 2021, ISSN: 21693536. DOI: 10.1109/ACCESS.2021.3053486.

[21] Y. Chen, W. Liu, Z. Niu, Z. Feng, Q. Hu, and T. Jiang, "Pervasive intelligent endogenous 6g wireless systems: Prospects, theories and key technologies," *Digital Communications and Networks*, vol. 6, no. 3, pp. 312–320, Aug. 2020, ISSN: 2352-8648. DOI: 10.1016/J.DCAN.2020.07.002.

[22] Y. Lu, X. Z.-J. o. I. I. Integration, and undefined 2020, "6g: A survey on technologies, scenarios, challenges, and the related issues," *Elsevier*,

[23] S. Chen, Y. C. Liang, S. Sun, S. Kang, W. Cheng, and M. Peng, "Vision, requirements, and technology trend of 6g: How to tackle the challenges of system coverage, capacity, user data-rate and movement speed," *IEEE Wireless Communications*, vol. 27, no. 2, pp. 218–228, Apr. 2020, ISSN: 15580687. DOI: 10.1109/MWC.001.1900333.

[24] S. Dang, O. Amin, B. Shihada, M. S. Alouini, B. Shihada, and O. A. M.-S. Alouini S. Dang, "What should 6g be?" *Nature Electronics*, vol. 3, no. 1, pp. 20–29, 2020, ISSN: 25201131. DOI: 10.1038/s41928-019-0355-6.

[25] T. S. Rappaport *et al.*, "Wireless communications and applications above 100 GHz: Opportunities and challenges for 6g and beyond," *IEEE Access*, vol. 7, pp. 78 729–78 757, 2019, ISSN: 21693536. DOI: 10.1109/ACCESS.2019.2921522.

[26] K. Nallappan, H. Guerboukha, C. Nerguizian, and M. Skorobogatiy, "Uncompressed HD and ultra-HD video streaming using terahertz wireless communications," *2018 11th Global Symposium on Millimeter Waves, GSMM 2018*, Aug. 2018. DOI: 10.1109/GSMM.2018.8439548.

[27] E. Basar, "Reconfigurable intelligent surface-based index modulation: A new beyond mimo paradigm for 6g," *IEEE Transactions on Communications*, vol. 68, no. 5, pp. 3187–3196, 2020. DOI: 10.1109/TCOMM.2020.2971486.

[28] M. D. Renzo *et al.*, "Smart radio environments empowered by reconfigurable intelligent surfaces: How it works, state of research, and the road ahead," *IEEE Journal on Selected Areas in Communications*, vol. 38, no. 11, pp. 2450–2525, Nov. 2020, ISSN: 15580008. DOI: 10.1109/JSAC.2020.3007211.

[29] BR, "Recommendation ITU-r m.2083-0 IMT vision-framework and overall objectives of the future development of IMT for 2020 and beyond m series mobile, radiodetermination, amateur and related satellite services,"

[30] B. Sliwa, R. Falkenberg, and C. Wietfeld, "Towards cooperative data rate prediction for future mobile and vehicular 6g networks," *2nd 6G Wireless Summit 2020: Gain Edge for the 6G Era, 6G SUMMIT 2020*, Mar. 2020. DOI: 10.1109/6GSUMMIT49458.2020.9083767.

[31] M. Banafaa, I. Shayea, J. Din, M. H. Azmi, *et al.*, "6g mobile communication technology: Requirements, targets, applications, challenges, advantages, and opportunities," *Alexandria Engineering Journal*, vol. 64, pp. 245–274, 2023, ISSN: 1110-0168. DOI: 10.1016/j.aej.2022.08.017.

[32] M. Bagaa, D. L. C. Dutra, T. Taleb, and H. Flinck, "Toward enabling network slice mobility to support 6g system," *IEEE Transactions on Wireless Communications*, vol. 21, no. 12, pp. 10 130–10 144, Dec. 2022, ISSN: 15582248. DOI: 10.1109/TWC.2022.3182591.

[33] S. Alraih *et al.*, "Revolution or evolution? technical requirements and considerations towards 6g mobile communications," *Sensors*, vol. 22, no. 3, 2022, ISSN: 14248220. DOI: 10.3390/s22030762.

[34] B. Liu, J. Luo, and X. Su, "The framework of 6g self-evolving networks and the decision-making scheme for massive iot," *Applied Sciences (Switzerland)*, vol. 11, no. 19, 2021, ISSN: 20763417. DOI: 10.3390/app11199353.

[35] A. Slalmi, H. Chaibi, A. Chehri, R. Saadane, and G. Jeon, "Toward 6g: Understanding network requirements and key performance indicators," *Transactions on Emerging Telecommunications Technologies*, vol. 32, no. 3, 2021, ISSN: 21613915. DOI: 10.1002/ett.4201.

[36] M. Alsabah *et al.*, "6g wireless communications networks: A comprehensive survey," *IEEE Access*, vol. 9, pp. 148 191–148 243, 2021. DOI: 10.1109/ACCESS.2021.3124812.

[37] W. Saad, M. Bennis, and M. Chen, "A vision of 6g wireless systems: Applications, trends, technologies, and open research problems," *IEEE Network*, vol. 34, no. 3, pp. 134–142, May 2020, ISSN: 1558156X. DOI: 10.1109/MNET.001.1900287.

[38] M. N. Mahdi, A. R. Ahmad, Q. S. Qassim, H. Natiq, M. A. Subhi, and M. Mahmoud, "From 5g to 6g technology: Meets energy, internet-of-things and machine learning: A survey," *Applied Sciences 2021, Vol. 11, Page 8117*, vol. 11, no. 17, p. 8117, Aug. 2021, ISSN: 2076-3417. DOI: 10.3390/APP11178117.

[39] S. Iyer, A. Patil, S. Bhairanatti, S. Halagatti, and R. J. Pandya, "A survey on technological trends to enhance spectrum-efficiency in 6g communications," *Transactions of the Indian National Academy of Engineering*, vol. 7, no. 4, pp. 1093–1120, Dec. 1, 2022, ISSN: 2662-5423. DOI: 10.1007/s41403-022-00372-w.

[40] E. Hossain and F. Fredj, "Editorial: Energy efficiency of machine-learning-based designs for future wireless systems and networks," *IEEE Transactions on Green Communications and Networking*, vol. 5, no. 3, pp. 1005–1010, Sep. 2021, ISSN: 24732400. DOI: 10.1109/TGCN.2021.3099580.

[41] N. Hu, Z. Tian, X. Du, and M. Guizani, "An energy-efficient in-network computing paradigm for 6g," *IEEE Transactions on Green Communications and Networking*, vol. 5, no. 4, pp. 1722–1733, Dec. 2021, ISSN: 24732400. DOI: 10.1109/TGCN.2021.3099804.

[42] T. Huang, W. U. Yang, J. Wu, *et al.*, "SPECIAL SECTION ON GREEN INTERNET OF THINGS a survey on green 6g network: Architecture and technologies," DOI: 10.1109/ACCESS.2019.2957648.

[43] K. B. Letaief, W. Chen, Y. Shi, J. Zhang, and Y. J. A. Zhang, "The roadmap to 6g: AI empowered wireless networks," *IEEE Communications Magazine*, vol. 57, no. 8, pp. 84–90, Aug. 2019, ISSN: 15581896. DOI: 10.1109/MCOM.2019.1900271.

[44] E. Basar, M. D. Renzo, J. D. Rosny, M. Debbah, M.-S. Alouini, and R. Zhang, "Wireless communications through reconfigurable intelligent surfaces," vol. 1, 2019. DOI: 10.1109/ACCESS.2019.2935192.

[45] R. Shafin, L. Liu, V. Chandrasekhar, H. Chen, J. Reed, and J. C. Zhang, "Artificial intelligence-enabled cellular networks: A critical path to beyond-5g and 6g," *IEEE Wireless Communications*, vol. 27, no. 2, pp. 212–217, Apr. 2020, ISSN: 15580687. DOI: 10.1109/MWC.001.1900323.

[46] Q. Xia and J. M. Jornet, "Expedited neighbor discovery in directional terahertz communication networks enhanced by antenna side-lobe information," 2015.

[47] X. Wang, L. Kong, *et al.*, "Millimeter wave communication: A comprehensive survey," *IEEE Communications Surveys and Tutorials*, vol. 20, no. 3, pp. 1616–1653, 2018. DOI: 10.1109/COMST.2018.2844322.

[48] T. Eichler and R. Ziegler, "Fundamentals of thz technology for 6g," Rohde & Schwarz, Tech. Rep., Nov. 2022.

[49] A. Y. Pawar, K. B. E. Deepak D. Sonawane, and D. V. Derle, "Terahertz technology and its applications," *Drug Invention Today*, vol. 5, pp. 157–163, 2 2013, ISSN: 0975-7619. DOI: 10.1016/j.dit.2013.03.009.

[50] Z. Qadir, K. N. Le, N. Saeed, and H. S. Munawar, "Towards 6g internet of things: Recent advances, use cases, and open challenges," *ICT Express*, vol. 9, no. 3, pp. 296–312, 2023, ISSN: 2405-9595. DOI: https://doi.org/10.1016/j.icte.2022.06.006.

[51] I. F. Akyildiz, J. M. Jornet, and C. Han, "Teranets: Ultra-broadband communication networks in the terahertz band," *IEEE Wireless Communications*, vol. 21, no. 4, pp. 130–135, 2014. DOI: 10.1109/MWC.2014.6882305.

[52] C. Chaccour, M. N. Soorki, W. Saad, M. Bennis, P. Popovski, and M. Debbah, "Seven defining features of terahertz (thz) wireless systems: A fellowship of communication and sensing," *IEEE Communications Surveys and Tutorials*, vol. 24, no. 2, pp. 967–993, 2022. DOI: 10.1109/COMST.2022.3143454.

[53] I. F. Akyildiz, C. Han, Z. Hu, S. Nie, and J. M. Jornet, "Terahertz band communication: An old problem revisited and research directions for the next decade," *IEEE Transactions on Communications*, vol. 70, no. 6, pp. 4250–4285, 2022. DOI: 10.1109/TCOMM.2022.3171800.

[54] K. M. S. Huq, S. A. Busari, J. Rodriguez, V. Frascolla, W. Bazzi, and D. C. Sicker, "Terahertz-enabled wireless system for beyond-5g ultra-fast networks: A brief survey," *IEEE Network*, vol. 33, no. 4, pp. 89–95, 2019. DOI: 10.1109/MNET.2019.1800430.

[55] V. Petrov, T. Kurner, and I. Hosako, "Ieee 802.15.3d: First standardization efforts for sub-terahertz band communications toward 6g," *IEEE Communications Magazine*, vol. 58, no. 11, pp. 28–33, 2020. DOI: 10.1109/MCOM.001.2000273.

[56] L. Zhang, X. Pang, S. Jia, S. Wang, and X. Yu, "Beyond 100 gb/s optoelectronic terahertz communications: Key technologies and directions," *IEEE Communications Magazine*, vol. 58, no. 11, pp. 34–40, 2020. DOI: 10.1109/MCOM.001.2000254.

[57] I. SA. "Ieee sa - ieee 802.15.3d-2017." (2017), [Online]. Available: https://standards.ieee.org/ieee/802.15.3d/6648/.

[58] J. A. Cabrera, H. Boche, C. Deppe, R. F. Schaefer, C. Scheunert, and F. H. P. Fitzek, "6g and the post-shannon theory," *Shaping Future 6G Networks: Needs, Impacts, and Technologies*, pp. 271–294, Jan. 2021. DOI: 10.1002/9781119765554.CH16.

[59] P. R. P. Hoole, "5 a new smart antenna for 5/6g wireless systems: Narrow 360° steerable beam with no reflectors," in *Smart Antennas and Electromagnetic Signal Processing for Advanced Wireless Technology: with Artificial Intelligence Applications and Coding*. 2020, pp. 147–166.

[60] C. Yue, V. Miloslavskaya, M. Shirvanimoghaddam, B. Vucetic, and Y. Li, "Efficient decoders for short block length codes in 6g urllc," *IEEE Communications Magazine*, vol. 61, no. 4, pp. 84–90, 2023. DOI: 10.1109/MCOM.001.2200275.

[61] M. E. Jbari and M. Moussaoui, "Energy efficient channel coding for terahertz communications in 6g networks," *2022 International Conference on Innovation and Intelligence for Informatics, Computing, and Technologies, 3ICT 2022*, pp. 481–488, 2022. DOI: 10.1109/3ICT56508.2022.9990857.

[62] W. Tong and P. Zhu, *6G: The Next Horizon: From Connected People and Things to Connected Intelligence*. Cambridge University Press, 2021.

[63] Y. Dong, J. Dai, K. Niu, S. Wang, and Y. Yuan, "Joint source-channel coding for 6g communications," *China Communications*, vol. 19, no. 3, pp. 101–115, 2022. DOI: 10.23919/JCC.2022.03.007.

[64] C. Yue, V. Miloslavskaya, M. Shirvanimoghaddam, B. Vucetic, and Y. Li, "Efficient decoders for short block length codes in 6g URLLC," *IEEE Communications Magazine*, vol. 61, no. 4, pp. 84–90, Apr. 2023, ISSN: 1558-1896. DOI: 10.1109/MCOM.001.2200275.

[65] X. Zhong, C.-W. Sham, *et al.*, "Joint source-channel coding system for 6g communication: Design, prototype and future directions," *IEEE Access*, vol. 12, pp. 17 708–17 724, 2024. DOI: 10.1109/ACCESS.2024.3360003.

[66] S. Huang and C. Ji, "Channel coding at finite blocklength and its application in 6g URLLC," *Journal of Computer and Communications*, vol. 11, pp. 132–142, 2023. DOI: 10.4236/jcc.2023.119008.

[67] S. S. B. Huang and C. Ji, "Channel coding at finite blocklength and its application in 6g urllc," *Journal of Computer and Communications*, vol. 11, pp. 132–142, 2023. DOI: 10.4236/jcc.2023.119008.

[68] K. Zhu and Z. Wu, "Comprehensive study on CC-LDPC, BC-LDPC and polar code; comprehensive study on CC-LDPC, BC-LDPC and polar code," in *2020 IEEE Wireless Communications and Networking Conference Workshops (WCNCW)*, 2020.

[69] A. Agarwal and S. N. Mehta, "PC-CC: An advancement in forward error correction using polar and convolutional codes for MIMO-OFDM system," *Journal of King Saud University*

- *Computer and Information Sciences*, vol. 32, no. 8, pp. 917–927, Oct. 2020, ISSN: 22131248. DOI: 10.1016/j.jksuci.2017.12.003.

[70] Q. Wang, P. Fu, and S. Zhang, "A comparison of concatenated polar codes with different interleaving and decoding schemes," *2020 5th International Conference on Computer and Communication Systems, ICCCS 2020*, pp. 570–574, May 2020. DOI: 10.1109/ICCCS49078.2020.9118473.

[71] P. Chen, B. Bai, J. Wang, and S. Sun, "SPECIAL SECTION ON ADVANCES IN CHANNEL CODING FOR 5g AND BEYOND hash-polar codes with application to 5g," DOI: 10.1109/ACCESS.2019.2892969.

[72] W. Li and Z. He, "An efficient CRC-aided parity-check concatenated polar coding; an efficient CRC-aided parity-check concatenated polar coding," *2021 IEEE Asia Conference on Information Engineering (ACIE)*, 2021. DOI: 10.1109/ACIE51979.2021.9381073.

[73] N. Doan, A. Hashemi, E. N. Mambou, T. Tonnellier, and W. J. Gross, *Neural Belief Propagation Decoding of CRC-Polar Concatenated Codes; Neural Belief Propagation Decoding of CRC-Polar Concatenated Codes*. 2019, ISBN: 978-1-5386-8088-9.

[74] X. You *et al.*, "Spatiotemporal 2-d channel coding for very low latency reliable mimo transmission," in *2022 IEEE Globecom Workshops (GC Wkshps)*, 2022, pp. 473–479. DOI: 10.1109/GCWkshps56602.2022.10008621.

[75] A. Sahin, I. Guvenc, and H. Arslan, "A survey on multicarrier communications: Prototype filters, lattice structures, and implementation aspects," *IEEE Communications Surveys and Tutorials*, vol. 16, no. 3, pp. 1312–1338, 2014, ISSN: 1553877X. DOI: 10.1109/SURV.2013.121213.00263.

[76] A. F. M. S. Shah, S. Member, A. N. Qasim, M. A. Karabulut, H. Ilhan, and M. B. Islam, "Survey and performance evaluation of multiple access schemes for next-generation wireless communication systems," DOI: 10.1109/ACCESS.2021.3104509.

[77] B. Farhang-Boroujeny, "Filter bank multicarrier modulation: A waveform candidate for 5g and beyond," *Advances in Electrical Engineering*, vol. 2014, pp. 1–25, Dec. 2014, ISSN: 2356-6655. DOI: 10.1155/2014/482805.

[78] W. Jiang and F.-L. Luo, "Adaptive and non-orthogonal multiple access systems in 6g," in *6G Key Technologies: A Comprehensive Guide*. 2023, pp. 475–540. DOI: 10.1002/9781119847502.ch10.

[79] A. Bansal, N. Agrawal, and K. Singh, "Rate-splitting multiple access for UAV-based RIS-enabled interference-limited vehicular communication system," *IEEE TRANSACTIONS ON INTELLIGENT VEHICLES*, vol. 8, no. 1, 2023. DOI: 10.1109/TIV.2022.3168159.

[80] O. M. K. Al-Dulaimi, A. M. K. Al-Dulaimi, M. O. Alexandra, and M. K. H. Al-Dulaimi, "Strategy for non-orthogonal multiple access and performance in 5g and 6g networks,"

Sensors 2023, Vol. 23, Page 1705, vol. 23, no. 3, p. 1705, Feb. 2023, ISSN: 1424-8220. DOI: 10.3390/S23031705.

[81] Y. Liu, S. Zhang, X. Mu, Z. Ding, R. S.-I. J. on . . ., and undefined 2022, "Evolution of NOMA toward next generation multiple access (NGMA) for 6g," *ieeexplore.ieee.org*,

[82] H. Yahya, A. Al-Dweik, and E. Alsusa, "Power-tolerant NOMA using data-aware adaptive power assignment for IoT systems," *IEEE Internet of Things Journal*, vol. 8, no. 19, pp. 14 896–14 907, Oct. 2021, ISSN: 23274662. DOI: 10.1109/JIOT.2021.3072985.

[83] I. Budhiraja *et al.*, "A systematic review on NOMA variants for 5g and beyond," *IEEE Access*, vol. 9, pp. 85 573–85 644, 2021, ISSN: 21693536. DOI: 10.1109/ACCESS.2021.3081601.

[84] B. Kim, Y. Park, and D. Hong, "Partial non-orthogonal multiple access (p-NOMA)," *IEEE Wireless Communications Letters*, vol. 8, no. 5, pp. 1377–1380, Oct. 2019, ISSN: 21622345. DOI: 10.1109/LWC.2019.2918780.

[85] J. B. Kim and I. H. Lee, "Non-orthogonal multiple access in coordinated direct and relay transmission," *IEEE Communications Letters*, vol. 19, no. 11, pp. 2037–2040, Nov. 2015, ISSN: 10897798. DOI: 10.1109/LCOMM.2015.2474856.

[86] Z. Ding, P. Fan, and H. V. Poor, "Impact of user pairing on 5g nonorthogonal multiple-access downlink transmissions," *IEEE Transactions on Vehicular Technology*, vol. 65, no. 8, pp. 6010–6023, Aug. 2016, ISSN: 00189545. DOI: 10.1109/TVT.2015.2480766.

[87] H. Xing, Y. Liu, A. Nallanathan, Z. Ding, and H. V. Poor, "Optimal throughput fairness tradeoffs for downlink non-orthogonal multiple access over fading channels," *IEEE Transactions on Wireless Communications*, vol. 17, no. 6, pp. 3556–3571, Jun. 2018, ISSN: 15361276. DOI: 10.1109/TWC.2018.2803177.

[88] S. Arzykulov, T. A. Tsiftsis, G. Nauryzbayev, and M. Abdallah, "Outage performance of cooperative underlay CR-NOMA with imperfect CSI," *IEEE Communications Letters*, vol. 23, no. 1, pp. 176–179, Jan. 2019, ISSN: 15582558. DOI: 10.1109/LCOMM.2018.2878730.

[89] P. Yang, Y. Xiao, M. Xiao, and Z. Ma, "NOMA-aided precoded spatial modulation for downlink MIMO transmissions," *IEEE Journal on Selected Topics in Signal Processing*, vol. 13, no. 3, pp. 729–738, Jun. 2019, ISSN: 19324553. DOI: 10.1109/JSTSP.2019.2901131.

[90] B. Xia, J. Wang, K. Xiao, Y. Gao, Y. Yao, and S. Ma, "Outage performance analysis for the advanced SIC receiver in wireless NOMA systems," *IEEE Transactions on Vehicular Technology*, vol. 67, no. 7, pp. 6711–6715, Jul. 2018, ISSN: 00189545. DOI: 10.1109/TVT.2018.2813524.

[91] "3rd generation partnership project; technical specification group radio access network; study on non-orthogonal multiple access (NOMA) for NR (release 16)," 2018.

[92] D. Pokamestov, Y. Kryukov, E. Rogozhnikov, G. Shalin, A. Shinkevich, and S. Novichkov, "Adaptation of signal with NOMA and polar codes to the rayleigh channel," *Symmetry*, vol. 14, no. 10, Oct. 2022, ISSN: 20738994. DOI: 10.3390/sym14102103.

[93] J. M. Hamamreh, M. Abewa, L. J. Poncha, and J. M. Hamamreh, "New non-orthogonal transmission schemes for achieving highly efficient, reliable, and secure multi-user communications," *RS Open Journal on Innovative Communication Technologies*, vol. 1, no. 2, Dec. 2020, ISSN: 3023-5014. DOI: 10.46470/03D8FFBD.324CC0FB.

[94] S. K. Ibrahim, N. Q. Ismaeel, and S. A. Abdulhussien, "Comparison study of channel coding on non-orthogonal multiple access techniques," *Bulletin of Electrical Engineering and Informatics*, vol. 11, no. 2, pp. 909–916, Apr. 2022, ISSN: 23029285. DOI: 10.11591/eei.v11i2.3348.

[95] H. Sarieddeen, M. S. Alouini, and T. Y. Al-Naffouri, "Terahertz-band ultra-massive spatial modulation MIMO," *IEEE Journal on Selected Areas in Communications*, vol. 37, no. 9, pp. 2040–2052, Sep. 2019, ISSN: 15580008. DOI: 10.1109/JSAC.2019.2929455.

[96] M. B. Shahab, R. Abbas, M. Shirvanimoghaddam, and S. J. Johnson, "Grant-free non-orthogonal multiple access for IoT: A survey," *IEEE Communications Surveys and Tutorials*, vol. 22, no. 3, pp. 1805–1838, Jul. 2020, ISSN: 1553877X. DOI: 10.1109/COMST.2020.2996032.

[97] Q. Luo, P. Gao, *et al.*, "An error rate comparison of power domain non-orthogonal multiple access and sparse code multiple access," *IEEE Open Journal of the Communications Society*, vol. 2, pp. 500–511, 2021, ISSN: 2644125X. DOI: 10.1109/OJCOMS.2021.3064504.

[98] P. R. Li, Z. Ding, and K. T. Feng, "Enhanced receiver based on FEC code constraints for uplink NOMA with imperfect CSI," *IEEE Transactions on Wireless Communications*, vol. 18, no. 10, pp. 4790–4802, Oct. 2019, ISSN: 15582248. DOI: 10.1109/TWC.2019.2929386.

[99] K. Xiao, B. Xia, L. Ma, and Y. Wei, "Design and analysis of probabilistic shaping scheme for uplink nonorthogonal multiple access systems," *IEEE Transactions on Communications*, vol. 67, no. 12, pp. 8818–8833, Dec. 2019, ISSN: 15580857. DOI: 10.1109/TCOMM.2019.2946831.

[100] X. Zou, M. Ganji, and H. Jafarkhani, "Trellis-coded non-orthogonal multiple access," *IEEE Wireless Communications Letters*, vol. 9, no. 4, pp. 538–542, Apr. 2020, ISSN: 21622345. DOI: 10.1109/LWC.2019.2961899.

[101] B. K. Ng and C. T. Lam, "A new two-user binary polar coded multiple access scheme with power and rate allocation," *IEEE Wireless Communications Letters*, vol. 10, no. 10, pp. 2299–2303, Oct. 2021, ISSN: 21622345. DOI: 10.1109/LWC.2021.3100132.

[102] C. Yan, A. Harada, A. Benjebbour, Y. Lan, A. Li, and H. Jiang, "Receiver design for downlink non-orthogonal multiple access (NOMA)," *IEEE Vehicular Technology Conference*, vol. 2015, Jul. 2015, ISSN: 15502252. DOI: 10.1109/VTCSPRING.2015.7146043.

[103] W. Abd-Alaziz, B. A. Jebur, H. Fakhrey, Z. Mei, and K. Rabie, "A low-complexity coding scheme for NOMA," *IEEE Systems Journal*, vol. 17, no. 3, pp. 4464–4473, Sep. 2023, ISSN: 19379234. DOI: 10.1109/JSYST.2023.3262174.

[104] V. C. Thirumavalavan and T. S. Jayaraman, "BER analysis of reconfigurable intelligent surface assisted downlink power domain NOMA system," *2020 International Conference on COMmunication Systems and NETworkS, COMSNETS 2020*, pp. 519–522, Jan. 2020. DOI: 10.1109/COMSNETS48256.2020.9027303.

[105] M. Aldababsa, A. A. Mwais, and M. Obaid, "Performance of STAR-RIS assisted NOMA networks in nakagami-m fading channels," *AEU - International Journal of Electronics and Communications*, vol. 166, p. 154 685, Jul. 2023, ISSN: 1434-8411. DOI: 10.1016/J.AEUE.2023.154685.

[106] L. Bariah, S. Muhaidat, P. C. Sofotasios, F. E. Bouanani, O. A. Dobre, and W. Hamouda, "Large intelligent surface-assisted nonorthogonal multiple access for 6g networks: Performance analysis," *IEEE Internet of Things Journal*, vol. 8, no. 7, pp. 5129–5140, Apr. 2021, ISSN: 23274662. DOI: 10.1109/JIOT.2021.3057416.

[107] A. Chauhan, S. Ghosh, and A. Jaiswal, "RIS partition-assisted non-orthogonal multiple access (NOMA) and quadrature-NOMA with imperfect SIC," *IEEE Transactions on Wireless Communications*, vol. 22, no. 7, pp. 4371–4386, Jul. 2023, ISSN: 15582248. DOI: 10.1109/TWC.2022.3224645.

[108] A. Alqahtani and E. Alsusa, "On the quality of service and experience in IRS-NOMA over generalized fading channels," *IEEE Open Journal of the Communications Society*, vol. 3, pp. 2272–2283, 2022, ISSN: 2644125X. DOI: 10.1109/OJCOMS.2022.3222177.

[109] M. Aldababsa, A. Khaleel, and E. Basar, "STAR-RIS-NOMA networks: An error performance perspective," *IEEE Communications Letters*, vol. 26, no. 8, pp. 1784–1788, Aug. 2022, ISSN: 15582558. DOI: 10.1109/LCOMM.2022.3179731.

[110] B. Y. D. Rito and K. H. Li, "RIS-assisted NOMA with interference-cancellation and interference-alignment scheme," *IEEE Communications Letters*, vol. 27, no. 3, pp. 1011–1015, Mar. 2023, ISSN: 15582558. DOI: 10.1109/LCOMM.2023.3235254.

[111] W. Jiang and F.-L. Luo, "Cellular and cell-free massive MIMO techniques in 6g," *6G Key Technologies*, pp. 417–474, Nov. 2022. DOI: 10.1002/9781119847502.CH9.

[112] Y. Huo *et al.*, "Technology trends for massive MIMO towards 6g," *Sensors*, vol. 23, no. 13, Jul. 2023, ISSN: 14248220. DOI: 10.3390/s23136062.

[113] E. Meyer *et al.*, "The state of the art in beyond 5g distributed massive multiple-input multiple-output communication system solutions," *Open Research Europe*, vol. 2, p. 106, Sep. 2022. DOI: 10.12688/openreseurope.14501.1.

[114] Y. Zhao, L. Dai, *et al.*, "Near-field communications: Characteristics, technologies, and engineering," *Frontiers of Information Technology & Electronic Engineering*, vol. 25, no. 12, pp. 1580–1626, 2024, ISSN: 2095-9230. DOI: 10.1631/FITEE.2400576.

[115] R. P. Selvam, K. Narayanasamy, and M. Ilayaraja, "Efficient deer hunting optimization algorithm based spectrum sensing approach for 6g communication networks," *AI-Enabled 6G Networks and Applications*, pp. 111–129, Jan. 2023. DOI: 10.1002/9781119812722.CH7.

[116] "The development of 6g and possible implications for spectrum needs and guidance on the rollout of future wireless broadband networks DRAFT RSPG opinion," 2023.

[117] W. Hong *et al.*, "The role of millimeter-wave technologies in 5g/6g wireless communications," *IEEE Journal of Microwaves*, vol. 1, no. 1, pp. 101–122, 2021. DOI: 10.1109/JMW.2020.3035541.

[118] Ericsson, *6G Spectrum: Unleashing Extreme Performance — ericsson.com*, https://www.ericsson.com/en/6g/spectrum.

[119] N. T. Nguyen, Q. D. Vu, K. Lee, and M. Juntti, "Hybrid relay-reflecting intelligent surface-assisted wireless communications," *IEEE Transactions on Vehicular Technology*, vol. 71, no. 6, pp. 6228–6244, Jun. 2022, ISSN: 19399359. DOI: 10.1109/TVT.2022.3158686.

[120] Z. Wan, Z. Gao, F. Gao, M. D. Renzo, and M. S. Alouini, "Terahertz massive MIMO with holographic reconfigurable intelligent surfaces," *IEEE Transactions on Communications*, vol. 69, no. 7, pp. 4732–4750, Jul. 2021, ISSN: 15580857. DOI: 10.1109/TCOMM.2021.3064949.

[121] R. Deng, B. Di, H. Zhang, D. Niyato, *et al.*, "Reconfigurable holographic surfaces for future wireless communications," Dec. 2021.

[122] C. Huang, Z. Yang, G. C. Alexandropoulos, *et al.*, "Multi-hop ris-empowered terahertz communications: A drl-based hybrid beamforming design," *IEEE Journal on Selected Areas in Communications*, vol. 39, no. 6, pp. 1663–1677, 2021. DOI: 10.1109/JSAC.2021.3071836.

[123] S. Abeywickrama, R. Zhang, Q. Wu, and C. Yuen, "Intelligent reflecting surface: Practical phase shift model and beamforming optimization," *IEEE Transactions on Communications*, vol. 68, no. 9, pp. 5849–5863, Sep. 2020, ISSN: 15580857. DOI: 10.1109/TCOMM.2020.3001125.

[124] A. Araghi *et al.*, "Reconfigurable intelligent surface (RIS) in the sub-6 GHz band: Design, implementation, and real-world demonstration," *IEEE Access*, vol. 10, pp. 2646–2655, 2022, ISSN: 21693536. DOI: 10.1109/ACCESS.2022.3140278.

[125] G. C. Alexandropoulos, N. Shlezinger, I. Alamzadeh, M. F. Imani, H. Zhang, and Y. C. Eldar, "Hybrid reconfigurable intelligent metasurfaces: Enabling simultaneous tunable reflections and sensing for 6g wireless communications," *IEEE Vehicular Technology Magazine*, pp. 2–11, 2023. DOI: 10.1109/MVT.2023.3332580.

[126] I. Alamzadeh, G. C. Alexandropoulos, N. Shlezinger, and M. F. Imani, "A reconfigurable intelligent surface with integrated sensing capability," *Scientific Reports*, vol. 11, p. 20 737, 123. DOI: 10.1038/s41598-021-99722-x.

[127] Z. Xing, R. Wang, and X. Yuan, "Joint active and passive beamforming design for reconfigurable intelligent surface enabled integrated sensing and communication," *IEEE Transactions on Communications*, vol. 71, no. 4, pp. 2457–2474, Apr. 2023, ISSN: 15580857. DOI: 10.1109/TCOMM.2023.3244246.

[128] I. Yildirim, F. Kilinc, E. Basar, and G. C. Alexandropoulos, "Hybrid RIS-empowered reflection and decode-and-forward relaying for coverage extension," *IEEE Communications Letters*, vol. 25, no. 5, pp. 1692–1696, May 2021, ISSN: 15582558. DOI: 10.1109/LCOMM.2021.3054819.

[129] Z. Chen, B. Ning, C. Han, Z. Tian, and S. Li, "Intelligent reflecting surface assisted terahertz communications toward 6g," *IEEE Wireless Communications*, vol. 28, no. 6, pp. 110–117, Dec. 2021, ISSN: 1536-1284. DOI: 10.1109/MWC.001.2100215.

[130] Q. Wu and R. Zhang, "Beamforming optimization for wireless network aided by intelligent reflecting surface with discrete phase shifts," *IEEE Transactions on Communications*, vol. 68, no. 3, pp. 1838–1851, Mar. 2020, ISSN: 15580857. DOI: 10.1109/TCOMM.2019.2958916.

[131] Z. Liu, W. Chen, Z. Li, J. Yuan, Q. Wu, and K. Wang, "Transmissive reconfigurable intelligent surface transmitter empowered cognitive RSMA networks," *IEEE Communications Letters*, vol. 27, no. 7, pp. 1829–1833, Jul. 2023, ISSN: 15582558. DOI: 10.1109/LCOMM.2023.3273561.

[132] J. Xu, Y. Liu, X. Mu, and O. A. Dobre, "STAR-RISs: Simultaneous transmitting and reflecting reconfigurable intelligent surfaces," *IEEE Communications Letters*, vol. 25, no. 9, pp. 3134–3138, Sep. 2021, ISSN: 15582558. DOI: 10.1109/LCOMM.2021.3082214.

[133] C. Wu, Y. Liu, X. Mu, X. Gu, and O. A. Dobre, "Coverage characterization of STAR-RIS networks: NOMA and OMA," *IEEE Communications Letters*, vol. 25, no. 9, pp. 3036–3040, Sep. 2021, ISSN: 15582558. DOI: 10.1109/LCOMM.2021.3091807.

[134] X. Mu, Y. Liu, L. Guo, J. Lin, and R. Schober, "Simultaneously transmitting and reflecting (STAR) RIS aided wireless communications," *IEEE Transactions on Wireless Communications*, vol. 21, no. 5, pp. 3083–3098, May 2022, ISSN: 15582248. DOI: 10.1109/TWC.2021.3118225.

[135] S. Zhang, H. Zhang, B. Di, Y. Tan, M. D. Renzo, *et al.*, "Intelligent omni-surfaces: Ubiquitous wireless transmission by reflective-refractive metasurfaces; intelligent omni-surfaces: Ubiquitous wireless transmission by reflective-refractive metasurfaces," *IEEE TRANSACTIONS ON WIRELESS COMMUNICATIONS*, vol. 21, no. 1, p. 219, 2022. DOI: 10.1109/TWC.2021.3094869.

[136] S. Zhang, H. Zhang, B. Di, Y. Tan, Z. Han, and L. Song, "Beyond intelligent reflecting surfaces: Reflective-transmissive metasurface aided communications for full-dimensional

coverage extension," *IEEE Transactions on Vehicular Technology*, vol. 69, no. 11, pp. 13 905–13 909, Nov. 2020, ISSN: 19399359. DOI: 10.1109/TVT.2020.3024756.

[137] Y. Liu, X. Mu, X. Liu, M. D. Renzo, Z. Ding, and R. Schober, "Reconfigurable intelligent surface-aided multi-user networks: Interplay between NOMA and RIS," *IEEE Wireless Communications*, vol. 29, no. 2, pp. 169–176, Apr. 2022, ISSN: 15580687. DOI: 10.1109/MWC.102.2100363.

[138] N. S. Perovic, M. D. Renzo, and M. F. Flanagan, "Channel capacity optimization using reconfigurable intelligent surfaces in indoor mmWave environments," *IEEE International Conference on Communications*, vol. 2020-June, Jun. 2020, ISSN: 15503607. DOI: 10.1109/ICC40277.2020.9148781.

[139] P. Wang, J. Fang, X. Yuan, Z. Chen, and H. Li, "Intelligent reflecting surface-assisted millimeter wave communications: Joint active and passive precoding design," *IEEE Transactions on Vehicular Technology*, vol. 69, no. 12, pp. 14 960–14 973, Dec. 2020, ISSN: 19399359. DOI: 10.1109/TVT.2020.3031657.

[140] Y. Pan, K. Wang, C. Pan, H. Zhu, and J. Wang, "Sum-rate maximization for intelligent reflecting surface assisted terahertz communications; sum-rate maximization for intelligent reflecting surface assisted terahertz communications," *IEEE Transactions on Vehicular Technology*, vol. 71, no. 3, 2022. DOI: 10.1109/TVT.2022.3140869.

[141] Q. Wu, Y. Zhang, C. Huang, Y. Chau, Z. Yang, and M. Shikh-Bahaei, "Energy efficient intelligent reflecting surface assisted terahertz communications," *2021 IEEE International Conference on Communications Workshops, ICC Workshops 2021 - Proceedings*, Jun. 2021. DOI: 10.1109/ICCWORKSHOPS50388.2021.9473736.

[142] W. Ni, X. Liu, Y. Liu, H. Tian, and Y. Chen, "Intelligent reflecting surface aided multi-cell NOMA networks," *2020 IEEE Globecom Workshops, GC Wkshps 2020 - Proceedings*, Dec. 2020. DOI: 10.1109/GCWKSHPS50303.2020.9367548.

[143] G. Yang, X. Xu, and Y. C. Liang, "Intelligent reflecting surface assisted non-orthogonal multiple access," *IEEE Wireless Communications and Networking Conference, WCNC*, vol. 2020-May, May 2020, ISSN: 15253511. DOI: 10.1109/WCNC45663.2020.9120476.

[144] H. Niu, Z. Chu, F. Zhou, P. Xiao, and N. Al-Dhahir, "Weighted sum rate optimization for STAR-RIS-assisted MIMO system," *IEEE Transactions on Vehicular Technology*, vol. 71, no. 2, pp. 2122–2127, Feb. 2022, ISSN: 19399359. DOI: 10.1109/TVT.2021.3131568.

[145] A. Papazafeiropoulos, Z. Abdullah, P. Kourtessis, S. Kisseleff, and I. Krikidis, "Coverage probability of STAR-RIS-assisted massive MIMO systems with correlation and phase errors," *IEEE Wireless Communications Letters*, vol. 11, no. 8, pp. 1738–1742, Aug. 2022, ISSN: 21622345. DOI: 10.1109/LWC.2022.3179653.

[146] C. Wu, C. You, Y. Liu, X. Gu, and Y. Cai, "Channel estimation for STAR-RIS-aided wireless communication," *IEEE Communications Letters*, vol. 26, no. 3, pp. 652–656, Mar. 2022, ISSN: 15582558. DOI: 10.1109/LCOMM.2021.3139198.

[147] T. Hou, J. Wang, Y. Liu, X. Sun, A. Li, and B. Ai, "A joint design for STAR-RIS enhanced NOMA-CoMP networks: A simultaneous-signal-enhancement-and-cancellation-based (SSECB) design," *IEEE Transactions on Vehicular Technology*, vol. 71, no. 1, pp. 1043–1048, Jan. 2022, ISSN: 19399359. DOI: 10.1109/TVT.2021.3129178.

[148] Y. Guo, F. Fang, D. Cai, and Z. Ding, "Energy-efficient design for a NOMA assisted STAR-RIS network with deep reinforcement learning," *IEEE Transactions on Vehicular Technology*, vol. 72, no. 4, pp. 5424–5428, Apr. 2023, ISSN: 19399359. DOI: 10.1109/TVT.2022.3224926.

[149] M. M. Elsherbini, O. A. Omer, and M. Salah, "Reconfigurable intelligent surface reliable cooperative beamforming based on cascade/parallel hybrid networking," *IEEE Access*, vol. 11, pp. 65 255–65 265, 2023, ISSN: 21693536. DOI: 10.1109/ACCESS.2023.3290220.

[150] Y. Xiu *et al.*, "Reconfigurable intelligent surfaces aided mmWave NOMA: Joint power allocation, phase shifts, and hybrid beamforming optimization mmWave-NOMA system without RIS, the proposed RIS-aided mmWave-NOMA system is capable of improving the achievable sum-rate. index terms-reconfigurable intelligent surface, millimeter wave, non-orthogonal multiple access, power allocation, phase shifts optimization, hybrid beamforming," *IEEE TRANSACTIONS ON WIRELESS COMMUNICATIONS*, vol. 20, no. 12, 2021. DOI: 10.1109/TWC.2021.3092597.

[151] V. Jamali, A. M. Tulino, G. Fischer, R. R. Muller, and R. Schober, "Intelligent surface-aided transmitter architectures for millimeter-wave ultra massive mimo systems," *IEEE Open Journal of the Communications Society*, vol. 2, pp. 144–167, 2021, ISSN: 2644125X. DOI: 10.1109/OJCOMS.2020.3048063.

[152] C. Pradhan, A. Li, L. Song, B. Vucetic, and Y. Li, "Hybrid precoding design for reconfigurable intelligent surface aided mmWave communication systems," *IEEE Wireless Communications Letters*, vol. 9, no. 7, pp. 1041–1045, Jul. 2020, ISSN: 21622345. DOI: 10.1109/LWC.2020.2980225.

[153] J. Zhu, Y. Huang, J. Wang, K. Navaie, and Z. Ding, "Power efficient IRS-assisted NOMA," *IEEE Transactions on Communications*, vol. 69, no. 2, pp. 900–913, Feb. 2021, ISSN: 15580857. DOI: 10.1109/TCOMM.2020.3029617.

[154] J. Zuo, Y. Liu, Z. Qin, and N. Al-Dhahir, "Resource allocation in intelligent reflecting surface assisted NOMA systems," *IEEE Transactions on Communications*, vol. 68, no. 11, pp. 7170–7183, Nov. 2020, ISSN: 15580857. DOI: 10.1109/TCOMM.2020.3016742.

[155] R. Karasik, O. Simeone, M. D. Renzo, and S. S. Shitz, "Beyond max-SNR: Joint encoding for reconfigurable intelligent surfaces," *IEEE International Symposium on Information Theory*

- *Proceedings*, vol. 2020-June, pp. 2965–2970, Jun. 2020, ISSN: 21578095. DOI: 10.1109/ISIT44484.2020.9174060.

[156] X. Qian, M. D. Renzo, J. Liu, A. Kammoun, and M. S. Alouini, "Beamforming through reconfigurable intelligent surfaces in single-user MIMO systems: SNR distribution and scaling laws in the presence of channel fading and phase noise," *IEEE Wireless Communications Letters*, vol. 10, no. 1, pp. 77–81, Jan. 2021, ISSN: 21622345. DOI: 10.1109/LWC.2020.3021058.

[157] G. Zhou, C. Pan, H. Ren, K. Wang, M. D. Renzo, and A. Nallanathan, "Robust beamforming design for intelligent reflecting surface aided MISO communication systems," *IEEE Wireless Communications Letters*, vol. 9, no. 10, pp. 1658–1662, Oct. 2020, ISSN: 21622345. DOI: 10.1109/LWC.2020.3000490.

[158] S. Liu, Z. Gao, J. Zhang, M. D. Renzo, and M. S. Alouini, "Deep denoising neural network assisted compressive channel estimation for mmwave intelligent reflecting surfaces," *IEEE Transactions on Vehicular Technology*, vol. 69, no. 8, pp. 9223–9228, Aug. 2020, ISSN: 19399359. DOI: 10.1109/TVT.2020.3005402.

[159] S. Zhou, W. Xu, K. Wang, M. D. Renzo, and M. S. Alouini, "Spectral and energy efficiency of IRS-assisted MISO communication with hardware impairments," *IEEE Wireless Communications Letters*, vol. 9, no. 9, pp. 1366–1369, Sep. 2020, ISSN: 21622345. DOI: 10.1109/LWC.2020.2990431.

[160] H. Han, J. Zhao, D. Niyato, M. D. Renzo, and Q. V. Pham, "Intelligent reflecting surface aided network: Power control for physical-layer broadcasting," *IEEE International Conference on Communications*, vol. 2020-June, Jun. 2020, ISSN: 15503607. DOI: 10.1109/ICC40277.2020.9148827.

[161] H. Kim, *Artificial Intelligence for 6G*. Springer, 2022.

[162] W. Jiang, B. Han, M. A. Habibi, and H. D. Schotten, "The road towards 6g: A comprehensive survey," *IEEE Open Journal of the Communications Society*, vol. 2, pp. 334–366, 2021. DOI: 10.1109/OJCOMS.2021.3057679.

[163] W. Jiang and H. D. Schotten, "The kick-off of 6g research worldwide: An overview," in *2021 7th International Conference on Computer and Communications (ICCC)*, 2021, pp. 2274–2279. DOI: 10.1109/ICCC54389.2021.9674614.

[164] M. B. Khan, X. An, and C. Peng, "Towards native support for federated learning in 6g," in *2023 IEEE Wireless Communications and Networking Conference (WCNC)*, 2023, pp. 1–6. DOI: 10.1109/WCNC55385.2023.10119083.

[165] S. Yrjölä, P. Ahokangas, and M. Matinmikko-Blue, "Visions for 6g futures: A causal layered analysis," in *2022 Joint European Conference on Networks and Communications and 6G Summit (EuCNC/6G Summit)*, 2022, pp. 535–540. DOI: 10.1109/EuCNC/6GSummit54941.2022.9815809.

[166] C. Yeh, G. D. Jo, Y.-J. Ko, and H. K. Chung, "Perspectives on 6g wireless communications," *ICT Express*, vol. 9, no. 1, pp. 82–91, 2023, ISSN: 2405-9595. DOI: https://doi.org/10.1016/j.icte.2021.12.017.

[167] A. Gautam, P. Thakur, and G. Singh, "Advanced channel coding schemes for b5g/6g networks: State-of-the-art analysis, research challenges and future directions," *International Journal of Communication Systems*, 2024. DOI: 10.1002/dac.5855.

[168] C. Ngene, P. Thakur, and G. Singh, "Power allocation strategies for 6g communication in vl-noma systems: An overview," *Smart Science*, vol. 11, no. 3, pp. 475–518, 2023. DOI: 10.1080/23080477.2023.2225944.

[169] A. Balieiro, K. Dias, and P. Guarda, "Addressing the cqi feedback delay in 5g/6g networks via machine learning and evolutionary computing," *Intelligent and Converged Networks*, vol. 3, no. 3, pp. 271–281, 2022. DOI: 10.23919/ICN.2022.0012.

[170] R. Ahmad, H. Elgala, S. Almajali, H. Bany Salameh, and M. Ayyash, "Unified physical-layer learning framework toward vlc-enabled 6g indoor flying networks," *IEEE Internet of Things Journal*, vol. 11, no. 3, pp. 5545–5557, 2024. DOI: 10.1109/JIOT.2023.3307224.

[171] A. Salh *et al.*, "Development of a fully data-driven artificial intelligence and deep learning for urllc application in 6g wireless systems: A survey," 1, vol. 2564, 2023. DOI: 10.1063/5.0122677.

[172] L. Mucchi *et al.*, "Signal processing techniques for 6g," *Journal of Signal Processing Systems*, vol. 95, no. 4, pp. 435–457, 2023. DOI: 10.1007/s11265-022-01827-7.

[173] T.-M. Dang, E. Cho, and S.-H. Kim, "Current trends on deep learning-aided channel coding," vol. 2022-October, 2022, pp. 1222–1225. DOI: 10.1109/ICTC55196.2022.9952535.

[174] L. Miuccio, D. Panno, and S. Riolo, "A flexible encoding/decoding procedure for 6g scma wireless networks via adversarial machine learning techniques," *IEEE Transactions on Vehicular Technology*, vol. 72, no. 3, pp. 3288–3303, 2023. DOI: 10.1109/TVT.2022.3216028.

[175] X. Wang, X. Xie, W. Wang, W. Qi, Y. He, and L. Lu, "Dnn-based physical-layer network coding with low-complexity codec," 2023, pp. 713–718. DOI: 10.1109/ICCC59590.2023.10507537.

[176] J. Shi *et al.*, "Ai-enabled intelligent visible light communications: Challenges, progress, and future," *Photonics*, vol. 9, no. 8, 2022. DOI: 10.3390/photonics9080529.

[177] M. Vaezi *et al.*, "Cellular, wide-area, and non-terrestrial iot: A survey on 5g advances and the road toward 6g," *IEEE Communications Surveys and Tutorials*, vol. 24, no. 2, pp. 1117–1174, 2022. DOI: 10.1109/COMST.2022.3151028.

[178] C. Xu, N. Ishikawa, *et al.*, "Sixty years of coherent versus non-coherent tradeoffs and the road from 5g to wireless futures," *IEEE Access*, vol. 7, pp. 178 246–178 299, 2019. DOI: 10.1109/ACCESS.2019.2957706.

[179] M. Rowshan, M. Qiu, Y. Xie, X. Gu, and J. Yuan, "Channel coding toward 6g: Technical overview and outlook," *IEEE Open Journal of the Communications Society*, vol. 5, pp. 2585–2685, 2024. DOI: 10.1109/OJCOMS.2024.3390000.

[180] A. Gunturu, A. Agrawal, A. K. R. Chavva, and S. Pedamalli, "Machine learning based early termination for turbo and ldpc decoders," vol. 2021-March, 2021. DOI: 10.1109/WCNC49053.2021.9417420.

[181] R. Devnikar and V. Hendre, "Comprehensive literature survey for mm-wave massive mimo using machine learning for 6g," *Lecture Notes in Electrical Engineering*, vol. 828, pp. 765–774, 2022. DOI: 10.1007/978-981-16-7985-8$_$80.

[182] F. Kschischang, B. Frey, and H.-A. Loeliger, "Factor graphs and the sum-product algorithm," *IEEE Transactions on Information Theory*, vol. 47, no. 2, pp. 498–519, 2001. DOI: 10.1109/18.910572.

[183] E. Arikan, "Channel polarization: A method for constructing capacity-achieving codes for symmetric binary-input memoryless channels," *IEEE Transactions on Information Theory*, vol. 55, no. 7, pp. 3051–3073, 2009, ISSN: 1557-9654. DOI: 10.1109/TIT.2009.2021379.

[184] C. Mao, Z. Mu, Q. Liang, I. Schizas, and C. Pan, "Deep learning in physical layer communications: Evolution and prospects in 5g and 6g networks," *IET Communications*, vol. 17, no. 16, pp. 1863–1876, 2023. DOI: https://doi.org/10.1049/cmu2.12669. eprint: https://ietresearch.onlinelibrary.wiley.com/doi/pdf/10.1049/cmu2.12669.

[185] Y. Wang, S. Zhang, C. Zhang, X. Chen, and S. Xu, "A low-complexity belief propagation based decoding scheme for polar codes - decodability detection and early stopping prediction," *IEEE Access*, vol. 7, pp. 159 808–159 820, 2019. DOI: 10.1109/ACCESS.2019.2950766.

[186] F. Liang, C. Shen, and F. Wu, "An iterative bp-cnn architecture for channel decoding," *IEEE Journal of Selected Topics in Signal Processing*, vol. 12, no. 1, pp. 144–159, 2018. DOI: 10.1109/JSTSP.2018.2794062.

[187] T. Gruber, S. Cammerer, J. Hoydis, and S. t. Brink, "On deep learning-based channel decoding," in *2017 51st Annual Conference on Information Sciences and Systems (CISS)*, 2017, pp. 1–6. DOI: 10.1109/CISS.2017.7926071.

[188] S. Cammerer, T. Gruber, J. Hoydis, and S. ten Brink, "Scaling deep learning-based decoding of polar codes via partitioning," in *GLOBECOM 2017 - 2017 IEEE Global Communications Conference*, 2017, pp. 1–6. DOI: 10.1109/GLOCOM.2017.8254811.

[189] A. M. Elbir, A. Papazafeiropoulos, P. Kourtessis, and S. Chatzinotas, "Deep channel learning for large intelligent surfaces aided mm-wave massive mimo systems," *IEEE Wireless Communications Letters*, vol. 9, no. 9, pp. 1447–1451, 2020. DOI: 10.1109/LWC.2020.2993699.

[190] A. Taha, M. Alrabeiah, and A. Alkhateeb, "Enabling large intelligent surfaces with compressive sensing and deep learning," *IEEE Access*, vol. 9, pp. 44 304–44 321, 2021. DOI: 10.1109/ACCESS.2021.3064073.

[191] S. Khan, K. S. Khan, N. Haider, and S. Y. Shin, *Deep-learning-aided detection for reconfigurable intelligent surfaces*, 2020. arXiv: 1910.09136 [eess.SP].

[192] S. Liu, Z. Gao, J. Zhang, M. D. Renzo, and M.-S. Alouini, "Deep denoising neural network assisted compressive channel estimation for mmwave intelligent reflecting surfaces," *IEEE Transactions on Vehicular Technology*, vol. 69, no. 8, pp. 9223–9228, 2020. DOI: 10.1109/TVT.2020.3005402.

[193] Y. Jin, J. Zhang, X. Zhang, H. Xiao, B. Ai, and D. W. K. Ng, "Channel estimation for semi-passive reconfigurable intelligent surfaces with enhanced deep residual networks," *IEEE Transactions on Vehicular Technology*, vol. 70, no. 10, pp. 11 083–11 088, 2021. DOI: 10.1109/TVT.2021.3109937.

[194] N. K. Kundu and M. R. McKay, "Channel estimation for reconfigurable intelligent surface aided miso communications: From lmmse to deep learning solutions," *IEEE Open Journal of the Communications Society*, vol. 2, pp. 471–487, 2021. DOI: 10.1109/OJCOMS.2021.3063171.

[195] L. Dai and X. Wei, "Distributed machine learning based downlink channel estimation for ris assisted wireless communications," *IEEE Transactions on Communications*, vol. 70, no. 7, pp. 4900–4909, 2022. DOI: 10.1109/TCOMM.2022.3175175.

[196] J. He, H. Wymeersch, M. Di Renzo, and M. Juntti, "Learning to estimate ris-aided mmwave channels," *IEEE Wireless Communications Letters*, vol. 11, no. 4, pp. 841–845, 2022. DOI: 10.1109/LWC.2022.3147250.

[197] M. Wu, Z. Gao, Y. Huang, Z. Xiao, D. W. K. Ng, and Z. Zhang, "Deep learning-based rate-splitting multiple access for reconfigurable intelligent surface-aided tera-hertz massive mimo," *IEEE Journal on Selected Areas in Communications*, vol. 41, no. 5, pp. 1431–1451, 2023. DOI: 10.1109/JSAC.2023.3240781.

[198] A. Taha, M. Alrabeiah, and A. Alkhateeb, "Deep learning for large intelligent surfaces in millimeter wave and massive mimo systems," in *2019 IEEE Global Communications Conference (GLOBECOM)*, 2019, pp. 1–6. DOI: 10.1109/GLOBECOM38437.2019.9013256.

[199] Ö. Özdoğan and E. Björnson, "Deep learning-based phase reconfiguration for intelligent reflecting surfaces," in *2020 54th Asilomar Conference on Signals, Systems, and Computers*, 2020, pp. 707–711. DOI: 10.1109/IEEECONF51394.2020.9443516.

[200] J. Gao, C. Zhong, X. Chen, H. Lin, and Z. Zhang, "Unsupervised learning for passive beamforming," *IEEE Communications Letters*, vol. 24, no. 5, pp. 1052–1056, 2020. DOI: 10.1109/LCOMM.2020.2965532.

[201] T. Jiang, H. V. Cheng, and W. Yu, "Learning to reflect and to beamform for intelligent reflecting surface with implicit channel estimation," *IEEE Journal on Selected Areas in Communications*, vol. 39, no. 7, pp. 1931–1945, 2021. DOI: 10.1109/JSAC.2021.3078502.

[202] B. Peng, F. Siegismund-Poschmann, and E. A. Jorswieck, "Risnet: A dedicated scalable neural network architecture for optimization of reconfigurable intelligent surfaces," in *WSA and SCC 2023; 26th International ITG Workshop on Smart Antennas and 13th Conference on Systems, Communications, and Coding*, 2023, pp. 1–6.

[203] C. Huang, R. Mo, and C. Yuen, "Reconfigurable intelligent surface assisted multiuser miso systems exploiting deep reinforcement learning," *IEEE Journal on Selected Areas in Communications*, vol. 38, no. 8, pp. 1839–1850, 2020. DOI: 10.1109/JSAC.2020.3000835.

[204] B. Saglam, D. Gurgunoglu, and S. S. Kozat, "Deep reinforcement learning based joint downlink beamforming and ris configuration in ris-aided mu-miso systems under hardware impairments and imperfect csi," in *2023 IEEE International Conference on Communications Workshops (ICC Workshops)*, 2023, pp. 66–72. DOI: 10.1109/ICCWorkshops57953.2023.10283517.

[205] W. Wang and W. Zhang, "Intelligent reflecting surface configurations for smart radio using deep reinforcement learning," *IEEE Journal on Selected Areas in Communications*, vol. 40, no. 8, pp. 2335–2346, 2022. DOI: 10.1109/JSAC.2022.3180787.

[206] H. Mei, K. Yang, Q. Liu, and K. Wang, "3d-trajectory and phase-shift design for ris-assisted uav systems using deep reinforcement learning," *IEEE Transactions on Vehicular Technology*, vol. 71, no. 3, pp. 3020–3029, 2022. DOI: 10.1109/TVT.2022.3143839.

[207] H. Peng and L.-C. Wang, "Energy harvesting reconfigurable intelligent surface for uav based on robust deep reinforcement learning," *IEEE Transactions on Wireless Communications*, vol. 22, no. 10, pp. 6826–6838, 2023. DOI: 10.1109/TWC.2023.3245820.

[208] M.-L. Tham, Y. J. Wong, A. Iqbal, N. B. Ramli, Y. Zhu, and T. Dagiuklas, "Deep reinforcement learning for secrecy energy- efficient uav communication with reconfigurable intelligent surface," in *2023 IEEE Wireless Communications and Networking Conference (WCNC)*, 2023, pp. 1–6. DOI: 10.1109/WCNC55385.2023.10118891.

[209] Z. Wang, J. Qiu, *et al.*, "Federated learning via intelligent reflecting surface," *IEEE Transactions on Wireless Communications*, vol. 21, no. 2, pp. 808–822, 2022. DOI: 10.1109/TWC.2021.3099505.

[210] L. Zhao, H. Xu, J. Wang, Y. Chen, X. Chen, and Z. Wang, "Computation–communication resource allocation for federated learning system with intelligent reflecting surfaces," *Arabian Journal for Science and Engineering*, vol. 47, no. 8, pp. 10 203–10 209, 2022, ISSN: 2191-4281. DOI: 10.1007/s13369-021-06438-1.

[211] T. Zhang and S. Mao, "Energy-efficient federated learning with intelligent reflecting surface," *IEEE Transactions on Green Communications and Networking*, vol. 6, no. 2, pp. 845–858, 2022. DOI: 10.1109/TGCN.2021.3126795.

[212] H. Liu, X. Yuan, and Y.-J. A. Zhang, "Reconfigurable intelligent surface enabled federated learning: A unified communication-learning design approach," *IEEE Transactions on Wireless Communications*, vol. 20, no. 11, pp. 7595–7609, 2021. DOI: 10.1109/TWC.2021.3086116.

[213] M. A. S. Sejan, M. H. Rahman, and H.-K. Song, "Demod-cnn: A robust deep learning approach for intelligent reflecting surface-assisted multiuser mimo communication," *Sensors*, vol. 22, no. 16, 2022, ISSN: 1424-8220. DOI: 10.3390/s22165971.

[214] M. H. Rahman, M. A. S. Sejan, M. A. Aziz, D.-S. Kim, Y.-H. You, and H.-K. Song, "Deep convolutional and recurrent neural-network-based optimal decoding for ris-assisted mimo communication," *Mathematics*, vol. 11, no. 15, 2023, ISSN: 2227-7390. DOI: 10.3390/math11153397.

[215] E. Basar and I. Yildirim, "Simris channel simulator for reconfigurable intelligent surface-empowered communication systems," in *2020 IEEE Latin-American Conference on Communications (LATINCOM)*, 2020, pp. 1–6. DOI: 10.1109/LATINCOM50620.2020.9282349.

[216] C. Liaskos, A. Tsioliaridou, S. Nie, A. Pitsillides, S. Ioannidis, and I. Akyildiz, "An interpretable neural network for configuring programmable wireless environments," in *2019 IEEE 20th International Workshop on Signal Processing Advances in Wireless Communications (SPAWC)*, 2019, pp. 1–5. DOI: 10.1109/SPAWC.2019.8815428.

[217] M. M. Azari *et al.*, "Evolution of non-terrestrial networks from 5g to 6g: A survey," *IEEE Communications Surveys and Tutorials*, vol. 24, no. 4, pp. 2633–2672, 2022, ISSN: 1553877X. DOI: 10.1109/COMST.2022.3199901.

[218] C. De Lima *et al.*, "Convergent communication, sensing and localization in 6g systems: An overview of technologies, opportunities and challenges," *IEEE Access*, vol. 9, pp. 26 902–26 925, 2021, ISSN: 21693536. DOI: 10.1109/ACCESS.2021.3053486.

[219] S. Kavaiya, N. Chauhan, P. Dalal, M. Parmar, R. Patel, and S. Patel, "Inverse reinforcement learning to enhance physical layer security in 6g ris-assisted connected cars," *Communications in Computer and Information Science*, vol. 2031, pp. 41–53, 2024, ISSN: 18650929. DOI: 10.1007/978-3-031-53728-8_4.

[220] L.-H. Shen, K.-T. Feng, T.-S. Lee, *et al.*, "Ai-enabled unmanned vehicle-assisted reconfigurable intelligent surfaces: Deployment, prototyping, experiments, and opportunities," *IEEE Network*, pp. 1–1, 2024, ISSN: 08908044. DOI: 10.1109/MNET.2024.3381783.

[221] P. S. Bouzinis, N. A. Mitsiou, P. D. Diamantoulakis, D. Tyrovolas, and G. K. Karagiannidis, "Intelligent over-the-air computing environment," *IEEE Wireless Communications Letters*, vol. 12, no. 1, pp. 134–137, 2023, ISSN: 21622337. DOI: 10.1109/LWC.2022.3219250.

[222] S. Zhang, D. Zhu, and Y. Liu, "Artificial intelligence empowered physical layer security for 6g: State-of-the-art, challenges, and opportunities," *Computer Networks*, vol. 242, 2024, ISSN: 13891286. DOI: 10.1016/j.comnet.2024.110255.

[223] B. Adhikari, M. Jaseemuddin, and A. Anpalagan, "Resource allocation for co-existence of embb and urllc services in 6g wireless networks: A survey," *IEEE Access*, vol. 12, pp. 552–581, 2024, ISSN: 21693536. DOI: 10.1109/ACCESS.2023.3343250.

[224] N. K. Daghari, T. Y. Elganimi, and K. M. Rabie, "Energy-efficient hybrid precoding schemes for ris-assisted millimeter-wave massive mimo," Institute of Electrical and Electronics Engineers Inc., 2021, pp. 294–299, ISBN: 978-166544505-4. DOI: 10.1109/MeditCom49071.2021.9647463.

[225] B. D. Son *et al.*, "Adversarial attacks and defenses in 6g network-assisted iot systems," *IEEE Internet of Things Journal*, vol. 11, no. 11, pp. 19 168–19 187, 2024, ISSN: 23274662. DOI: 10.1109/JIOT.2024.3373808.

[226] M. M. Sahin, H. Arslan, and K.-C. Chen, "Control of electromagnetic radiation on coexisting smart radio environment," *IEEE Open Journal of the Communications Society*, vol. 3, pp. 557–573, 2022, ISSN: 2644125X. DOI: 10.1109/OJCOMS.2022.3162142.

[227] S. J. Nawaz, S. K. Sharma, B. Mansoor, M. N. Patwary, and N. M. Khan, "Non-coherent and backscatter communications: Enabling ultra-massive connectivity in 6g wireless networks," *IEEE Access*, vol. 9, pp. 38 144–38 186, 2021, ISSN: 21693536. DOI: 10.1109/ACCESS.2021.3061499.

[228] J. Li, W. Wang, R. Jiang, and S. Huang, "Csinet-former network for bilateral user 3d localization in star-ris-assisted miso systems," Institute of Electrical and Electronics Engineers Inc., 2023, pp. 1886–1891. DOI: 10.1109/GCWkshps58843.2023.10464850.

[229] I. P. Chochliouros *et al.*, "6g-bricks: Developing a modern experimentation facility for validation, testing and showcasing of 6g breakthrough technologies and devices," *IFIP Advances in Information and Communication Technology*, vol. 677, pp. 17–31, 2023, ISSN: 18684238. DOI: 10.1007/978-3-031-34171-7_1.

[230] Y. Liu, X. Liu, *et al.*, "Reconfigurable intelligent surfaces: Principles and opportunities," *IEEE Communications Surveys and Tutorials*, vol. 23, no. 3, pp. 1546–1577, 2021, ISSN: 1553877X. DOI: 10.1109/COMST.2021.3077737.

[231] R. Chataut, M. Nankya, and R. Akl, "6g networks and the ai revolution—exploring technologies, applications, and emerging challenges," *Sensors*, vol. 24, no. 6, 2024, ISSN: 14248220. DOI: 10.3390/s24061888.

[232] G. Xia, H. Liu, and K. Long, "Transformer-empowered parallel channel prediction for fast-paced and dynamic ris-aided wireless communication systems," *IEEE Communications Letters*, pp. 1–1, 2024, ISSN: 10897798. DOI: 10.1109/LCOMM.2024.3383427.

[233] B. Clerckx *et al.*, "A primer on rate-splitting multiple access: Tutorial, myths, and frequently asked questions," *IEEE Journal on Selected Areas in Communications*, vol. 41, no. 5, pp. 1265–1308, 2023, ISSN: 07338716. DOI: 10.1109/JSAC.2023.3242718.

[234] K. Shafique and M. Alhassoun, "Going beyond a simple ris: Trends and techniques paving the path of future ris," *IEEE Open Journal of Antennas and Propagation*, vol. 5, no. 2, pp. 256–276, 2024, ISSN: 26376431. DOI: 10.1109/OJAP.2024.3360900.

[235] F. A. P. de Figueiredo, "Unlocking the power of reconfigurable intelligent surfaces: From wireless communication to energy efficiency and beyond," *Applied Sciences (Switzerland)*, vol. 13, no. 21, 2023, ISSN: 20763417. DOI: 10.3390/app132111750.

[236] R. Kaur, B. Bansal, S. Majhi, S. Jain, C. Huang, and C. Yuen, "A survey on reconfigurable intelligent surface for physical layer security of next-generation wireless communications," *IEEE Open Journal of Vehicular Technology*, vol. 5, pp. 172–199, 2024, ISSN: 26441330. DOI: 10.1109/OJVT.2023.3348658.

[237] S. K. Das, F. Benkhelifa, *et al.*, "Comprehensive review on ml-based ris-enhanced iot systems: Basics, research progress and future challenges," *Computer Networks*, vol. 224, 2023, ISSN: 13891286. DOI: 10.1016/j.comnet.2023.109581.

[238] G. C. Alexandropoulos, K. Stylianopoulos, C. Huang, C. Yuen, M. Bennis, and M. Debbah, "Pervasive machine learning for smart radio environments enabled by reconfigurable intelligent surfaces," *Proceedings of the IEEE*, vol. 110, no. 9, pp. 1494–1525, 2022, ISSN: 00189219. DOI: 10.1109/JPROC.2022.3174030.

[239] N. U. Saqib, S. Hou, S. H. Chae, and S.-W. Jeon, "Reconfigurable intelligent surface aided hybrid beamforming: Optimal placement and beamforming design," *IEEE Transactions on Wireless Communications*, pp. 1–1, 2024, ISSN: 15361276. DOI: 10.1109/TWC.2024.3387449.

[240] L.-C. Wang, H. Peng, A. C.-S. Huang, and A.-H. Tsai, "Latest advances in spectrum management for 6g communications," Institute of Electrical and Electronics Engineers Inc., 2021, pp. 295–297, ISBN: 978-166542772-2. DOI: 10.1109/WOCC53213.2021.9603218.

[241] H. Zhou, M. Erol-Kantarci, Y. Liu, and H. V. Poor, "A survey on model-based, heuristic, and machine learning optimization approaches in ris-aided wireless networks," *IEEE Communications Surveys and Tutorials*, vol. 26, no. 2, pp. 781–823, 2024, ISSN: 1553877X. DOI: 10.1109/COMST.2023.3340099.

[242] "Sacvlc 2021 - proceedings: 2021 3rd south american colloquium on visible light communications," Institute of Electrical and Electronics Engineers Inc., 2021, ISBN: 978-166544225-1.

[243] R. F. Ibarra-Hernández, F. R. Castillo-Soria, C. A. Gutiérrez, A. García-Barrientos, L. A. Vásquez-Toledo, and J. A. Del-Puerto-Flores, "Machine learning strategies for reconfigurable intelligent surface-assisted communication systems—a review," *Future Internet*, vol. 16, no. 5, 2024, ISSN: 19995903. DOI: 10.3390/fi16050173.

[244] S. Tewes, M. Heinrichs, K. Weinberger, R. Kronberger, and A. Sezgin, "A comprehensive dataset of ris-based channel measurements in the 5ghz band," vol. 2023-June, Institute of Electrical and Electronics Engineers Inc., 2023. DOI: 10.1109/VTC2023-Spring57618.2023.10200973.

[245] W. Khalid, M. A. U. Rehman, T. Van Chien, Z. Kaleem, H. Lee, and H. Yu, "Reconfigurable intelligent surface for physical layer security in 6g-iot: Designs, issues, and advances," *IEEE Internet of Things Journal*, vol. 11, no. 2, pp. 3599–3613, 2024, ISSN: 23274662. DOI: 10.1109/JIOT.2023.3297241.

[246] M. Ahmed Ouameur, L. D. T. Anh, D. Massicotte, G. Jeon, and F. A. P. de Figueiredo, "Adversarial bandit approach for ris-aided ofdm communication," *Eurasip Journal on Wireless Communications and Networking*, vol. 2022, no. 1, 2022, ISSN: 16871472. DOI: 10.1186/s13638-022-02184-6.

[247] A. Daurembekova and H. D. Schotten, "Opportunities and limitations of space-air-ground integrated network in 6g systems," Institute of Electrical and Electronics Engineers Inc., 2023, ISBN: 978-166546483-3. DOI: 10.1109/PIMRC56721.2023.10294000.

[248] X. Zeng, Y. Mao, and Y. Shi, "Star-ris assisted over-the-air vertical federated learning in multi-cell wireless networks," Institute of Electrical and Electronics Engineers Inc., 2023, pp. 361–366. DOI: 10.1109/ICCWorkshops57953.2023.10283612.

[249] F. Xu, T. Hussain, *et al.*, "The state of ai-empowered backscatter communications: A comprehensive survey," *IEEE Internet of Things Journal*, vol. 10, no. 24, pp. 21 763–21 786, 2023, ISSN: 23274662. DOI: 10.1109/JIOT.2023.3299210.

[250] T. M. Hoang, S. Dinh-Van, B. Barn, R. Trestian, and H. X. Nguyen, "Ris-aided smart manufacturing: Information transmission and machine health monitoring," *IEEE Internet of Things Journal*, vol. 9, no. 22, pp. 22 930–22 943, 2022, ISSN: 23274662. DOI: 10.1109/JIOT.2022.3187189.

[251] M. Elamassie and M. Uysal, "Free space optical communication: An enabling backhaul technology for 6g non-terrestrial networks," *Photonics*, vol. 10, no. 11, 2023, ISSN: 23046732. DOI: 10.3390/photonics10111210.

[252] T. Y. Elganimi, N. K. Daghari, and K. M. Rabie, "Impact of channel imperfection on the performance of ris-assisted energy-efficient hybrid precoding," Institute of Electrical and Electronics Engineers Inc., 2021, ISBN: 978-166544913-7. DOI: 10.1109/CITS52676.2021.9618475.

[253] N. Gonzalez-Prelcic *et al.*, "The integrated sensing and communication revolution for 6g: Vision, techniques, and applications," *Proceedings of the IEEE*, pp. 1–, 2024, ISSN: 00189219. DOI: 10.1109/JPROC.2024.3397609.

[254] V. Pathak, R. J. Pandya, V. Bhatia, and O. A. Lopez, "Qualitative survey on artificial intelligence integrated blockchain approach for 6g and beyond," *IEEE Access*, vol. 11, pp. 105 935–105 981, 2023, ISSN: 21693536. DOI: 10.1109/ACCESS.2023.3319083.

[255] H. Taghvaee *et al.*, "Radiation pattern prediction for metasurfaces: A neural network-based approach," *Sensors*, vol. 21, no. 8, 2021, ISSN: 14248220. DOI: 10.3390/s21082765.

[256] N. H. Mahmood, G. Berardinelli, E. J. Khatib, R. Hashemi, C. De Lima, and M. Latva-Aho, "A functional architecture for 6g special-purpose industrial iot networks," *IEEE Transactions on Industrial Informatics*, vol. 19, no. 3, pp. 2530–2540, 2023, ISSN: 15513203. DOI: 10.1109/TII.2022.3182988.

[257] Z. Yang, M. Chen, K.-K. Wong, H. V. Poor, and S. Cui, "Federated learning for 6g: Applications, challenges, and opportunities," *Engineering*, vol. 8, pp. 33–41, 2022, ISSN: 20958099. DOI: 10.1016/j.eng.2021.12.002.

[258] Microwaves and RF. "Non-terrestrial network technology from a 3gpp perspective." (2022), [Online]. Available: https://www.mwrf.com/technologies/embedded/systems/article/21252945/rohde-schwarz-nonterrestrial-network-technology-from-a-3gpp-perspective.

[259] X. JIANG, M. SHENG, N. ZHAO, C. XING, W. LU, and X. WANG, "Green UAV communications for 6g: A survey," *Chinese Journal of Aeronautics*, vol. 35, no. 9, pp. 19–34, Sep. 2022, ISSN: 1000-9361. DOI: 10.1016/J.CJA.2021.04.025.

[260] Stellar-IoT, *How satellite constellations are redefining global iot connectivity*, 2024.

[261] Y. Zeng, Q. Wu, and R. Zhang, "Accessing from the sky: A tutorial on UAV communications for 5g and beyond," *Proceedings of the IEEE*, vol. 107, no. 12, pp. 2327–2375, Dec. 2019, ISSN: 15582256. DOI: 10.1109/JPROC.2019.2952892.

[262] Y. Zeng, R. Zhang, and T. J. Lim, "Wireless communications with unmanned aerial vehicles: Opportunities and challenges," *IEEE Communications Magazine*, vol. 54, no. 5, pp. 36–42, May 2016, ISSN: 01636804. DOI: 10.1109/MCOM.2016.7470933.

[263] S. A. H. Mohsan, N. Q. H. Othman, Y. Li, M. H. Alsharif, and M. A. Khan, "Unmanned aerial vehicles (UAVs): Practical aspects, applications, open challenges, security issues, and future trends," *Intelligent Service Robotics 2023 16:1*, vol. 16, no. 1, pp. 109–137, Jan. 2023, ISSN: 1861-2784. DOI: 10.1007/S11370-022-00452-4.

[264] D. E. Martin and M. A. Latheef, "Payload capacities of remotely piloted aerial application systems affect spray pattern and effective swath," *Drones 2022, Vol. 6, Page 205*, vol. 6, no. 8, p. 205, Aug. 2022, ISSN: 2504-446X. DOI: 10.3390/DRONES6080205.

[265] E. Drones. "Exploring the pros and cons of uav drones for aerial photography." (), [Online]. Available: https://www.equinoxsdrones.com/10-major-pros-cons-of-unmanned-aerial-vehicleuav-drones/.

[266] A. Erceg, B. Činčurak, E. Josip, J. Strossmayer, A. Vasilj, and J. J. Strossmayer, "Unmanned aircraft systems in logistics-legal regulation and worldwide examples toward use in croatia," 2017.

[267] T.-C. Yu, W.-T. Huang, W.-B. Lee, C.-W. Chow, S.-W. Chang, and H.-C. Kuo, "Visible light communication system technology review: Devices, architectures, and applications," *Crystals*, vol. 11, no. 9, 2021, ISSN: 2073-4352. DOI: 10.3390/cryst11091098.

[268] S. Vappangi and V. V. Mani, "A survey on the integration of visible light communication with power line communication: Conception, applications and research challenges," *Optik*, vol. 266, p. 169 582, Sep. 2022, ISSN: 0030-4026. DOI: 10.1016/J.IJLEO.2022.169582.

[269] H. Yoshikawa *et al.*, "Optimal spatial coherence of a light-emitting diode in a digital holographic display," *Applied Sciences 2022, Vol. 12, Page 4176*, vol. 12, no. 9, p. 4176, Apr. 2022, ISSN: 2076-3417. DOI: 10.3390/APP12094176.

[270] N. Chi, Y. Zhou, Y. Wei, and F. Hu, "Visible light communication in 6g: Advances, challenges, and prospects," *IEEE Vehicular Technology Magazine*, vol. 15, no. 4, pp. 93–102, Dec. 2020, ISSN: 15566080. DOI: 10.1109/MVT.2020.3017153.

[271] A. Haas, "Physical layer security for visible light communication systems: A survey," *IEEE Communications Surveys and Tutorials*, vol. 22, no. 3, pp. 1887–1908, DOI: 10.1109/COMST.2020.2988615.

[272] G. A. Mapunda, R. Ramogomana, L. Marata, B. Basutli, A. S. Khan, and J. M. Chuma, "Indoor visible light communication: A tutorial and survey," *Wireless Communications and Mobile Computing*, vol. 2020, 2020, ISSN: 15308677. DOI: 10.1155/2020/8881305.

[273] Huawei, *Visible light communication (vlc)*, 2023.

[274] Z. Zhang, Y. Xiao, Z. Ma, M. Xiao, Z. D.-I. Vehicular . . ., and undefined 2019, "6g wireless networks: Vision, requirements, architecture, and key technologies," *ieeexplore.ieee.org*,

[275] H. Viswanathan and P. E. Mogensen, "Communications in the 6g era," *IEEE Access*, vol. 8, pp. 57 063–57 074, 2020. DOI: 10.1109/ACCESS.2020.2981745.

[276] S. Rajbhandari *et al.*, "A comprehensive survey on MIMO visible light communication: Current research, machine learning and future trends," *Sensors 2023, Vol. 23, Page 739*, vol. 23, no. 2, p. 739, Jan. 2023, ISSN: 1424-8220. DOI: 10.3390/S23020739.

[277] M. S. M. Gismalla *et al.*, "Survey on device to device (d2d) communication for 5gb/6g networks: Concept, applications, challenges, and future directions," *IEEE Access*, vol. 10, pp. 30 792–30 821, 2022, ISSN: 21693536. DOI: 10.1109/ACCESS.2022.3160215.

[278] M. F. Ali, D. N. K. Jayakody, and Y. Li, "Recent trends in underwater visible light communication (UVLC) systems," *IEEE Access*, vol. 10, pp. 22 169–22 225, 2022, ISSN: 21693536. DOI: 10.1109/ACCESS.2022.3150093.

[279] L. Teixeira, F. Loose, J. M. Alonso, C. H. Barriquello, V. A. Reguera, and M. A. D. Costa, "A review of visible light communication LED drivers," *IEEE Journal of Emerging and Selected Topics in Power Electronics*, vol. 10, no. 1, pp. 919–933, Feb. 2022, ISSN: 21686785. DOI: 10.1109/JESTPE.2021.3092284.

[280] P. Dwivedy, V. Dixit, and A. Kumar, "A survey on visible light communication for 6g: Architecture, application and challenges," *2023 International Conference on Computer, Electronics and Electrical Engineering and their Applications, IC2E3 2023*, 2023. DOI: 10.1109/IC2E357697.2023.10262462.

[281] S. Ariyanti and M. Suryanegara, "Visible light communication (VLC) for 6g technology: The potency and research challenges," *Proceedings of the World Conference on Smart Trends in Systems, Security and Sustainability, WS4 2020*, pp. 490–493, Jul. 2020. DOI: 10.1109/WORLDS450073.2020.9210383.

[282] M. Katz and I. Ahmed, "Opportunities and challenges for visible light communications in 6g," *2nd 6G Wireless Summit 2020: Gain Edge for the 6G Era, 6G SUMMIT 2020*, Mar. 2020. DOI: 10.1109/6GSUMMIT49458.2020.9083805.

[283] F. Tariq, M. R. A. Khandaker, K. K. Wong, M. A. Imran, M. Bennis, and M. Debbah, "A speculative study on 6g," *IEEE Wireless Communications*, vol. 27, no. 4, pp. 118–125, Aug. 2020, ISSN: 15580687. DOI: 10.1109/MWC.001.1900488.

[284] Y. Siriwardhana, P. Porambage, M. Liyanage, and M. Ylianttila, "A survey on mobile augmented reality with 5g mobile edge computing: Architectures, applications, and technical aspects," *IEEE Communications Surveys and Tutorials*, vol. 23, no. 2, pp. 1160–1192, Apr. 2021, ISSN: 1553877X. DOI: 10.1109/COMST.2021.3061981.

[285] I. D. F. .-. IxDF. "What is extended reality (xr)?" (2024), [Online]. Available: https://www.interaction-design.org/literature/topics/extended-reality-xr.

[286] Imisi 3D, *Welcome to xr wonderland: Unravelling the magic of extended reality (xr)*, 2023.

[287] S. Elmeadawy and R. M. Shubair, "6g wireless communications: Future technologies and research challenges," *2019 International Conference on Electrical and Computing Technologies and Applications, ICECTA 2019*, Nov. 2019. DOI: 10.1109/ICECTA48151.2019.8959607.

[288] W. Hou, B. Bai, and L. Lyu, "Evaluation model of holographic communication experience in the 6g era based on light field display," *Applied Sciences*, vol. 13, no. 22, p. 12 381, Nov. 2023, ISSN: 2076-3417. DOI: 10.3390/app132212381.

[289] A. Masaracchia, V. Sharma, B. Canberk, O. A. Dobre, and T. Q. Duong, "Digital twin for 6g: Taxonomy, research challenges, and the road ahead," *IEEE Open Journal of the Communications Society*, vol. 3, pp. 2137–2150, 2022, ISSN: 2644125X. DOI: 10.1109/OJCOMS.2022.3219015.

[290] R. Beams *et al.*, "Evaluation challenges for the application of extended reality devices in medicine," *Journal of Digital Imaging*, vol. 35, no. 5, pp. 1409–1418, Oct. 2022, ISSN: 1618-727X. DOI: 10.1007/s10278-022-00622-x.

[291] I. F. Akyildiz, "Metaverse: Challenges for extended reality and holographic-type communication in the next decade," *2022 ITU Kaleidoscope - Extended Reality - How to Boost Quality of Experience and Interoperability, ITU K 2022 - Proceedings*, 2022. DOI: 10.23919/ITUK56368.2022.10003048.

[292] R. Petkova, V. Poulkov, A. Manolova, and K. Tonchev, "Challenges in implementing low-latency holographic-type communication systems," *Sensors 2022, Vol. 22, Page 9617*, vol. 22, no. 24, p. 9617, Dec. 2022, ISSN: 1424-8220. DOI: 10.3390/S22249617.

[293] "S-JNL-VOL3.ISSUE2-2022-a33-PDF-e,"

[294] C. Tellambura *et al.*, "Toward immersive communications in nG."

[295] M. Arif, F. Ajesh, S. Shamsudheen, and M. Shahzad, "Secure and energy-efficient computational offloading using lstm in mobile edge computing," *Security and Communication Networks*, vol. 2022, pp. 1–13, Jan. 2022. DOI: 10.1155/2022/4937588.

[296] TSGS, "TS 123 288 - v17.9.0 - 5g; architecture enhancements for 5g system (5gs) to support network data analytics services (3gpp TS 23.288 version 17.9.0 release 17)," 2023.

[297] G. S. M. Association, "Definition of quality of service parameters and their computation," *Etsi Ts 102 250-2*, vol. 1, pp. 1–252, 2017.

[298] Y. Zhang, "Mobile edge computing for beyond 5g/6g," in *Mobile Edge Computing*. Cham: Springer International Publishing, 2022, pp. 37–45, ISBN: 978-3-030-83944-4. DOI: 10.1007/978-3-030-83944-4_4.

[299] Y. Wang and J. Zhao, "Mobile edge computing, metaverse, 6g wireless communications, artificial intelligence, and blockchain: Survey and their convergence," *2022 IEEE 8th World Forum on Internet of Things, WF-IoT 2022*, 2022. DOI: 10.1109/WF-IOT54382.2022.10152245.

[300] L. Lovén *et al.*, "EdgeAI: A vision for distributed, edge-native artificial intelligence in future 6g networks,"

[301] S. S. Sonone, K. Saini, S. Jadhav, M. S. Sankhla, and V. Nagar, "The future of edge computing," *Advances in Computers*, vol. 127, pp. 333–358, Jan. 2022, ISSN: 0065-2458. DOI: 10.1016/BS.ADCOM.2022.02.009.

[302] Y. Zhang, "SIMULA SPRINGER BRIEFS ON COMPUTING 9 mobile edge computing."

[303] A. Alawadhi, A. Almogahed, and E. Azrag, "Towards edge computing for 6g internet of everything: Challenges and opportunities," *1st International Conference in Advanced Innovation on Smart City, ICAISC 2023 - Proceedings*, 2023. DOI: 10.1109/ICAISC56366.2023.10085007.

[304] L. Wu, G. Yang, J. Yan, S. Ran, B. Zhao, and H. Zhou, "Simulation for urban computing scenarios: An overview and research challenges," *Proceedings - 2023 IEEE 10th International Conference on Cyber Security and Cloud Computing and 2023 IEEE 9th International Conference on Edge Computing and Scalable Cloud, CSCloud-EdgeCom 2023*, pp. 12–17, 2023. DOI: 10.1109/CSCLOUD-EDGECOM58631.2023.00012.

[305] G. Nencioni, R. G. Garroppo, and R. F. Olimid, "5g multi-access edge computing: A survey on security, dependability, and performance," *IEEE Access*, vol. 11, pp. 63 496–63 533, 2023, ISSN: 21693536. DOI: 10.1109/ACCESS.2023.3288334.

[306] N. Abbas, Y. Zhang, A. Taherkordi, and T. Skeie, "Mobile edge computing: A survey," *IEEE Internet of Things Journal*, vol. 5, no. 1, pp. 450–465, Feb. 2018, ISSN: 23274662. DOI: 10.1109/JIOT.2017.2750180.

[307] F. Vhora and J. Gandhi, "A comprehensive survey on mobile edge computing: Challenges, tools, applications," *Proceedings of the 4th International Conference on Computing Methodologies and Communication, ICCMC 2020*, pp. 49–55, Mar. 2020. DOI: 10.1109/ICCMC48092.2020.ICCMC-0009.

[308] S. N. Shirazi, A. Gouglidis, A. Farshad, and D. Hutchison, "The extended cloud: Review and analysis of mobile edge computing and fog from a security and resilience perspective," *IEEE JOURNAL ON SELECTED AREAS IN COMMUNICATIONS*, vol. 1,

[309] S. Zhou, W. Jadoon, and I. A. Khan, "Computing offloading strategy in mobile edge computing environment: A comparison between adopted frameworks, challenges, and future directions," *Electronics 2023, Vol. 12, Page 2452*, vol. 12, no. 11, p. 2452, May 2023, ISSN: 2079-9292. DOI: 10.3390/ELECTRONICS12112452.

[310] M. A. Khan, E. Baccour, *et al.*, "A survey on mobile edge computing for video streaming: Opportunities and challenges," *IEEE Access*, vol. 10, pp. 120 514–120 550, 2022, ISSN: 21693536. DOI: 10.1109/ACCESS.2022.3220694.

[311] W. Wang, D. T. Hoang, *et al.*, "A survey on consensus mechanisms and mining strategy management in blockchain networks," *IEEE Access*, vol. 7, pp. 22 328–22 370, 2019, ISSN: 21693536. DOI: 10.1109/ACCESS.2019.2896108.

[312] A. Singh, S. C. Satapathy, A. Roy, and A. Gutub, "AI-based mobile edge computing for IoT: Applications, challenges, and future scope," *Arabian Journal for Science and Engineering 2021 47:8*, vol. 47, no. 8, pp. 9801–9831, Jan. 2022, ISSN: 2191-4281. DOI: 10.1007/S13369-021-06348-2.

[313] S. M. A. Huda and S. Moh, "Survey on computation offloading in UAV-enabled mobile edge computing," *Journal of Network and Computer Applications*, vol. 201, p. 103 341, May 2022, ISSN: 1084-8045. DOI: 10.1016/J.JNCA.2022.103341.

[314] Z. Song, X. Qin, Y. Hao, T. Hou, J. Wang, and X. Sun, "A comprehensive survey on aerial mobile edge computing: Challenges, state-of-the-art, and future directions," *Computer*

Communications, vol. 191, pp. 233–256, Jul. 2022, ISSN: 0140-3664. DOI: 10.1016/J.COMCOM.2022.05.004.

[315] D. C. Nguyen, P. N. Pathirana, M. Ding, and A. Seneviratne, "Blockchain for 5g and beyond networks: A state of the art survey," *Journal of Network and Computer Applications*, vol. 166, p. 102 693, Sep. 2020, ISSN: 1084-8045. DOI: 10.1016/J.JNCA.2020.102693.

[316] D. C. Nguyen, P. N. Pathirana, M. Ding, and A. Seneviratne, "Blockchain for 5g and beyond networks: A state of the art survey," *Journal of Network and Computer Applications*, vol. 166, p. 102 693, 2020, ISSN: 1084-8045. DOI: https://doi.org/10.1016/j.jnca.2020.102693.

[317] H. Xu, P. V. Klaine, O. Onireti, B. Cao, M. Imran, and L. Zhang, "Blockchain-enabled resource management and sharing for 6g communications," *Digital Communications and Networks*, vol. 6, no. 3, pp. 261–269, Aug. 2020, ISSN: 23528648. DOI: 10.1016/J.DCAN.2020.06.002.

[318] J. Wang, X. Ling, Y. Le, Y. Huang, and X. You, "Blockchain-enabled wireless communications: A new paradigm towards 6g," *National Science Review*, vol. 8, no. 9, Sep. 2021, ISSN: 2053714X. DOI: 10.1093/NSR/NWAB069.

[319] G. Bindu, I. T. J. S, V. R. Kanakala, G. L. K. Niharika, and B. E. Raj, "Impact of blockchain technology in 6g network: A comprehensive survey," *5th International Conference on Inventive Computation Technologies, ICICT 2022 - Proceedings*, pp. 328–334, 2022. DOI: 10.1109/ICICT54344.2022.9850463.

[320] N. Krishnaraj, K. Bellam, B. Sivakumar, and A. Daniel, "The future of cloud computing: Blockchain-based decentralized cloud/fog solutions – challenges, opportunities, and standards," in *Blockchain Security in Cloud Computing*, K. M. Baalamurugan, S. R. Kumar, A. Kumar, V. Kumar, and S. Padmanaban, Eds. Cham: Springer International Publishing, 2022, pp. 207–226, ISBN: 978-3-030-70501-5. DOI: 10.1007/978-3-030-70501-5_10.

[321] Y. Zuo, J. Guo, N. Gao, Y. Zhu, S. Jin, and X. Li, "A survey of blockchain and artificial intelligence for 6g wireless communications," *IEEE Communications Surveys and Tutorials*, 2023, ISSN: 1553877X. DOI: 10.1109/COMST.2023.3315374.

[322] S. Das, S. Namasudra, and V. H. C. d. Albuquerque, "Blockchain technology: Fundamentals, applications, and challenges," *Blockchain Technology in e-Healthcare Management*, pp. 1–30, Dec. 2022. DOI: 10.1049/PBHE048E_CH110.1049/PBHE048E10.1049/PBHE048E_CH1.

[323] E. W. D. Mauro, "Smart contracts operating on blockchain: Advantages and disadvantages," *Italian Law Journal*, vol. 8, 2022.

[324] E. Atay and J. L. Y. T. Tong, "The impact of blockchain technology on human resource management," *https://services.igi-global.com/resolvedoi/resolve.aspx?doi=10.4018/978-1-7998-9035-5.ch009*, pp. 136–151, DOI: 10.4018/978-1-7998-9035-5.CH009.

[325] J. Golosova and A. Romanovs, "The advantages and disadvantages of the blockchain technology," *2018 IEEE 6th Workshop on Advances in Information, Electronic and Electrical Engineering, AIEEE 2018 - Proceedings*, Dec. 2018. DOI: 10.1109/AIEEE.2018.8592253.

[326] V. M. Ammbika and D. S. Rao, "Limitations of blockchain technology with its applications," *International Journal of Recent Technology and Engineering*, vol. 8, no. 2, pp. 3646–3652, Sep. 2019, ISSN: 22773878. DOI: 10.35940/IJRTE.B1459.0982S1119.

[327] W. Viriyasitavat, L. D. Xu, Z. Bi, and V. Pungpapong, "Blockchain and internet of things for modern business process in digital economy - the state of the art," *IEEE Transactions on Computational Social Systems*, vol. 6, no. 6, pp. 1420–1432, Dec. 2019, ISSN: 2329924X. DOI: 10.1109/TCSS.2019.2919325.

[328] W. Viriyasitavat, L. D. Xu, Z. Bi, D. Hoonsopon, and N. Charoenruk, "Managing QoS of internet-of-things services using blockchain," *IEEE Transactions on Computational Social Systems*, vol. 6, no. 6, pp. 1357–1368, Dec. 2019, ISSN: 2329924X. DOI: 10.1109/TCSS.2019.2919667.

[329] M. H. Miraz and M. Ali, "Applications of blockchain technology beyond cryptocurrency," *Annals of Emerging Technologies in Computing*, vol. 2, no. 1, pp. 1–6, Jan. 2018, ISSN: 2516029X. DOI: 10.33166/AETIC.2018.01.001.

[330] Y. Lu, "Blockchain and the related issues: A review of current research topics," *Journal of Management Analytics*, vol. 5, no. 4, pp. 231–255, Oct. 2018, ISSN: 23270039. DOI: 10.1080/23270012.2018.1516523.

[331] Y. Lu, "Blockchain: A survey on functions, applications and open issues," *Journal of Industrial Integration and Management*, vol. 3, no. 4, Dec. 2018, ISSN: 24248630. DOI: 10.1142/S242486221850015X.

[332] Y. Lu, "The blockchain: State-of-the-art and research challenges," *Journal of Industrial Information Integration*, vol. 15, pp. 80–90, Sep. 2019, ISSN: 2452-414X. DOI: 10.1016/J.JII.2019.04.002.

[333] M. Z. Ali, A. Abohmra, *et al.*, "Quantum for 6g communication: A perspective," *IET Quantum Communication*, vol. 4, no. 3, pp. 112–124, Sep. 2023, ISSN: 26328925. DOI: 10.1049/QTC2.12060.

[334] M. M. Wilde and M. H. Hsieh, "The quantum dynamic capacity formula of a quantum channel," *Quantum Information Processing*, vol. 11, no. 6, pp. 1431–1463, Sep. 2012, ISSN: 15700755. DOI: 10.1007/S11128-011-0310-6/METRICS.

[335] A. Manzalini, "Quantum communications in future networks and services," *Quantum Reports 2020, Vol. 2, Pages 221-232*, vol. 2, no. 1, pp. 221–232, Mar. 2020, ISSN: 2624-960X. DOI: 10.3390/QUANTUM2010014.

[336] Q. Ruihong and M. Ying, "Research progress of quantum repeaters," *Journal of Physics: Conference Series*, vol. 1237, no. 5, p. 052 032, Jun. 2019, ISSN: 1742-6596. DOI: 10.1088/1742-6596/1237/5/052032.

[337] C. Elliott, "Building the quantum network*," *New Journal of Physics*, vol. 4, no. 1, p. 46, Jul. 2002, ISSN: 1367-2630. DOI: 10.1088/1367-2630/4/1/346.

[338] A. Reiserer, "Colloquium: Cavity-enhanced quantum network nodes," *Reviews of Modern Physics*, vol. 94, no. 4, p. 041 003, Oct. 2022, ISSN: 15390756. DOI: 10.1103/REVMODPHYS.94.041003/FIGURES/11/MEDIUM.

[339] K. Chakraborty, F. Rozpedek, A. Dahlberg, and S. Wehner, "Distributed routing in a quantum internet," Jul. 2019.

[340] K. Chakraborty, D. Elkouss, B. Rijsman, and S. Wehner, "Entanglement distribution in a quantum network: A multicommodity flow-based approach," *IEEE Transactions on Quantum Engineering*, vol. 1, 2020, ISSN: 26891808. DOI: 10.1109/TQE.2020.3028172.

[341] F. Sun, "Performance analysis of quantum channels," *Quantum Engineering*, vol. 2, no. 2, Jun. 2020, ISSN: 2577-0470. DOI: 10.1002/QUE2.35.

[342] M. Pompili *et al.*, "Realization of a multinode quantum network of remote solid-state qubits," *Science*, vol. 372, no. 6539, pp. 259–264, Apr. 2021, ISSN: 10959203. DOI: 10.1126/science.abg1919.

[343] S.-H. Wei, B. Jing, *et al.*, "Towards real-world quantum networks: A review," *Laser and Photonics Reviews*, vol. 16, no. 3, p. 2 100 219, Mar. 2022, ISSN: 1863-8899. DOI: 10.1002/LPOR.202100219.

[344] V. Ziegler and S. Yrjola, "6g indicators of value and performance," in *2020 2nd 6G Wireless Summit (6G SUMMIT)*, 2020, pp. 1–5. DOI: 10.1109/6GSUMMIT49458.2020.9083885.

[345] H. Viswanathan and P. E. Mogensen, "Communications in the 6g era," *IEEE Access*, vol. 8, pp. 57 063–57 074, 2020. DOI: 10.1109/ACCESS.2020.2981745.

[346] P. Mach and Z. Becvar, "Device-to-device relaying: Optimization, performance perspectives, and open challenges towards 6g networks," *IEEE Communications Surveys and Tutorials*, vol. 24, no. 3, pp. 1336–1393, Sep. 2022, ISSN: 1553877X. DOI: 10.1109/COMST.2022.3180887.

[347] S. Zhang, J. Liu, H. Guo, M. Qi, N. K.-I. Network, and undefined 2020, "Envisioning device-to-device communications in 6g," *ieeexplore.ieee.org*,

[348] A. Shahraki, A. Taherkordi, O. Haugen, and F. Eliassen, "A survey and future directions on clustering: From WSNs to IoT and modern networking paradigms," *IEEE Transactions on Network and Service Management*, vol. 18, no. 2, pp. 2242–2274, Jun. 2021, ISSN: 19324537. DOI: 10.1109/TNSM.2020.3035315.

[349] C. Suraci, S. Pizzi, A. Molinaro, and G. Araniti, "MEC and d2d as enabling technologies for a secure and lightweight 6g eHealth system," *IEEE Internet of Things Journal*, vol. 9, no. 13, pp. 11 524–11 532, Jul. 2022, ISSN: 23274662. DOI: 10.1109/JIOT.2021.3130666.

[350] R. Fantacci and B. Picano, "A d2d-aided federated learning scheme with incentive mechanism in 6g networks," *IEEE Access*, vol. 11, pp. 107–117, 2023, ISSN: 21693536. DOI: 10.1109/ACCESS.2022.3232440.

[351] Q. Guo, F. Tang, and N. Kato, "Federated reinforcement learning-based resource allocation for d2d-aided digital twin edge networks in 6g industrial IoT," *IEEE Transactions on Industrial Informatics*, vol. 19, no. 5, pp. 7228–7236, May 2023, ISSN: 19410050. DOI: 10.1109/TII.2022.3227655.

[352] M. Zhou, J. Li, *et al.*, "An architecture for AoI and cache hybrid multicast/unicast/d2d with cell-free massive MIMO systems," *IEEE Access*, vol. 11, pp. 43 080–43 088, 2023, ISSN: 21693536. DOI: 10.1109/ACCESS.2023.3271519.

[353] W. Khalid, H. Yu, D. T. Do, Z. Kaleem, and S. Noh, "RIS-aided physical layer security with full-duplex jamming in underlay d2d networks," *IEEE Access*, vol. 9, pp. 99 667–99 679, 2021, ISSN: 21693536. DOI: 10.1109/ACCESS.2021.3095852.

[354] I. I. Ioannou, C. Christophorou, V. Vassiliou, M. Lestas, and A. Pitsillides, "Dynamic d2d communication in 5g/6g using a distributed AI framework," *IEEE Access*, vol. 10, pp. 62 772–62 799, 2022, ISSN: 21693536. DOI: 10.1109/ACCESS.2022.3182388.

[355] D. Zucchetto and A. Zanella, "Uncoordinated access schemes for the iot: Approaches, regulations, and performance," *IEEE Communications Magazine*, vol. 55, pp. 48–54, 2017.

[356] Q. Bi, "Ten trends in the cellular industry and an outlook on 6g," *IEEE Communications Magazine*, vol. 57, pp. 31–36, 2019.

[357] M. B. Shahab, R. Abbas, M. Shirvanimoghaddam, and S. J. Johnson, "Grant-free non-orthogonal multiple access for iot: A survey," *IEEE Communications Surveys and Tutorials*, vol. 22, pp. 1805–1838, 2019.

[358] N. I. Bernardo, "Improving error resiliency of sparse code multiple access using precoding and non-orthogonal signaling techniques," in *2018 11th International Symposium on Communication Systems, Networks and Digital Signal Processing (CSNDSP)*, 2018, pp. 1–6. DOI: 10.1109/CSNDSP.2018.8471755.

[359] W. Kim, H. Ji, and B. Shim, "Channel aware sparse signaling for ultra low-latency communication in tdd systems," in *2018 IEEE 88th Vehicular Technology Conference (VTC-Fall)*, 2018, pp. 1–5. DOI: 10.1109/VTCFall.2018.8690971.

[360] G. Wunder, H. Boche, T. Strohmer, and P. Jung, "Sparse signal processing concepts for efficient 5g system design," *IEEE Access*, vol. 3, pp. 195–208, 2014.

[361] H. Sarieddeen, M.-S. Alouini, and T. Y.Al-Naffouri, "An overview of signal processing techniques for terahertz communications," *Proceedings of the IEEE*, vol. 109, pp. 1628–1665, 2020.

[362] C. Huang, S. Hu, *et al.*, "Holographic mimo surfaces for 6g wireless networks: Opportunities, challenges, and trends," *IEEE Wireless Communications*, vol. 27, pp. 118–125, 2019.

[363] R. Deng, Y. Zhang, *et al.*, "Reconfigurable holographic surfaces for ultra-massive mimo in 6g: Practical design, optimization and implementation," *IEEE Journal on Selected Areas in Communications*, vol. 41, no. 8, pp. 2367–2379, 2023. DOI: 10.1109/JSAC.2023.3288248.

[364] R. Deng, B. Di, H. Zhang, H. V. Poor, and L. Song, "Holographic mimo for leo satellite communications aided by reconfigurable holographic surfaces," *IEEE Journal on Selected Areas in Communications*, vol. 40, no. 10, pp. 3071–3085, 2022. DOI: 10.1109/JSAC.2022.3196110.

[365] T. Frey, M. Döring, C. Waldschmidt, and T. Chaloun, "Towards holographic antenna systems for mimo radar and communication applications," in *2022 16th European Conference on Antennas and Propagation (EuCAP)*, 2022, pp. 1–5. DOI: 10.23919/EuCAP53622.2022.9769556.

[366] A. Adhikary *et al.*, "An artificial intelligence framework for holographic beamforming: Coexistence of holographic mimo and intelligent omni-surface," in *2023 International Conference on Information Networking (ICOIN)*, 2023, pp. 19–24. DOI: 10.1109/ICOIN56518.2023.10048994.

[367] M. Giordani, M. Polese, M. Mezzavilla, S. Rangan, and M. Zorzi, "Toward 6g networks: Use cases and technologies," *IEEE Communications Magazine*, vol. 58, pp. 55–61, 2020.

[368] J. Sun, G. Gui, H. Sari, H. Gačanin, and F. Adachi, "Aviation data lake: Using side information to enhance future air-ground vehicle networks," *IEEE Vehicular Technology Magazine*, vol. 16, pp. 40–48, 2021.

[369] L. Wang, T. Han, Q. Li, J. Yan, X. Liu, and D. Deng, "Cell-less communications in 5g vehicular networks based on vehicle-installed access points," *IEEE Wireless Communications*, vol. 24, pp. 64–71, 2017.

[370] M. Z. Chowdhury, M. Shahjalal, S. Ahmed, and Y. M. Jang, "6g wireless communication systems: Applications, requirements, technologies, challenges, and research directions," *IEEE Open Journal of the Communications Society*, vol. 1, pp. 957–975, 2019.

[371] L. U. Khan, I. Yaqoob, M. Imran, Z. Han, and C. S. Hong, "6g wireless systems: A vision, architectural elements, and future directions," *IEEE Access*, vol. 8, pp. 147 029–147 044, 2020, ISSN: 2169-3536. DOI: 10.1109/ACCESS.2020.3015289.

[372] C. Merlhe and C. Gueguen, "Dynamic cell-less radio access network meta-scheduler for high system capacity increase," in *2020 IEEE 21st International Symposium on "A*

World of Wireless, Mobile and Multimedia Networks" (WoWMoM), 2020, pp. 108–116. DOI: 10.1109/WoWMoM49955.2020.00031.

[373] A. Viterbi, "Error bounds for convolutional codes and an asymptotically optimum decoding algorithm," *IEEE Transactions on Information Theory*, vol. 13, no. 2, pp. 260–269, 1967, ISSN: 1557-9654. DOI: 10.1109/TIT.1967.1054010.

[374] P. Elias, "Error-free coding," *Transactions of the IRE Professional Group on Information Theory*, vol. 4, no. 4, pp. 29–37, 1954, ISSN: 2168-2704. DOI: 10.1109/TIT.1954.1057464.

[375] G. Forney, "Generalized minimum distance decoding," *IEEE Transactions on Information Theory*, vol. 12, no. 2, pp. 125–131, 1966. DOI: 10.1109/TIT.1966.1053873.

[376] C. Berrou, A. Glavieux, and P. Thitimajshima, "Near shannon limit error-correcting coding and decoding: Turbo-codes. 1," in *Proceedings of ICC '93 - IEEE International Conference on Communications*, vol. 2, 1993, 1064–1070 vol.2. DOI: 10.1109/ICC.1993.397441.

[377] S. M. R. Islam, N. Avazov, O. A. Dobre, and K. S. Kwak, "Power-domain non-orthogonal multiple access (NOMA) in 5g systems: Potentials and challenges," *IEEE Communications Surveys and Tutorials*, vol. 19, no. 2, pp. 721–742, 2017, ISSN: 1553877X. DOI: 10.1109/COMST.2016.2621116.

[378] "Kronecker product," in *Matrix Calculus, Kronecker Product and Tensor Product*, ch. Chapter 2, pp. 107–178. DOI: 10.1142/9789811202520_0002. eprint: https://www.worldscientific.com/doi/pdf/10.1142/9789811202520_0002.

[379] P. Elias, "Predictive coding–i," *IRE Transactions on Information Theory*, vol. 1, no. 1, pp. 16–24, 1955, ISSN: 2168-2712. DOI: 10.1109/TIT.1955.1055126.

[380] A. A. Andi and O. Gazi, "Fast decoding of polar codes using tree structure," *IET Communications*, vol. 13, no. 14, pp. 2063–2068, 2019. DOI: https://doi.org/10.1049/iet-com.2018.5019. eprint: https://ietresearch.onlinelibrary.wiley.com/doi/pdf/10.1049/iet-com.2018.5019.

[381] A. Viterbi, "Error bounds for convolutional codes and an asymptotically optimum decoding algorithm," *IEEE Transactions on Information Theory*, vol. 13, no. 2, pp. 260–269, 1967, ISSN: 1557-9654. DOI: 10.1109/TIT.1967.1054010.

[382] J. Zhang and M. Wang, "Belief propagation decoder with multiple bit-flipping sets and stopping criteria for polar codes," *IEEE Access*, vol. 8, pp. 83 710–83 717, 2020, ISSN: 2169-3536. DOI: 10.1109/ACCESS.2020.2988878.

[383] W. M. Waggener, *Pulse Code Modulation Techniques*. Springer New York, NY, 1994, ISBN: 978-0-442-01436-0.

[384] M. Vaezi *et al.*, "Cellular, wide-area, and non-terrestrial iot: A survey on 5g advances and the road toward 6g," *IEEE Communications Surveys and Tutorials*, vol. 24, no. 2, pp. 1117–1174, 2022. DOI: 10.1109/COMST.2022.3151028.

[385] L.-H. Shen, K.-T. Feng, and L. Hanzo, "Five facets of 6g: Research challenges and opportunities," *ACM Comput. Surv.*, vol. 55, no. 11, Feb. 2023, ISSN: 0360-0300. DOI: 10.1145/3571072.

[386] M. Banafaa, I. Shayea, J. Din, M. Hadri Azmi, *et al.*, "6g mobile communication technology: Requirements, targets, applications, challenges, advantages, and opportunities," *Alexandria Engineering Journal*, vol. 64, pp. 245–274, 2023, ISSN: 1110-0168. DOI: https://doi.org/10.1016/j.aej.2022.08.017.

[387] H. F. Alhashimi *et al.*, "A survey on resource management for 6g heterogeneous networks: Current research, future trends, and challenges," *Electronics*, vol. 12, no. 3, 2023, ISSN: 2079-9292. DOI: 10.3390/electronics12030647.

[388] V. P. Rekkas, S. Sotiroudis, P. Sarigiannidis, S. Wan, G. K. Karagiannidis, and S. K. Goudos, "Machine learning in beyond 5g/6g networks—state-of-the-art and future trends," *Electronics*, vol. 10, no. 22, 2021, ISSN: 2079-9292. DOI: 10.3390/electronics10222786.

[389] "Deep learning-enabled polar code decoders for 5g networks and beyond," *AEU - International Journal of Electronics and Communications*, vol. 177, 2024, ISSN: 1434-8411.

[390] A. Nauman, T. N. Nguyen, Y. A. Qadri, Z. Nain, K. Cengiz, and S. W. Kim, "Artificial intelligence in beyond 5g and 6g reliable communications," *IEEE Internet of Things Magazine*, vol. 5, no. 1, pp. 73–78, 2022. DOI: 10.1109/IOTM.001.2100140.

[391] L. Mucchi *et al.*, "Signal processing techniques for 6g," *Journal of Signal Processing Systems*, vol. 95, no. 4, pp. 435–457, Apr. 1, 2023, ISSN: 1939-8115. DOI: 10.1007/s11265-022-01827-7.

[392] B. Ozpoyraz, A. T. Dogukan, Y. Gevez, U. Altun, and E. Basar, "Deep learning-aided 6g wireless networks: A comprehensive survey of revolutionary phy architectures," *IEEE Open Journal of the Communications Society*, vol. 3, pp. 1749–1809, 2022. DOI: 10.1109/OJCOMS.2022.3210648.

[393] M. Shafi, R. K. Jha, and S. Jain, "6g: Technology evolution in future wireless networks," *IEEE Access*, pp. 1–1, 2024. DOI: 10.1109/ACCESS.2024.3385230.

[394] N. V. Huynh *et al.*, "Generative ai for physical layer communications: A survey," *IEEE Transactions on Cognitive Communications and Networking*, pp. 1–1, 2024. DOI: 10.1109/TCCN.2024.3384500.

[395] M. Abd Elaziz *et al.*, "Evolution toward intelligent communications: Impact of deep learning applications on the future of 6g technology," *WIREs Data Mining and Knowledge Discovery*, vol. 14, no. 1, e1521, 2024. DOI: https://doi.org/10.1002/widm.1521. eprint: https://wires.onlinelibrary.wiley.com/doi/pdf/10.1002/widm.1521.

[396] R. Chataut, M. Nankya, and R. Akl, "6g networks and the ai revolution—exploring technologies, applications, and emerging challenges," *Sensors*, vol. 24, no. 6, 2024, ISSN: 1424-8220. DOI: 10.3390/s24061888.

[397] M. Rowshan, M. Qiu, Y. Xie, X. Gu, and J. Yuan, "Channel coding towards 6g: Technical overview and outlook," *IEEE Open Journal of the Communications Society*, pp. 1–1, 2024. DOI: 10.1109/OJCOMS.2024.3390000.

[398] A. Irawan, G. Witjaksono, and W. K. Wibowo, "Deep learning for polar codes over flat fading channels," in *2019 International Conference on Artificial Intelligence in Information and Communication (ICAIIC)*, 2019, pp. 488–491. DOI: 10.1109/ICAIIC.2019.8669025.

[399] B. He, S. Wu, Y. Deng, H. Yin, J. Jiao, and Q. Zhang, "A machine learning based multi-flips successive cancellation decoding scheme of polar codes," May 2020, pp. 1–5. DOI: 10.1109/VTC2020-Spring48590.2020.9128875.

[400] S. Dehdashtian, M. Hashemi, and S. Salehkaleybar, "Deep-learning-based blind recognition of channel code parameters over candidate sets under awgn and multi-path fading conditions," *IEEE Wireless Communications Letters*, vol. 10, no. 5, pp. 1041–1045, 2021. DOI: 10.1109/LWC.2021.3056631.

[401] M. Yang, C. Bian, and H.-S. Kim, "Deep joint source channel coding for wireless image transmission with ofdm," in *ICC 2021 - IEEE International Conference on Communications*, 2021, pp. 1–6. DOI: 10.1109/ICC42927.2021.9500996.

[402] K. Chahine, N. Ye, and H. Kim, "Deepic: Coding for interference channels via deep learning," in *2021 IEEE Global Communications Conference (GLOBECOM)*, 2021, pp. 01–06. DOI: 10.1109/GLOBECOM46510.2021.9685430.

[403] T. Dozat, "Incorporating nesterov momentum into adam," 2016.

[404] Y. Nesterov, "A method for unconstrained convex minimization problem with the rate of convergence $o(\frac{1}{k^2})$," 1983.

[405] Y. A. LeCun, L. Bottou, G. B. Orr, and K.-R. Müller, "Efficient BackProp," in *Neural Networks: Tricks of the Trade: Second Edition*, G. Montavon, G. B. Orr, and K.-R. Müller, Eds., Berlin, Heidelberg: Springer Berlin Heidelberg, 2012, pp. 9–48, ISBN: 978-3-642-35289-8. DOI: 10.1007/978-3-642-35289-8_3.

[406] G. Montavon, G. Orr, and K.-R. Müller, *Neural Networks: Tricks of the Trade: Second Edition*. Jan. 2012, ISBN: 978-3-642-35288-1. DOI: 10.1007/978-3-642-35289-8.

[407] S. Eliason, *Maximum Likelihood Estimation: Logic and Practice* (Maximum Likelihood Estimation no. 96). SAGE Publications, 1993, ISBN: 9780803941076.

[408] O. Jumira and S. Zeadally, *Energy Efficiency in Wireless Networks* (FOCUS Series). Wiley, 2013, ISBN: 9781118580011.

[409] R. Y. Wu, L. W. Wu, S. He, S. Liu, and T. J. Cui, "Programmable metamaterials," *Programmable Materials*, vol. 1, e4, 2023. DOI: 10.1017/pma.2023.1.

[410] K. He, T. Tang, *et al.*, "Polarization-dependent reconfigurable light field manipulation by liquid-immersion metasurface," *Opt. Express*, vol. 31, no. 9, pp. 13 739–13 750, Apr. 2023. DOI: 10.1364/OE.483593.

[411] Z. Zhang, L. Dai, *et al.*, "Active ris vs. passive ris: Which will prevail in 6g?" *IEEE Transactions on Communications*, vol. 71, no. 3, pp. 1707–1725, 2023. DOI: 10.1109/TCOMM.2022.3231893.

[412] P. Li and J. Bian, "Active RIS-assisted transmission design for wireless secrecy network with energy harvesting," *Mathematical Problems in Engineering*, vol. 2023, J. Hu, Ed., p. 8 897 781, Feb. 1, 2023, ISSN: 1024-123X. DOI: 10.1155/2023/8897781.

[413] R. Long, Y.-C. Liang, Y. Pei, and E. G. Larsson, "Active reconfigurable intelligent surface-aided wireless communications," *IEEE Transactions on Wireless Communications*, vol. 20, no. 8, pp. 4962–4975, 2021. DOI: 10.1109/TWC.2021.3064024.

[414] L. Dong and W. Yan, "Active reconfigurable intelligent surface (ris) aided secure wireless transmission under a shared power source between transmitter and ris," in *2022 14th International Conference on Wireless Communications and Signal Processing (WCSP)*, 2022, pp. 996–1000. DOI: 10.1109/WCSP55476.2022.10039260.

[415] Z. Peng, Z. Zhang, C. Pan, M. Di Renzo, O. A. Dobre, and J. Wang, "Beamforming optimization for active ris-aided multiuser communications with hardware impairments," *IEEE Transactions on Wireless Communications*, pp. 1–1, 2024. DOI: 10.1109/TWC.2024.3367131.

[416] S. Hassouna *et al.*, "A survey on reconfigurable intelligent surfaces: Wireless communication perspective," *IET Communications*, vol. 17, no. 5, pp. 497–537, 2023. DOI: https://doi.org/10.1049/cmu2.12571. eprint: https://ietresearch.onlinelibrary.wiley.com/doi/pdf/10.1049/cmu2.12571.

[417] X. Zhai, G. Han, Y. Cai, Y. Liu, and L. Hanzo, "Simultaneously transmitting and reflecting (star) ris assisted over-the-air computation systems," *IEEE Transactions on Communications*, vol. 71, no. 3, pp. 1309–1322, 2023. DOI: 10.1109/TCOMM.2023.3235915.

[418] H. Jia, L. Ma, and S. Valaee, "Star-ris enabled downlink secure noma network under imperfect csi of eavesdroppers," *IEEE Communications Letters*, vol. 27, no. 3, pp. 802–806, 2023. DOI: 10.1109/LCOMM.2023.3233980.

[419] R. Zhong, X. Mu, Y. Liu, Y. Chen, J. Zhang, and P. Zhang, "Star-riss assisted noma networks: A distributed learning approach," *IEEE Journal of Selected Topics in Signal Processing*, vol. 17, no. 1, pp. 264–278, 2023. DOI: 10.1109/JSTSP.2022.3229567.

[420] R. Zhong, X. Mu, X. Xu, Y. Chen, and Y. Liu, "Star-riss assisted noma networks: A tile-based passive beamforming approach," in *2022 International Symposium on Wireless Communication Systems (ISWCS)*, 2022, pp. 1–6. DOI: 10.1109/ISWCS56560.2022.9940329.

[421] H. Luo, R. Liu, M. Li, and Q. Liu, "Ris-aided integrated sensing and communication: Joint beamforming and reflection design," *IEEE Transactions on Vehicular Technology*, vol. 72, no. 7, pp. 9626–9630, 2023. DOI: 10.1109/TVT.2023.3248657.

[422] R. Liu, M. Li, Q. Liu, and A. L. Swindlehurst, "Snr/crb-constrained joint beamforming and reflection designs for ris-isac systems," *IEEE Transactions on Wireless Communications*, pp. 1–1, 2023. DOI: 10.1109/TWC.2023.3341429.

[423] L. Cao, H. Yin, L. Tan, and X. Pei, "Ris with insufficient phase shifting capability: Modeling, beamforming, and experimental validations," *IEEE Transactions on Communications*, pp. 1–1, 2024. DOI: 10.1109/TCOMM.2024.3392784.

[424] J. Rao, Y. Zhang, S. Tang, Z. Li, C.-Y. Chiu, and R. Murch, "An active reconfigurable intelligent surface utilizing phase-reconfigurable reflection amplifiers," *IEEE Transactions on Microwave Theory and Techniques*, vol. 71, no. 7, pp. 3189–3202, 2023. DOI: 10.1109/TMTT.2023.3237029.

[425] J. Xu, C. Yuen, *et al.*, "Reconfiguring wireless environments via intelligent surfaces for 6g: Reflection, modulation, and security," *Science China Information Sciences*, vol. 66, no. 3, p. 130 304, Feb. 20, 2023, ISSN: 1869-1919. DOI: 10.1007/s11432-022-3626-5.

[426] M. Barbuto *et al.*, "Reflective intelligent surfaces: Enabling reconfigurability with composite vortices," in *2023 XXXVth General Assembly and Scientific Symposium of the International Union of Radio Science (URSI GASS)*, 2023, pp. 1–3. DOI: 10.23919/URSIGASS57860.2023.10265449.

[427] H. Chen, N. Li, R. Long, and Y.-C. Liang, "Channel estimation and training design for active ris aided wireless communications," *IEEE Wireless Communications Letters*, vol. 12, no. 11, pp. 1876–1880, 2023. DOI: 10.1109/LWC.2023.3297231.

[428] W. U. Khan, E. Lagunas, *et al.*, "Integration of noma with reflecting intelligent surfaces: A multi-cell optimization with sic decoding errors," *IEEE Transactions on Green Communications and Networking*, vol. 7, no. 3, pp. 1554–1565, 2023. DOI: 10.1109/TGCN.2023.3263121.

[429] H. Kim, S. Oh, S. Bang, H. Yang, B. Kim, and J. Oh, "Independently polarization manipulable liquid- crystal -based reflective metasurface for 5g reflectarray and reconfigurable intelligent surface," *IEEE Transactions on Antennas and Propagation*, vol. 71, no. 8, pp. 6606–6616, 2023. DOI: 10.1109/TAP.2023.3283136.

[430] X. Jin, X. Li, Z. Wu, and M. Wen, "Ris-aided joint transceiver space shift keying reflection modulation," *IEEE Communications Letters*, vol. 27, no. 3, pp. 891–895, 2023. DOI: 10.1109/LCOMM.2023.3236619.

[431] R. Singh, A. Kaushik, W. Shin, G. C. Alexandropoulos, M. Toka, and M. Di Renzo, "Indexed multiple access with reconfigurable intelligent surfaces: The reflection tuning potential," *IEEE Communications Magazine*, vol. 62, no. 4, pp. 120–126, 2024. DOI: 10.1109/MCOM.020.2300073.

[432] T. Lu, L. Chen, J. Han, Y. Wang, and K. Yu, "Ris-assisted physical layer key generation by exploiting randomness from channel coefficients of reflecting elements and ofdm subcarriers," *Ad Hoc Networks*, vol. 138, p. 103 002, 2023, ISSN: 1570-8705. DOI: https://doi.org/10.1016/j.adhoc.2022.103002.

[433] D. Badheka, J. Sapis, S. R. Khosravirad, and H. Viswanathan, "Accurate modeling of intelligent reflecting surface for communication systems," *IEEE Transactions on Wireless Communications*, vol. 22, no. 9, pp. 5871–5883, 2023. DOI: 10.1109/TWC.2023.3237955.

[434] W. Jiang and H. D. Schotten, "Opportunistic reflection in reconfigurable intelligent surface-assisted wireless networks," in *2023 IEEE 34th Annual International Symposium on Personal, Indoor and Mobile Radio Communications (PIMRC)*, 2023, pp. 1–6. DOI: 10.1109/PIMRC56721.2023.10293900.

[435] J. Zhang, R. Xiong, J. Liu, T. Mi, and R. C. Qiu, *Design and prototyping of transmissive ris-aided wireless communication*, 2024. arXiv: 2402.05570 [eess.SY].

[436] A. Rabault *et al.*, "On the tacit linearity assumption in common cascaded models of ris-parametrized wireless channels," *IEEE Transactions on Wireless Communications*, pp. 1–1, 2024. DOI: 10.1109/TWC.2024.3367953.

[437] V. Sharma, R. Allu, S. K. Singh, K. Singh, T. Q. Duong, and T. A. Tsiftsis, "Robust transmission design in multi-objective ris-aided swipt iot communications," *IEEE Internet of Things Journal*, pp. 1–1, 2024. DOI: 10.1109/JIOT.2024.3364392.

[438] J. Liu, Y. Huang, J. Zhang, R. Xiong, and R. C. Qiu, *Trtar: Transmissive ris-assisted through-the-wall human activity recognition*, 2024. arXiv: 2401.05170 [eess.SY].

[439] A. M. Huroon, Y.-C. Huang, and L.-C. Wang, "Uav-ris assisted multiuser communications through transmission strategy optimization: Gbd application," *IEEE Transactions on Vehicular Technology*, pp. 1–14, 2024. DOI: 10.1109/TVT.2024.3362066.

[440] Y. Xu, Y. Li, and T. Q. S. Quek, *Robust transmission design for ris-assisted integrated sensing and communication systems*, 2024. arXiv: 2401.13882 [cs.IT].

[441] Z. Liu, W. Chen, Q. Wu, *et al.*, *Rate-splitting multiple access for transmissive reconfigurable intelligent surface transceiver empowered isac system*, 2024. arXiv: 2402.12127 [cs.IT].

[442] V. Sharma, A. Paul, S. K. Singh, K. Singh, and S. Biswas, "Robust transmission for energy-efficient sub-connected active ris-assisted wireless networks: Drl versus traditional optimization," *IEEE Transactions on Green Communications and Networking*, pp. 1–1, 2024. DOI: 10.1109/TGCN.2024.3370691.

[443] K. Ntougias, S. Chatzinotas, and I. Krikidis, *Hybrid ris with sub-connected active partitions: Performance analysis and transmission design*, 2024. arXiv: 2402.11547 [cs.IT].

[444] R. Dong, B. Wang, K. Cao, J. Tian, and T. Cheng, "Secure transmission design of ris enabled uav communication networks exploiting deep reinforcement learning," *IEEE Transactions on Vehicular Technology*, pp. 1–15, 2024. DOI: 10.1109/TVT.2024.3357821.

[445] J. Zhang, X. Huang, Y. Han, K. Xu, S. Jin, and S. Ma, "Transmission design for hybrid ris and dma assisted mimo multiple-access channel over spatially correlated rician fading," *IEEE Transactions on Communications*, pp. 1–1, 2024. DOI: 10.1109/TCOMM.2024.3351356.

[446] L. Zhai, Y. Zou, and J. Zhu, "Robust transmission design for ris-assisted multi-cluster wireless powered communications with hardware impairments," *IEEE Transactions on Communications*, pp. 1–1, 2024. DOI: 10.1109/TCOMM.2024.3351758.

[447] R. P. Naik, M. Salman, J. Bolboli, S. Shetty C S, and W.-Y. Chung, "Multiuser data transmission aided by simultaneous transmit and reflect reconfigurable intelligent surface in underwater wireless optical communications," *IEEE Transactions on Vehicular Technology*, pp. 1–14, 2024. DOI: 10.1109/TVT.2024.3357838.

[448] K. Li, H. Du, and S. Li, "Reconfigurable intelligent surface assisted multi-user secrecy transmission with low-resolution dacs," *IEEE Transactions on Green Communications and Networking*, pp. 1–1, 2024. DOI: 10.1109/TGCN.2024.3362866.

[449] X. Xie, C. He, X. Ma, F. Gao, Z. Han, and Z. J. Wang, "Joint precoding for active intelligent transmitting surface empowered outdoor-to-indoor communication in mmwave cellular networks," *IEEE Transactions on Wireless Communications*, vol. 22, no. 10, pp. 7072–7086, 2023. DOI: 10.1109/TWC.2023.3247906.

[450] Z. Lin *et al.*, "Refracting ris-aided hybrid satellite-terrestrial relay networks: Joint beamforming design and optimization," *IEEE Transactions on Aerospace and Electronic Systems*, vol. 58, no. 4, pp. 3717–3724, 2022. DOI: 10.1109/TAES.2022.3155711.

[451] M. Ahmed, A. Wahid, *et al.*, "A survey on star-ris: Use cases, recent advances, and future research challenges," *IEEE Internet of Things Journal*, vol. 10, no. 16, pp. 14 689–14 711, 2023. DOI: 10.1109/JIOT.2023.3279357.

[452] Z. Zhang, J. Chen, Y. Liu, Q. Wu, B. He, and L. Yang, "On the secrecy design of star-ris assisted uplink noma networks," *IEEE Transactions on Wireless Communications*, vol. 21, no. 12, pp. 11 207–11 221, 2022. DOI: 10.1109/TWC.2022.3190563.

[453] S. Xu, C. Liu, H. Wang, M. Qian, and J. Li, "On secrecy performance analysis of multi-antenna STAR-RIS-assisted downlink NOMA systems," *EURASIP Journal on Advances in Signal Processing*, vol. 2022, no. 1, p. 118, Dec. 5, 2022, ISSN: 1687-6180. DOI: 10.1186/s13634-022-00953-5.

[454] Y. Liu, X. Mu, R. Schober, and H. V. Poor, "Simultaneously transmitting and reflecting (star)-riss: A coupled phase-shift model," *ICC 2022 - IEEE International Conference on Communications*, pp. 2840–2845, 2021.

[455] J. Xu, Y. Liu, X. Mu, and O. A. Dobre, "Star-riss: Simultaneous transmitting and reflecting reconfigurable intelligent surfaces," *IEEE Communications Letters*, vol. 25, no. 9, pp. 3134–3138, 2021. DOI: 10.1109/LCOMM.2021.3082214.

[456] M. Li, S. Zhang, Y. Ge, Z. Li, F. Gao, and P. Fan, "Star-ris aided integrated sensing and communication over high mobility scenario," *IEEE Transactions on Communications*, 2024.

[457] Y. Wen, G. Chen, S. Fang, Z. Chu, P. Xiao, and R. Tafazolli, "Star-ris-assisted-full-duplex jamming design for secure wireless communications system," *IEEE Transactions on Information Forensics and Security*, 2024.

[458] W. Wei, X. Pang, C. Xing, N. Zhao, and D. Niyato, "Star-ris aided secure noma integrated sensing and communication," *IEEE Transactions on Wireless Communications*, 2024.

[459] Y. Eghbali, S. K. Taskou, M. R. Mili, M. Rasti, and E. Hossain, "Providing urllc service in multi-star-ris assisted and full-duplex cellular wireless systems: A meta-learning approach," *IEEE Communications Letters*, 2024.

[460] X. Mu, J. Xu, Y. Liu, and L. Hanzo, "Reconfigurable intelligent surface-aided near-field communications for 6g: Opportunities and challenges," *IEEE Vehicular Technology Magazine*, 2024.

[461] M. Toka *et al.*, "Ris-empowered leo satellite networks for 6g: Promising usage scenarios and future directions," *arXiv preprint arXiv:2402.07381*, 2024.

[462] M. Katwe, R. Deshpande, K. Singh, C. Pan, P. H. Ghare, and T. Q. Duong, "Spectrally-efficient beamforming design for star-ris-aided urllc noma systems," *IEEE Transactions on Communications*, 2024.

[463] Y. Liu, J. Xu, Z. Wang, X. Mu, J. Zhang, and P. Zhang, "Simultaneously transmitting and reflecting (star) riss for 6g: Fundamentals, recent advances, and future directions," *Frontiers of Information Technology and Electronic Engineering*, vol. 24, no. 12, pp. 1689–1707, 2023.

[464] M. Ahmed, A. Wahid, *et al.*, "A survey on star-ris: Use cases, recent advances, and future research challenges," *IEEE Internet of Things Journal*, 2023.

[465] X. Mu, J. Xu, and Y. Liu, "Reconfigurable intelligent surfaces toward 6g: From reflection only to simultaneous transmission and reflection (star)," in *Fundamentals of 6G Communications and Networking*, X. Lin, J. Zhang, Y. Liu, and J. Kim, Eds., Cham: Springer International Publishing, 2024, pp. 399–424, ISBN: 978-3-031-37920-8. DOI: 10.1007/978-3-031-37920-8_15.

[466] T. Wang, F. Fang, and Z. Ding, "Joint phase shift and beamforming design in a multi-user miso star-ris assisted downlink noma network," *IEEE Transactions on Vehicular Technology*, vol. 72, no. 7, pp. 9031–9043, 2023. DOI: 10.1109/TVT.2023.3248789.

[467] A. Papazafeiropoulos, A. M. Elbir, P. Kourtessis, I. Krikidis, and S. Chatzinotas, "Cooperative ris and star-ris assisted mmimo communication: Analysis and optimization," *IEEE Transactions on Vehicular Technology*, vol. 72, no. 9, pp. 11 975–11 989, 2023. DOI: 10.1109/TVT.2023.3264724.

[468] Q. Wu, S. Zhang, B. Zheng, C. You, and R. Zhang, "Intelligent reflecting surface-aided wireless communications: A tutorial," *IEEE Transactions on Communications*, vol. 69, no. 5, pp. 3313–3351, 2021. DOI: 10.1109/TCOMM.2021.3051897.

[469] J. Fink, R. L. Cavalcante, and S. Stanczak, "Multicast beamforming using semidefinite relaxation and bounded perturbation resilience," in *ICASSP 2019 - 2019 IEEE International Conference on Acoustics, Speech and Signal Processing (ICASSP)*, 2019, pp. 4749–4753. DOI: 10.1109/ICASSP.2019.8682325.

[470] H. Huang, X. Wang, C. Zhang, K. Qiu, and Z. Han, "Reward-maximization-based passive beamforming for multi-ris-aided multi-user miso systems," in *2021 IEEE Global Communications Conference (GLOBECOM)*, Madrid, Spain: IEEE Press, 2021, pp. 01–06. DOI: 10.1109/GLOBECOM46510.2021.9685372.

[471] X. Cao, Y. Zhang, and P. Du, "Robust mmse beamforming of downlink multi-user miso systems in the presence of beam pointing error," in *2021 13th International Conference on Wireless Communications and Signal Processing (WCSP)*, 2021, pp. 1–5. DOI: 10.1109/WCSP52459.2021.9613507.

[472] I. Ahmad, R. Narmeen, Z. Becvar, and I. Guvenc, "Machine learning-based beamforming for unmanned aerial vehicles equipped with reconfigurable intelligent surfaces," *IEEE Wireless Communications*, vol. 29, no. 4, pp. 32–38, 2022. DOI: 10.1109/MWC.004.2100694.

[473] P. Susarla, Y. Deng, M. Juntti, and O. Sílven, "Hierarchial-dqn position-aided beamforming for uplink mmwave cellular-connected uavs," in *GLOBECOM 2022 - 2022 IEEE Global Communications Conference*, 2022, pp. 1308–1313. DOI: 10.1109/GLOBECOM48099.2022.10001044.

[474] R. Zhong, Y. Liu, X. Mu, Y. Chen, X. Wang, and L. Hanzo, "Hybrid reinforcement learning for star-riss: A coupled phase-shift model based beamformer," *IEEE Journal on Selected Areas in Communications*, vol. 40, no. 9, pp. 2556–2569, 2022. DOI: 10.1109/JSAC.2022.3192053.

[475] M. Liu, R. Wang, Z. Xing, and J. Yu, "Complex-valued reinforcement learning based dynamic beamforming design for irs aided time-varying downlink channel," in *2022 IEEE 95th Vehicular Technology Conference: (VTC2022-Spring)*, 2022, pp. 1–5. DOI: 10.1109/VTC2022-Spring54318.2022.9860446.

[476] Y. Ge and J. Fan, "Beamforming optimization for intelligent reflecting surface assisted miso: A deep transfer learning approach," *IEEE Transactions on Vehicular Technology*, vol. 70, no. 4, pp. 3902–3907, 2021. DOI: 10.1109/TVT.2021.3062870.

[477] A. Abdallah, A. Celik, M. M. Mansour, and A. M. Eltawil, "Deep reinforcement learning based beamforming codebook design for ris-aided mmwave systems," in *2023 IEEE 20th Consumer Communications and Networking Conference (CCNC)*, 2023, pp. 1020–1026. DOI: 10.1109/CCNC51644.2023.10060056.

[478] A. Faisal, I. Al-Nahhal, O. A. Dobre, and T. M. N. Ngatched, "Distributed ris-assisted fd systems with discrete phase shifts: A reinforcement learning approach," in *GLOBECOM 2022 - 2022 IEEE Global Communications Conference*, 2022, pp. 5862–5867. DOI: 10.1109/GLOBECOM48099.2022.10001723.

[479] P. S. Aung, L. X. Nguyen, Y. K. Tun, Z. Han, and C. S. Hong, "Deep reinforcement learning-based joint spectrum allocation and configuration design for star-ris-assisted v2x communications," *IEEE Internet of Things Journal*, vol. 11, no. 7, pp. 11 298–11 311, 2024. DOI: 10.1109/JIOT.2023.3329893.

[480] S. Yadav and R. Rishi, "Deep reinforcement learning based energy-efficient design for star-irs assisted v2v users," in *Recent Trends in Image Processing and Pattern Recognition*, K. Santosh *et al.*, Eds., Cham: Springer Nature Switzerland, 2024, pp. 130–143, ISBN: 978-3-031-53082-1.

[481] L. Guo, J. Jia, J. Chen, and X. Wang, "Secure communication optimization in noma systems with uav-mounted star-ris," *IEEE Transactions on Information Forensics and Security*, vol. 19, pp. 2300–2314, 2024. DOI: 10.1109/TIFS.2023.3348242.

[482] C. Meng, K. Xiong, W. Chen, B. Gao, P. Fan, and K. B. Letaief, "Sum-rate maximization in star-ris-assisted rsma networks: A ppo-based algorithm," *IEEE Internet of Things Journal*, vol. 11, no. 4, pp. 5667–5680, 2024. DOI: 10.1109/JIOT.2023.3309859.

[483] T.-H. Nguyen, H. Park, and L. Park, "Recent studies on deep reinforcement learning in ris-uav communication networks," in *2023 International Conference on Artificial Intelligence in Information and Communication (ICAIIC)*, 2023, pp. 378–381. DOI: 10.1109/ICAIIC57133.2023.10067052.

[484] Z. Hu, R. Zhong, C. Fang, and Y. Liu, "Caching-at-stars: The next generation edge caching," *IEEE Transactions on Wireless Communications*, pp. 1–1, 2024. DOI: 10.1109/TWC.2023.3349230.

[485] M. Jamal, Z. Ullah, M. Naeem, M. Abbas, and A. Coronato, "A hybrid multi-agent reinforcement learning approach for spectrum sharing in vehicular networks," *Future Internet*, vol. 16, no. 5, 2024, ISSN: 1999-5903. DOI: 10.3390/fi16050152.

[486] M. Naqqash Tariq, J. Wang, S. Memon, M. Siraj, M. Altamimi, and M. A. Mirza, "Toward energy-efficiency: Integrating drl and ze-ris for task offloading in uav-mec environments," *IEEE Access*, vol. 12, pp. 65 530–65 542, 2024. DOI: 10.1109/ACCESS.2024.3397890.

[487] Z. Huang, Z. Kuang, S. Lin, F. Hou, and A. Liu, "Energy-efficient joint trajectory and reflecting design in irs-enabled uav edge computing," *IEEE Internet of Things Journal*, pp. 1–1, 2024. DOI: 10.1109/JIOT.2024.3380747.

[488] S. Soltani, R. S. Ehsan Ghafourian, and M. V. Diego Martín, "A deep reinforcement learning-based technique for optimal power allocation in multiple access communications," *Intelligent Automation and Soft Computing*, vol. 39, no. 1, pp. 93–108, 2024, ISSN: 2326-005X. DOI: 10.32604/iasc.2024.042693.

[489] Z. Li, W. Chen, Q. Wu, H. Cao, K. Wang, and J. Li, "Robust beamforming design and time allocation for irs-assisted wireless powered communication networks," *IEEE Transactions on Communications*, vol. 70, no. 4, pp. 2838–2852, 2022. DOI: 10.1109/TCOMM.2022.3152576.

[490] S. Liu, M. Lei, and M.-J. Zhao, "Deep learning based channel estimation for intelligent reflecting surface aided miso-ofdm systems," in *2020 IEEE 92nd Vehicular Technology Conference (VTC2020-Fall)*, 2020, pp. 1–5. DOI: 10.1109/VTC2020-Fall49728.2020.9348697.